APPROXIMATE SOLUTIONS OF SOME PREDATOR-PREY ECOLOGICAL MODELS

by

John R. Brearley

B.Eng. (Honours) McGill University, 1976

A THESIS SUBMITTED IN PARTIAL FULFILMENT OF

THE REQUIREMENTS FOR THE DEGREE OF

MASTER OF APPLIED SCIENCE

in

THE FACULTY OF GRADUATE STUDIES

in the Department

of

Electrical Engineering

We accept this thesis as conforming to

the required standard

THE UNIVERSITY OF BRITISH COLUMBIA

June, 1978

In presenting this thesis in partial fulfilment of the requirements for an advanced degree at the University of British Columbia, I agree that the Library shall make it freely available for reference and study. I further agree that permission for extensive copying of this thesis for scholarly purposes may be granted by the Head of my Department or by his representatives. It is understood that copying or publication of this thesis for financial gain shall not be allowed without my written permission.

Department of ELECTRICAL ENGINEERING.

The University of British Columbia
2075 Wesbrook Place
Vancouver, Canada
V6T 1W5

Date Aug. 17, 1978.

ABSTRACT

The purpose of this thesis is to develop and evaluate approximate analytical solutions of nonlinear differential equations that purport to model physical ecological systems of a predator-prey nature. A variety of analytical techniques, some well known and some new are used to obtain analytical solutions for these models. Solutions are obtained for five different predator-prey systems, and simulations show that these solutions are accurate over wide ranges of initial conditions and system parameters. These literal parameter solutions allow the user to readily determine which components of the solutions are sensitive to which parameters, and thus avoid the traditional heuristic computer sensitivity studies.

TABLE OF CONTENTS

LIST OF ILLUSTRATIONS

ACKNOWLEDGEMENTS

It is with great pleasure that I acknowledge the invaluable advice of Dr. A.C. Soudack, whose weekly interaction provided a continuing source of drive and inspiration, without which this undertaking would not have been completed.

This research was supported by National Research Council Grant A-3138, as well as a U.B.C. Fellowship. This support is gratefully acknowledged.

INTRODUCTION

The purpose of this thesis is to develop and evaluate approximate analytical solutions of systems of nonlinear differential equations that purport to model physical ecological systems of a predator prey nature. These analytical solutions will give insight into the system behaviour and the effect of system parameter variations without resorting to extensive computer simulation studies. A variety of analytical techniques, some well known and some new, are used to obtain the analytical solutions and are outlined in the following chapters.

The ecological systems of interest usually consist of one or more interacting species whose population dynamics are influenced by many factors, such as carrying capacity of the environment (see Gilpen 21), age and spatial distributions (see Hoppenstead 27 & Sanchez 50), natural evolution (see Zwanzig 57), prey nutrient control (see Rosenzweig 47), harvesting (see Brauer 7,8 & San Goh 51), and time delays (see Murray 41 & Mazanov 38) to name just a few.

There are numerous methods for mathematically describing the various observed biological phenomena. To begin with, the time variable may be modelled as continuous or discrete. The actual population variables are of the integer type in reality, but for large populations these are approximated by continuous variables. The model will consist of a system of difference, integral (see Greenberg 24), or differential equations. The differential equations may be either partial or ordinary, and either deterministic or stochastic in formulation.

In this thesis, we will be considering only pairs of first order coupled, continuous, time invariant, ordinary differential equations

modelling predator-prey systems. For those interested in discrete time models, the papers by May (36) and Oster (45) are recommended as introductory reading. Diamond (14) discusses some stability theory and results, while Comins (12) discusses the effects of a predator which can choose between several prey species. The mathematical phenomenon of bifurcation and the so-called "chaos" problem is expounded upon by Hoppenstead (26 & 28), May (35 & 37), and Smale (52). Some results concerning linear time varying systems are given by Mulholland (40). The joys and complications of third and higher order coupled systems are elaborated on by McGehee (39), Oaten (43), Rapport (46), and Rosenzweig (49).

The major current problem in ecological modelling lies in that the more elegent the biologically observed phenomena becomes, the less tractable the associated mathematics becomes, and vice versa. In an attempt to comprehend the dynamics of a given ecological system, the researchers have often neglected the second order effects when formulating their mathematical models. In practice, it is usually very difficult to backtrack and experimentally verify the validity of the complete model. The individual terms in the models are experimentally justified, however the combination given in the model may still not be enough to adequately describe the system at hand. In the models that will be presented in the following chapters, application, data, and results for the models will be given when available.

A single predator, single prey biological system is modelled (see Brauer 7) by a pair of first order, coupled, ordinary differential equations of the form

$$\begin{aligned} \dot{x} &= xf(x,y) \\ \dot{y} &= yg(x,y) \end{aligned} \qquad \text{with} \qquad \begin{aligned} x_o &\triangleq x(0) \\ y_o &\triangleq y(0) \end{aligned}$$

where x(t) and y(t) are, respectively, the prey and the predator populations. It should be noted that with this form of model, populations initially at zero remain there. Here it is assumed that the growth rates of the populations are dependant only on the present population sizes. Thus the model neglects the numerous factors which may influence real populations as previously mentioned. In a more general model, the expression for $\dot{y}(t)$ might contain a second term to include the effects of harvesting the predator (see Brauer 7, or Rapport, 46). These effects are not included in the models considered in this thesis, and permits the mathematics to remain tractable.

For the system of differential equations to represent a predator prey system, we must impose the following conditions

$$f_y(x,y) < 0 \quad g_x(x,y) > 0 \quad g_y(x,y) \leq 0$$

and

$$x \geq 0 \quad y \geq 0$$

where the subscripts indicate partial derivatives (see Brauer 7). The last two conditions are characteristic of all ecological systems, as negative populations are meaningless. The first two conditions imply that the prey population is decreased by increasing predator population and that the predator growth is dependant of the existence of the prey. The third condition expresses the possibility that competition amongst the predators for the prey may exist. Often g(x,y) is independant of y, implying that there is no competition amongst the predators.

In the following chapters, a number of ecological models will be introduced. Several different analytical techniques will be discussed and applied to the models to yield analytic approximate solutions, and these will be evaluated in detail.

CHAPTER ONE

LOTKA-VOLTERRA SYSTEM PROTOTYPE

1. Introduction

The Lotka-Volterra predator-prey system was selected for a prototype study. Predator-prey systems have been the subject of much mathematical study since the original work of Lotka (33) and Volterra (55), but to our knowledge, no one has developed approximate solutions that show the functional relation of the system parameters in the solution.

While there are many valid objections to the use of the Lotka-Volterra equations for describing physical predator prey systems (see May 34, or Ayala 1), it has been found that these equations do characterize some natural systems, such as the lynx and the Arctic hare populations, and some fish populations. With some modification, the equations can be used to model multi-species predator prey systems. It is this use of the Lotka-Volterra equations as the basic building block of a number of more complicated models (see Rapport 46) that motivates the analytical study of the system behaviour.

1.2 Analytical Technique

The Equivalent Ritz Method, also known as the Principle of Harmonic Balance, was developed about 60 years ago by W. Ritz (see Cunningham, 13), and will be used to determine approximate solutions of the Lotka-Volterra equations.

The Ritz method finds an approximate solution, $\tilde{x}(t)$ to the equation $\ddot{x} + f(x) = 0$ such that the functional

$$J = \int_{t_a}^{t_b} F(x,\dot{x},t)\ dt$$

is a minimum, and $F(x,\dot{x},t)$ is chosen such that the solution for the minimum of J, the Euler-Lagrange equation, is the differential equation we wish to solve, that is

$$\frac{\partial F}{\partial x} - \frac{d}{dt}\left[\frac{\partial F}{\partial \dot{x}}\right] = \ddot{x} + f(x) = E(x) = 0$$

The approximate solution $\tilde{x}(t)$ is of the form $\tilde{x}(t) = \sum_i a_i \phi_i(t)$, where the $\phi_i(t)$ form a linearly independant set, and are chosen from an à prior knowledge of the differential equation's behaviour. To obtain $\tilde{x}(t)$, the functional J must be minimized with respect to the n coefficients a_i. If we specify that $\phi_i(t_a) = \phi_i(t_b) = 0$, or ϕ_i is periodic in $t_a - t_b$, we obtain the conditions

$$\int_{t_b}^{t_a} \phi_i(t) E(\tilde{x}(t))\,dt = 0, \qquad i = 1, \ldots, n$$

For oscillatory systems the Equivalent Ritz Method eliminates the necessity of performing the above n integrations. If we take $\tilde{x}(t) = A \cos \omega t$ as an approximate solution to $\ddot{x} + f(x) = 0$, it is found by evaluating the above integral that the Ritz method is equivalent to choosing ω and A such that $\tilde{x}(t)$ satisfies the differential equation with the harmonic terms generated by $f(\tilde{x})$ being neglected (see Cunningham 13). That is to say that the sum of the coefficients of $\cos \omega t$ in $E(\tilde{x}(t))$ is identically zero. Similarly, if we take $\tilde{x}(t) = \sum_0^N a_n \cos n\omega t$, we find that we must have the coefficients of $\cos n\omega t$, for $n = 0, \ldots, N$, in $E(\tilde{x}(t))$ must balance to zero (hence the name Principle of Harmonic Balance).

1.3 Application to the Lotka-Volterra Equations

Consider the Lotka-Volterra predator prey system

$$\dot{x} = xf(x,y) \qquad f(x,y) = \alpha - \beta y$$

$$\dot{y} = yg(x,y) \qquad g(x,y) = -\gamma + \delta x$$

where $\alpha, \beta, \gamma, \delta > 0$.

This model was formulated by retaining the first terms of the double Taylor series expansion of $f(x,y)$ and $g(x,y)$. The coefficient γ represents the predator's natural mortality rate. The coefficients β and δ represent the magnitude of the predator prey interactions. The system has two signularities, at $(x_{sing}, y_{sing}) = (0,0)$ and $(\gamma/\delta, \alpha/\beta)$. Linearization of the differential equation about the singularities shows the former to be a saddle point and the latter to be a centre. We will apply the equivalent Ritz method to obtain approximate solutions in the neighbourhood of the centre.

The saddle point is of little interest to the discussion, the associated separatrices being the x and y axes. Thus we are guaranteed that if we start with both x and y greater than zero, they will always remain so.

An approximate solution of the form

$$x(t) = A + B \cos \omega t + C \sin \omega t$$

$$y(t) = D + E \cos \omega t + F \sin \omega t$$

is postulated, where A, B, C, D, E, F and ω have yet to be found. Substituting the above solutions into the differential equations and equating the coefficients of $\cos \omega t$, $\sin \omega t$ and the constant terms to zero, we obtain the following equations

$$\alpha C - \beta AF - \beta CD + \omega B = 0$$

$$C\omega - \alpha B + \beta AE + \beta BD = 0$$

$$\alpha A - \beta AD - \frac{\beta BE}{2} - \frac{\beta CF}{2} = 0$$

$$\omega E - \gamma F + \delta AF + \delta CD = 0$$

$$\omega F + \gamma E - \delta AE - \delta BD = 0$$

$$\delta AD - \gamma D + \frac{\delta BE}{2} + \frac{\delta CF}{2} = 0$$

By matching initial values, we obtain

$$x(0) = A + B$$

$$y(0) = D + E$$

We à priori assume that $A = \gamma/\delta$ and $D = \alpha/\beta$ in order to obtain closed trajectories about the desired equilibrium point in the x-y plane, (x_{sing}, y_{sing}). Solving the above set of equations, we obtain

$$B = x(0) - \gamma/\delta$$

$$C = \pm(y(0) - \alpha/\beta)(\beta/\delta)\sqrt{\gamma/\alpha}$$

$$E = y(0) - \alpha/\beta$$

$$F = \mp(x(0) - \gamma/\delta)(\delta/\beta)\sqrt{\alpha/\gamma}$$

$$\omega = \mp\sqrt{\gamma\alpha}$$

Thus the approximate solutions are given by

$$x(t) = \gamma/\delta + (x(0) - \gamma/\delta)\cos\sqrt{\gamma\alpha}t$$
$$-(y(0) - \alpha/\beta)(\beta/\delta)\sqrt{\gamma/\alpha}\sin\sqrt{\gamma\alpha}t$$

$$y(t) = \alpha/\beta + (y(0) - \alpha/\beta)\cos\sqrt{\gamma\alpha}t$$
$$+(x(0) - \gamma/\delta)(\delta/\beta)\sqrt{\alpha/\gamma}\sin\sqrt{\gamma\alpha}t$$

These solutions describe an ellipse in the x-y plane, and if the technique used is adequate, should compare favourably with numerical solutions of the Lotka-Volterra equations. Subsequent analysis reveals that

these solutions are identical to those obtained by linearizing about the singular point, even though this was not the method used to obtain them. As a general rule, the Ritz method will not normally generate linearized solutions as it did in this case.

1.4 Simulation Study of Ritz Solutions

To test the validity of the approximate solutions developed in the previous section, the Lotka-Volterra equations were simulated on the University of British Columbia's IBM 370/168 Computer using a variable step Runge-Kutta integration routine. The numerical and approximate solutions are plotted in the phase (x-y) plane, and also as functions of time.

In the simulation, the calculations were perfomed with the centre singularity located at (50,50) using the arbitrary parameter choice $\alpha = \gamma = 500$, and $\beta = \delta = 10$. Valid data for this model is difficult to locate. The trajectories were computed for initial conditions in the ranges $10 \leq x(0) \leq y(0) \leq 90$ in increments of 5. The trajectories and phase plane curves are shown in Figures 1.1 to 1.9 for the initial conditions $(x(0),y(0)) = (35,10)$, $(60,35)$ and $(85,35)$. It is seen that there is close agreement between the two solutions for initial conditions local to the center singularity.

From the time plots of the numerical solution, the actual frequency of the oscillation is computed, and the frequency error is given as the percentage difference between the Ritz frequency and the actual frequency. Also from the time plots of the solutions, the amplitude error is computed, being the worst case percentage difference between the Ritz solution amplitude peaks and the actual solution amplitude peaks. This method of computing amplitude errors neglects any phase error between the peaks and thus gives a measure of error of the solution amplitude envelope.

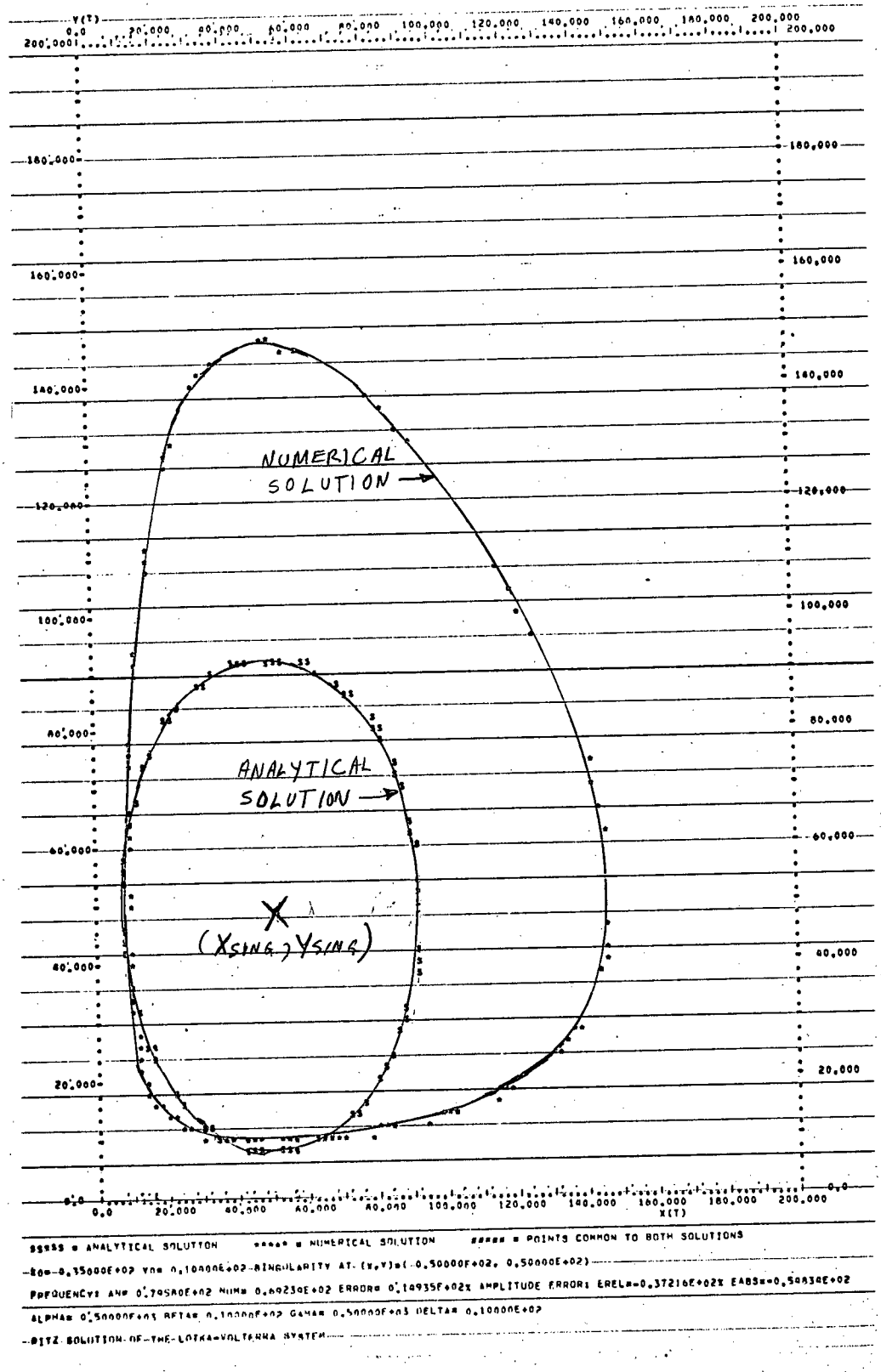

Fig. 1.1 "Lotka-Volterra Model Ritz solution for $(x_o, y_o) = (35, 10)$

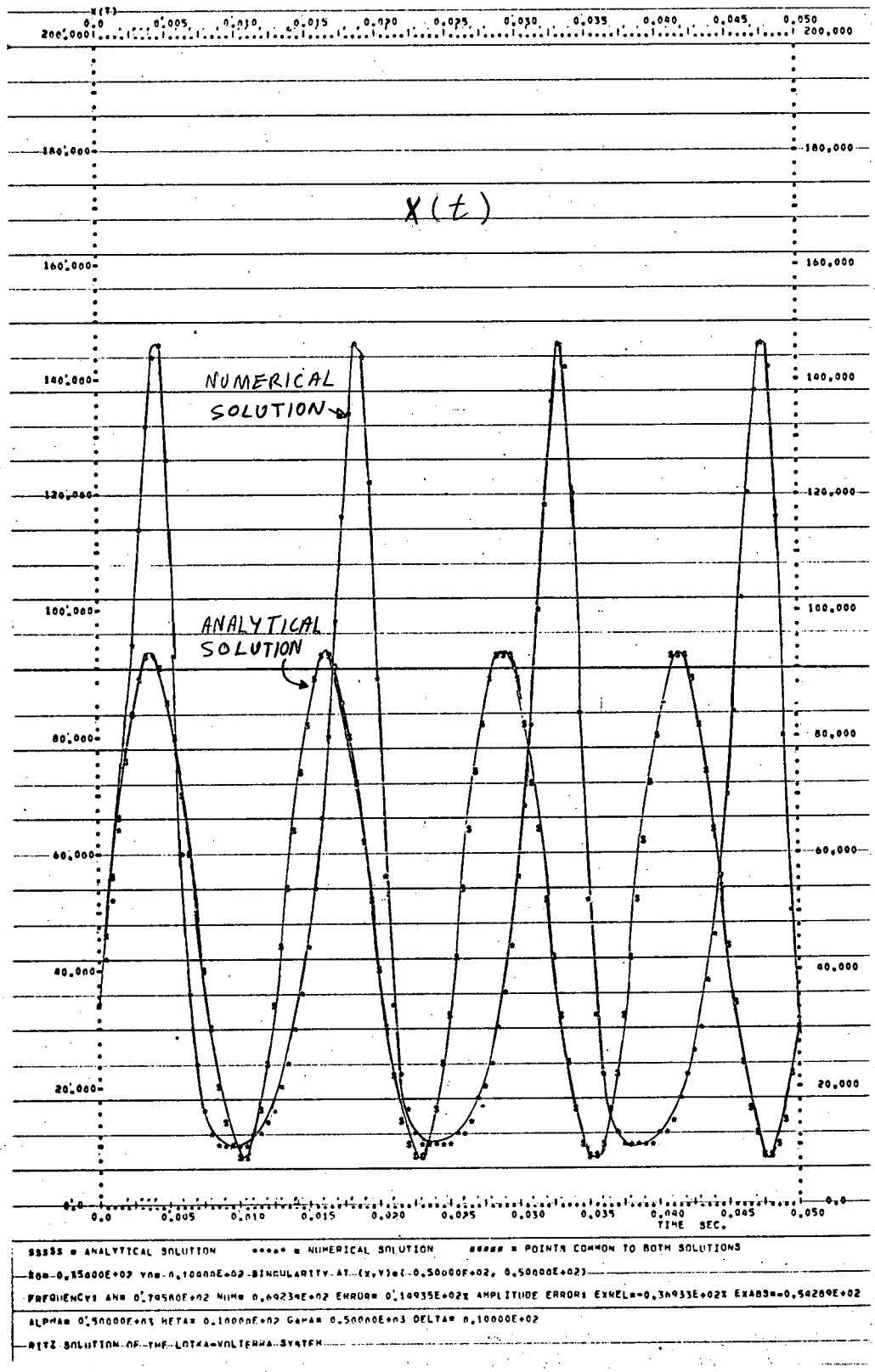

Fig. 1.2 Lotka-Volterra Model Ritz solution for $(x_o, y_o) = (35, 10)$

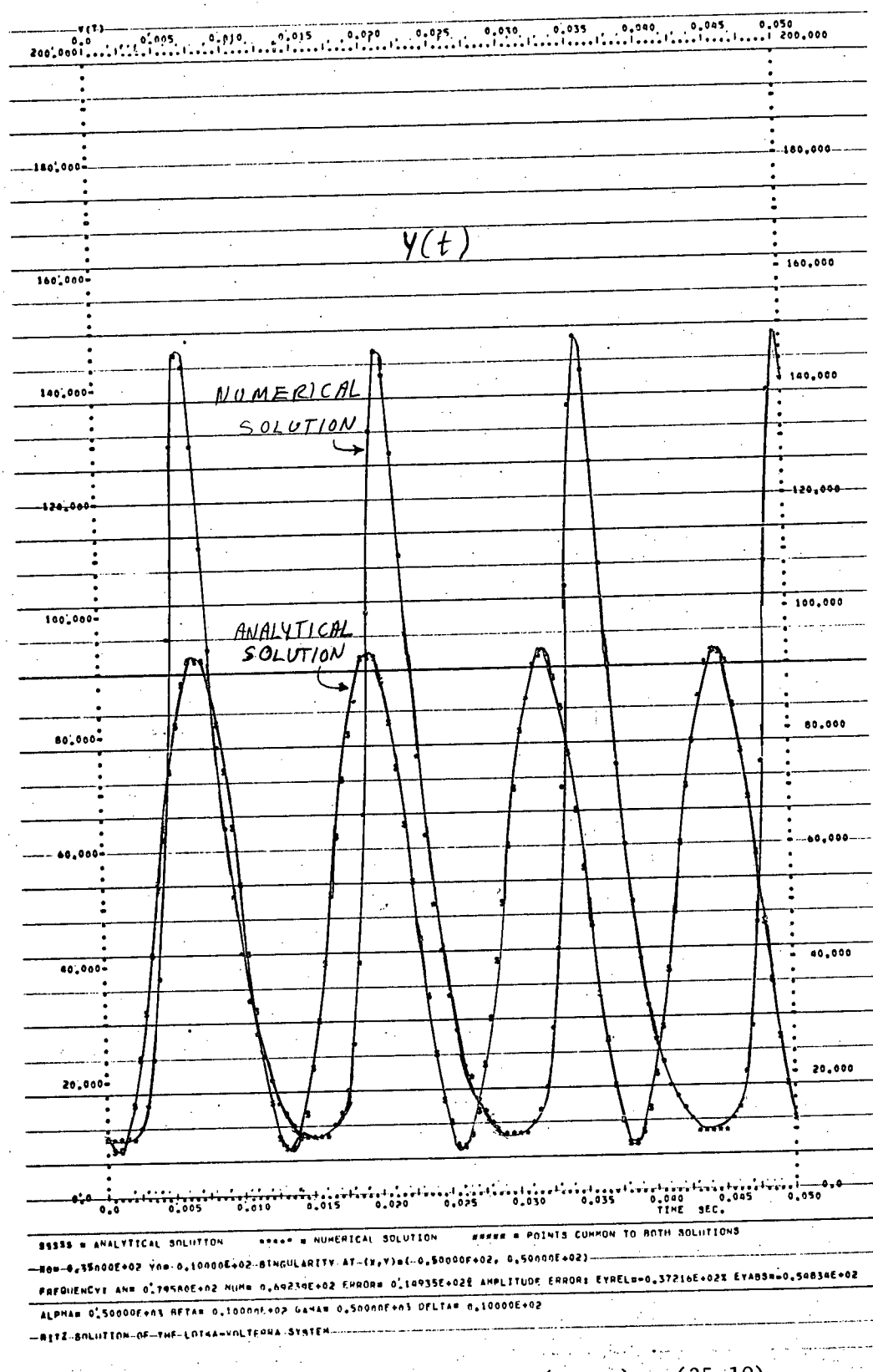

Fig. 1.3 Lotka-Volterra Model Ritz Solution for $(x_o, y_o) = (35, 10)$

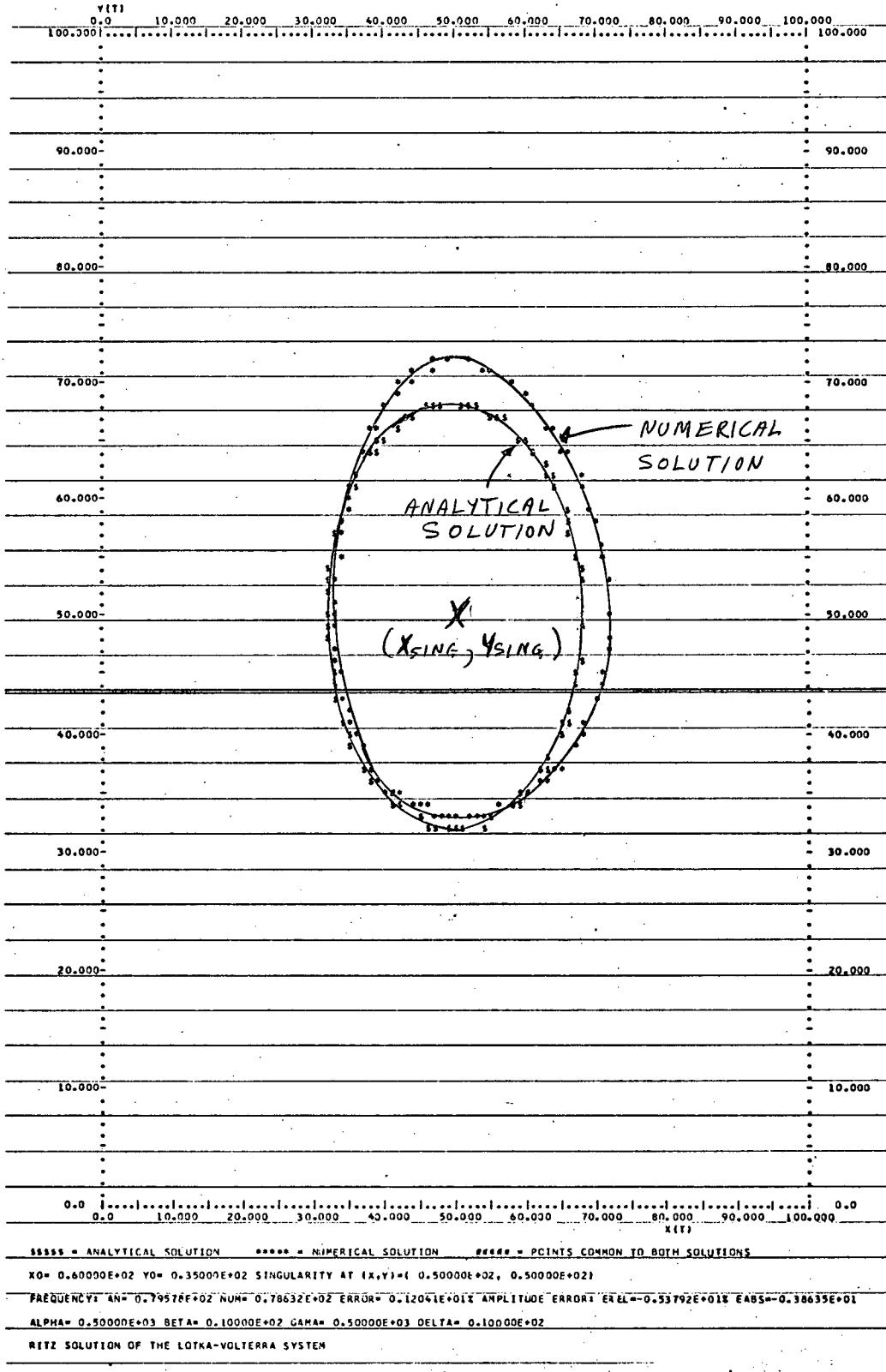

Fig. 1.4 Lotka-Volterra Model Ritz Solution for $(x_o, y_o) = (60, 35)$

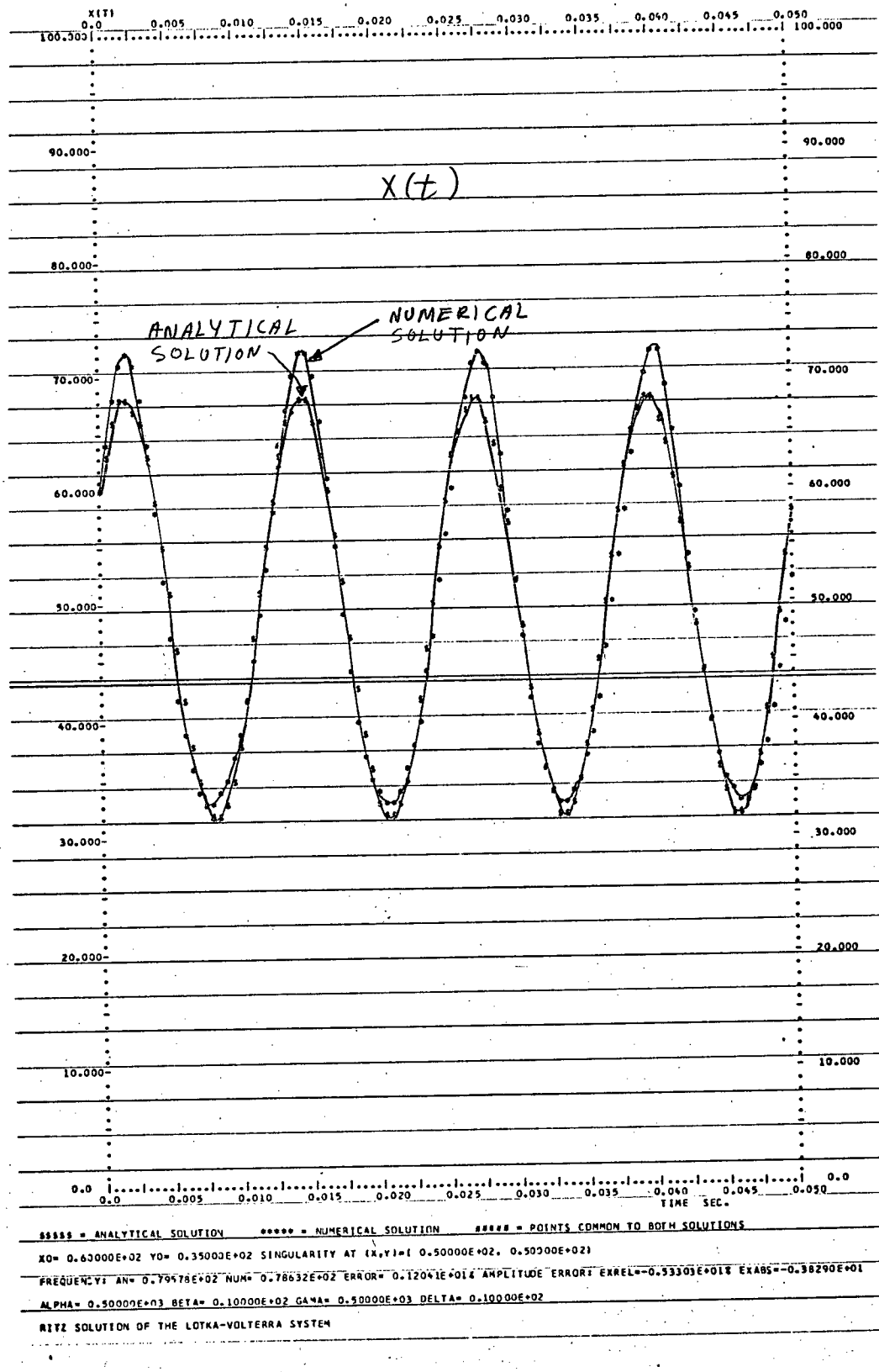

Fig. 1.5 Lotka-Volterra Model Ritz Solution for $(x_o, y_o) = (60, 35)$

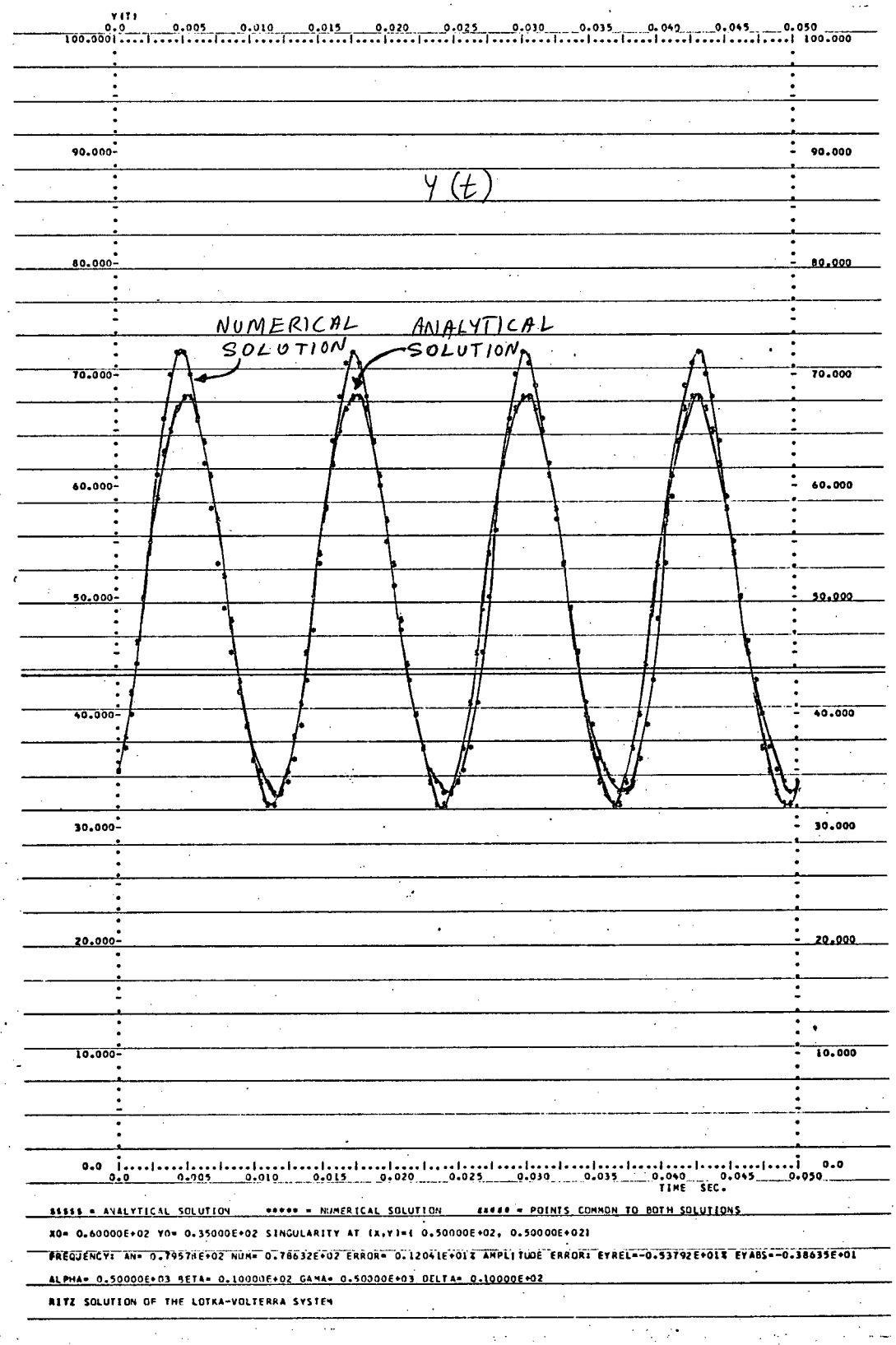

Fig. 1.6 Lotka-Volterra Model Ritz Solution for $(x_o, y_o) = (60, 35)$

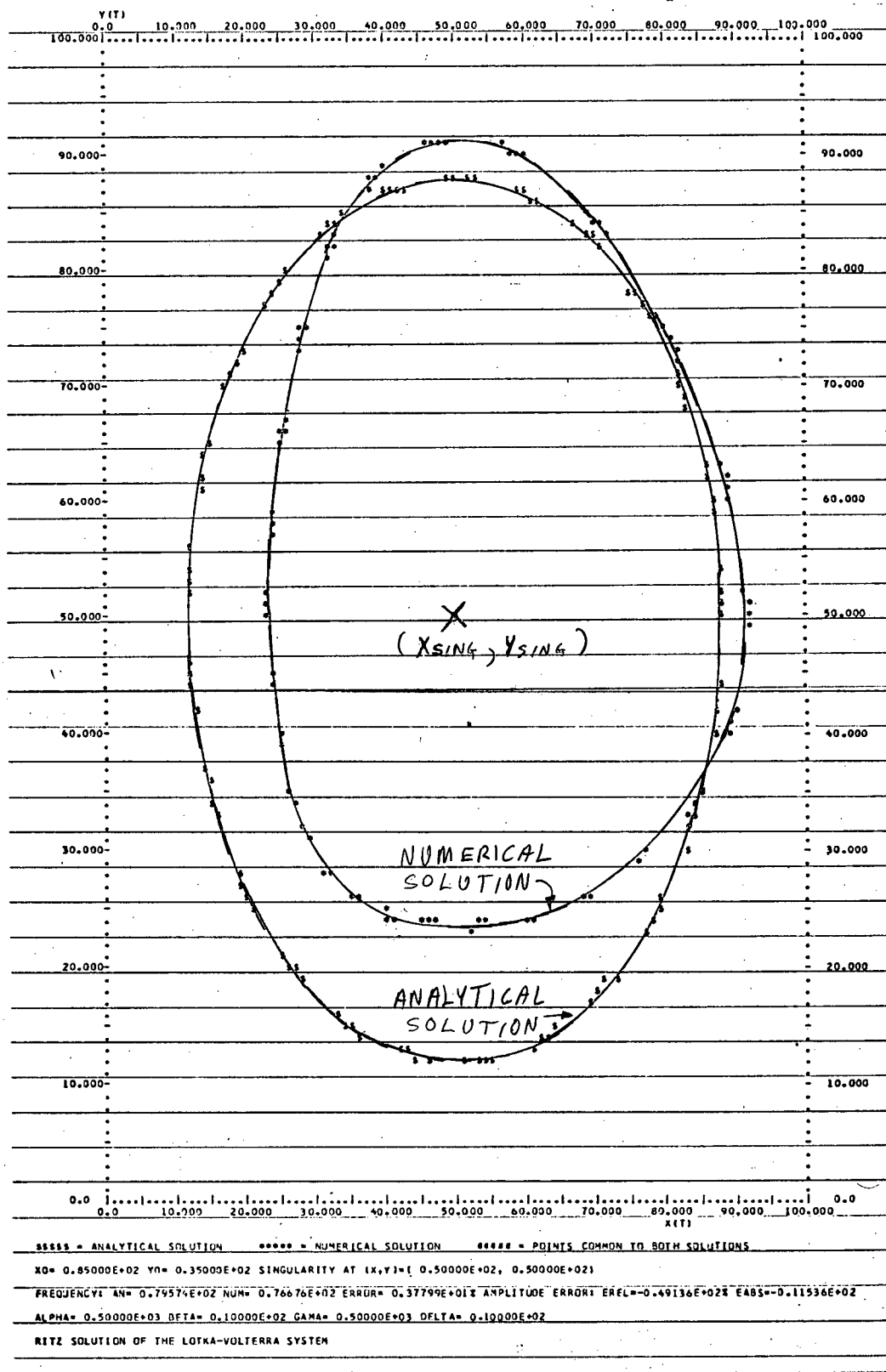

Fig. 1.7 Lotka-Volterra Model Ritz Solution for $(x_o, y_o) = (85, 35)$

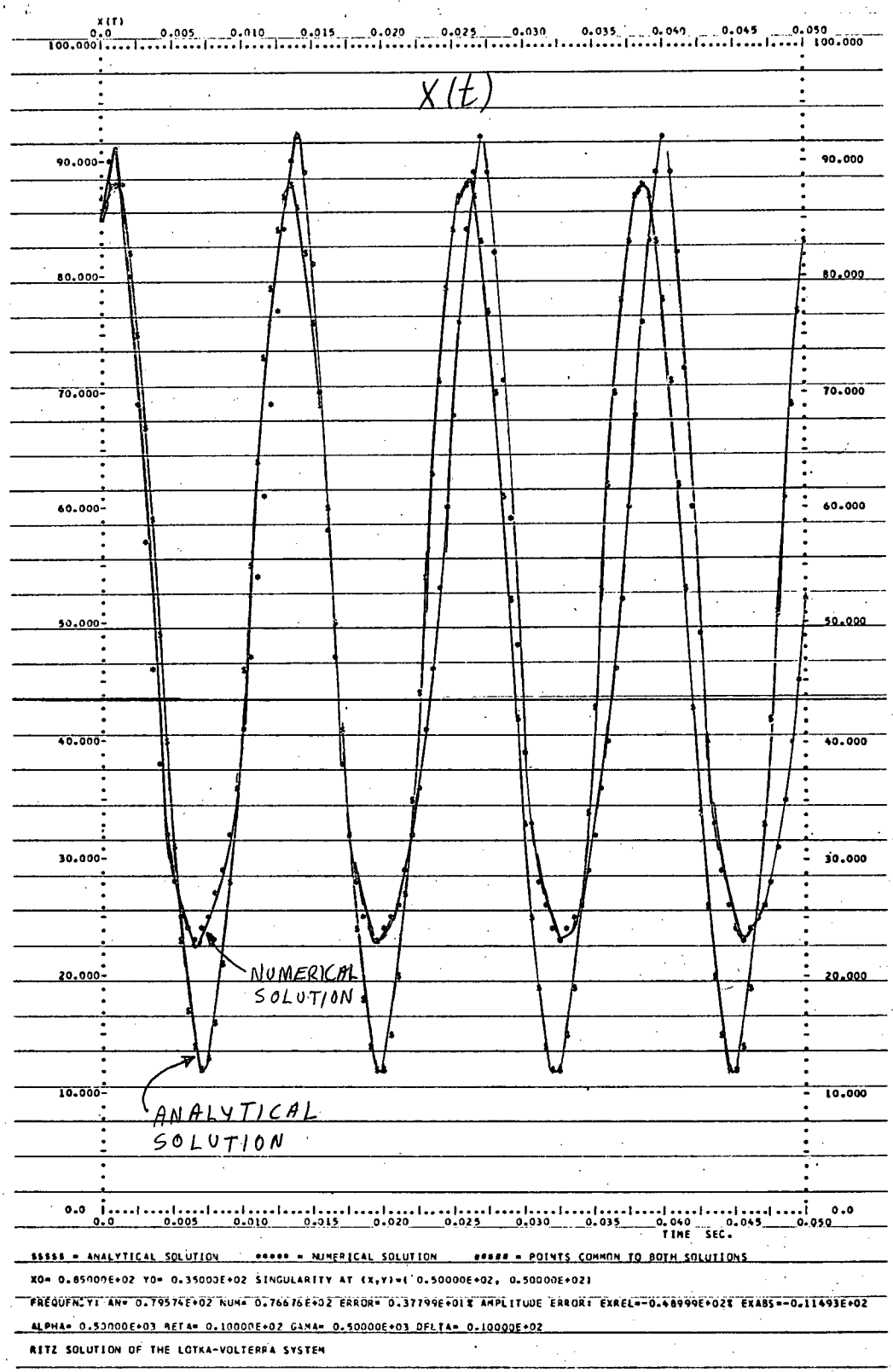

Fig. 1.8 Lotka-Volterra Model Ritz Solution for $(x_o, y_o) = (85, 35)$

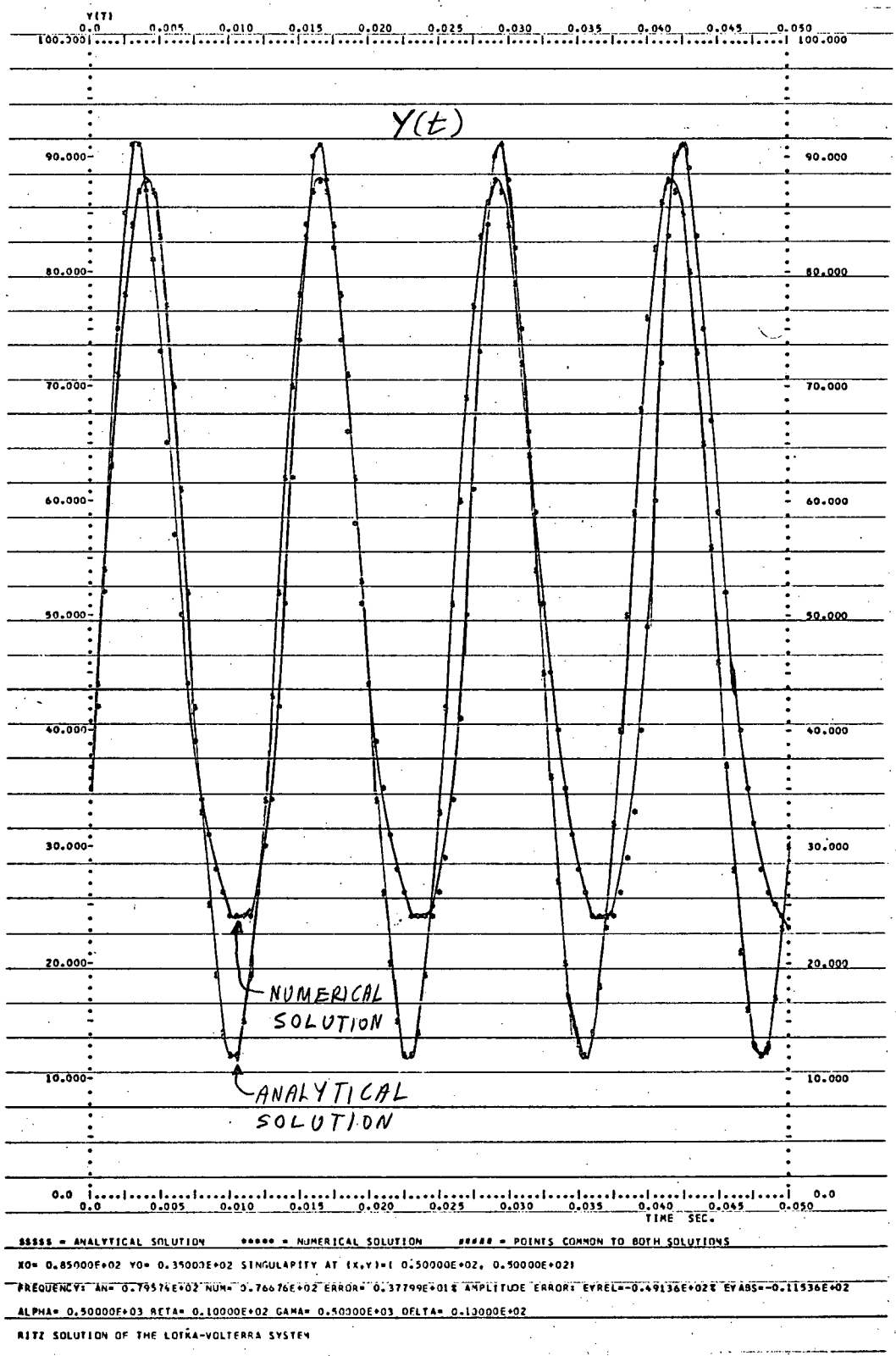

Fig. 1.9 Lotka-Volterra Model Ritz Solution for $(x_o, y_o) = (85, 35)$

In the simulation, amplitude and frequency errors were stored for each set of initial conditions, and from this data, loci of constant error, as a function of initial conditions, are plotted in Figures 1.10 and 1.11. From these curves it is seen that Ritz frequency is quite accurate for a large region of initial conditions, while the amplitude of the Ritz solution is accurate over a smaller region of initial conditions.

In this case (and future ones similar to it) where the data is either arbitrary of of questionable accuracy, we shall be arbitrarily assuming that certain stated percentage accuracies of the approximate solutions are acceptable for use with the model. It is seen that in the region of acceptable amplitude error (say 20%), the corresponding frequency error is much less (about 5%). We observe from additional runs with different parameters that the general shapes of the error loci remain the same for different centre singularity locations. We also note that the farther the centre singularity from the origin, the larger the regions enclosed by the error loci become, thus extending the region of initial conditions for which the approximate solutions are useful. It is essential to remember that both the amplitude and frequency error loci plots should be studied when deciding on the useful ranges of initial conditions of the solutions, as information in the frequency error loci is not reflected in the amplitude error loci, and vice versa. The actual relation between the amplitude and frequency error plots is, at present, unknown and may be pursued at a later date. The preceding results have been summarized in a paper by Brearley and Soudack (9).

At this point it should be mentioned that a number of other researchers have developed formulae for the period of the solution of the Lotka-Volterra system. Frame (17) has given the exact formula for the period

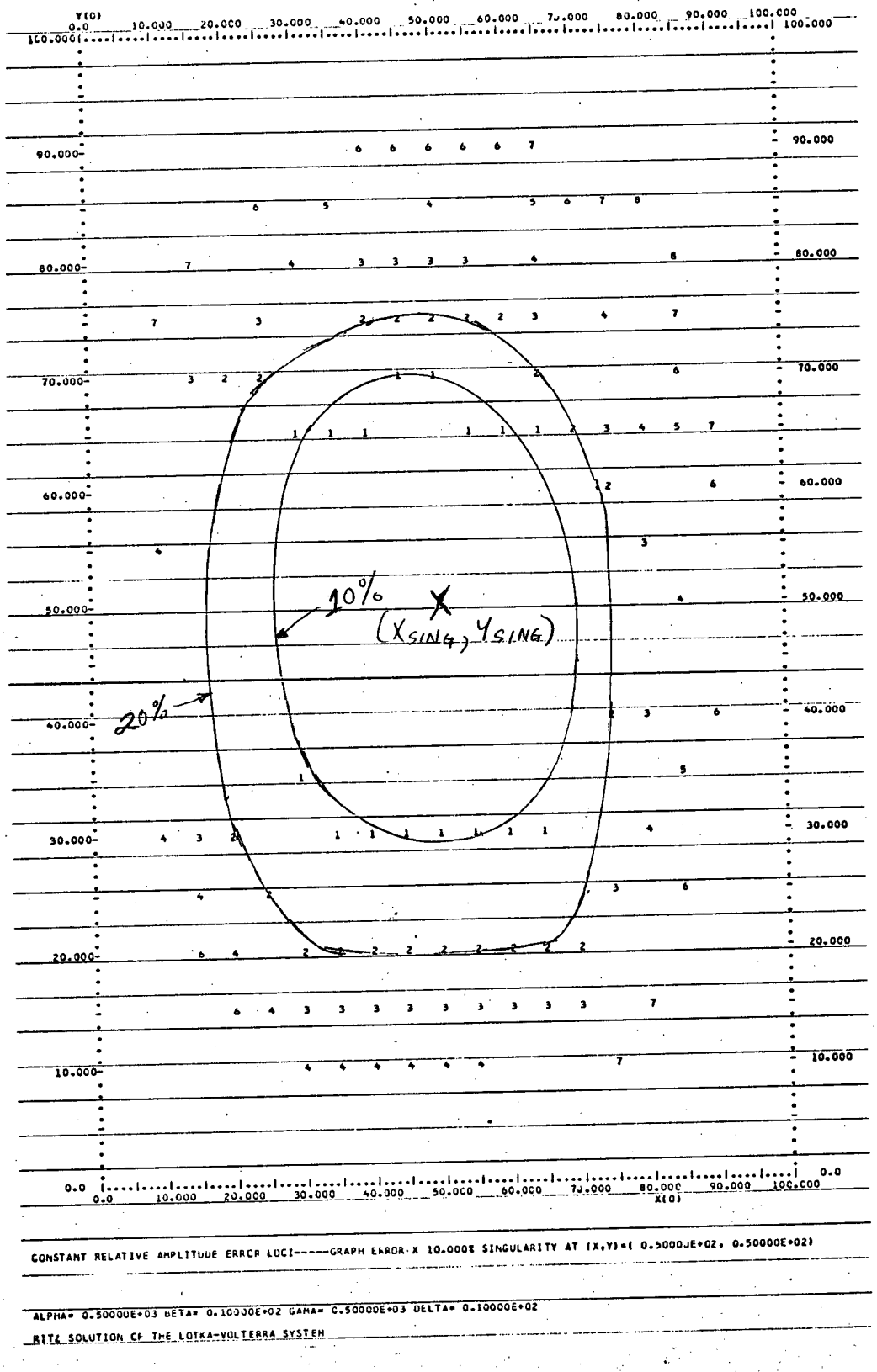

Fig. 1.10 Lotka-Volterra Ritz Solution Amplitude Error Loci

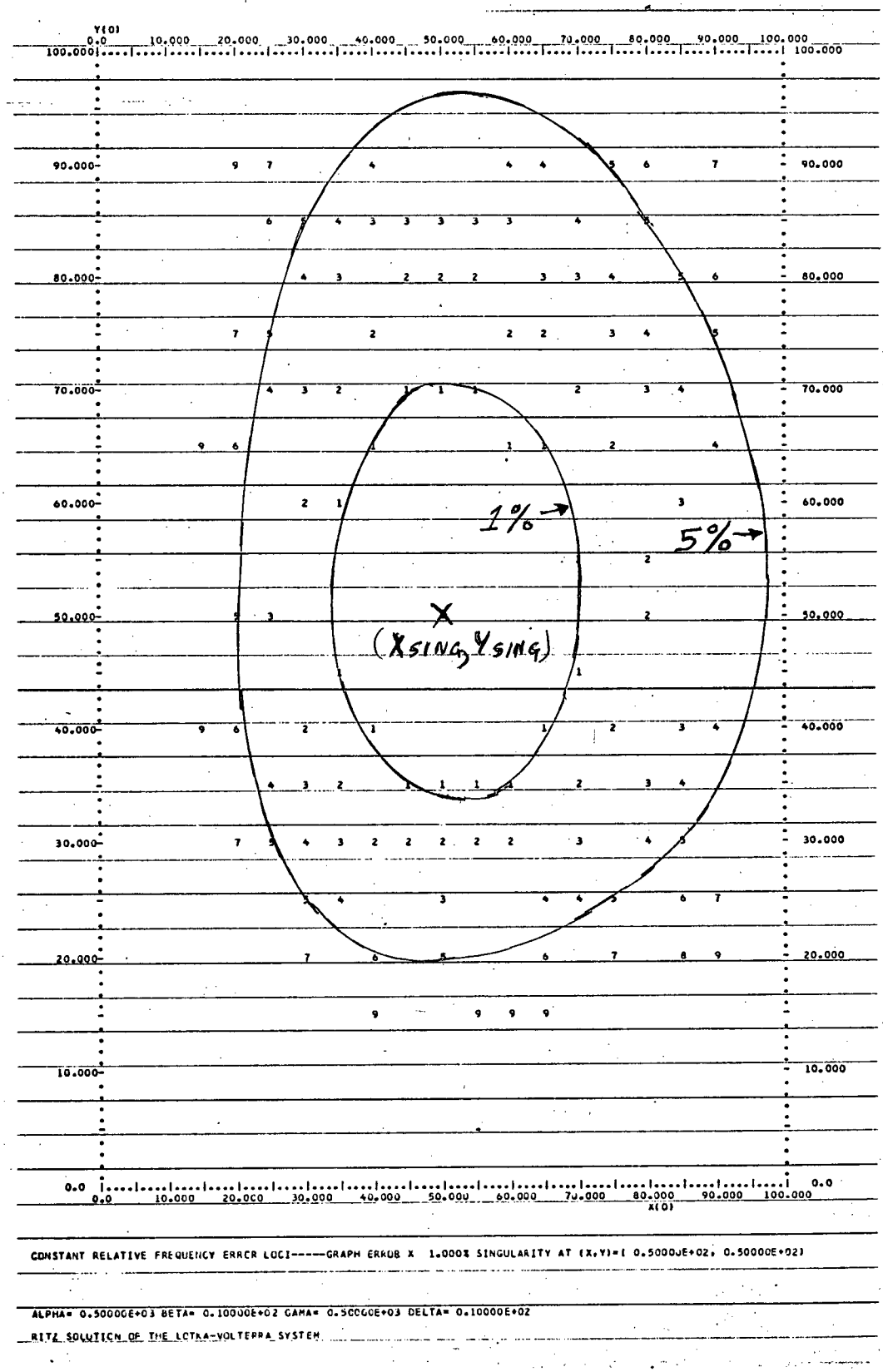

Fig. 1.11 Lotka-Volterra Model Ritz Solution Frequency Error Loci

in the form of an infinite series, which he then approximates by a series of Bessel functions. Grassman (23) develops a complicated asymptotic formula which works under certain initial conditions. Both these methods of determining the frequency are rather long and tedious, and do not yield much insight into the system behaviour. The extra accuracy gained for the labor involved is of dubious value. For these reasons, the simple, concise Ritz frequency formula seems to be the most practical solution. We now proceed to another method of obtaining solutions for the Lotka-Volterra system.

1.5 Improved Approximate Amplitude Solution

Being encouraged by the results of the previous section, we attempted to improve the amplitude of the Ritz solution. It was desired to be able to more accurately estimate the peaks of the solutions of the Lotka-Volterra system. The differential equations may be integrated directly in the phase plane to give the exact solution as follows:

$$\dot{x} = \alpha x - \beta xy$$

$$\dot{y} = \gamma y + \delta xy$$

$$\therefore \quad \frac{dx}{dy} = \frac{\alpha x - \beta xy}{-\gamma y + \delta xy}$$

$$\therefore \quad dx\left(-\frac{\delta}{x} + \delta\right) = dy\left(\frac{\alpha}{y} - \beta\right)$$

which upon integration, becomes

$$-\gamma \ln(x) + \delta x = \alpha \ln(y) - \beta y + C$$

where

$$C = \delta x_o + \beta y_o - \gamma \ln(x_o) - \alpha \ln(y_o)$$

This is a well known result which gives the exact phase plane solution. Graphical techniques (see Clark 11) have been developed which permit the sketching of the solutions only in the phase plane.

To obtain the peaks of the solutions, we proceed as follows. At the peaks of $x(t)$, we have $\dot{x}(t) = 0$, which implies from the differential equation that $y = \alpha/\beta$. Substituting this value of y in the phase plane solution we obtain

$$-\gamma \ln(x) + \delta x = \alpha(\ln(\alpha/\beta)-1) + C$$

This equation has two roots which correspond to the maxima and minima of the $x(t)$ oscillation. This equation could be solved by any number of standard numerical analysis methods. To provide a comparitively simple estimate of the actual roots, we approximate $\ln(x)$ by its truncated Taylor series

$$\ln(x) \simeq \ln(a) - 1 + x/a$$

where a is some suitable point to develop a Taylor series about. This yields

$$x_{peak} = \frac{\alpha(\ln(\alpha/\beta)-1) + C + \gamma(\ln(a) - 1)}{\delta - \gamma/a}$$

A first approximation to the peak deviation from the singular point is given by the initial displacement from the singular point

$$r_o = \sqrt{(x_o - x_{sing})^2 + (y_o - y_{sing})^2}$$

Thus we choose a as follows

$$a = \begin{cases} x_{sing} - r_o & \text{for } x_{min} \\ x_{sing} + r_o & \text{for } x_{max} \end{cases}$$

subject to the constraint $a > 0$.

Having estimated the peaks of the solution, we construct a solution that oscillates between the peak points at the Ritz frequency. The solution is given by

$$x(t) = x_{DC} + A_x \cos(\omega t + \phi_x)$$

where

$$x_{DC} = (x_{max} + x_{min})/2$$

$$A_x = (x_{max} - x_{min})/2$$

Note: if $\dot{x}(t) > 0$, put $A_x = -A_x$ so that the initial derivative has the correct sign.

ω = Ritz frequency = $\sqrt{\alpha\gamma}$

$$\phi_x = \cos^{-1}\frac{(x_o - x_{DC})}{A_x}$$

The y(t) solution is constructed in exactly the same manner. This completes the second approximate solution of the Lotka-Volterra system.

1.6 Simulation Study of Approximate Amplitude Solution

We now wish to evaluate the second approximate solution of the Lotka-Volterra system. In the simulation study, the calculations were performed with the same parameters as the Ritz solution, and over the same ranges of initial conditions. The trajectories and phase plane curves for the same initial conditions are shown in figures 1.12 to 1.20. The corresponding amplitude error plots are shown in figure 1.21. The frequency error loci plots are the same as the Ritz solution plots, and need not be shown here.

It is seen that the 10% and 20% amplitude error loci cover a much wider range of initial conditions than the Ritz case, and the improvements are readily seen in the given time plots. Eventually, the true solution departs from a sinusoidal shape, and the approximate solution has little value. This completes our evaluation of the second approximate solution of the Lotka-Volterra system.

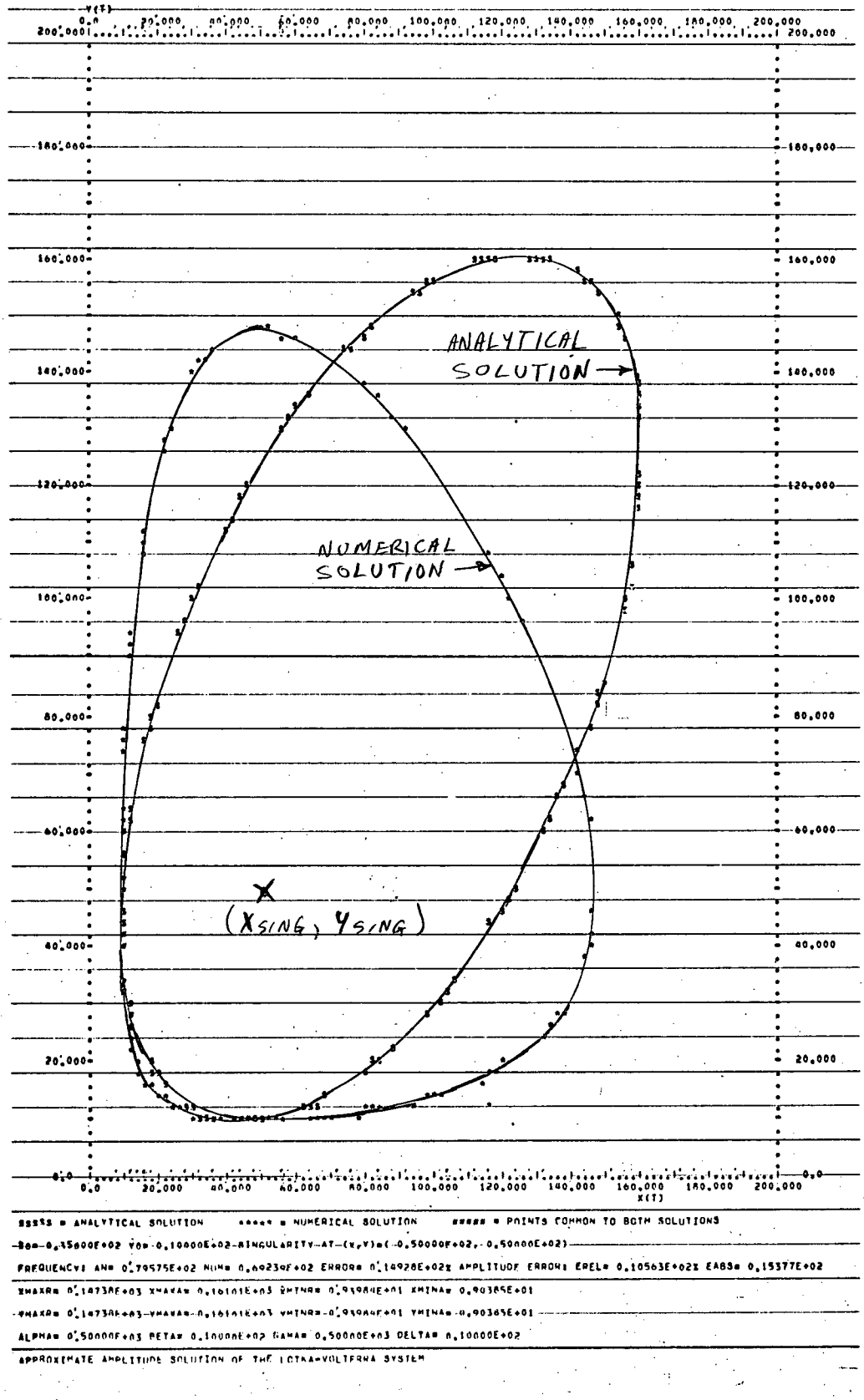

Fig. 1.12 Lotka-Volterra Model Approximate Amplitude Solution for $(x_o, y_o)=(35,10)$

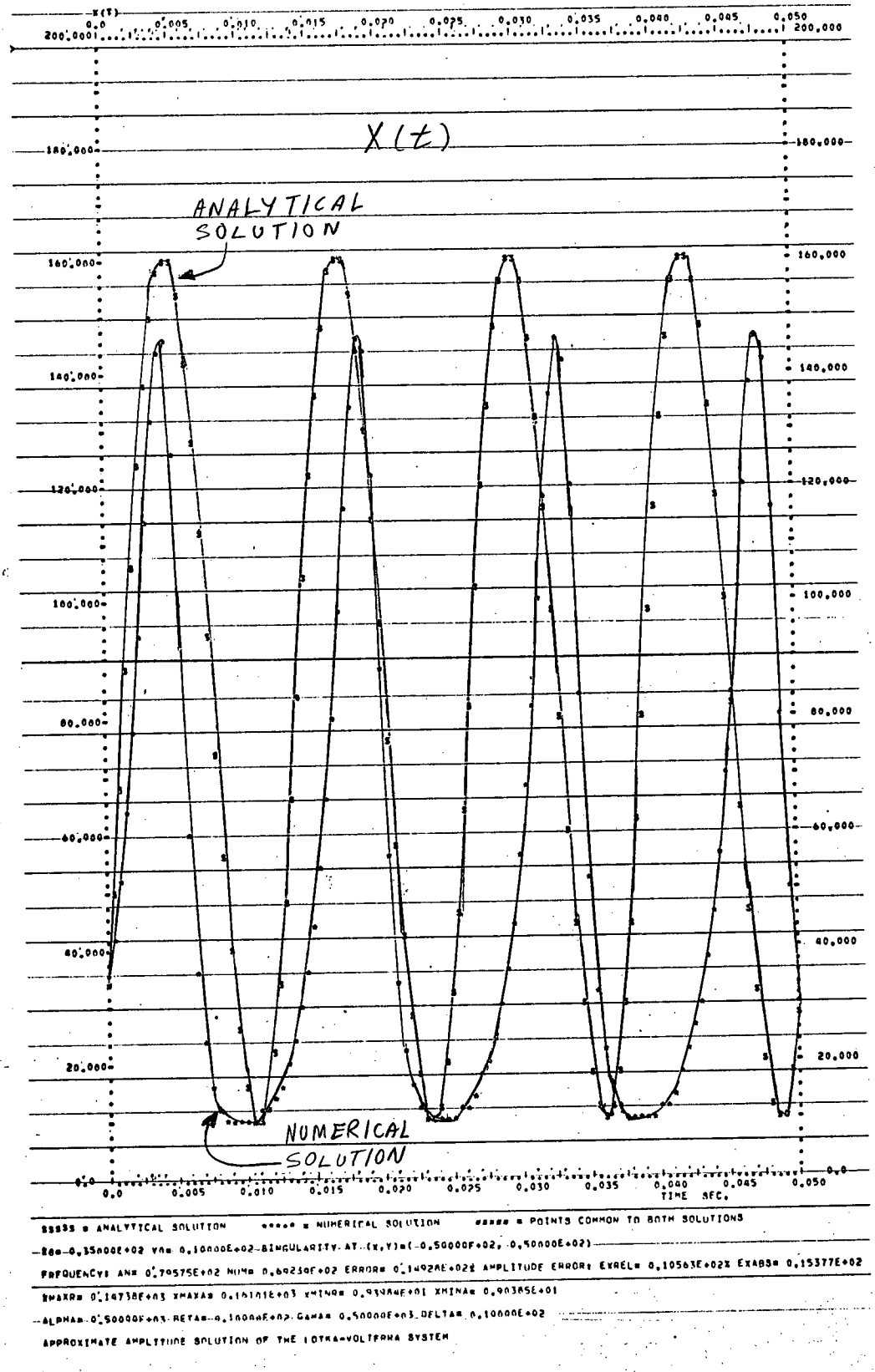

Fig.1.13 Lotka-Volterra Model Approximate Amplitude Solution for $(x_o, y_o) = (35,10)$

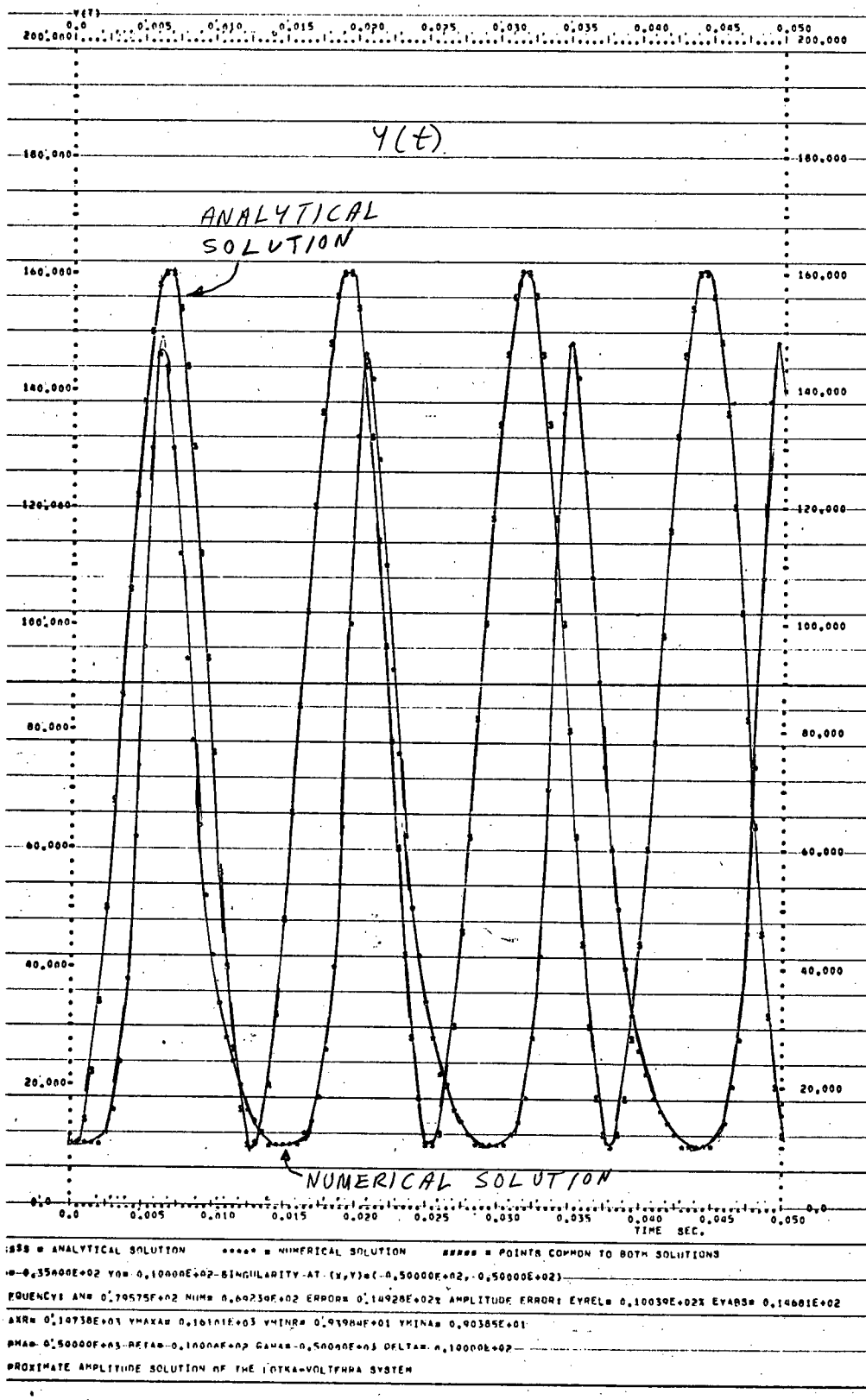

Fig. 1.14 Lotka-Volterra Model Approximate Amplitude Solution for $(x_o, y_o) = (35, 10)$

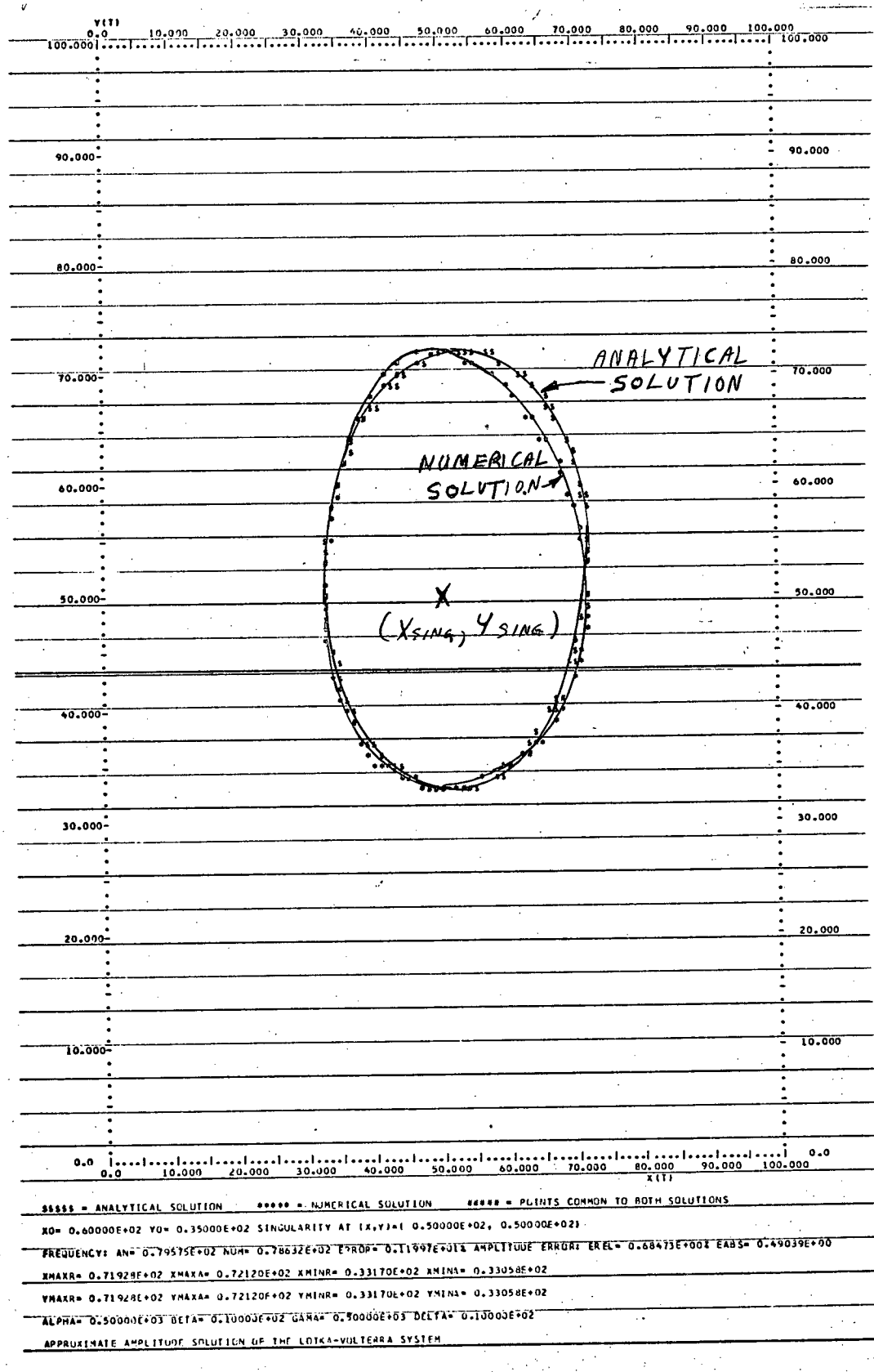

Fig. 1.15 Lotka-Volterra Model Approximate Amplitude Solution for $(x_o, y_o)=(60,35)$

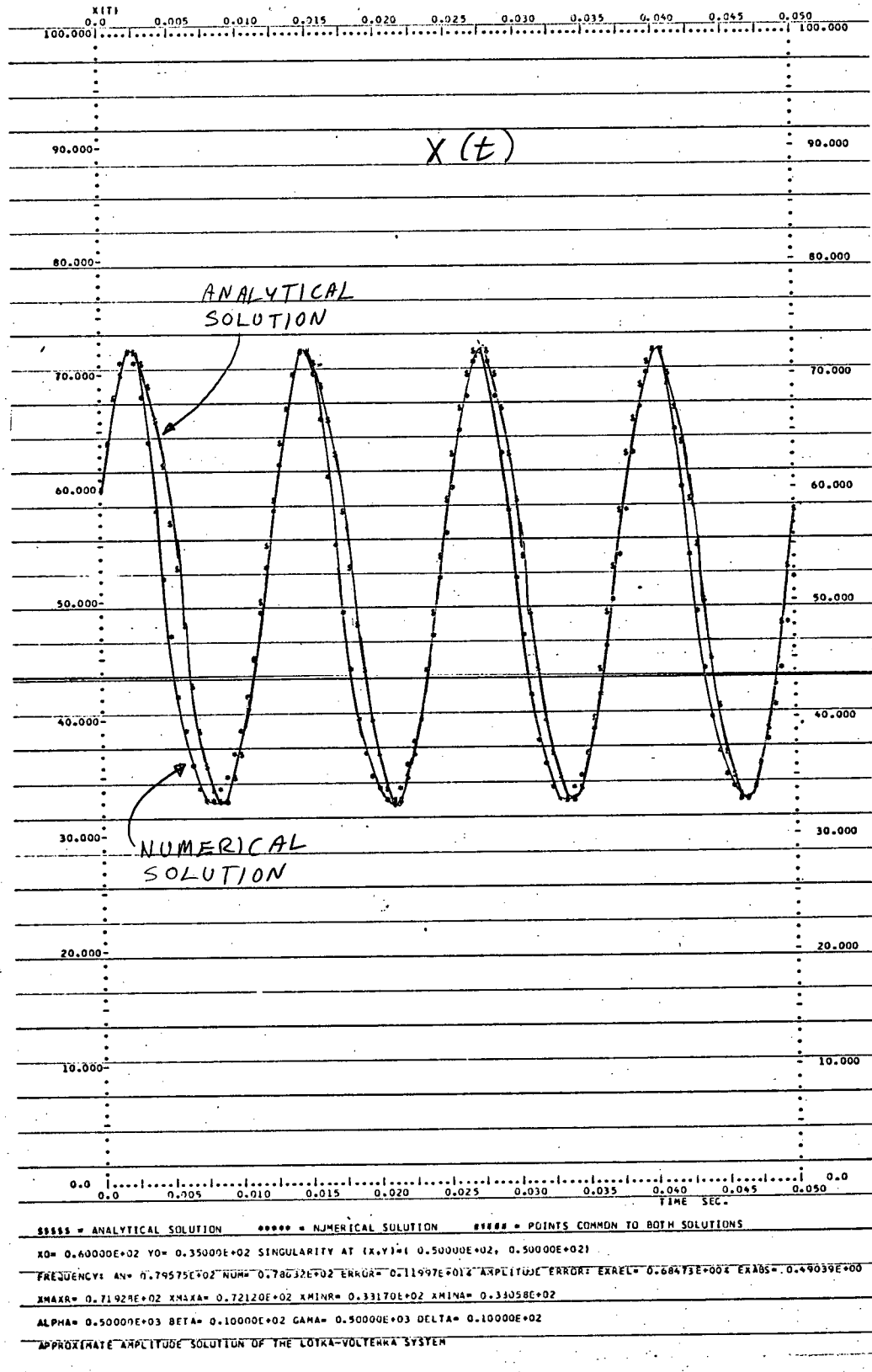

Fig. 1.16 Lotka-Volterra Model Approximate Amplitude Solution for $(x_o, y_o)=(60,35)$

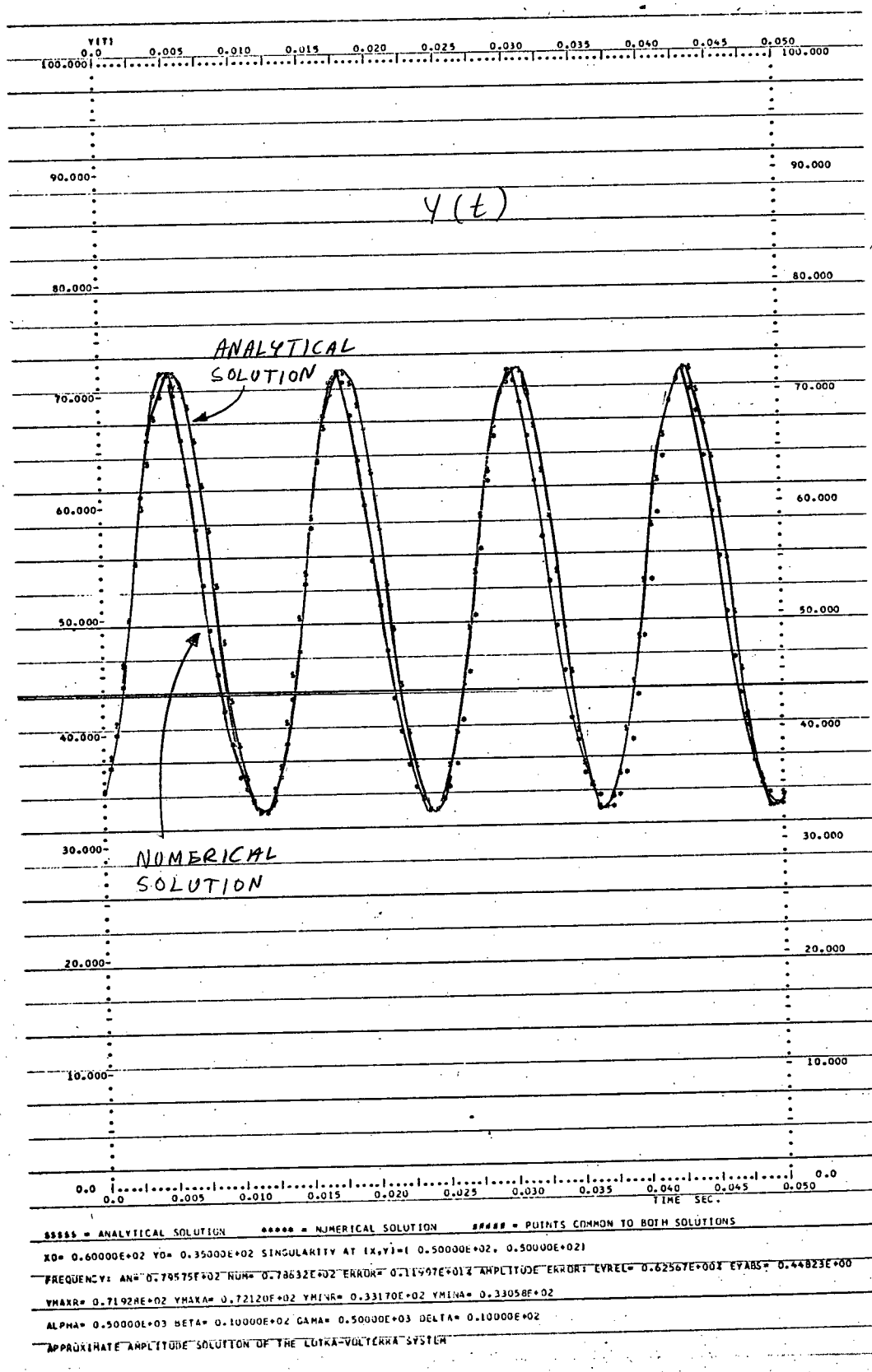

Fig. 1.17 Lotka-Volterra Model Approximate Amplitude Solution for $(x_o, y_o)=(60,35)$

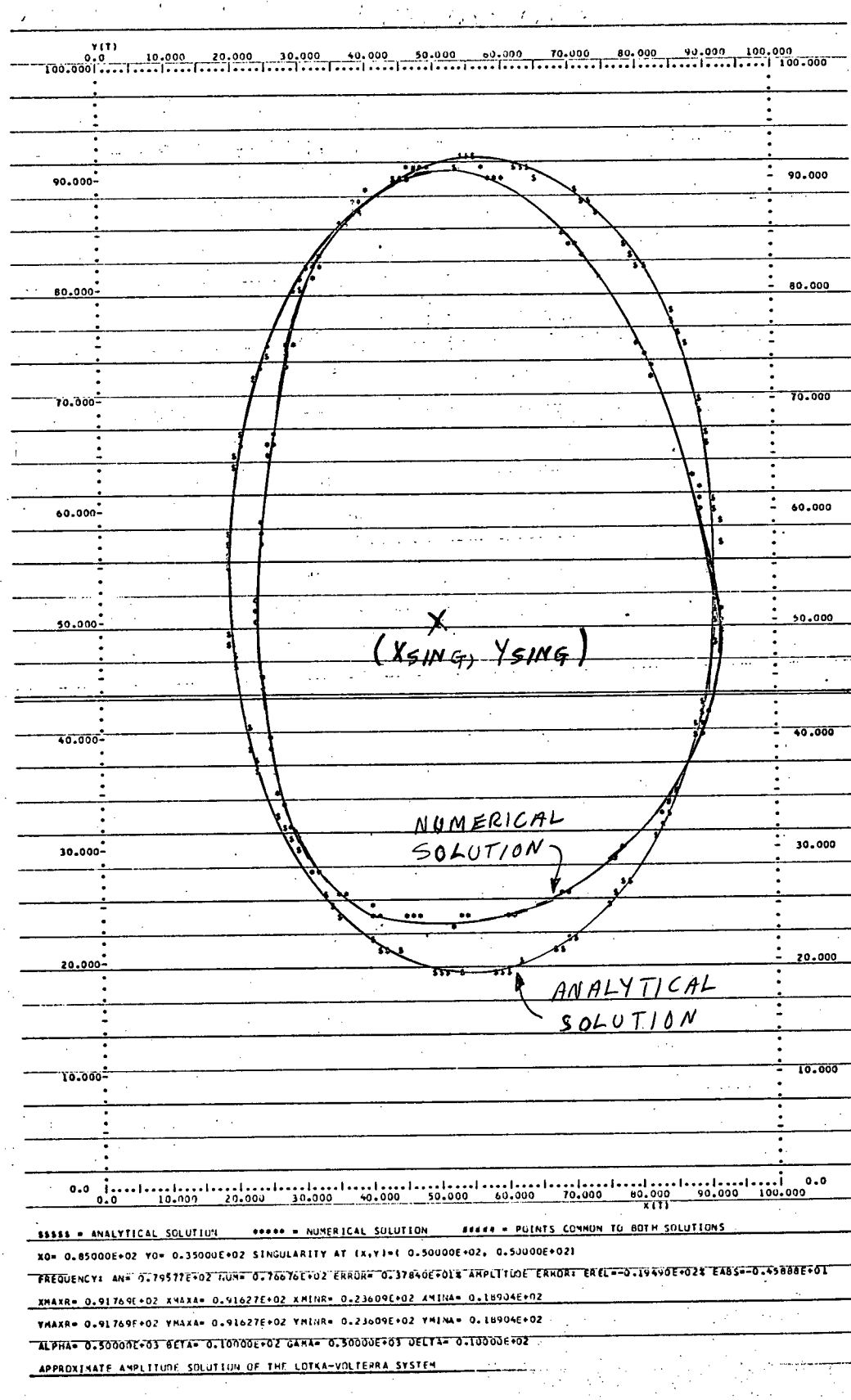

Fig. 1.18 Lotka-Volterra Model Approximate Amplitude Solution for $(x_o, y_o)=(85,35)$

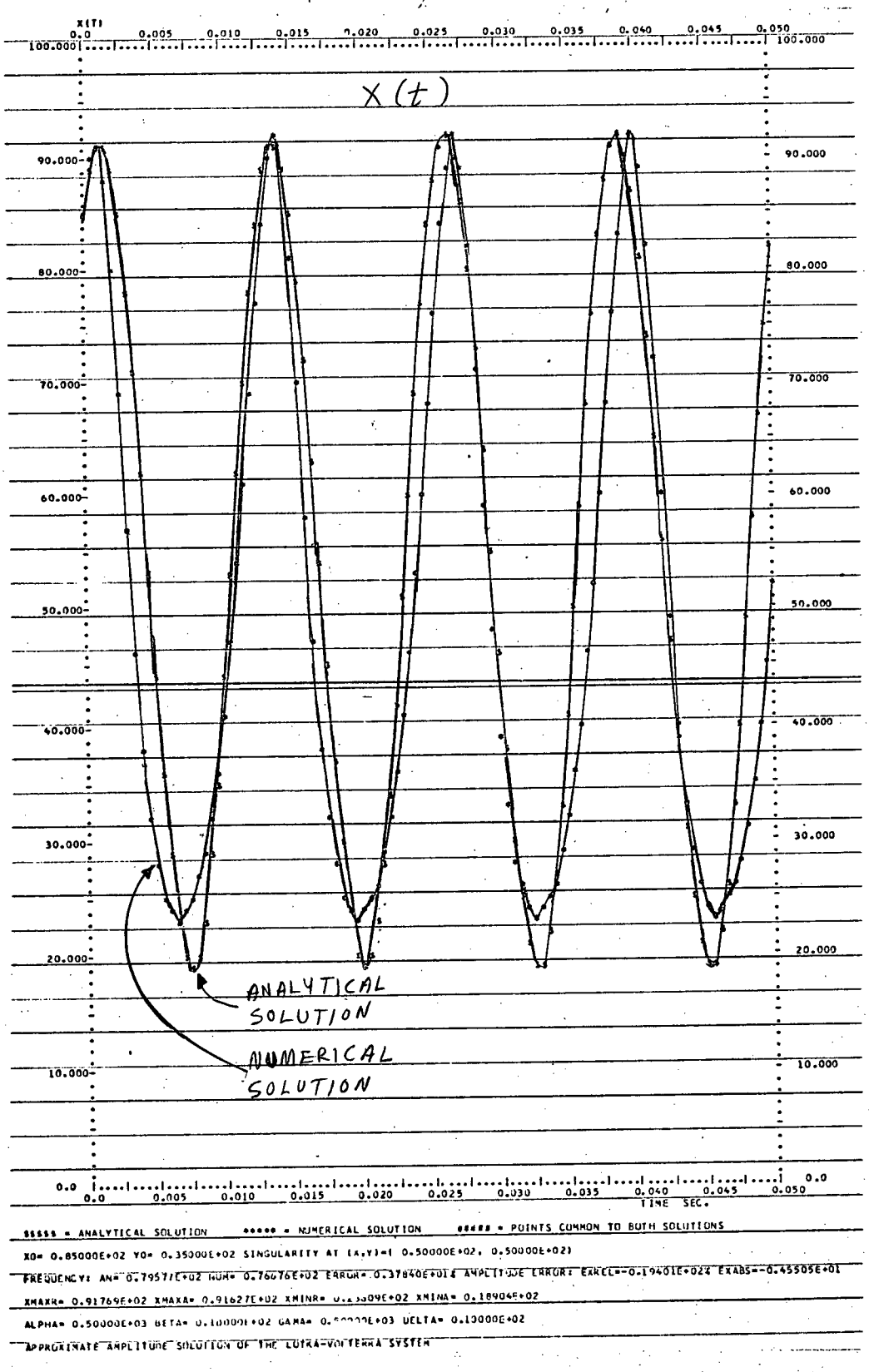

Fig. 1.19 Lotka-Volterra Model Approximate Amplitude Solution for $(x_o, y_o)=(85,35)$

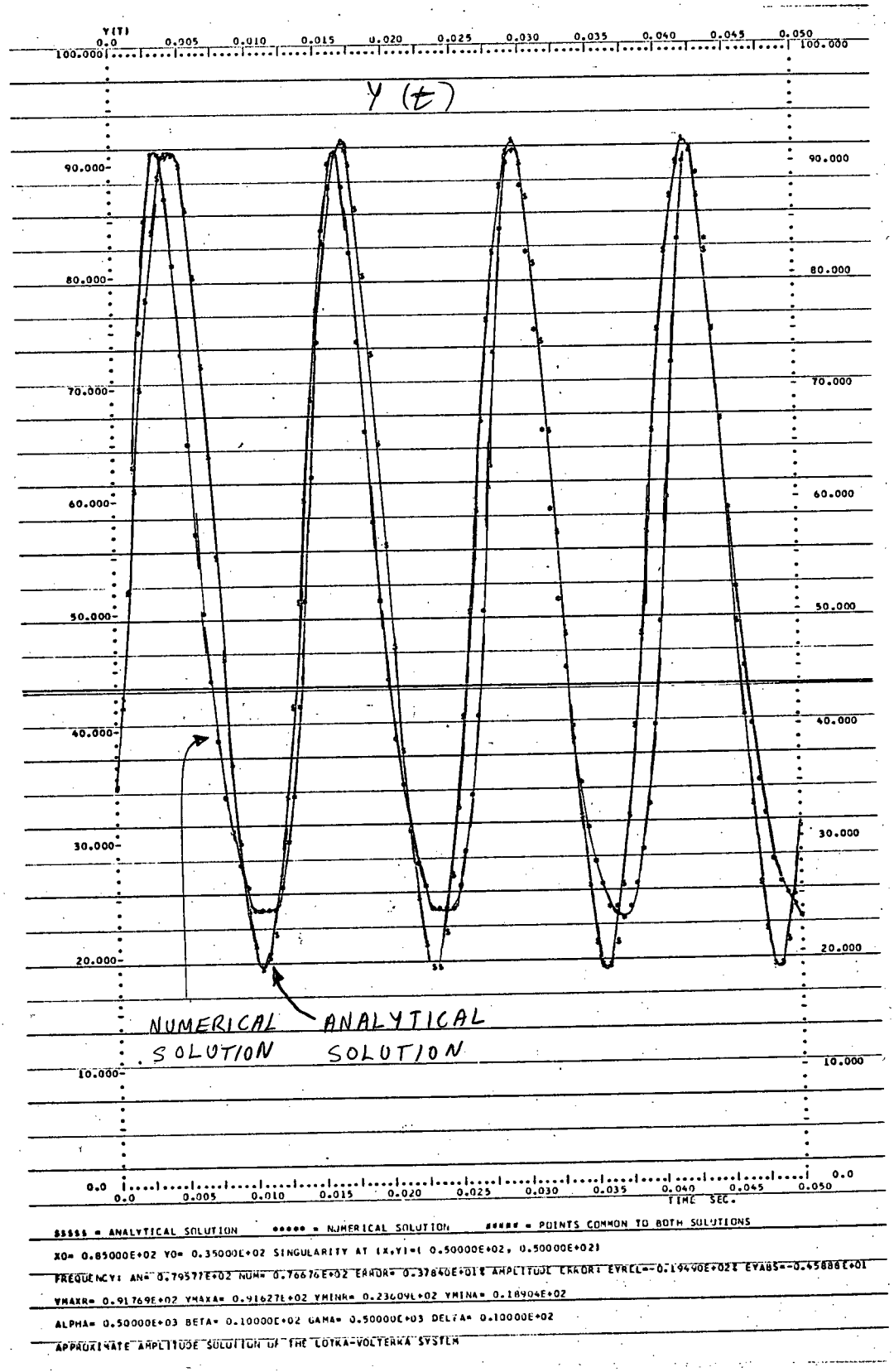

Fig. 1.20 Lotka-Volterra Model Approximate Amplitude Solution for $(x_o, y_o)=(85,35)$

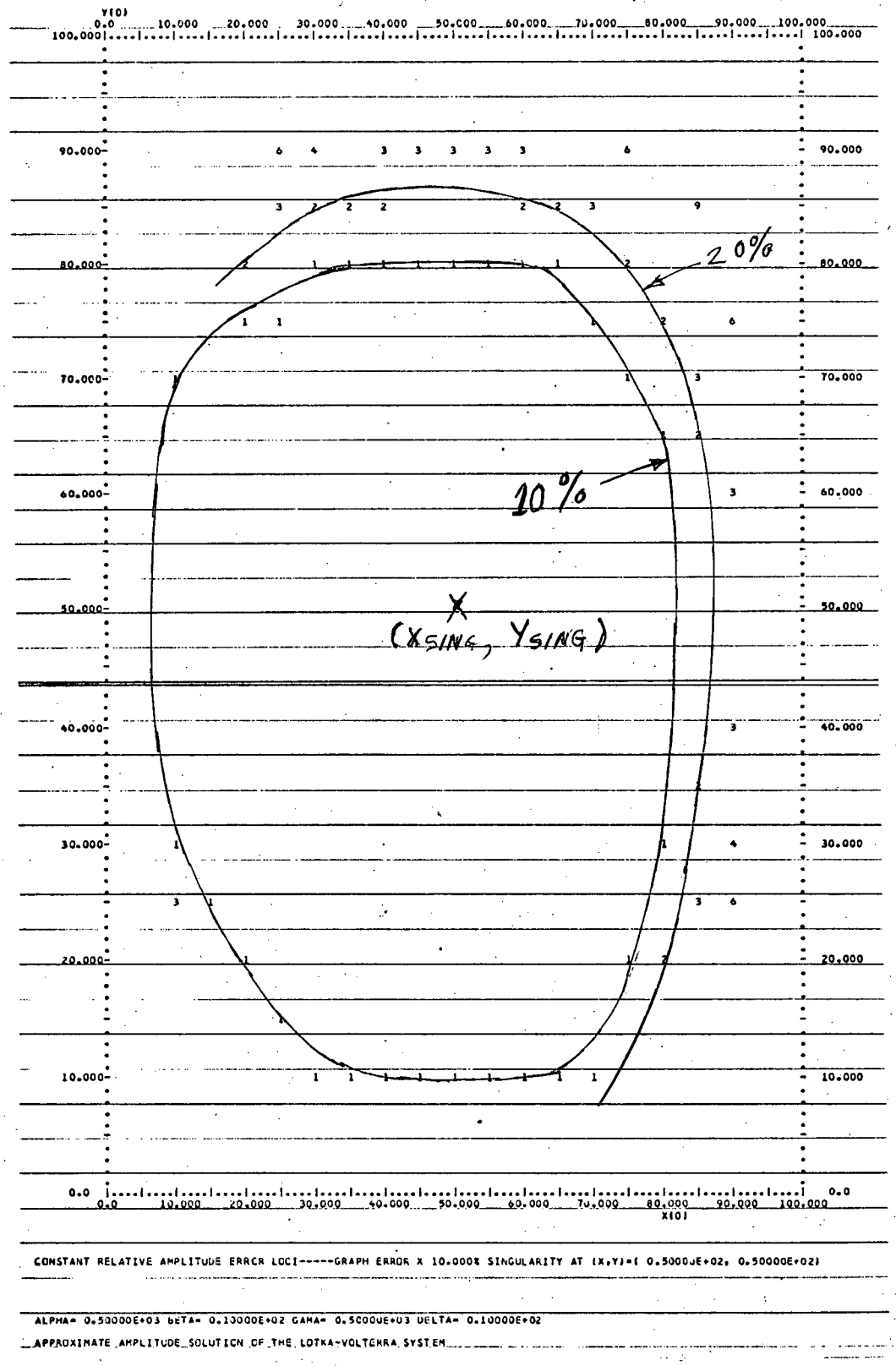

Fig. 1.21 Lotka-Volterra Model Approximate Amplitude Solution Amplitude Error Loci

1.7 Summary

We have developed two different analytical solutions to the Lotka-Volterra predator-prey system, using first of all, the classical Ritz method (which for the case at hand yielded the linearized solution), and secondly, an approximate solution which uses a combination of two different approximating techniques. The solutions (see page 7) permit great insight into the system behaviour and the effects of each system parameter without resorting to computer studies. We should note here that in general, the Ritz method will not generate linearized solutions as it did with this example.

As a rule of thumb, the Ritz solution is valid (< 20% amplitude error and 5% frequency error) in the set of initial conditions enclosed by an ellipse centred on the centre singularity with major and minor axes equal to 50% ofthe perpendicular distance between the singularity and the x & y axes. The amplitude error is the limiting factor in this case.

For the case of the approximate amplitude solution, the limiting factor is the frequency. The corresponding ellipse has axes that are 70% of the distance between the singularity and the axes.

These results raise the possiblity of developing approximate solutions for more complex (and more realistic) models. Such models and techniques for determining the approximate solutions are considered in the following chapters.

CHAPTER TWO

ADVANCED MODELS AND LINEAR SOLUTIONS

2.1 The Linear Solution

The first and simplest technique of obtaining solutions to the nonlinear models is to linearize the differential equations about the singular point of interest, (x_{sing}, y_{sing}).

We shall write the differential equations as follows:-

$$\dot{x} = F(x,y), \qquad x(0) = x_o$$

$$\dot{y} = G(x,y), \qquad y(0) = y_o$$

where

$$F(x,y) = xf(x,y)$$

$$G(x,y) = yg(x,y)$$

The matrix of partial derivatives is computed to yield the coefficients a_{ij}.

$$A = \begin{vmatrix} \frac{\partial F}{\partial x} & \frac{\partial F}{\partial y} \\ \frac{\partial G}{\partial x} & \frac{\partial G}{\partial y} \end{vmatrix} = \begin{vmatrix} a_{11} & -a_{12} \\ a_{21} & a_{22} \end{vmatrix}$$

The differential equation is reduced to the linear form(where the partials are evaluated at the equilibrium point).

$$\dot{x} = a_{11}x - a_{12}y$$

$$\dot{y} = a_{21}x + a_{22}y$$

where x and y are the variables translated to the singular point of interest.

The eigenvalues, s_i of the system are computed from $\det(A-sI) = 0$. These are used to determine the stability of the singular points, and thus determine the phase plane behaviour.

We may use the well known transition matrix technique of linear, time invariant differential equation theory to solve the above equations. If the eigenvalues of A are complex, the complete solution is given by:

$$x(t) = x_{sing} + (x_o - x_{sing})e^{\sigma t}(\cos\omega t + \frac{(a_{11}-\sigma)}{\omega}\sin\omega t)$$

$$- e^{\sigma t}(y_o - y_{sing})\frac{a_{12}}{\omega}\sin\omega t$$

$$y(t) = y_{sing} + (y_o - y_{sing})e^{\sigma t}(\cos\omega t + \frac{(a_{22} - \sigma)}{\omega}\sin\omega t)$$

$$+ e^{\sigma t}(x_o - x_{sing})\frac{a_{21}}{\omega}\sin\omega t$$

where

$$\sigma = (a_{11} + a_{22})/2$$

$$\omega = \tfrac{1}{2}\sqrt{4(a_{12}a_{21} + a_{11}a_{22}) - (a_{22} + a_{11})^2}$$

If the eigenvalues are real, the solution is given by:

$$x(t) = x_{sing} + (x_o - x_{sing})((a_{11} - \sigma_2)e^{\sigma_1 t}$$

$$+(\sigma_1 - a_{11})e^{\sigma_2 t})/(\sigma_1 - \sigma_2)$$

$$- a_{12}(y_o - y_{sing})(e^{\sigma_1 t} - e^{\sigma_2 t})/(\sigma_1 - \sigma_2)$$

$$y(t) = y_{sing} + (y_o - y_{sing})((a_{22} - \sigma_2)e^{\sigma_1 t}$$

$$+ (\sigma_1 - a_{22})e^{\sigma_2 t}) /(\sigma_1 - \sigma_2)$$

$$+ a_{21}(x_o - x_{sing})(e^{\sigma_1 t} - e^{\sigma_2 t})/(\sigma_1 - \sigma_2)$$

where

$$\sigma_{1,2} = \tfrac{1}{2}(a_{11}+a_{22} \pm \sqrt{(a_{11} + a_{22})^2 - 4(a_{12}a_{21} + a_{11}a_{22})}\ )$$

For very large initial conditions, these local solutions depart from the true solutions. The regions of initial conditions where these solution are valid will be determined in the following sections. We now have another

solution which explicitly relates the system parameters and initial conditions to the system behaviour. We will now discuss some models and apply this method to obtain some specific solutions.

2.2 The Volterra-Gause-Witt Model

The Volterra-Gause-Witt (VGW) (See Dutt 15) model is the first model to be considered and is a modification of the Lotka-Volterra model discussed in chapter one. A quadratic term is added to the prey equation, which will limit the prey population in the absence of the predator, and reflects the capacity of the environment to support the prey (see Gilpen 21). The model is:

$$\dot{x} = \alpha x - \lambda x^2 - \beta xy$$
$$\dot{y} = -\gamma y + \delta xy \qquad \alpha,\beta,\gamma,\delta,\lambda > 0$$

The model has three singularities which are located at $(0,0)$, $(\alpha/\lambda,0)$, $(\gamma/\delta, \frac{\alpha - \lambda\gamma/\delta}{\beta})$ and these will be discussed in greater detail in the next section.

Gause (19&20) applied this model to two species of yeast with a good measure of success and also to two species of protozoa with some success.

2.3 Linear Solution of the Volterra-Gause-Witt Model

We start our evaluation of the linear solution by applying this method to the Volterra-Gause-Witt model. We compute the A matrix of the VGW model to obtain:

$$A = \begin{bmatrix} \alpha - 2\lambda x - \beta y & -\beta x \\ +\delta y & -\delta + \delta x \end{bmatrix}$$

We now wish to examine the phase plane behaviour of the system (see fig. 2.1). For the singularity at (0,0), we obtain the eigenvalues $s_1 = \alpha > 0$, $s_2 = -\gamma < 0$ from which we conclude that this is a saddle point. The eigenvalues of the signularity at $(\alpha/\lambda, 0)$ are $s_1 = -\alpha < 0$ and $s_2 = -\gamma + \frac{\delta\alpha}{\lambda}$. If we have $\frac{\delta\alpha}{\delta} < \lambda$ (see figure 2.1A), the singularity is a stable node. Also, in this case, the third singular point has moved into the fourth quadrant of the phase plane, where it is of no interest to us, as we are only interested nonnegative populations, which occur only in the first quadrant of the phase plane. If we have $\frac{\delta\alpha}{\gamma} > \lambda$, the singular point at $(\alpha/\lambda, 0)$ is a saddle point. The third singular point $(x_{sing}, y_{sing}) = (\gamma/\delta, \frac{\alpha - \lambda\gamma/\delta}{\beta})$ is a stable focus (see figure 2.1B) if we have $0 < \lambda < 2\delta(-1 + \sqrt{1 + \alpha/\gamma})$ and has eigenvalues

$$s_{1,2} = -\frac{\lambda\gamma}{2\delta} \pm y\sqrt{\alpha\gamma - \frac{\lambda\gamma^2}{\delta} - \frac{\lambda^2\gamma^2}{\delta^2}} \quad .$$

If we have $2\delta(-1 + \sqrt{1 + \alpha/\gamma} < \lambda < \delta\alpha/\gamma$, the third singular point is a stable node (see Figure 2.1C), and is the singularity about which we wish to obtain solutions. The coefficients of the linearized differential equations at the third singularity, (x_{sing}, y_{sing}) are:

$$a_{11} = -\frac{\lambda\gamma}{\delta} \qquad a_{12} = \beta\gamma/\delta$$

$$a_{21} = \frac{\alpha\delta - \lambda\gamma}{\beta} \qquad a_{22} = 0$$

The system is always stable. The question of stability in the general n'th order VGW model is explored by Gilpen (22). This completes the determination of the linear solution of the VGW model.

2.4 Simulation Study of the Volterra-Gause-Witt Model

We now wish to evaluate the linear solution of the VGW model. The solutions were computed for the arbitrary parameter choice $\alpha = \gamma = 500$, $\beta = \delta = 10$, $\lambda = 1$(for which (x_{sing}, y_{sing}) is arbitrary a stable focus) over

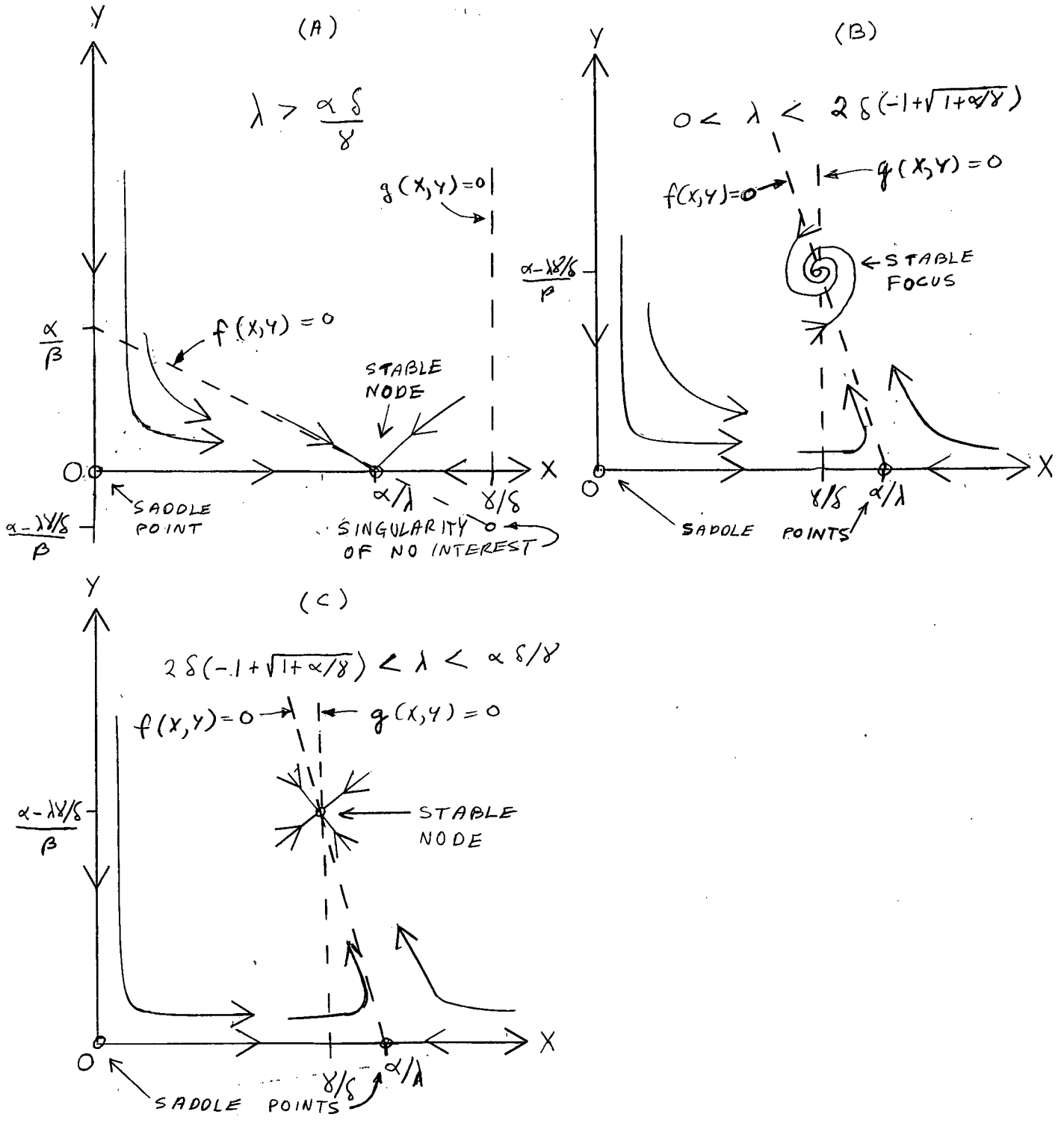

Fig. 2.1 Possible Singularity Types and Positions for the VGW Model

the initial conditions ranges of $10 < x_o < 90$, and $10 < y_o < 90$ in increments of 5. The time plots and phase plane curves for the initial conditions (85,60) are given in figures 2.2 to 2.4. The corresponding amplitude and frequency error loci are shown in figures 2.5 and 2.6. As was the case with Ritz solution, the frequency was found to be substantially more accurate than the amplitude for given initial conditions. We shall assume that a 10% or 20% error in the solution is acceptable.

Another arbitrary set of parameters was used for which (x_{sing}, y_{sing}) is a stable node. These were $\alpha = 275$, $\beta = \delta = 10$, $\gamma = 50$, $\lambda = 45$. The computations were done over the ranges of initial conditions $1 < x_o < 9$, and $1 < y_o < 9$ in increments of $\frac{1}{2}$. The time plots and phase plane curves for the initial conditions (3.5, 1.0) and (6.0, 3.5) are given in figures 2.7 to 2.12. The corresponding amplitude error loci curves, which are the only ones needed for solution evaluation, are given in figure 2.13. For the case of the stable node, the amplitude error is taken as the worst case percentage difference, on a point by point basis between the actual and approximate solutions. It should be noted here that with the stable node, if there is a slight error in the initial derivative, there may be a large difference between successive time plot points, which results in a large solution error even though the solution is visibly quite good. As a result, we may consider solutions with up to 40% amplitude error as acceptable. For the case of the stable focus, this "problem" in solution evaluation does not occur, as the amplitude and frequency errors are treated separately, and do not influence each other.

We have evaluated the linear solution of the VGW model and found that it is a good approximate solution (see error loci figures) over a wide range of initial conditions. We now proceed to study another ecological model.

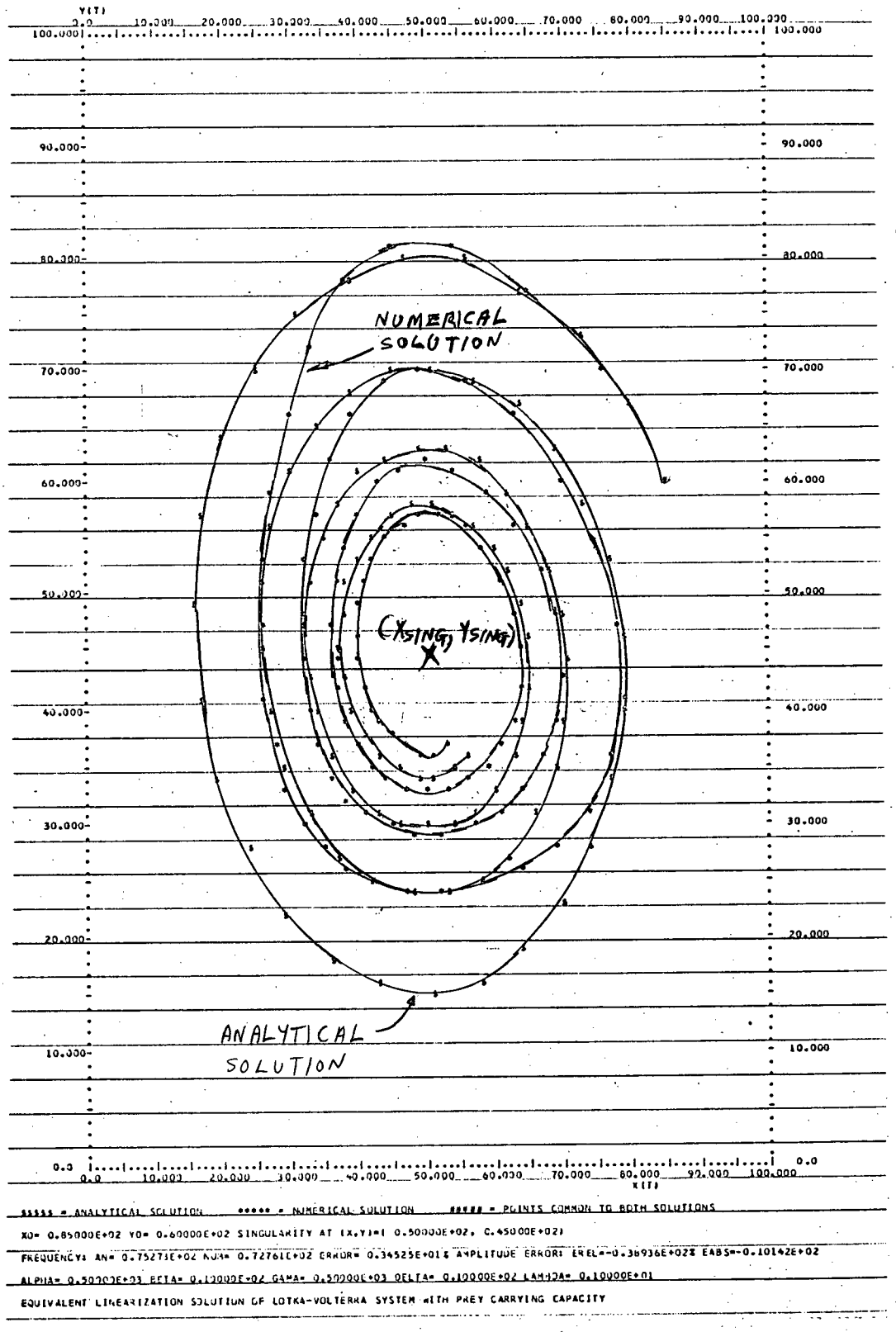

Fig. 2.2 VGW Model Linear Soltuions for $(x_o, y_o) = (85,60)$

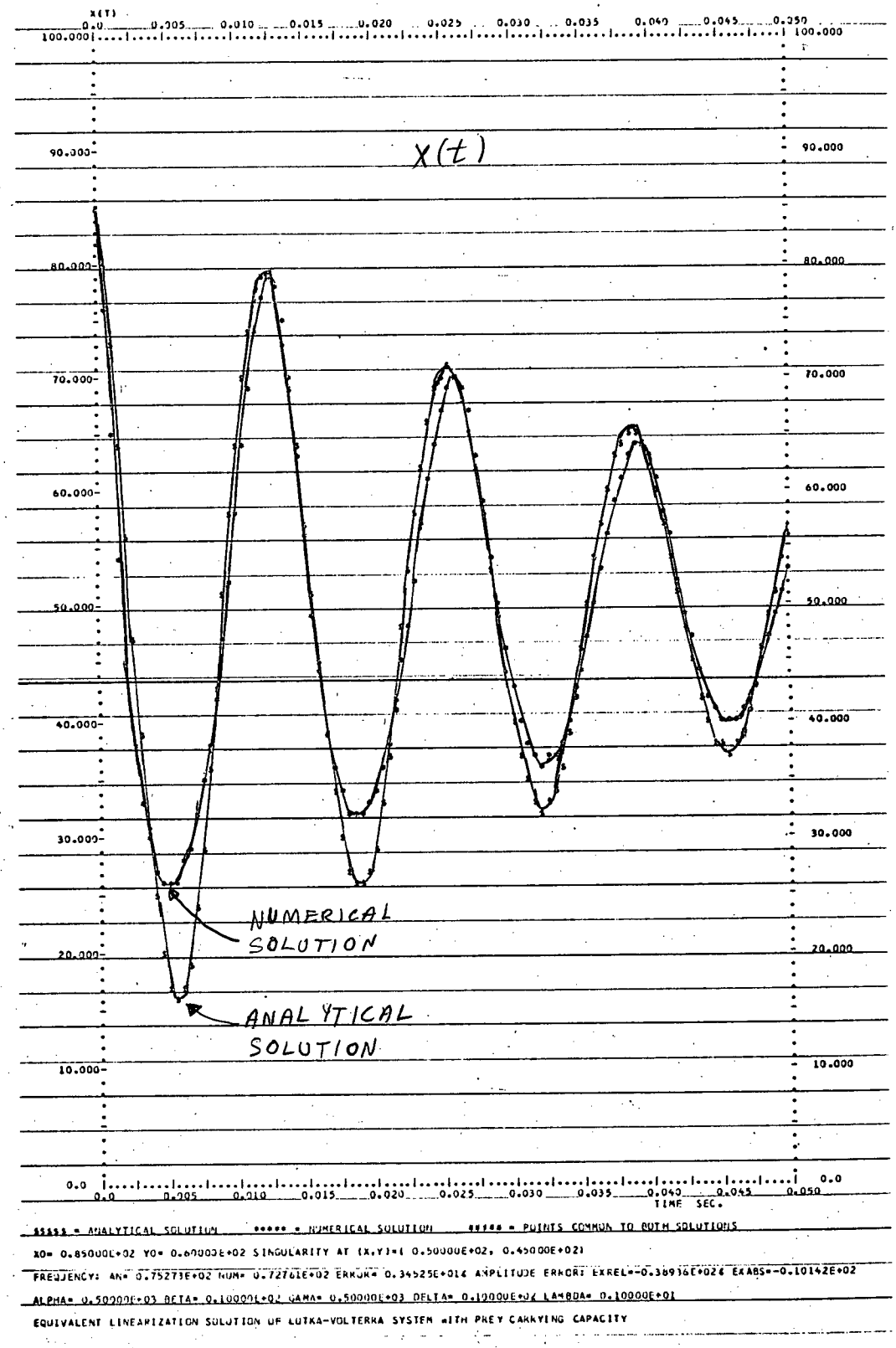

Fig. 2.3 VGW Model Linear Solution for $(x_o, y_o) = (85,60)$

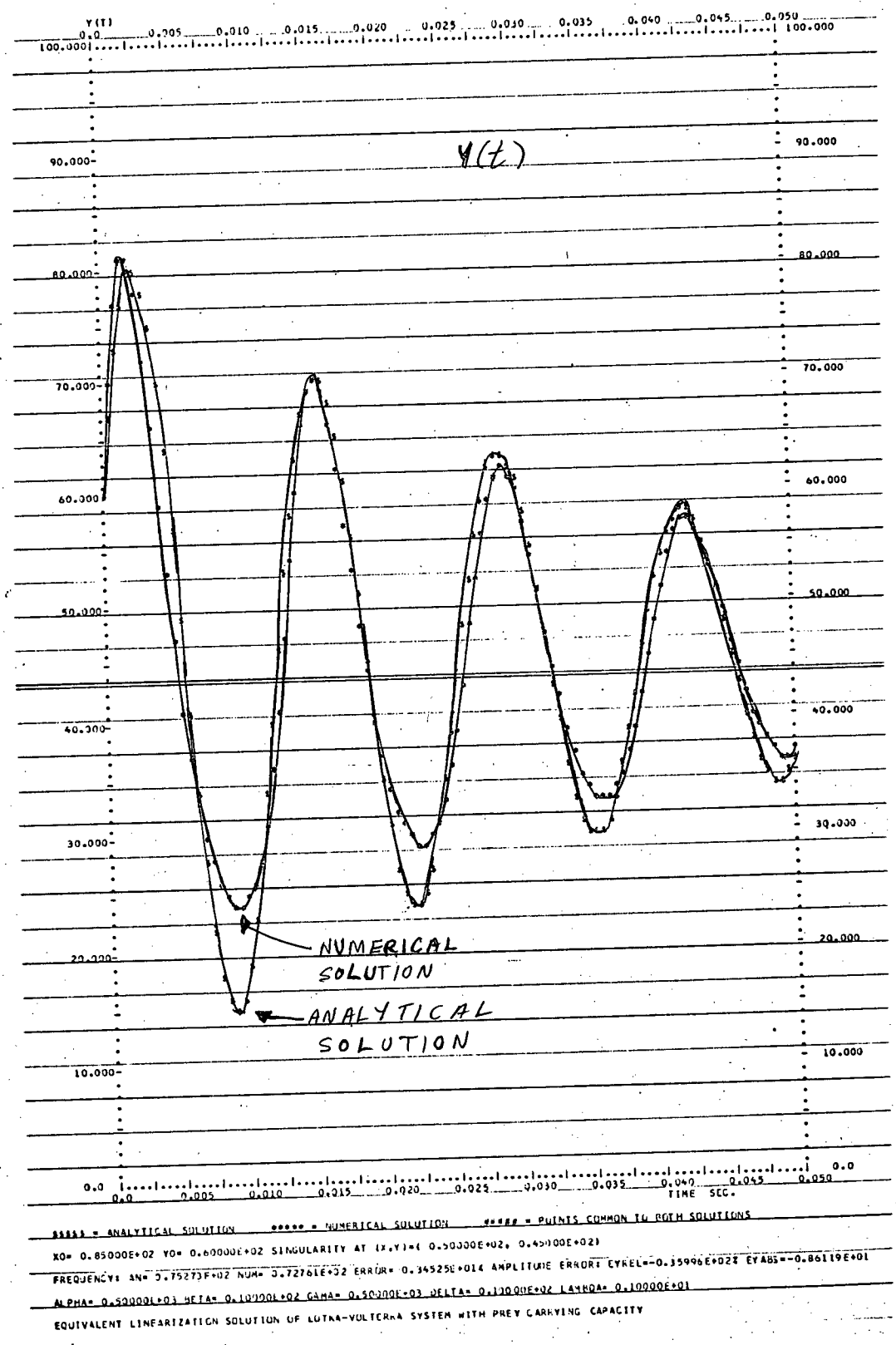

Fig. 2.4 VGW Model Linear Solution for $(x_o, y_o) = (85,60)$

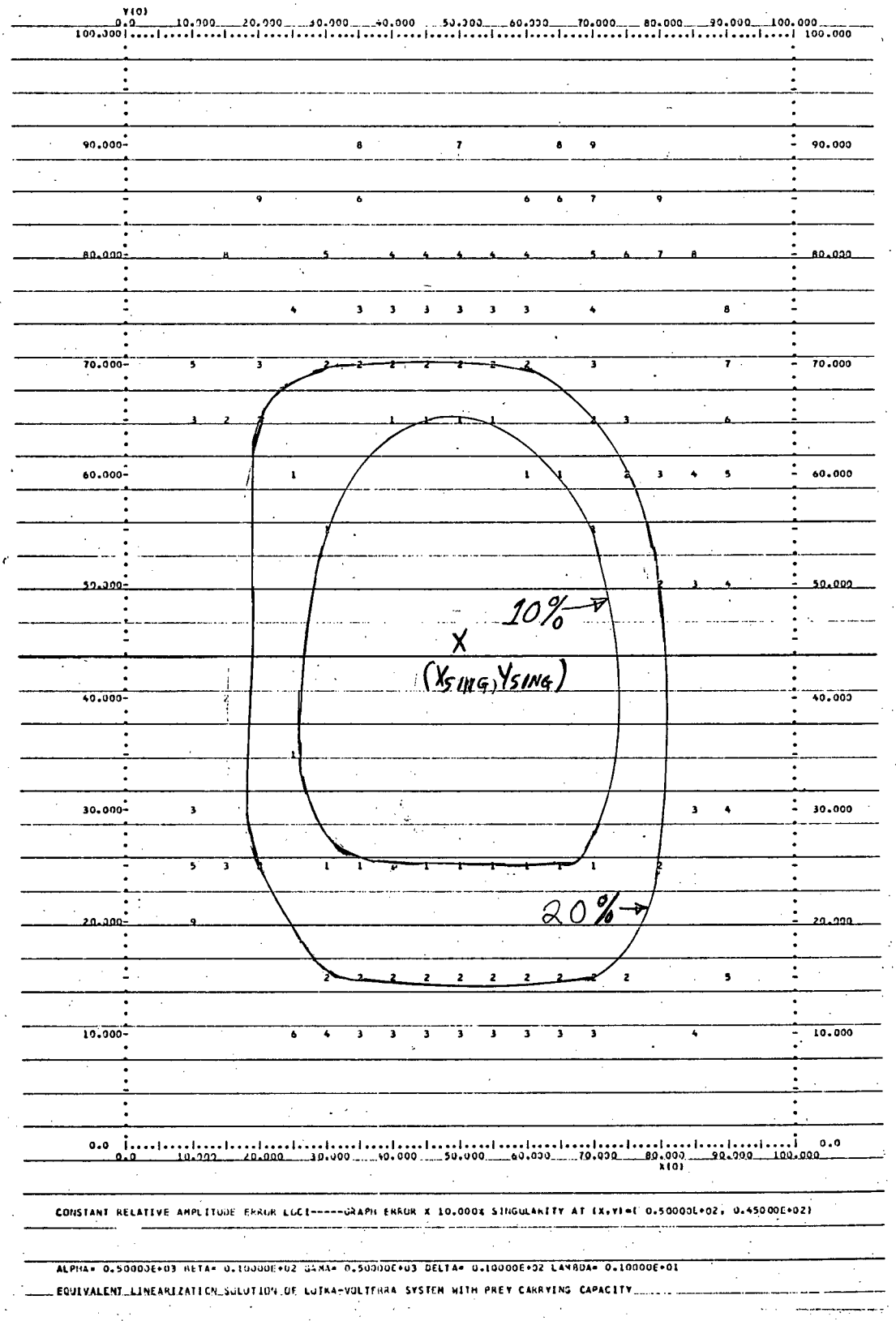

Fig. 2.5 VGW Model Linear Solution Amplitude Error Loci

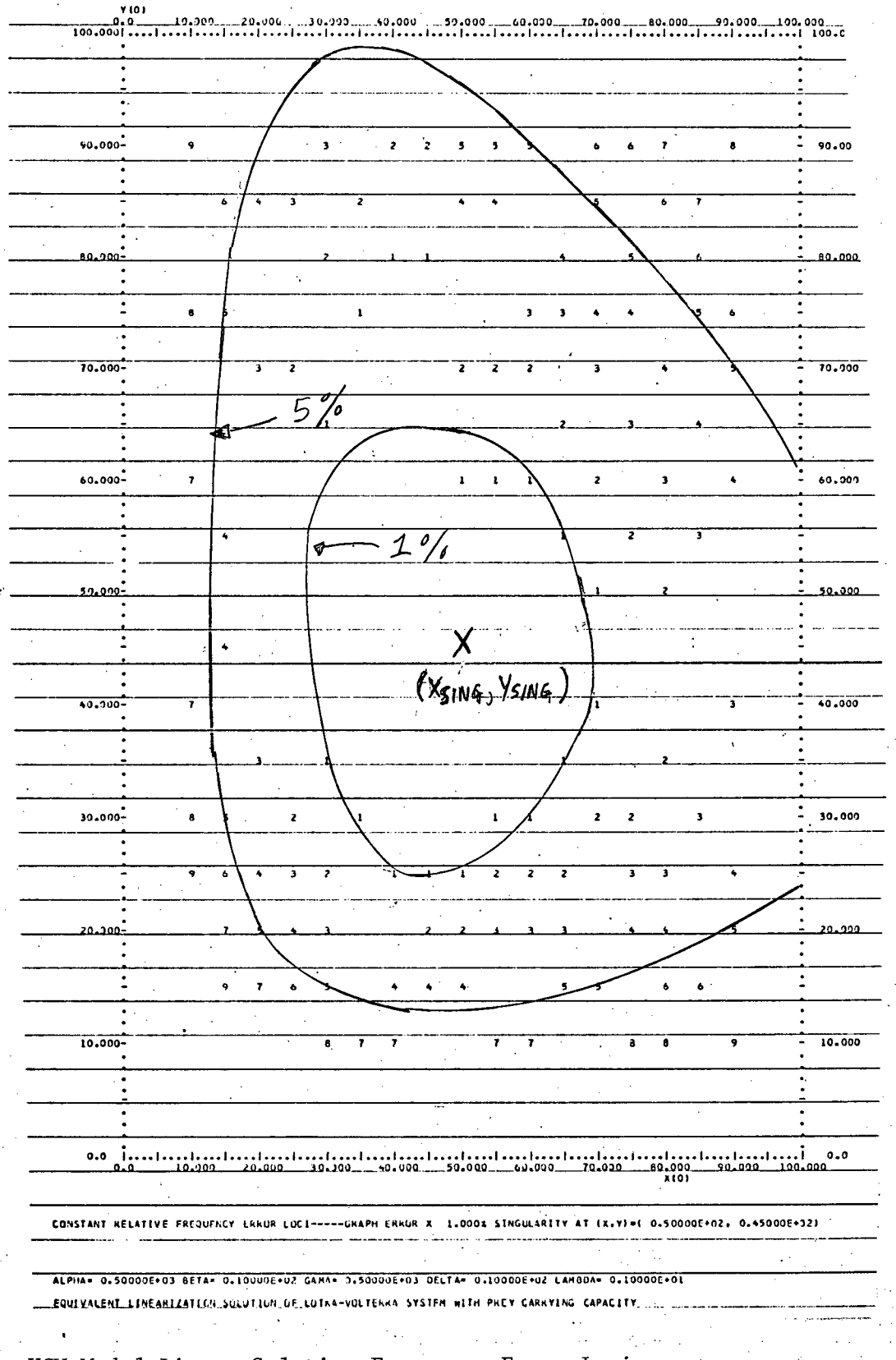

Fig. 2.6 VGW Model Linear Solution Frequency Error Loci

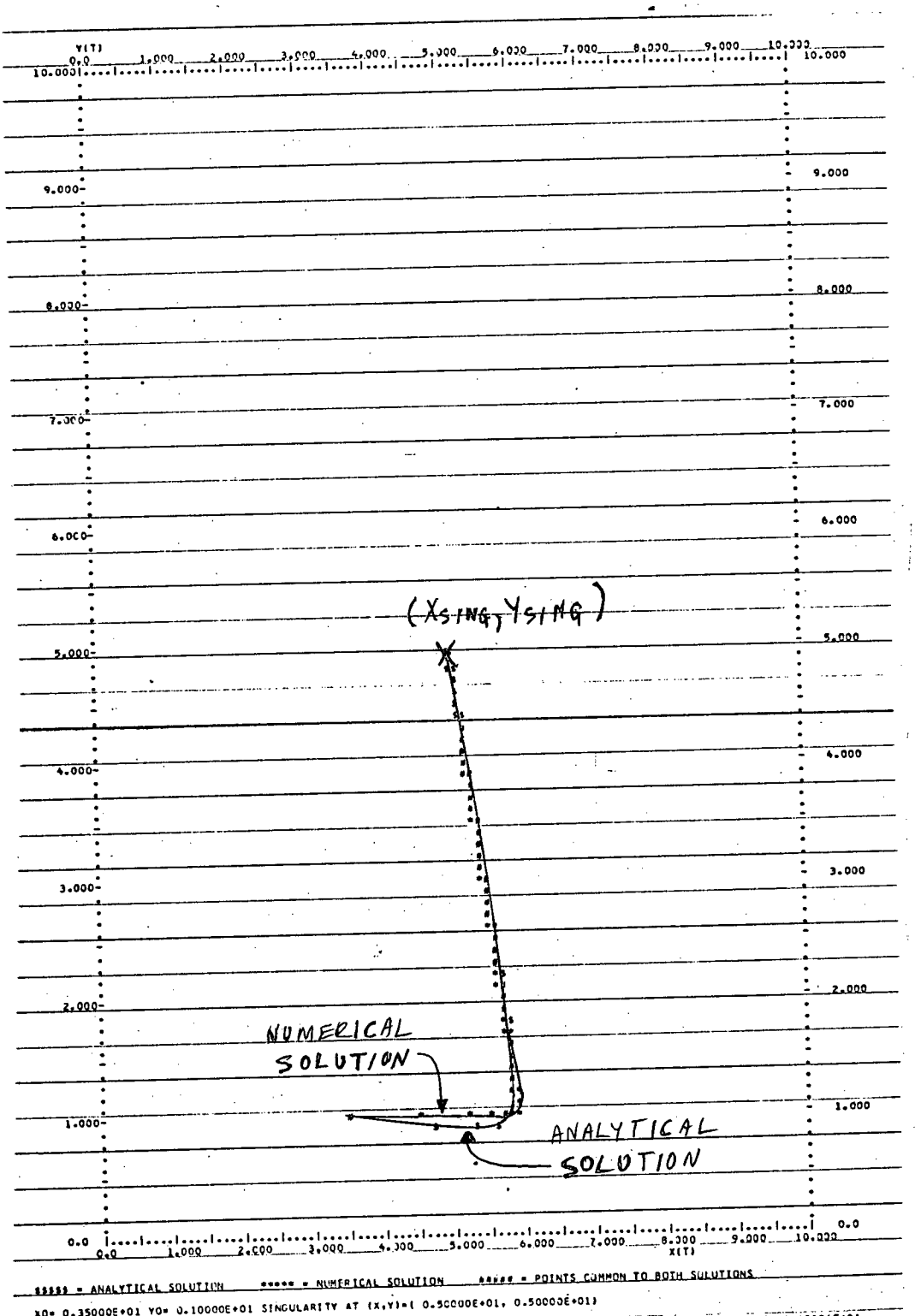

Fig. 2.7 VGW Model Linear Solution for $(x_o, y_o) = (3.5, 1)$

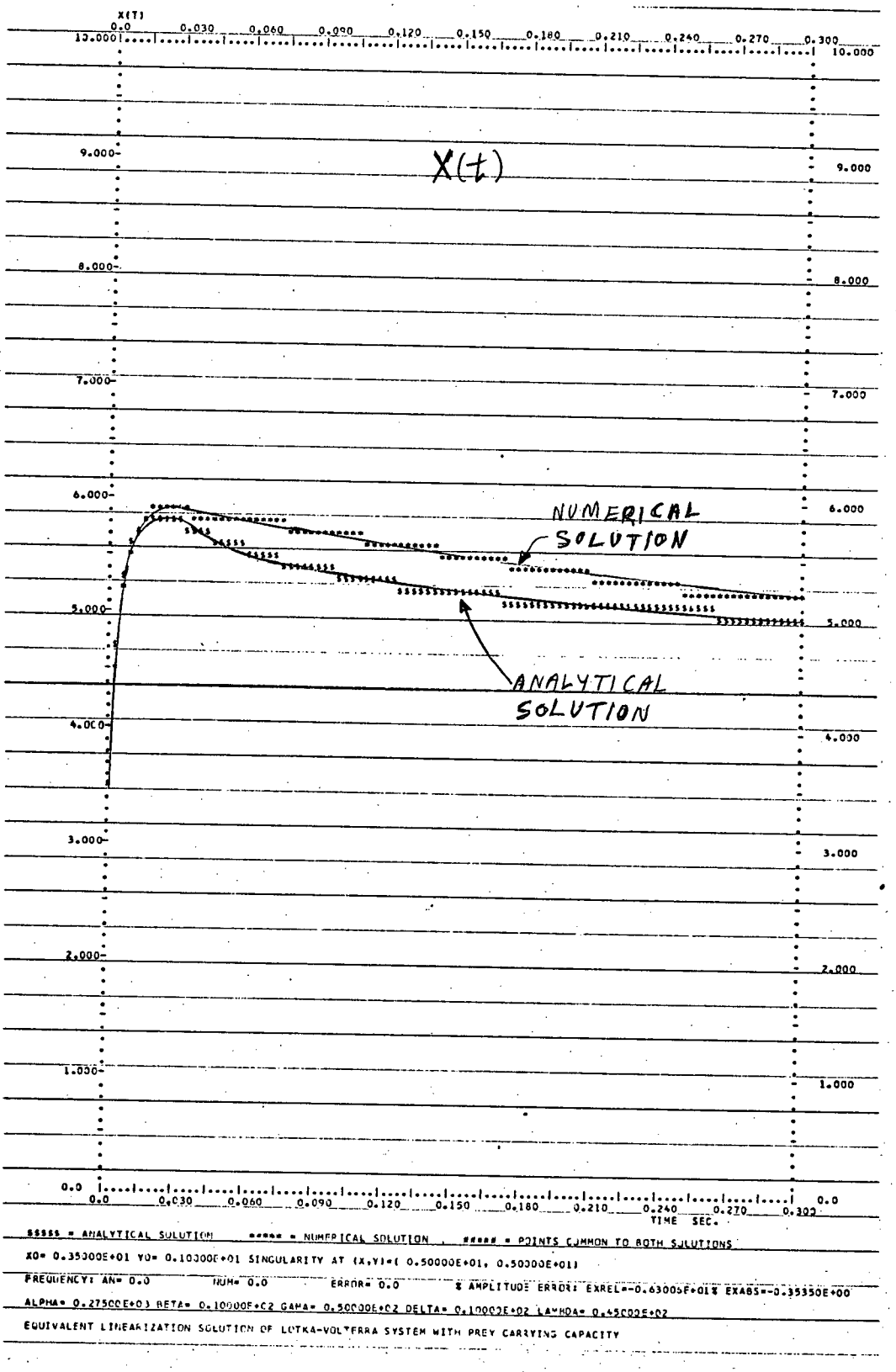

Fig. 2.8 VGW Model Linear Solution for $(x_o, y_o) = (3.5, 1)$

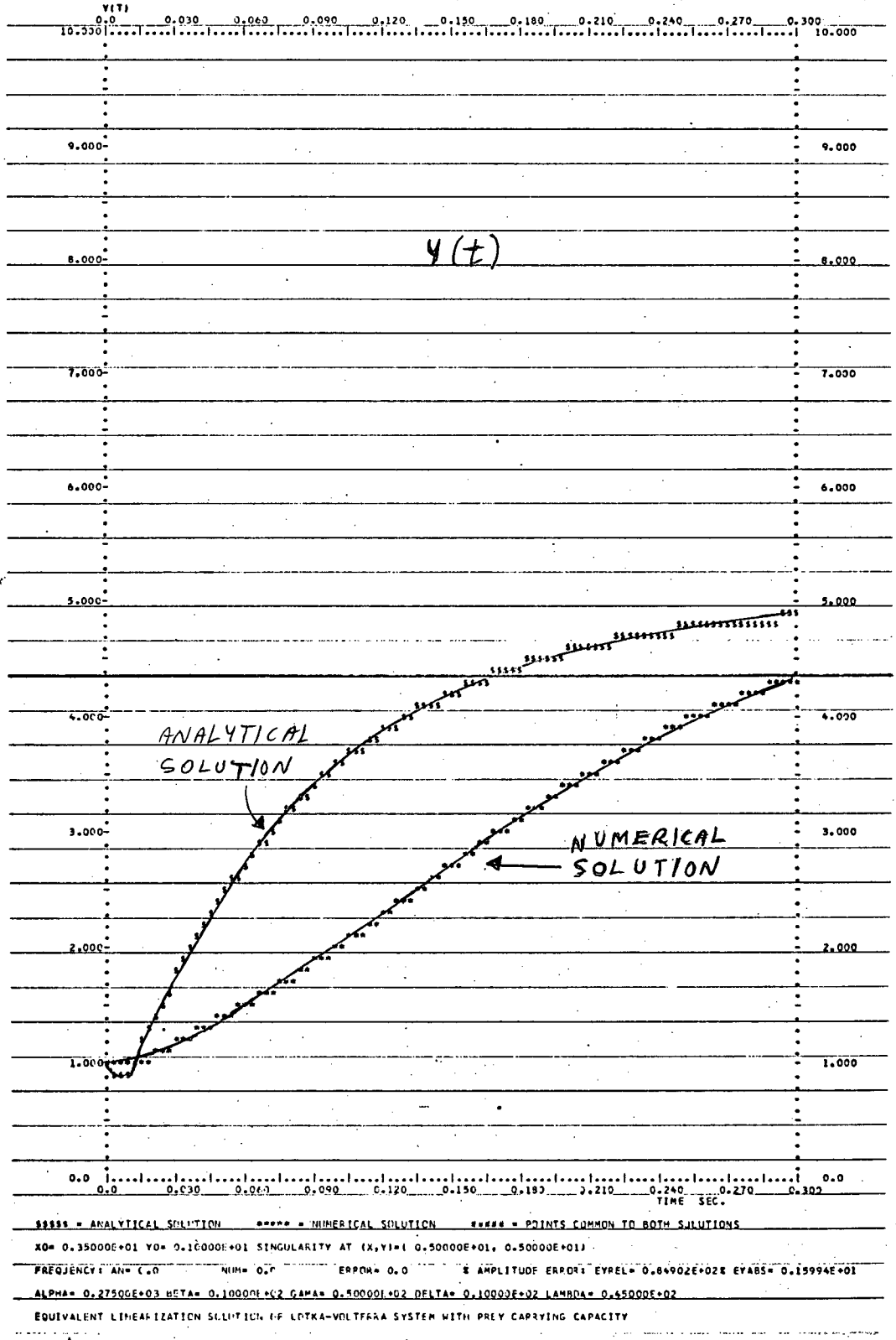

Fig. 2.9 VGW Model Linear Solutions for $(x_o, y_o) = (3.5, 1)$

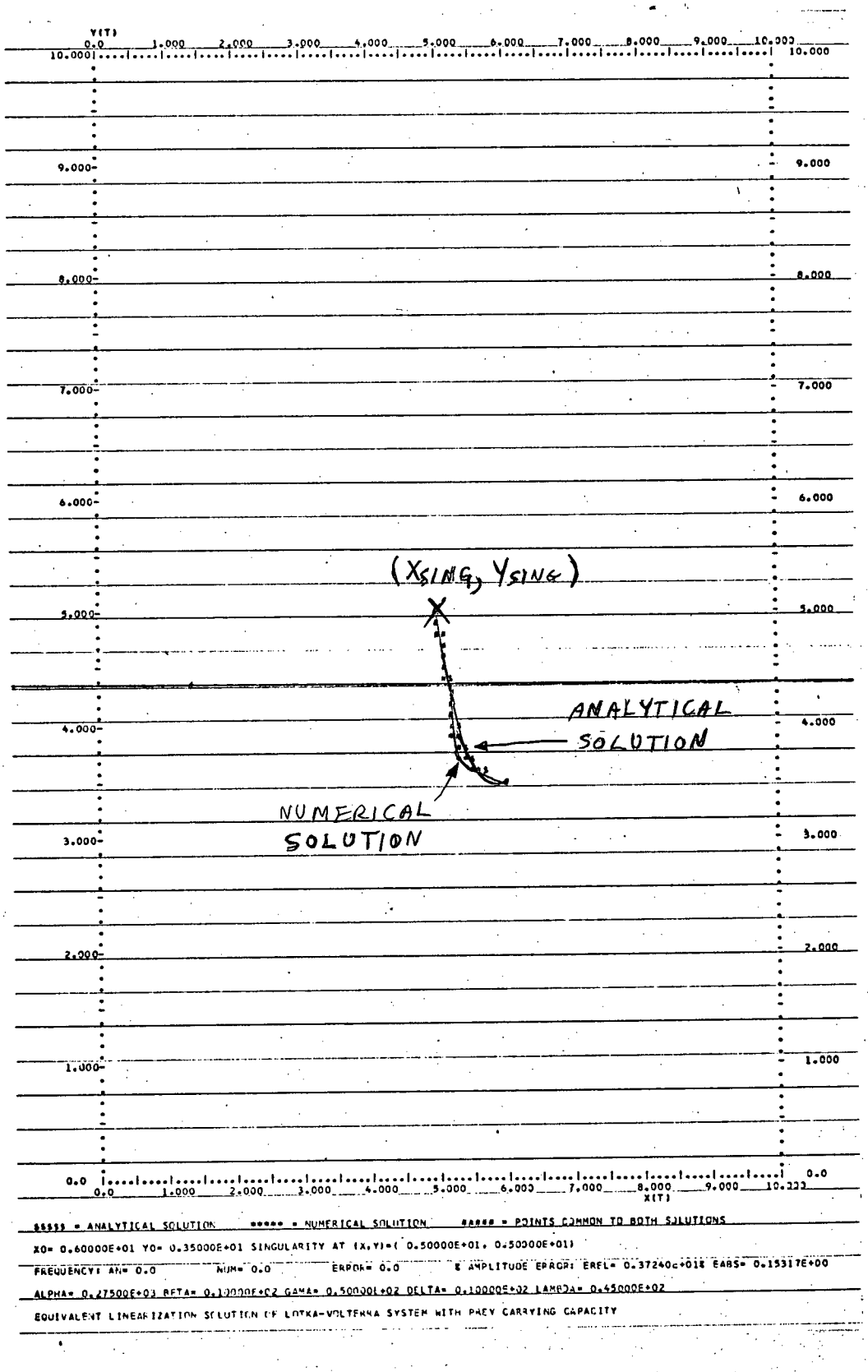

Fig. 2.10 VGW Model Linear Solution for $(x_o, y_o) = (6, 3.5)$

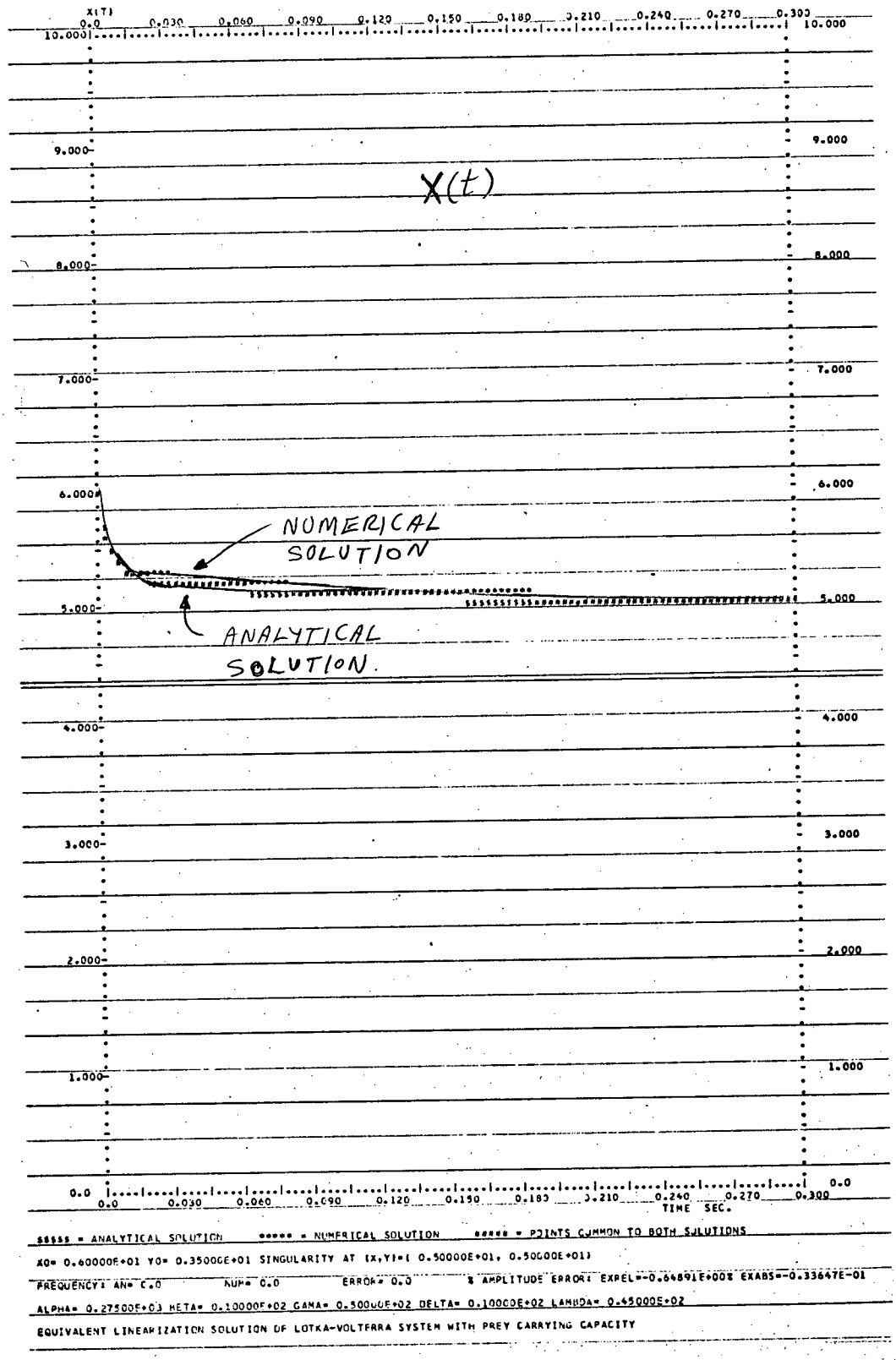

Fig. 2.11 VGW Model Linear Solutions for $(x_1, y_o) = (6, 3.5)$

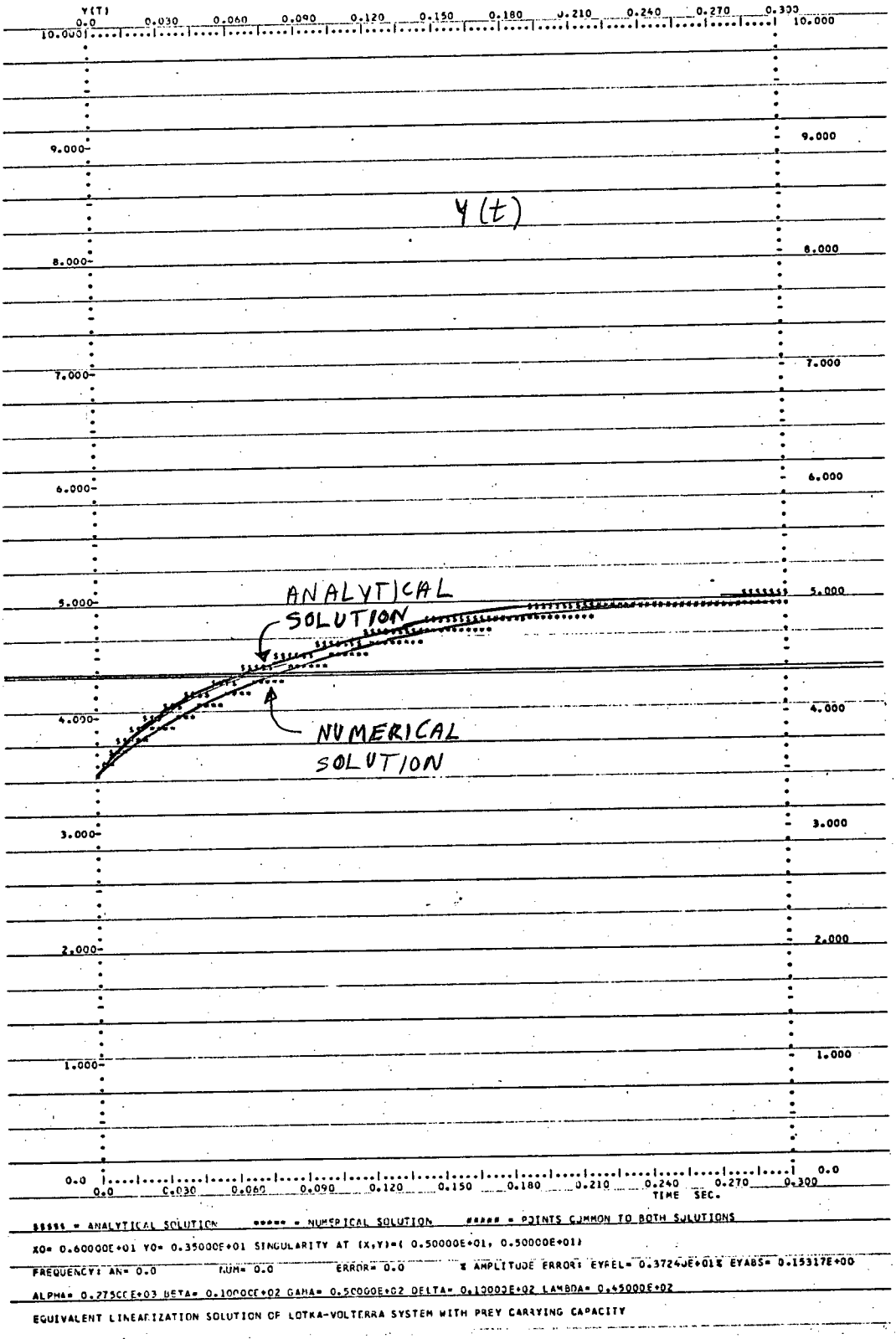

Fig. 2.12 VGW Model Linear Solution for $(x_1, y_o) = (6, 3.5)$

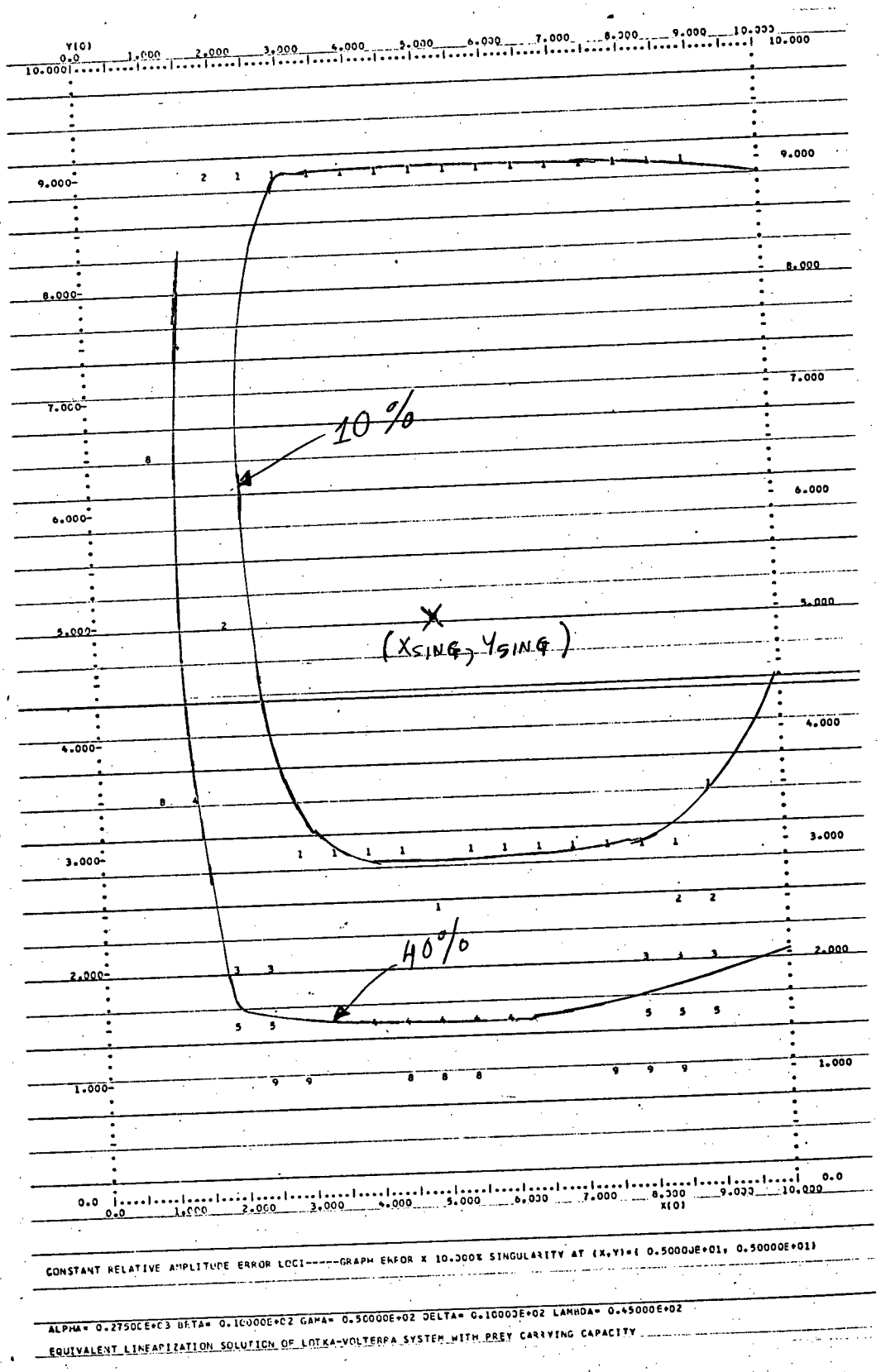

Fig. 2.13 YGW Model Linear Solution Amplitude Error Loci

2.5 Holling's Model

The next model we wish to study is Holling's model (see Holling 25). This model is one in which another physical characteristic of real ecological systems is incorporated, that of finite killing capacity of the predator, which is also dependant on the quantity of prey available. The model is:

$$\dot{x} = rx(1 - x/K) - xy/(A + x) \qquad r,K,A,s,J > 0$$

$$\dot{y} = \frac{sAy(x - J)}{(J + A)\ (A + x)}$$

In the prey equation, r governs the growth rate for small populations, while K is the carrying capacity of the environment. For large prey populations, the predator-prey interaction term, $xy/(A+x)$, (known as a Michaelis - Menton type interaction) indicates that the predators kill prey at the maximum rate of one prey per unit time per predator, which is the upper limit of the saturating term. For small populations, the prey are more difficult to locate and thus the killing capacity of the predator drops in a nonlinear manner. The parameter A controls the prey population level at which this effect becomes noticable. Note that for $A >> x$, the equations reduce to the VGW model. A complete derivation of this effect is given by Frederikson (18) and Holling (25). In the predator equation, the parameters s & J control the natural mortality rate of the predator and the magnitude of the predator-prey interaction. This model has three singularities, which are located at $(0,0)$, $(K,0)$, $(J,(J + A)r(1-J/K))$, and are discussed in the next section.

Holling (25) has numerous examples of ecological systems that obey the Michaelis-Menten type interaction. Two of these are short tailed shrew (predator) and sawflies in cocoons (prey); and the mantidae and adult

housefly. Validation of the complete model is still pending.

2.6 Linear Solution of Holling's Model

We now proceed to determine the linear solution of Holling's model. The A matrix corresponding to Holling's model is

$$A = \begin{vmatrix} r - 2rx/K - Ay/(A + x)^2 & -x/(A + x) \\ sAy/(A + x)^2 & \dfrac{sA(x - J)}{(J + A)(A + x)} \end{vmatrix}$$

For the singularity at (0,0), we have the eigenvalues $s_1 = r > 0$ and $s_2 = -sJ/(J + A) < 0$ which indicates that this is a saddle point. The eigenvalues of the singularity at (K,0) are $s_1 = -r < 0$ and $s_2 = \frac{sA(K - J)}{(J+A)(K+A)}$. If K > J, we have a saddle point. If J > K, we have a stable node (see figure 2.14A), with the third singularity having moved down into the fourth quadrant of the phase plane, where it is of no interest.

For K > J, the third singularity, $(x_{sing}, y_{sing}) = (J,(J + A)r(1 - J/K))$ is the one of interest to us. If $K_c < J < K$ (where K_c can be determined from the system eigenvalues with some difficulty, see Brauer 7). we have a stable focus (see figure 2.14B). If $\frac{1}{2}(K-A) < J < K_c$, we have a stable node (see figure 2.14C). If we have $0 < J < \frac{1}{2}(K-A)$, the singularity becomes unstable, and Kolmogorov's theorem (see Brauer) reveals that this gives rise to a limit cycle (see figure 2.14D). The major difference between Holling's model and the VGW model is that the prey isocline in Hollings model is humped and allows for the possiblity of a limit cycle, while the prey isocline of the VGW model is linear. The linearized system coefficients at the third singularity (x_{sing}, y_{sing}) are:

$$a_{11} = r(1 - 2J/K) - Ar(1 - J/K)/(J + A) \qquad a_{12} = J/(J + A)$$

$$a_{21} = sAr(1 - J/K)/(J + A) \qquad a_{22} = 0$$

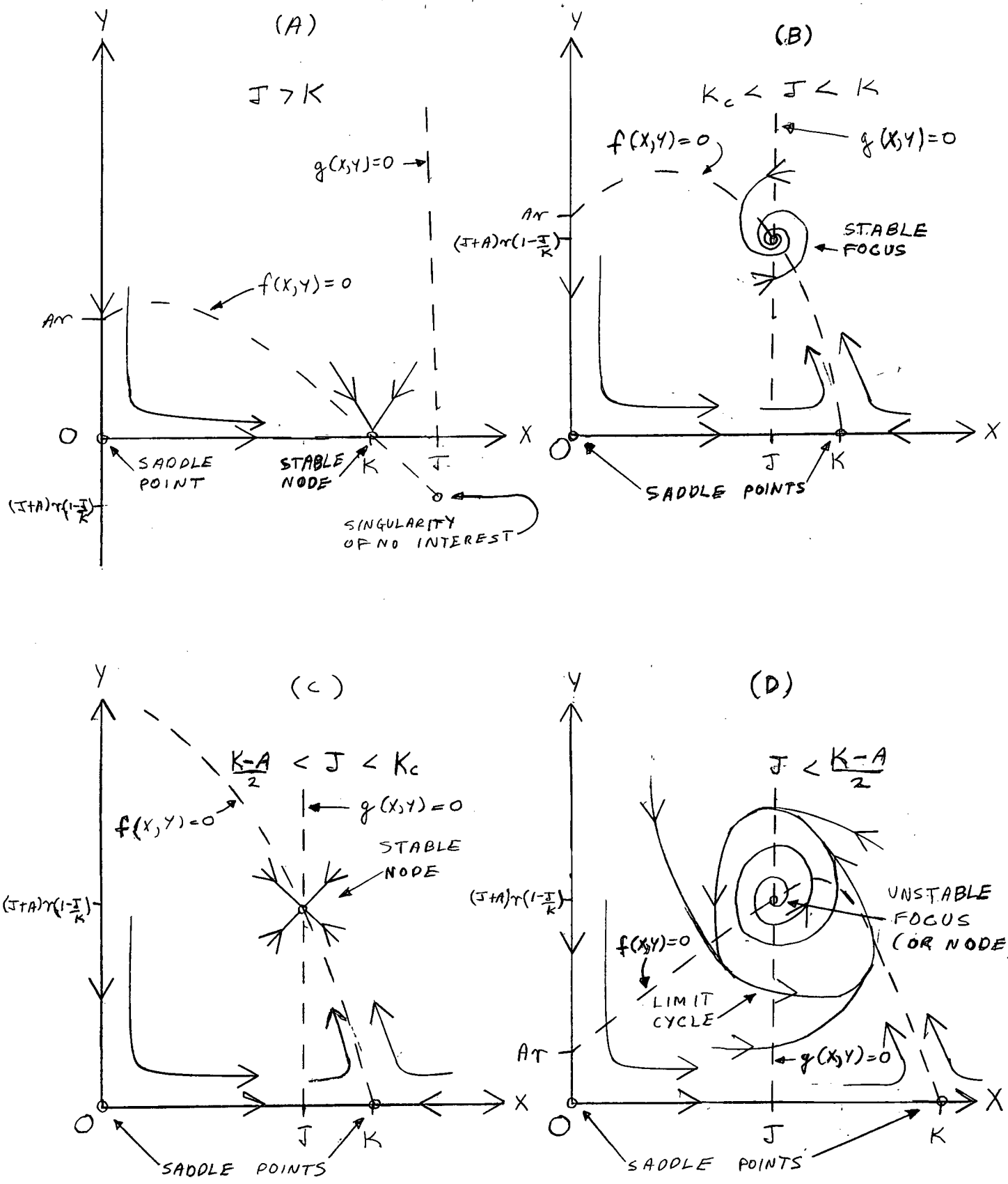

Fig. 2.14 Possible Singularity Types and Positions for Holling's Model

The problem of determining solutions for the limit cycle have not been considered in this thesis. This completes the determination of the linear solution of Holling's model.

2.7 Simulation Study of Holling's Model

We now wish to revaluate the linear solution of Holling's model. The solutions were computed for the arbitrary parameter choice of r=2, K=45, s=1, A=10, J=20 (for which (x_{sing},y_{sing}) is a stable focus), over the ranges of initial conditions $5<x_o<45$ and $5<y_o<45$ in increments of 2.5. The time plots and phase plane curves for the initial conditions (17.5, 42.5) and (30.0, 30.0) are shown in figures 2.15 to 2.20. The corresponding amplitude and frequency error loci are shown in figures 2.21 and 2.22. As before, the frequency is much more accurate then the amplitude for given initial conditions. The above computations were repeated for K=25, for which (x_{sing},y_{sing}) is a stable node, and the corresponding amplitude error loci are shown in figure 2.23.

We have evaluated the linear solution of Holling's model and found that it is a good approximate solution (see error loci curves). We now proceed onwards to study a third ecological model.

2.8 Rosenzweig's Model

The third model we wish to study is Rosenzweig's model (see Rosenzweig 48). The same physical phenomenon found in Holling's model are incorporated in Rosenzweig's model. The model is:

$$\dot{x} = rx(1 - x/K) - b(1 - e^{-cx})y \qquad r,K,b,c,s,J>0$$

$$\dot{y} = sy(e^{-cJ} - e^{-cx})$$

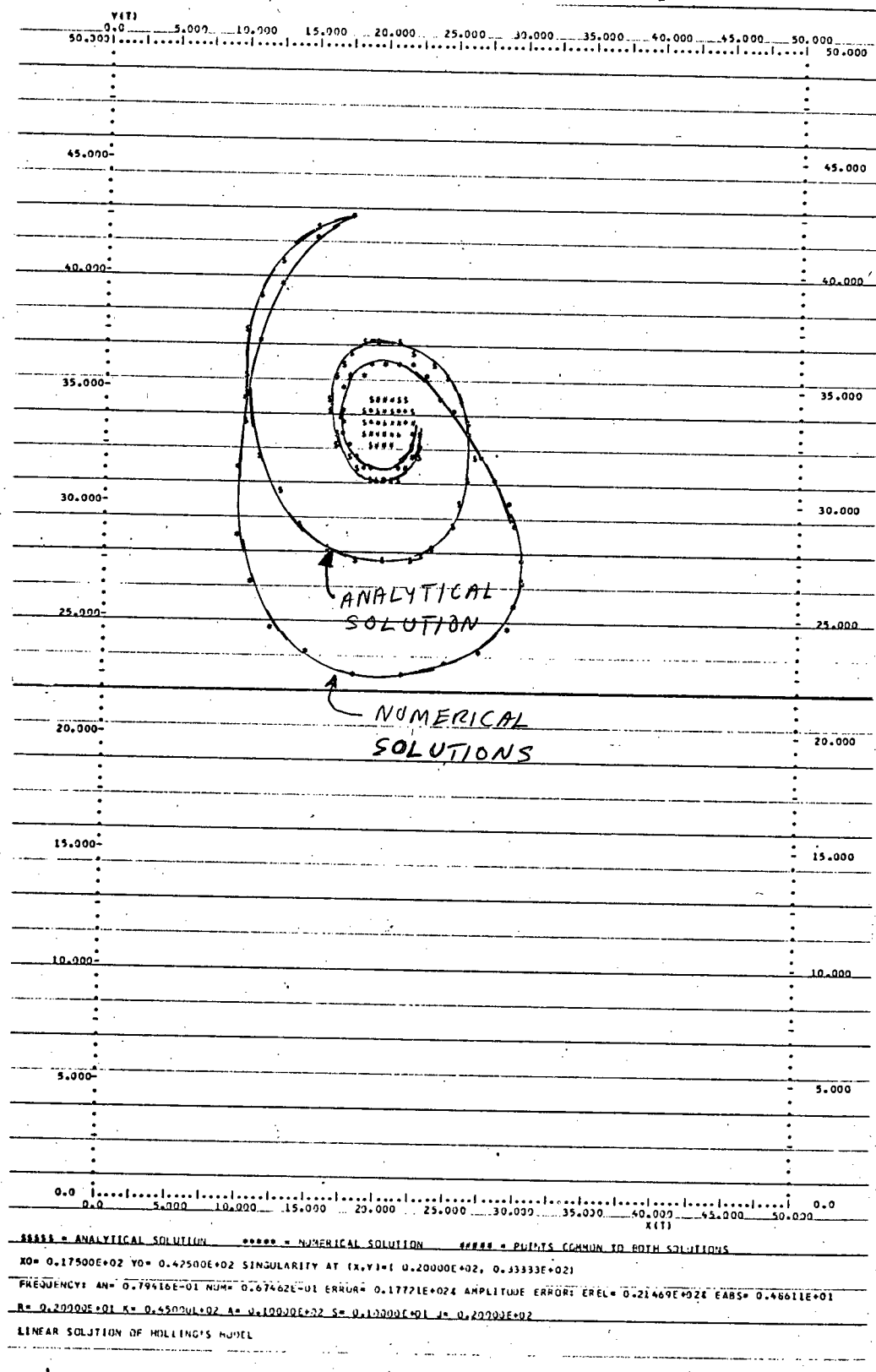

Fig. 2.15 Hollings Model Linear Solution for $(x_o, y_o) = (17.5, 42.5)$

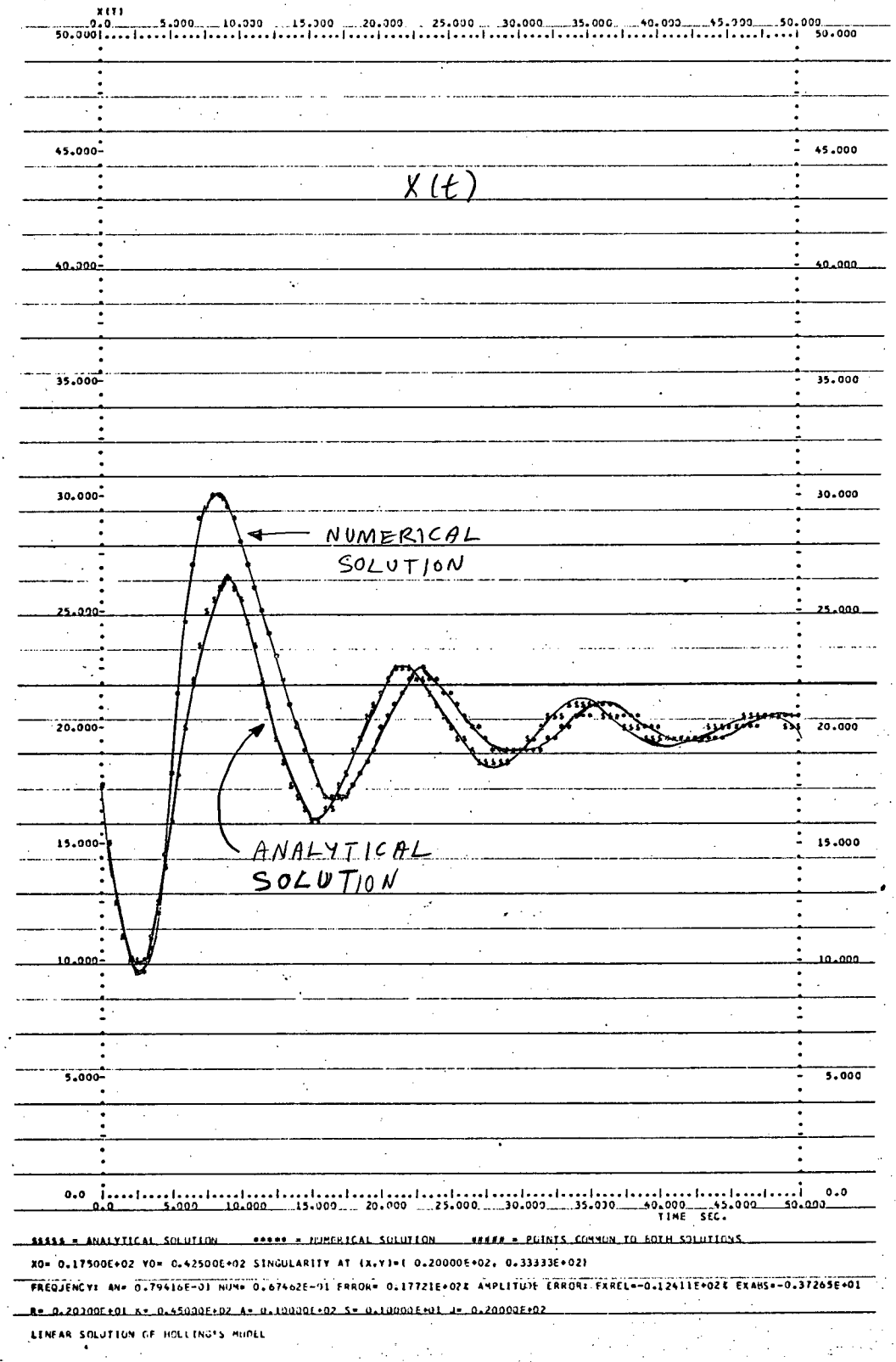

Fig. 2.16 Holling's Model Linear Solution for $(x_o, y_o) = (17.5, 42.5)$

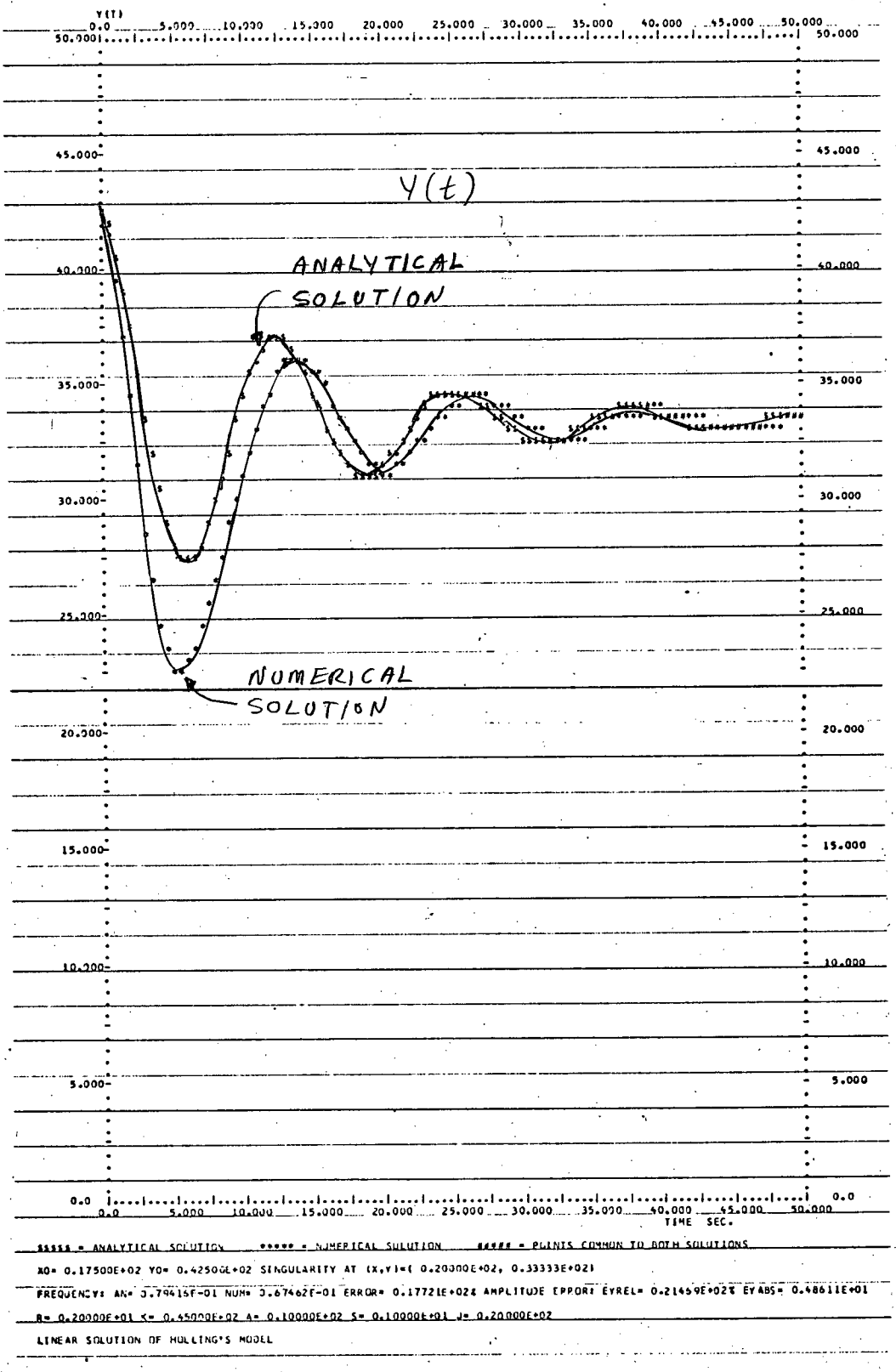

Fig. 2.17 Holling's Model Linear Solution for $(x_o, y_o) = (17.5, 42.5)$

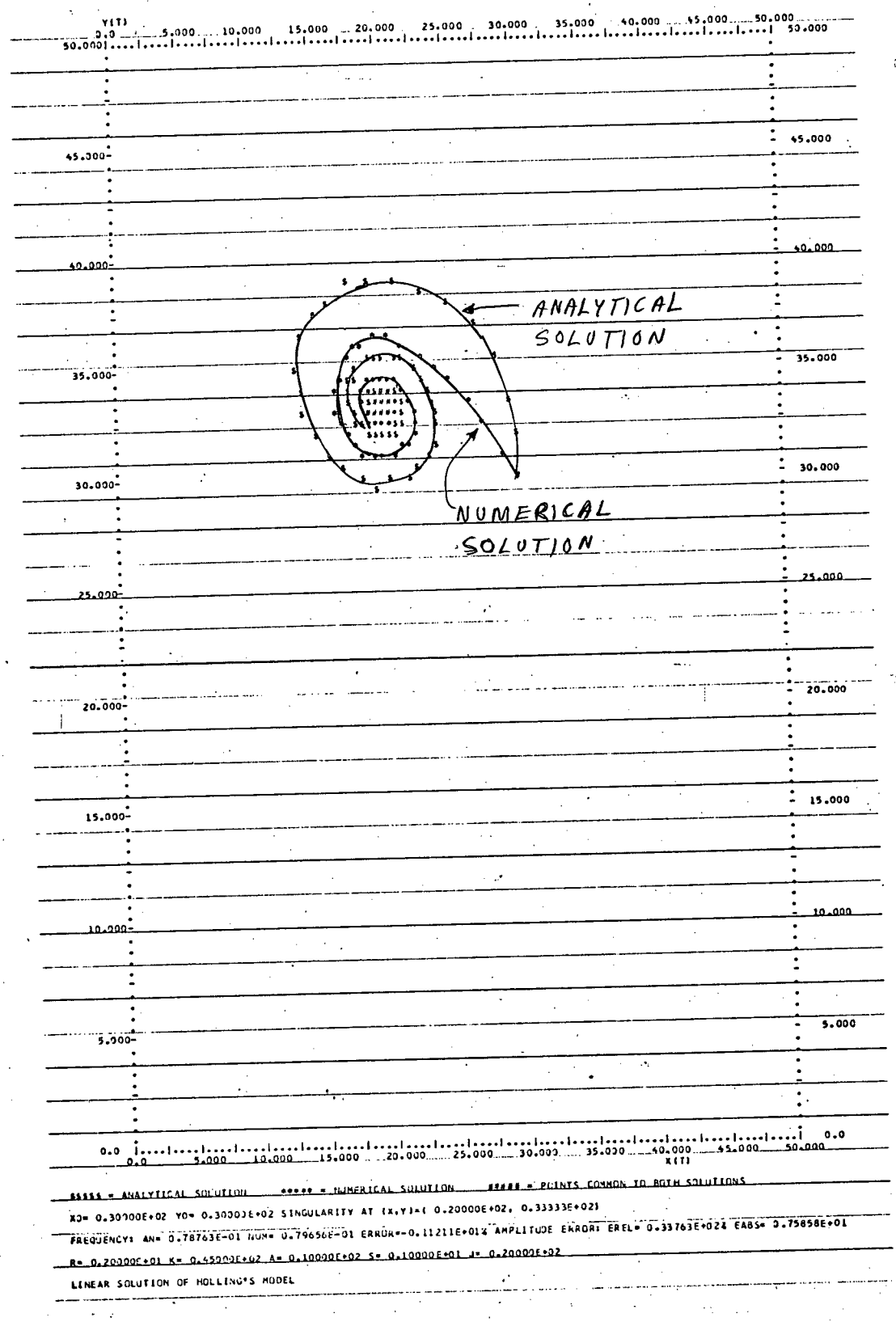

Fig. 2.18 Holling's Model Linear Solution for $(x_o, y_o) = (30, 30)$

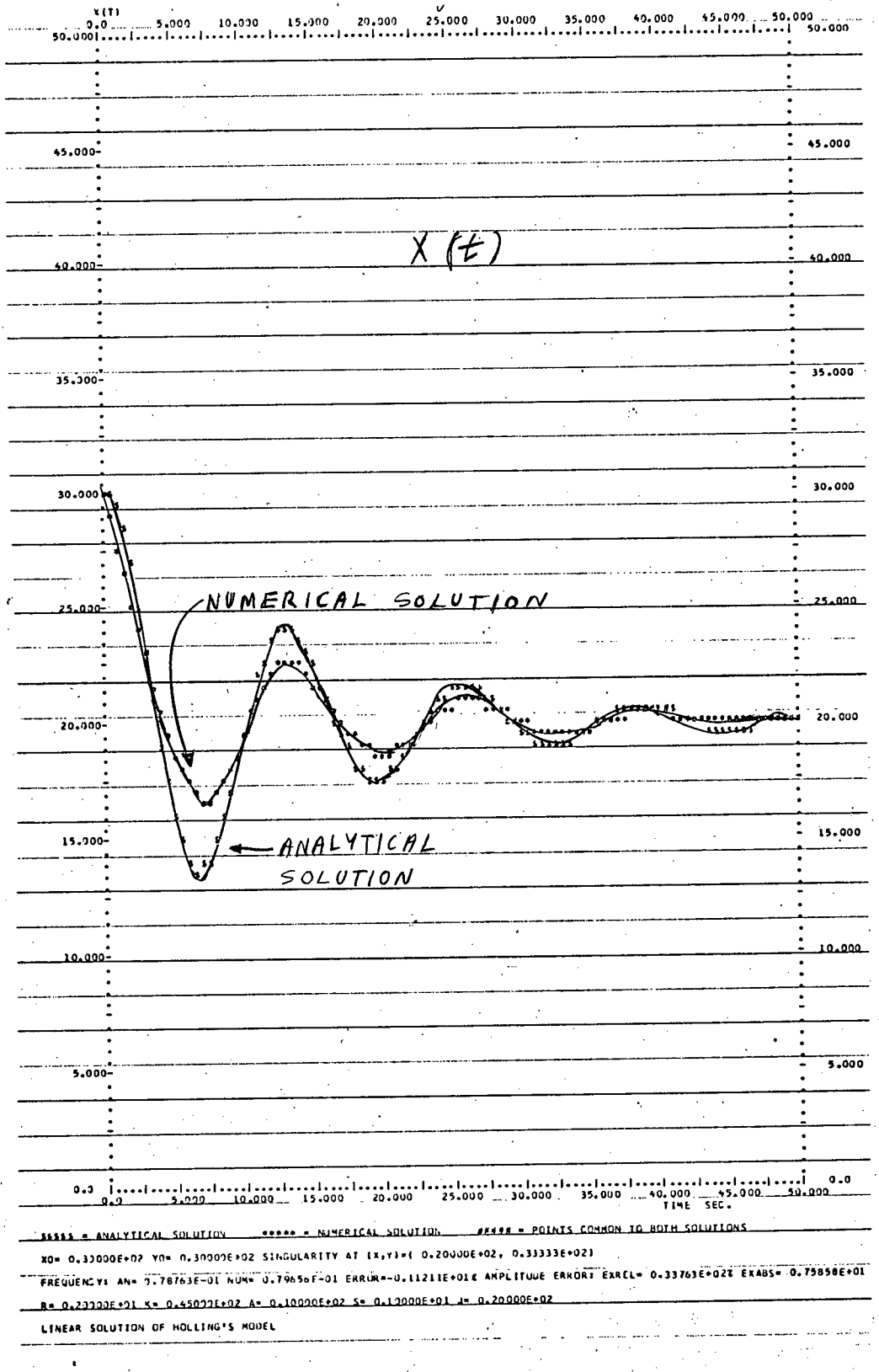

Fig. 2.19 Holling's Model Linear Solution for $(x_o, y_o) = (30, 30)$

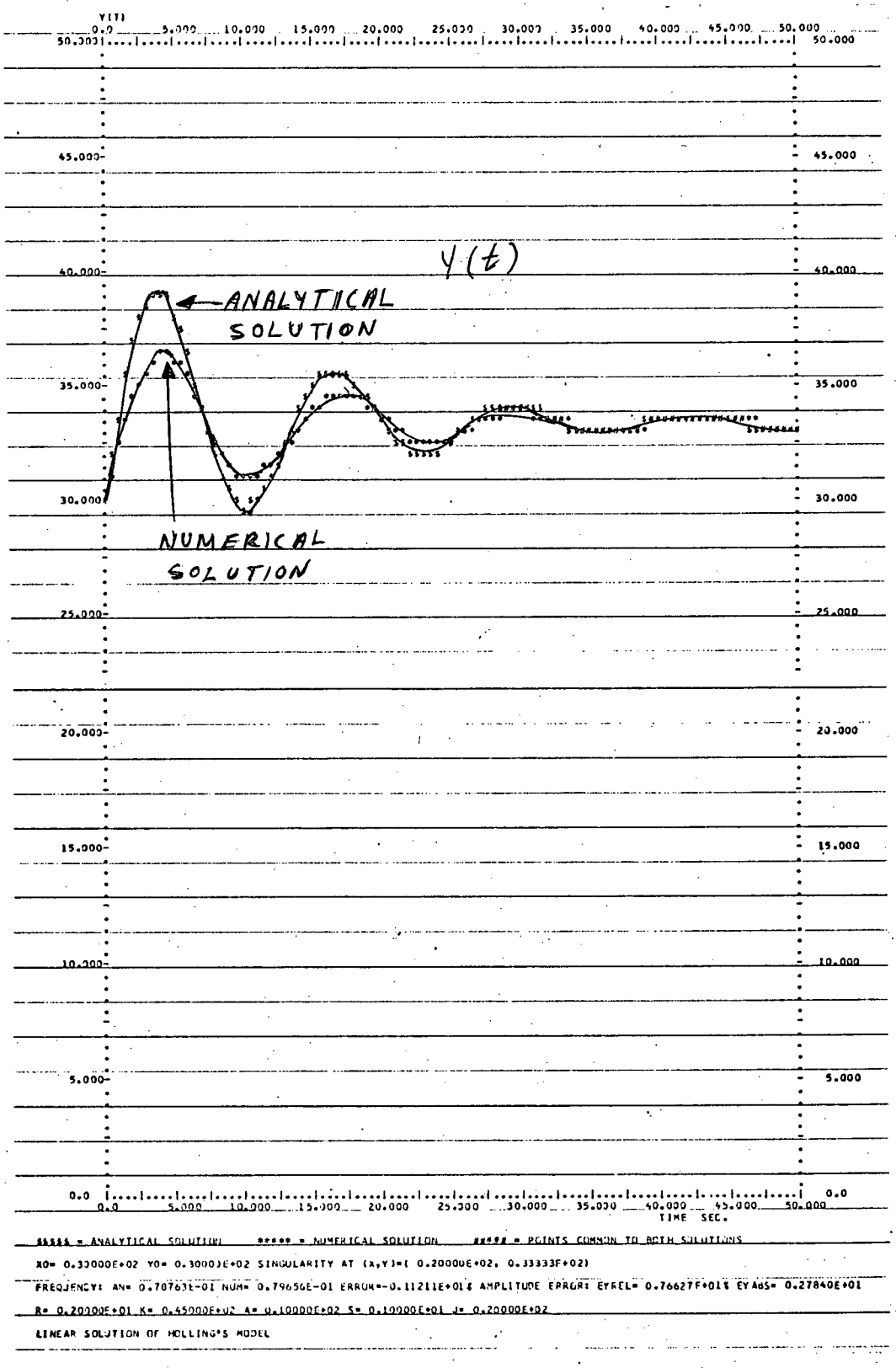

Fig. 2.20 Holling's Model Linear Solution for $(x_o, y_o) = (30, 30)$

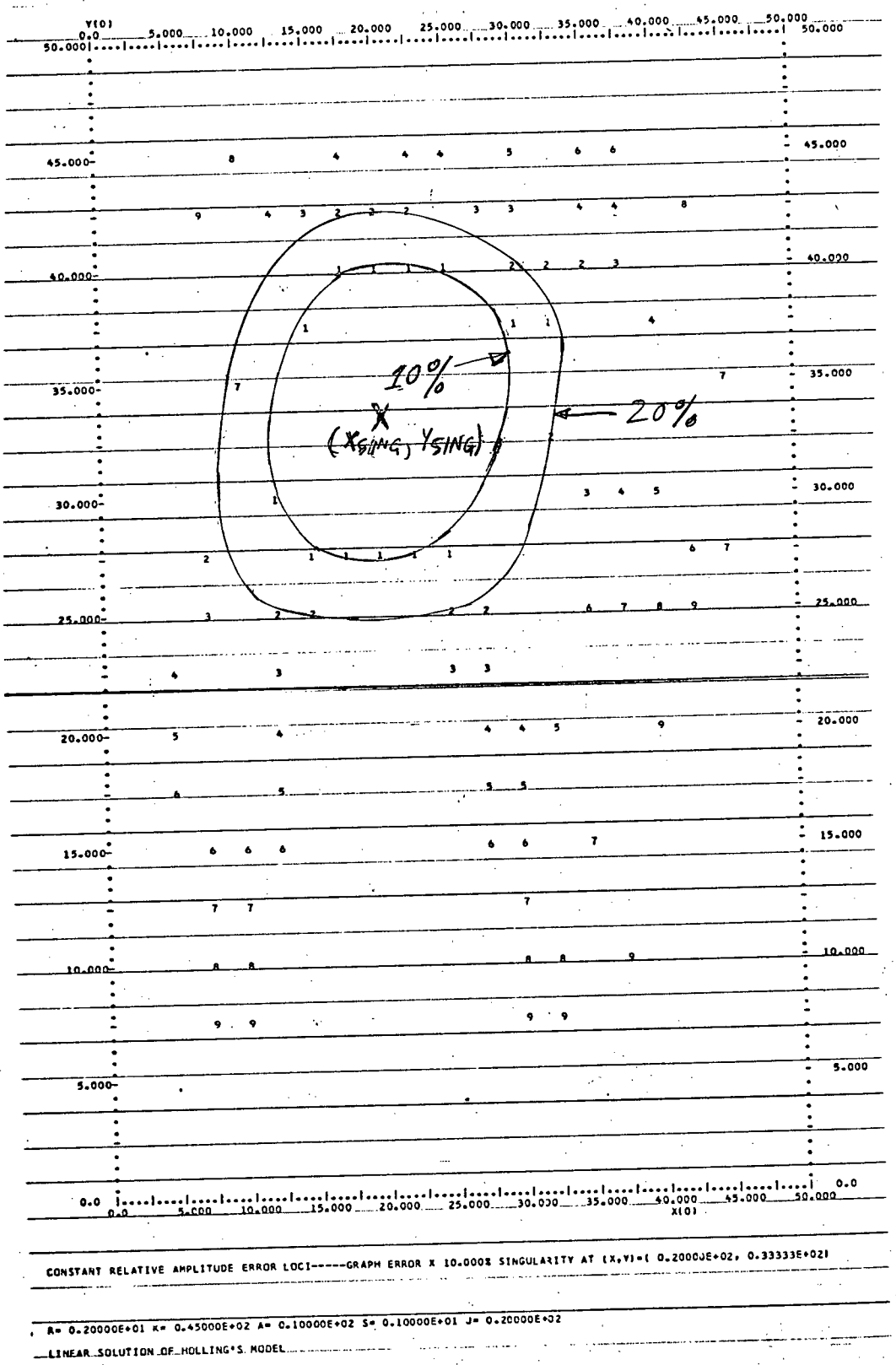

Fig. 2.21 Holling's Model Linear Solution Amplitude Error Loci

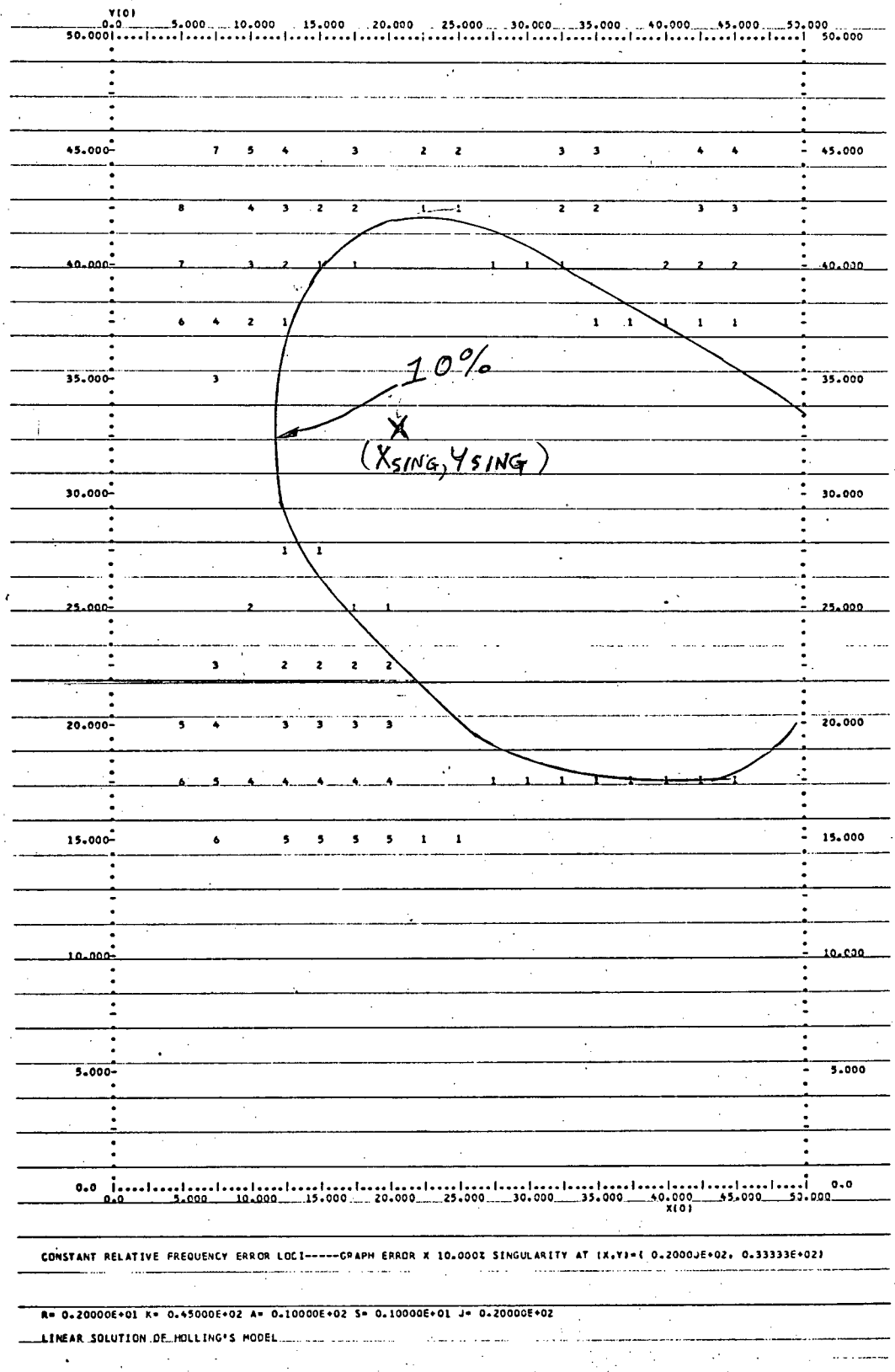

Fig. 2.22 Holling's Model Linear Solution Frequency Error Loci

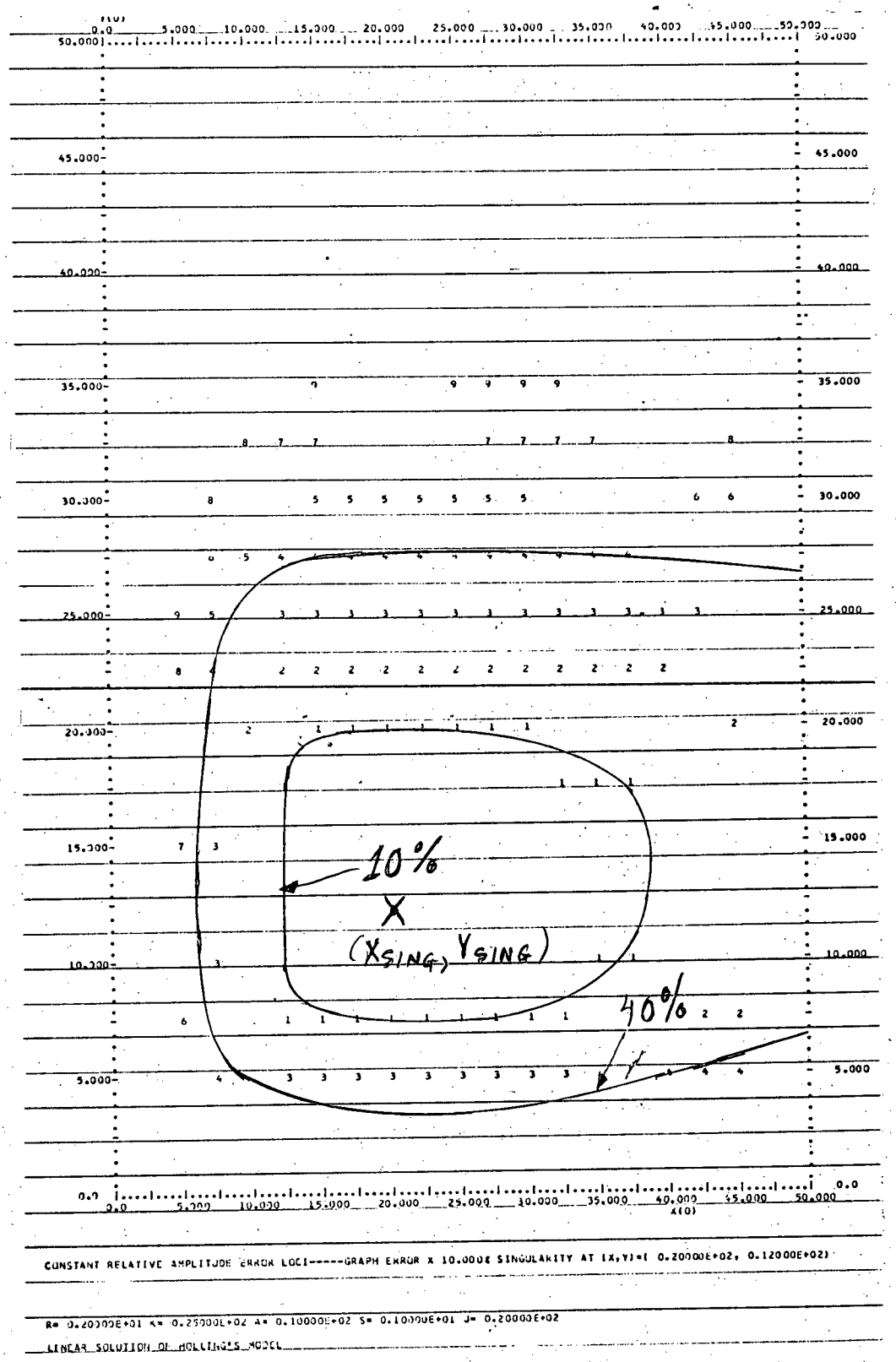

Fig. 2.23 Holling's Model Linear Solution Amplitude Error Loci

In this model, the saturation of the predator appetite is expressed in terms of exponentials (known as the Ivlev type interaction), instead of a ratio of polynomials as in Holling's model. Here, the parameter b represents the maximum killing capacity of the predator, while c governs the prey level at which the predator appetite saturation effect occurs. Rosenzweig's model behaves similarly to Holling's model, as the same physical phenomenon are modelled in each. As was the case with Holling's model, the prey isocline is humped. The model has three singularities which are located at (0,0), (K,0), $(J, \frac{rJ(1 - J/K)}{b(1 - \exp(-cJ))})$ and these are discussed in the next section.

Ivlev (29) has several examples of ecological systems that obey the above type of predator-prey interaction. Some of these are carp fed on nonliving food; roaches fed on chironomid larvae; and bleak fed on Daphnia pulex. Again, the validation of the complete model for specific ecological systems is pending.

2.9 Linear Solution of Rosenzweig's Model

We now proceed to determine the linear solution of Rosenzweig's model. The A matrix corresponding to Rosenzweig's model is:

$$A = \begin{vmatrix} r - 2rx/K - bcye^{-cx} & -b(1 - e^{-cx}) \\ scye^{-cx} & s(e^{-cJ} - e^{-cx}) \end{vmatrix}$$

For the singularity at (0,0), we have the eigenvalues $s_1 = r > 0$ and $s_2 = s(e^{-cJ} - 1) < 0$, which indicates that this is a saddle point. The eigenvalues at the singularity (K,0) are $s_1 = -r < 0$ and $s_2 = se^{-cJ}(1 - e^{-c(K-J)})$. If J<K, we have a saddle point. If J>K, we have a stable node, with the third singularity having moved down into the fourth quadrant of the phase plane, where it is of no interest (see Figure 2.24A).

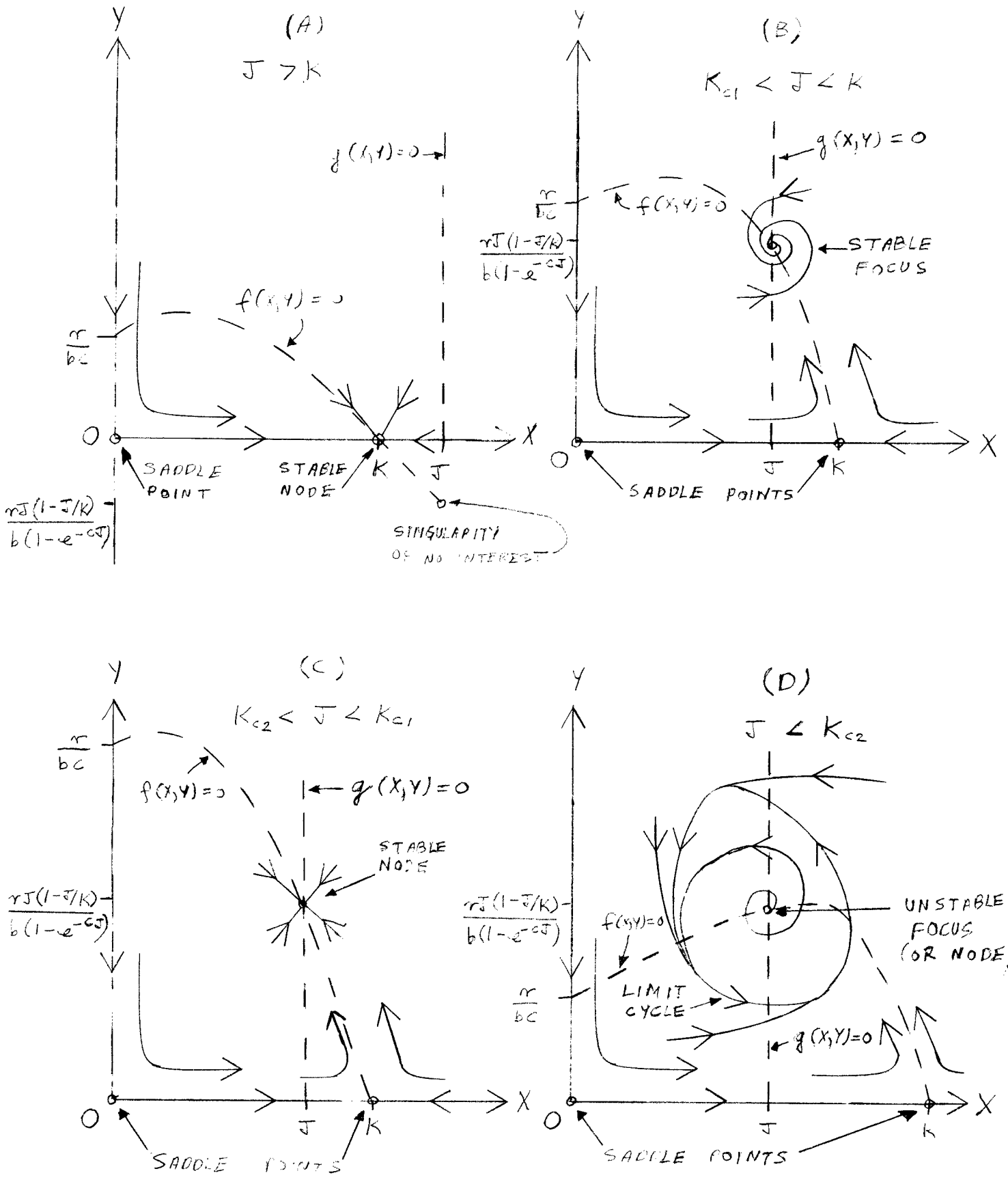

Fig. 2.24 Possible Singularity Types and Positions for Rosenzweig's Model

The third singularity, $(x_{sing}, y_{sing}) = (J, \frac{rJ(1 - J/K)}{b(1 - \exp(-cJ))}$ is normally (for K>J) the one of interest. If $K_c < J < K$, (where K_c can be determined from the system eigevnalues we have either a stable node or a stable focus (see figure 2.24 B & C). If $J < K_c$, the singularity becomes unstable (see figure 2.24D), and Kolmogorov's theorem (see Brauer 7) reveals that this gives rise to a limit cycle. The linearized system coefficients at the third singularity, (x_{sing}, y_{sing}) are:

$$a_{11} = r(1 - 2J/K) - rcJ(1 - J/K)/(e^{cJ} - 1) \qquad a_{12} = b(1 - e^{-cJ})$$

$$a_{21} = scrJ(1 - J/K)/b/(e^{cJ} - 1) \qquad a_{22} = 0$$

The problem of determining solutions for the limit cycle has not been considered in this thesis. This completes the determination of the linear solution of Rosenweig's model.

2.10 Simulation Study of Rosenzweig's Model

We now wish to evaluate the linear solution of Rosenzweig's model. The solutions were computed for the arbitrary parameter choice r = 2, K = 45, b=1, c=0.1, s=1, & J=20, (for which x_{sing}, y_{sing}) is a stable focus) over the range of initial conditions $5<x_o<45$ and $5<y_o<45$ in increments of 2.5 The amplitude and frequency error loci are shown in figures 2.25 & 2.26. As before, the frequency is more accurate than the amplitude for given initial conditions. The above computations were repeated for K=25, for which (x_{sing}, y_{sing}) is a stable node, and the corresponding amplitude error loci are shown if figure 2.27.

We have evaluated the linear solution of Rosenzweig's model and found it to be a good approximate solution (see error loci figures) over a wide range of initial conditions. We now proceed onward to study one final ecological model.

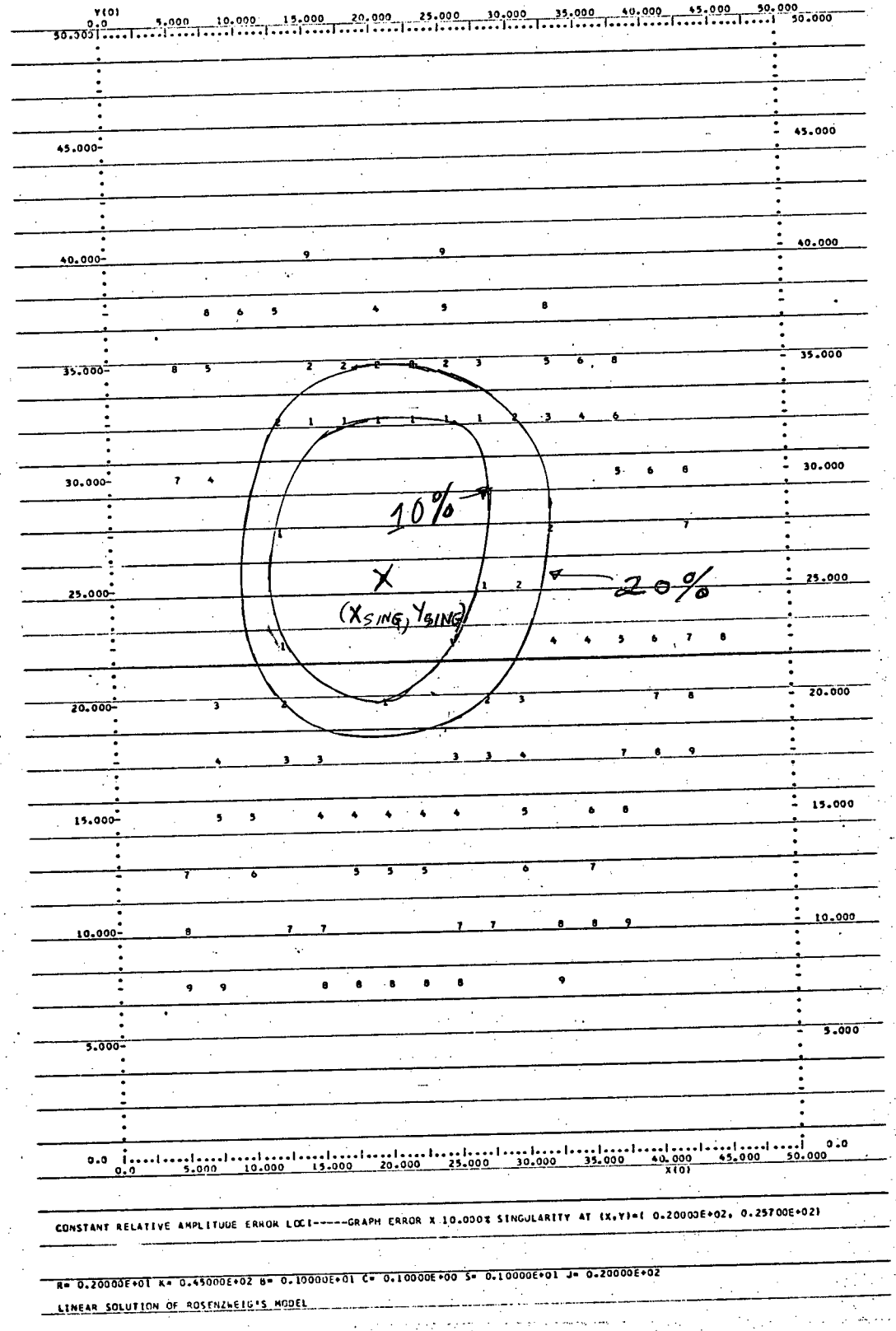

Fig. 2.25 Rosenzweig's Model Linear Solution Amplitude Error Loci

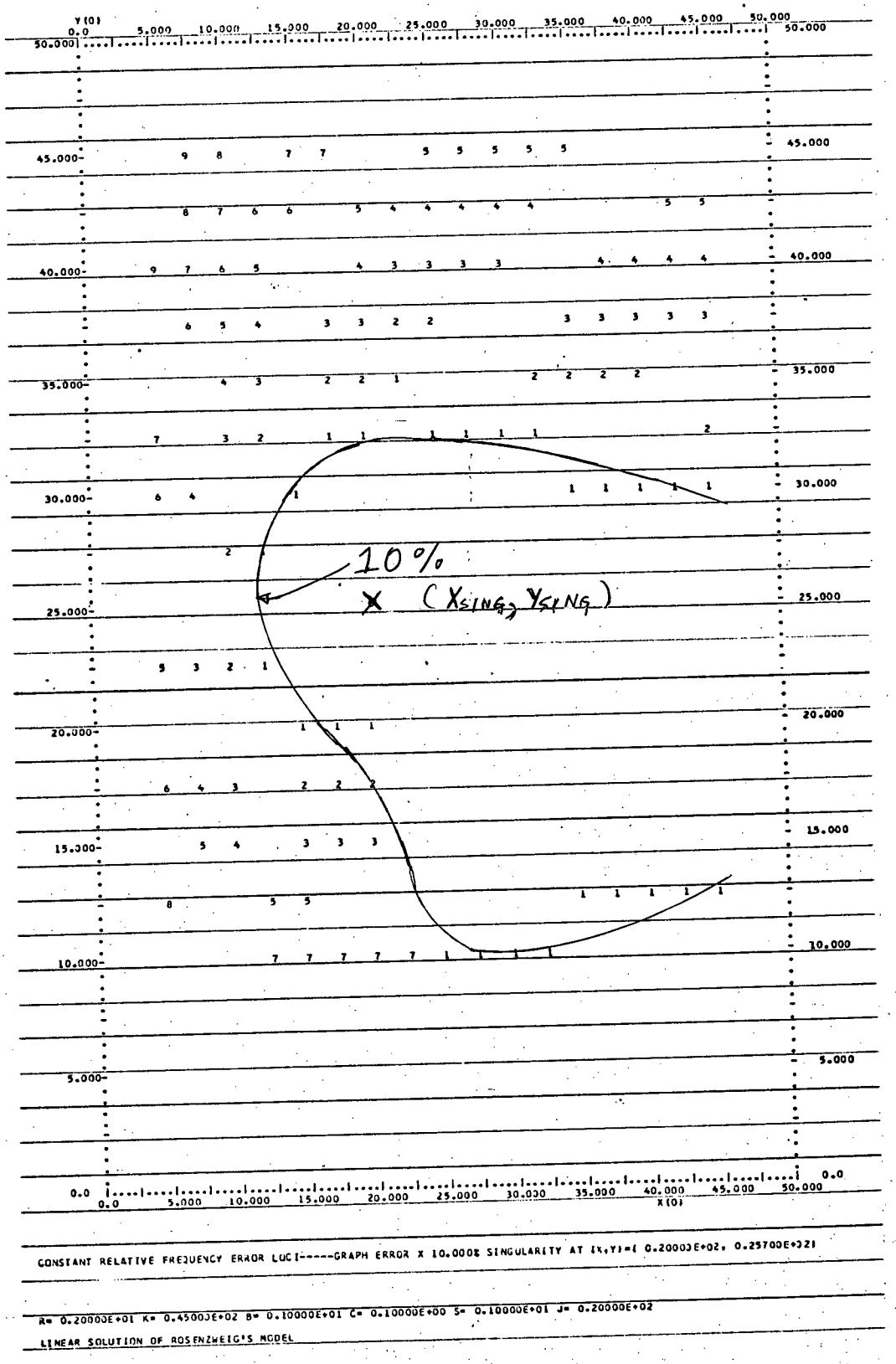

Fig. 2.26 Rosenzweig's Model Linear Solution Frequency Error Loci

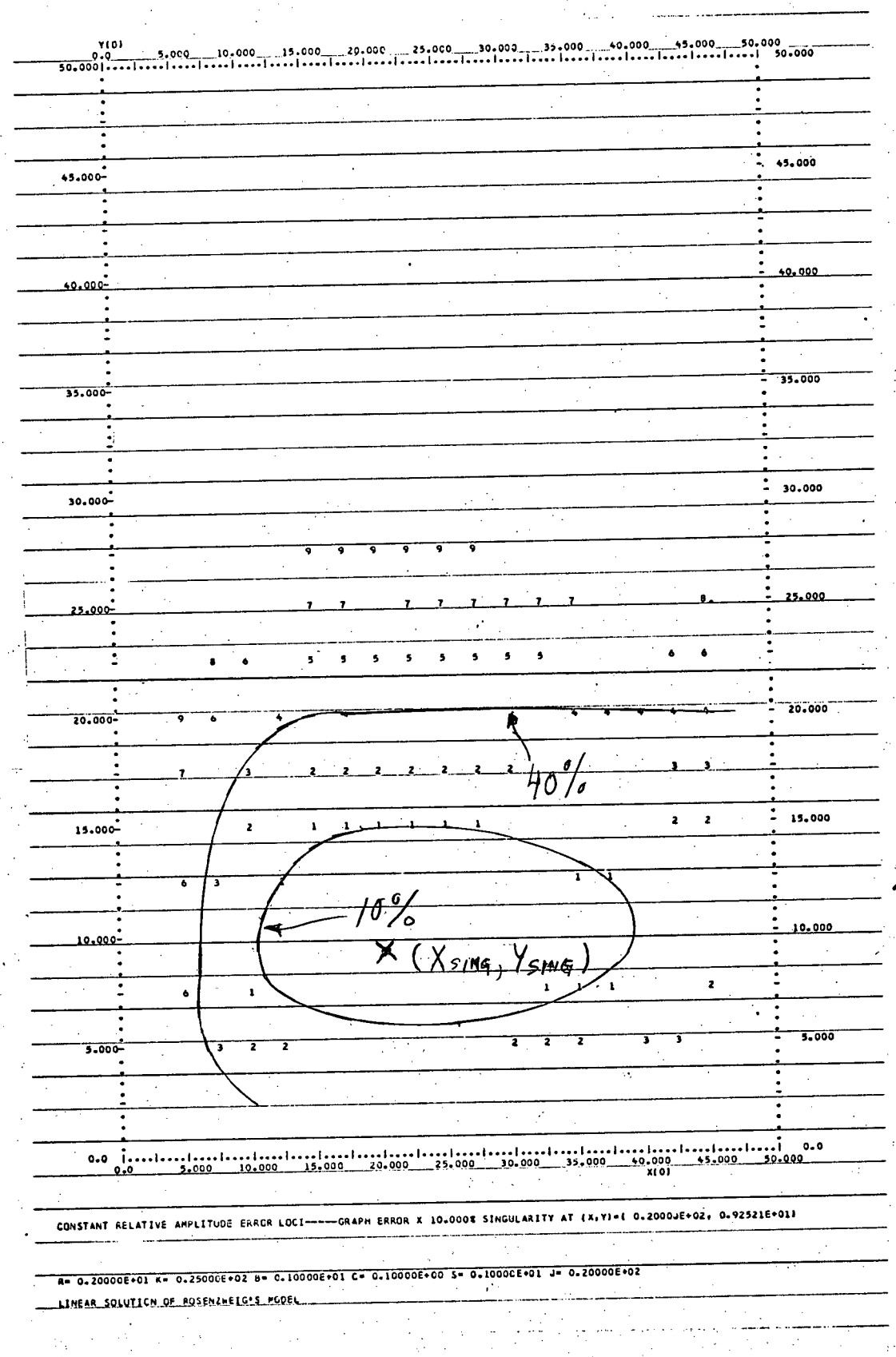

Fig. 2.27 Rosenzweig's Model Linear Solution Amplitude Error Loci

2.11 O'Brien's Model

The last ecological model to be studied is O'Brien's model (see O'Brien 44). This model has been successfully used in the study of phytoplankton dynamics. The model is:

$$\dot{x} = r - xy/(A + x)$$

$$\dot{y} = \frac{sAy(x - J)}{(J + A)(A + x)} \qquad r,A,S,J > 0$$

In the model, r is the rate at which prey (nutrient) is added to the system. As with the previous two models, the predator has a finite appetite. The predator equation is identical to Holling's predator equation. There is only one singularity in this model, which is located at $(J, r(J + A)/J)$, and it will be discussed in the next section.

2.12 Linear Solution of O'Brien's Model

We now proceed to determine the linear solution of O'Brien's model. The A matrix corresponding to O'Brien's model is:

$$A = \begin{vmatrix} -yA/(A + x)^2 & -x/(A + x) \\ sAy/(A + x)^2 & \frac{sA(x - J)}{(J + A)(A + x)} \end{vmatrix}$$

For the only singularity $(x_{sing}, y_{sing}) = (J, r(J + A)/J)$, we have the eigenvalues $s_{1,2} = \frac{-Ar}{2(J + A)J} \pm \frac{1}{2}\sqrt{\frac{A^2r^2}{(J + A)^2 J^2} - \frac{4sAr}{(J + A)^2}}$

The system is stable for all combinations of parameters. If $Ar > 4sJ^2$, then we have a stable node (see figure 2.28A). If we have $Ar < 4sJ^2$, then we have a stable focus (see figure 2.28B). The linearized system coefficients at the singularity are:

$$a_{11} = \frac{-Ar}{(J + A)J} \qquad a_{12} = J/(J + A)$$

$$a_{21} = \frac{sAr}{J(J + A)} \qquad a_{22} = 0$$

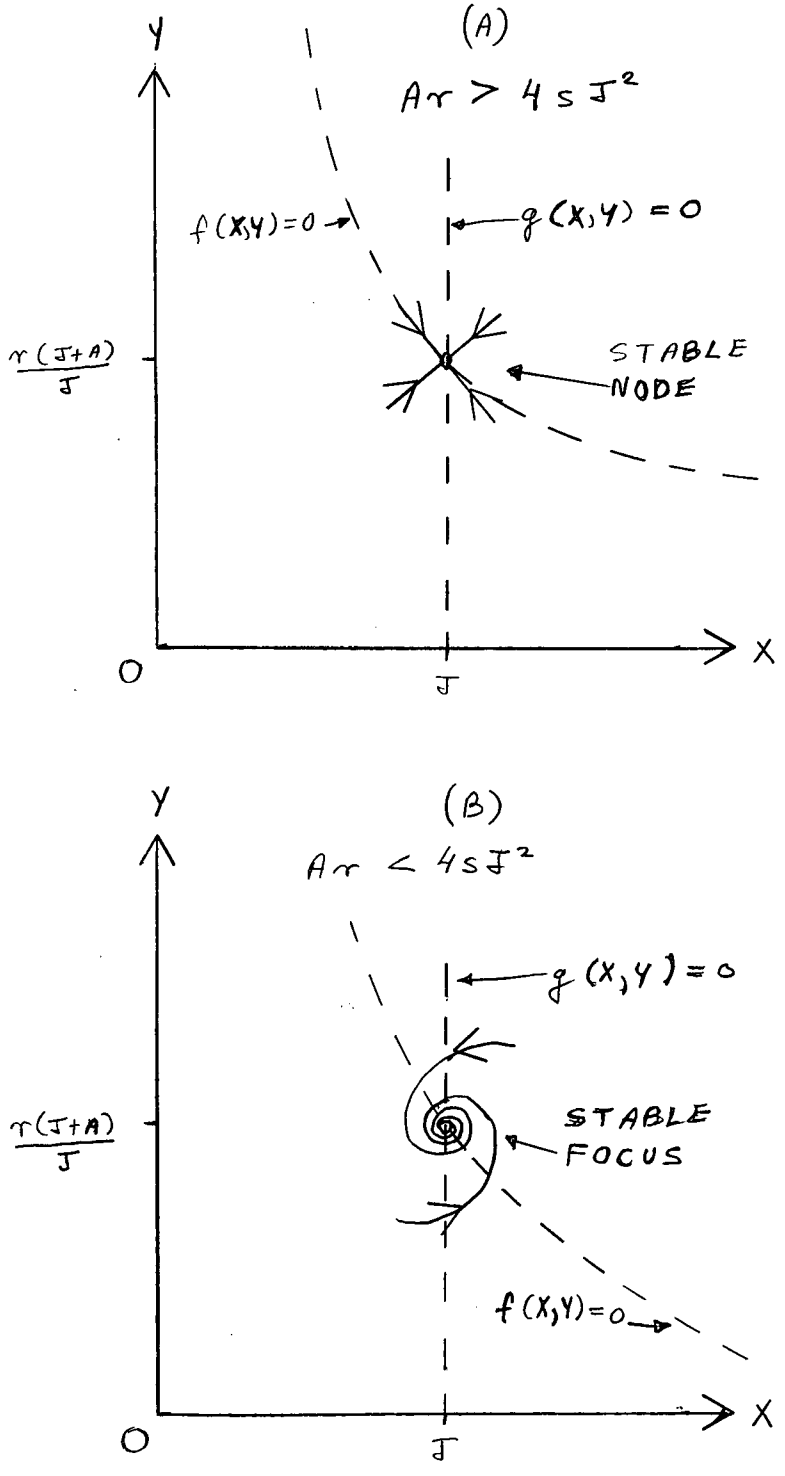

Fig. 2.28 Possible Singularity Types and Positions for O'Brien's Model

This completes the determination of the linear solution of O'Brien's model.

2.13 Simulation Study of O'Brien's Model

We now wish to evaluate the linear solution of O'Brien's model. The solutions were computed for the parameter choice r=2, A=10, s=2, J=5 (for which (x_{sing},y_{sing}) is a stable focus) over the ranges of initial conditions $1 < x_o < 9$, and $1 < y_o < 9$ with increments of $\frac{1}{2}$. These parameter values are scaled versions of those used by O'Brien in his model. The amplitude and frequency error loci are shown in figures 2.29 & 2.30. As before the frequency is more accurate then the amplitude for given initial conditions. The above computations were repeated for s = 0.1, for which (x_{sing},y_{sing}) is a stable node, and the corresponding amplitude error loci are shown in figure 2.31. We have evaluated the linear solution of O'Brien's model and found it to be a good approximate solution (see error loci figures) over a wide range of initial conditions. This completes our study of the method of linearizing nonlinear differential equation ecology models.

2.14 Summary

In this chapter we have started our study of advanced models by applying the classical principle of linearization to four nonlinear systems of differential equations that model predator-prey systems. These solutions accurately describe the behaviour of the systems for initial conditions that are more than a distance ε away from the singular point (see figures of error loci).

The value of these solutions is two fold. First of all, the complete literal parameter solution is made available. Secondly, one can quickly ascertain the effects of variations of a given parameter on the

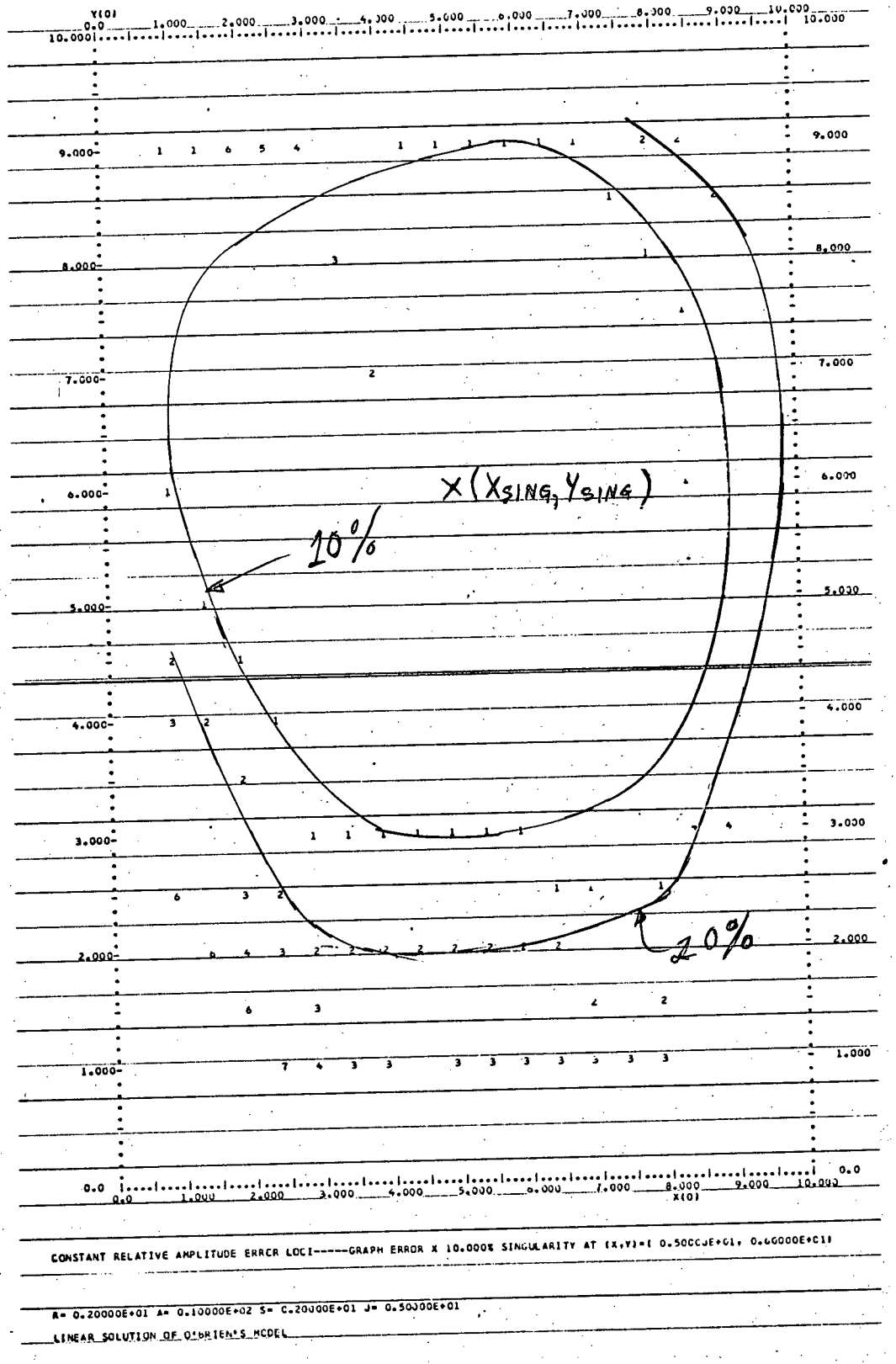

Fig. 2.29 O'Brien's Model Linear Solution Amplitude Error Loci

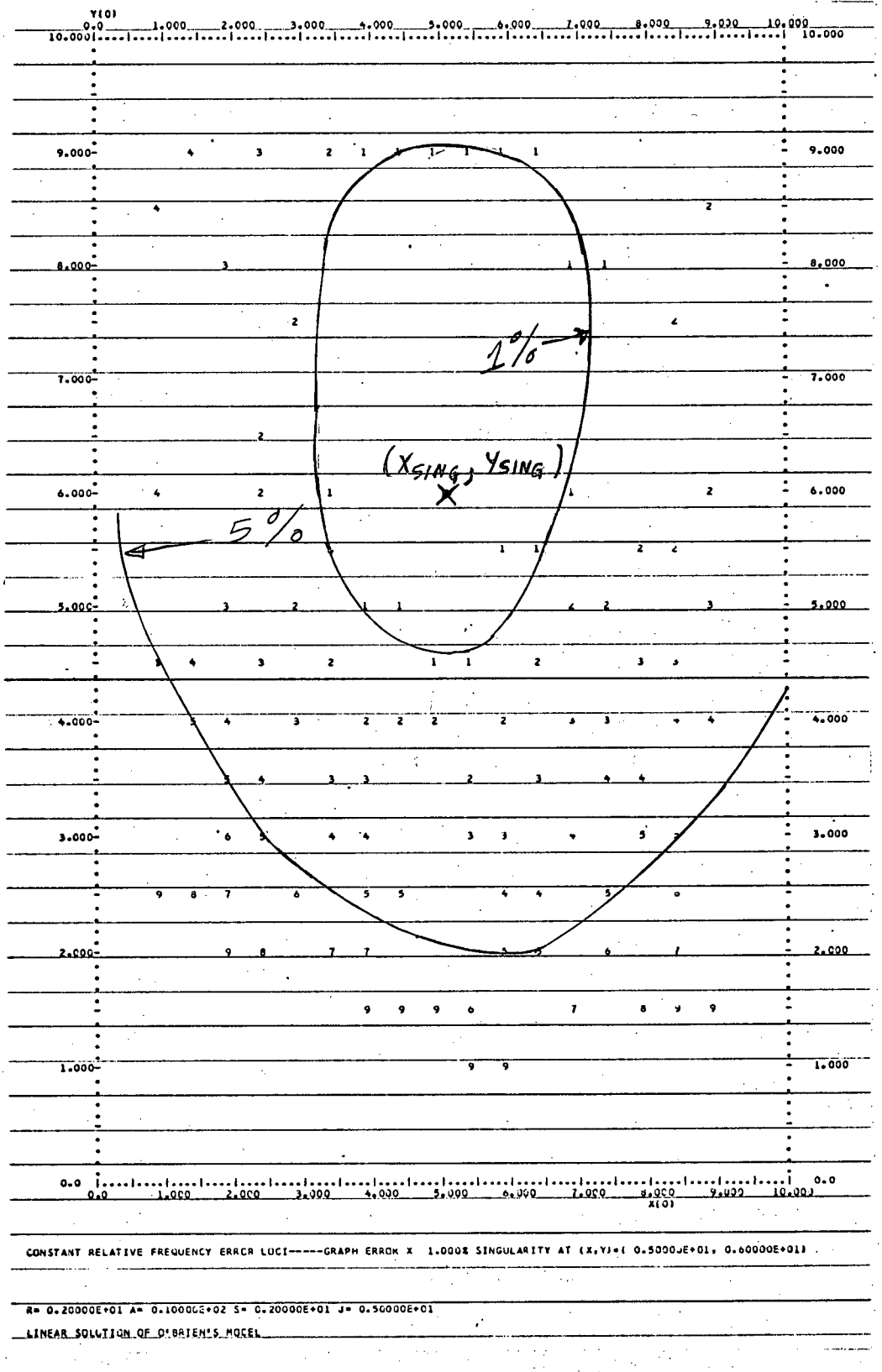

Fig. 2.30 O'Brien's Model Linear Solution Frequency Error Loci

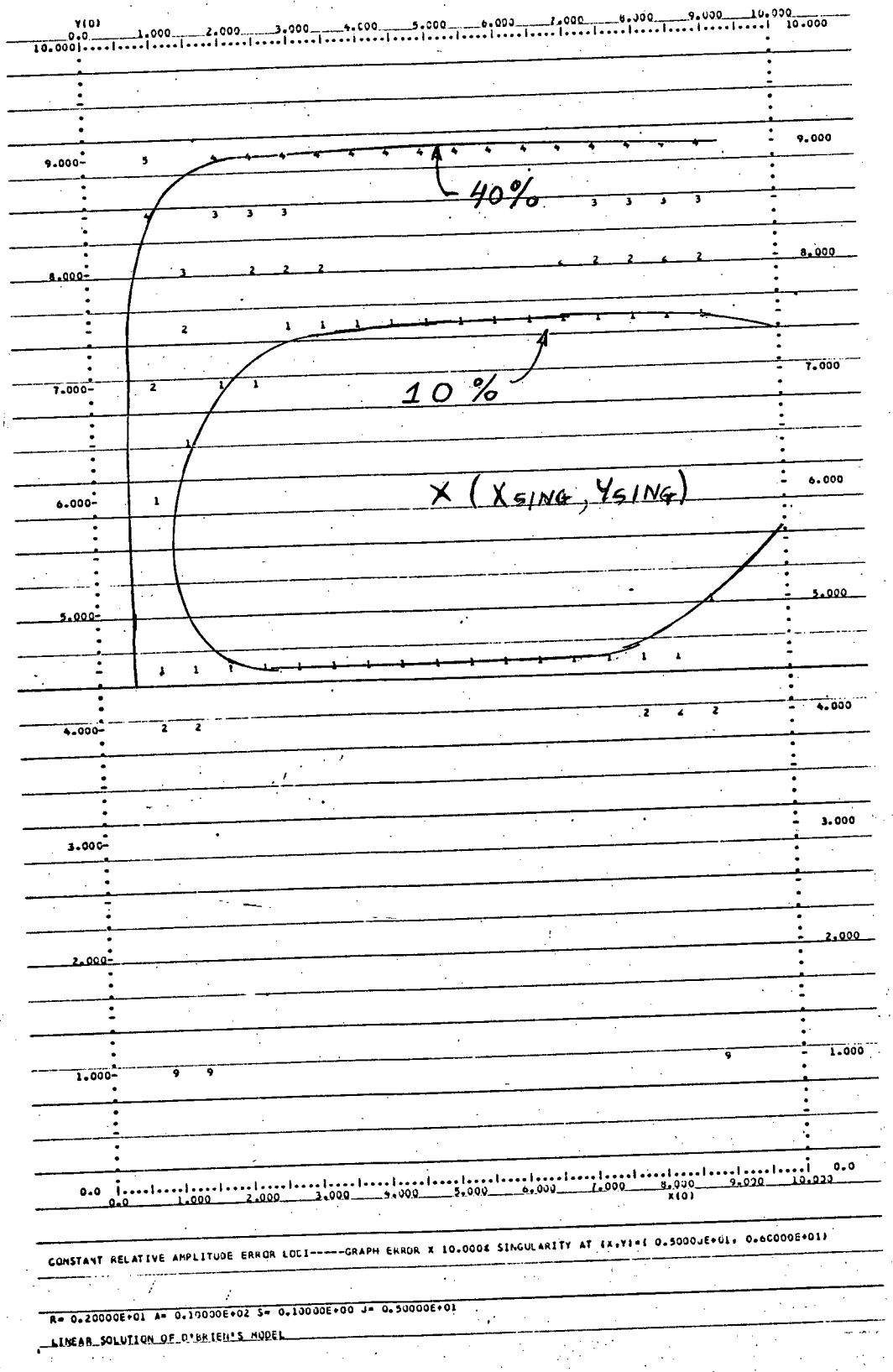

Fig. 2.31 O'Brien's Model Linear Solution Amplitude Error Loci

singular points, time constant and frequency of the solution. For some combinations of parameters, some terms in the individual a_{ij}'s may be negligible, or may be dominant. Thus, the user may readily determine which components of the solution will be sensitive or insensitive to variations in a given parameter without resorting to guesswork in computer simulations.

These solutions provide great insight into the system behaviour, and yield a basis on which more refined solutions are constructed in the following chapters.

CHAPTER THREE

EQUIVALENT LINEARIZATION SOLUTION OF ADVANCED MODELS

3.1 Introduction

A number of techniques were used in an attempt to develop solutions that were acceptable over a wider range of initial conditions than the linear solutions discussed in Chapter two. A brief discussion of the general formulation of nonlinear differential equations is necessary for comprehension of the nature of the problems encountered here.

Perturbation methods for approximating the solution of nonlinear differential equations have been studied (see Nayfeh 42 & Boguluibov 5) often took a form (such as $\ddot{x} + \omega^2 x + \varepsilon f(\dot{x},x) = 0$) in which the magnitude of the nonlinearity was controlled by a small parameter ε. Thus when $\varepsilon \to 0$, the differential equation degenerated to one that was solvable in terms of standard trigonometric functions or some other special functions, such as the elliptic functions (see Barkham 2 & 3). The frequency of the solution was usually readily discernable. The techniques used to approximate the solution when $\varepsilon \neq 0$ were such that the solution would degenerate to the exact solution when ε was set to zero.

Turning to the ecological models at hand, several important points should be emphasized. First of all, in the absence of nonlinear terms, the differential equation's behaviour usually becomes exponential in nature (often unstable), instead of oscillatory, due to a lack of cross coupling terms. Secondly, there is no small parameter ε that governs the magnitude of the nonlinearity in both equations. Third, the nonlinearities involved are not small perturbations of a linear system, but large ones that determine

the qualitative behaviour of the systems. It is these factors that caused many of the previously developed techniques for nonlinear differential equations to be of little use for the cases at hand. The above information was obtained by much trial and error while working with the VGW model as a prototype.

A brief summary of the techniques that were applied to little avail is given below. The well known perturbation series techniques with $x(t) = \sum_i \varepsilon^i x_i(t)$ was tried (see also Dutt 15 & 16). A variety of ideas for artificially inserting a parameter ε (and then setting $\varepsilon = 1$) were tried, as well as means of adding in linear cross coupling terms to produce oscillations in the case of negligible nonlinearities. These methods yielded first order solutions that were several orders of magnitude too large. The techniques of Krylov-Boguluibov (KB) were modified to handle pairs of first order differential equations. This method failed due to a lack of a parameter ε, and due to a lack of oscillations in the absence of nonlinearities. The averaging techniques presented by Lin(32) are a modification of the KB method, and suffer the same problems as the KB method. A slight variation of Van der Pol's method was applied to the Volterra-Gause-Witt model. The results were not as good as those obtained for the linear solution, and thus do not justify a lengthy description of the convoluted method of solution.

3.2 The Method of Equivalent Linearization

We now turn our attention to the next method of solution which provided good results. The method of equivalent linearization is a means of approximating the solutions of non-linear differential equations, and was originally developed for second order systems by Krylov and Boguluibov. The extension to first order coupled systems is sketchily described by Lin (32).

A complete explanation and derivation is given below.

We start with the system

$$\dot{x} = F(x,y)$$

$$\dot{y} = G(x,y)$$

If the singularity of interest is nonzero, we translate the variables to the singular point so that the origin of the phase plane is now the singular point of interest. This is done to reduce the complexity of the algebra which follows. We wish to approximate the original differential equation by a linear differential equation of the form:

$$\dot{x} = a_{11}x - a_{12}y$$

$$\dot{y} = a_{21}x + a_{22}y$$

whose coefficients a_{ij} will be determined shortly. The solution of the linear differential equation is given in section 2.2.

As a criterion for choosing the a_{ij}, we decide to minimize the mean square derivative error (as only derivatives are available) over one period between the original system and the linear system. For the one period the linear system is equivalent to the original nonlinear differential equation, and hence the name of the method. For quasilinear differential equations, the linear description of the original system will continue to be valid after the initial period. Thus we minimize the functional J, with respect to the a_{ij}, where J is given by

$$J = \frac{1}{2\pi} \int_0^{2\pi} ((F(x,y)-a_{11}x + a_{12}y)^2 + (G(x,y)-a_{21}x-a_{22}y)^2)d\theta$$

For the minimum of J, we require that

$$\frac{\partial J}{\partial a_{11}} = \frac{\partial J}{\partial a_{12}} = \frac{\partial J}{\partial a_{21}} = \frac{\partial J}{\partial a_{22}} = 0$$

Upon computing the above partial derivatives, we obtain:

$$\frac{\partial J}{\partial a_{11}} = \frac{1}{2\pi} \int_o^{2\pi} (F(x,y) - a_{11}x + a_{12}y)x \, d\theta = 0$$

$$\frac{\partial J}{\partial a_{12}} = \frac{1}{2\pi} \int_o^{2\pi} (F(x,y) - a_{11}x + a_{12}y)y \, d\theta = 0$$

$$\frac{\partial J}{\partial a_{21}} = \frac{1}{2\pi} \int_o^{2\pi} (G(x,y) - a_{21}x - a_{22}y)x \, d\theta = 0$$

$$\frac{\partial J}{\partial a_{22}} = \frac{1}{2\pi} \int_o^{2\pi} (G(x,y) - a_{21}x - a_{22}y)y \, d\theta = 0$$

The above integrals will give two sets of two equations in two unknowns, which must be solved for the a_{ij}'s. The above integrals cannot be solved exactly as the solutions x(t) & y(t) are not know. Hence we must resort to approxmimations that will allow the integrals to be evaluated. We make the assumption that over one period of the solution, the envelope of the solution is slowly changing and may be taken as a constant. The solutions may thus be approximated by $x = r_1 \cos\theta$ & $y = r_2 \sin\theta$, over one period. Inserting these approximate solutions in the first of the four above integrals, we obtain:

$$\frac{\partial J}{\partial a_{11}} = \frac{1}{2\pi} \int_o^{2\pi} (F(r_1\cos\theta, r_2\sin\theta) - a_{11}r_1\cos\theta + a_{12}r_2\sin\theta)r_1\cos\theta \, d\theta = 0$$

$$\therefore \quad \frac{1}{2\pi} \int_o^{2\pi} F(r_1\cos\theta, r_2\sin\theta)r_1\cos\theta \, d\theta = \frac{a_{11}r_1^2}{2}$$

$$\text{or} \quad a_{11} = \frac{1}{\pi r_1} \int_o^{2\pi} F(r_1\cos\theta, r_2\sin\theta)\cos\theta \, d\theta$$

Similarly, we obtain:

$$a_{12} = \frac{-1}{\pi r_2} \int_o^{2\pi} F(r_1\cos\theta, r_2\sin\theta)\sin\theta \, d\theta$$

$$a_{21} = \frac{1}{\pi r_1} \int_o^{2\pi} G(r_1\cos\theta, r_2\sin\theta)\cos\theta \, d\theta$$

$$a_{22} = \frac{1}{\pi r_2} \int_o^{2\pi} G(r_1\cos\theta, r_2\sin\theta)\sin\theta \, d\theta$$

We now turn our attention to the constants r_1 & r_2. The choice of the approximate solution says that we are assuming the translated equivalent linear differential equation to be of the form $\dot{x} = -a_{12}y$ and $\dot{y} = a_{21}x$ over one period. This has a solution

$$x = r_1 \cos(\omega t + \phi_1)$$

$$y = r_2 \sin(\omega t + \phi_2) \qquad \text{where} \quad \omega = \sqrt{a_{12}\, a_{21}}$$

$$r_1 = \sqrt{(x_o - x_{sing})^2 + \frac{a_{12}}{a_{21}} (y_o - y_{sing})^2}$$

$$r_2 = \sqrt{\frac{a_{21}}{a_{12}} (x_o - x_{sing})^2 + (y_o - y_{sing})^2}$$

$$\phi_1 = \tan^{-1} \left(\frac{(y_o - y_{sing})\, a_{12}}{(x_o - x_{sing})\, \omega} \right)$$

$$\phi_2 = \tan^{-1} \left(\frac{(y_o - y_{sing})\, a_{21}}{(x_o - x_{sing})\, \omega} \right)$$

We now have all the equations necessary for the computation of the a_{ij}. We note that r_1 and r_2 are dependant only on a_{12} and a_{21}. Thus, in the equations for a_{12} and a_{21}, the same variables will probably appear on the right handside in the integrals, to give two nonlinear algebraic equations in two unknowns, a_{12} and a_{21} which must be solved. Once the coefficients a_{12} and a_{21} have been computed, the coefficients a_{11} and a_{22} are quickly determined, as the right hand sides of the equations for these coefficients will contain at most, only a_{12} and a_{21}. In general, we see that the coefficients a_{ij} depend on the initial conditions of the differential equation, which is an effect that does not occur in linear differential equations. It should be noted that the minimum mean square error criterion will correct large derivative errors (which occur near the time origin for dampled oscillations) while neglecting smaller errors. Thus we may expect the solution to be best near the time origin.

We now have a second technique for obtaining a literal parameter dependant solution (which will probably depend nonlinearly on the initial conditions of the system) of nonlinear differential equation models of ecological systems. We now proceed to apply this method to the models discussed in chapter two.

3.3 Equivalent Linearized Solution of the Volterra-Gause-Witt Model

The first model we wish to apply the technique of equivalent linearization to, is the VGW model. We begin by translating the singular point $(x_{sing}, y_{sing}) = (\gamma/\delta, (\alpha - \lambda\gamma/\delta)/\beta)$ to (0,0). The differential equations become:

$$\dot{x} = \frac{-\lambda\gamma}{\delta} x - y\frac{\beta\gamma}{\delta} - \beta xy - \lambda x^2 = F(x,y)$$

$$\dot{y} = \delta xy + \frac{(\alpha\delta - \lambda\gamma)}{\beta} x = G(x,y)$$

We compute the a_{ij} to obtain:

$$a_{11} = -\lambda\gamma/\delta \qquad a_{12} = \beta\gamma/\delta$$

$$a_{21} = (\alpha\delta - \lambda\gamma)/\beta \qquad a_{22} = 0$$

which are exactly the same as those for the linear solution obtained in Chapter Two. The equivalent linear a_{ij} of this very simple model are independant of initial conditions. Thus we may consult the results of section 2.4 for the evaluation of this solution. We now proceed onwards to the second model discussed in Chapter Two.

3.4 Equivalent Linearization Solution of Holling's Model

The next model we wish to study is Hollings (see section 2.5) model. We start by translating the singularity $(x_{sing}, y_{sing}) = (J, (J+A)r(1-J/K))$ to (0,0) to obtain:

$$\dot{x} = xr + Jr - (x^2+J^2+2Jx)\frac{r}{K} - \frac{(xy + x(J+A)r(1-J/K)+Jy+(J+A)r(1-J/K)}{A + J + x}$$

$$\dot{y} = sA\,\frac{(xy + x\,(J+A)r(1-J/K))}{(J+A)(J+A+x)}$$

Before we can evaluate the a_{ij}, we must pause to obtain some results in calculus. Using the method of contour integration of complex variables (see Wayland 56), we evaluate an integral needed in the computation of the a_{ij}.

$$\int_0^{2\pi} \frac{e^{jnx}\,dx}{(p + q\cos x)} = \frac{2\pi}{\sqrt{p^2 - q^2}} \left(\sqrt{\frac{p^2}{q^2} - 1} - \frac{p}{q} \right)^n, \quad p > q$$

$$\therefore \int_0^{2\pi} \frac{\sin nx\,dx}{(p+q\cos x)} = 0, \quad p > q$$

and $$\int_0^{2\pi} \frac{\cos nx\,dx}{(p+q\cos x)} = \frac{2\pi}{\sqrt{p^2 - q^2}} \left(\sqrt{\frac{p^2}{q^2} - 1} - \frac{p}{q} \right)^n, \quad p > q$$

We may now compute the a_{ij} as follows:

$$a_{11} = r(1-2J/K) - (J+A)r(1-J/K)\,\frac{\{1+(\sqrt{\frac{(J+A)^2}{r_1^2} - 1} - \frac{(J+A)}{r_1})^2\}}{\sqrt{(J+A)^2 - r_1^2}}$$

$$- \frac{2J\,(J+A)r(1-J/K)}{r_1\sqrt{(J+A)^2 - r_1^2}} \left(\sqrt{\frac{(J+A)^2}{r_1^2} - 1} - \frac{(J+A)}{r_1} \right)$$

$$a_{12} = \frac{r_1}{2}\left\{ \sqrt{\frac{(J+A)^2}{r_1^2} - 1} - \frac{(J+A)}{r_1} - \left(\sqrt{\frac{(J+A)^2}{r_1^2} - 1} - \frac{(J+A)}{r_1} \right)^3 \right\}$$

$$+ J\left\{1 - \left(\sqrt{\frac{(J+A)^2}{r_1^2} - 1} - \frac{(J+A)}{r_1} \right)^2 \right\}$$

$$\sqrt{(J+A)^2 - r_1^2}$$

$$a_{21} = \frac{sAr(1-J/k)}{\sqrt{(J+A)^2-r_1^2}} \left\{ 1 + \left(\sqrt{\frac{(J+A)^2}{r_1^2} - 1} - \frac{(J+A)}{r_1} \right)^2 \right\}$$

$$a_{22} = \frac{sAr_1}{2(J+A)\sqrt{(J+A)^2-r_1^2}} \left\{ \sqrt{\frac{(J+A)^2}{r_1^2} - 1} - \frac{(J+A)}{r_1} \right.$$

$$\left. - \left(\sqrt{\frac{(J+A)^2}{r_1^2} - 1} - \frac{(J+A)}{r_1} \right)^3 \right\}$$

The equations for a_{12} & a_{21} are not yet in usable form. To solve for a_{12} & a_{21}, we define $\xi = a_{12}/a_{21}$. Thus we have $r_1 = \sqrt{(x_o - x_{sing})^2 - \xi(y_o - y_{sing})^2}$

By taking the ratio of the equations for a_{12} & a_{21}, we obtain an equation of the form $\xi = h(\xi)$, which we solve for ξ. We then back substitute to obtain the four parameters a_{ij}. We observe that as the initial conditions of the system tend to the singular point of interest, the coefficients a_{ij} tend to the values obtained for the linear solutions. Computer simulation has shown that we may approximate the solution of the equation for ξ by the ratio of the linear solution's a_{12} & a_{21}, ie: $\xi = \frac{J}{sAr(rJ/K)}$. This does not affect the solution accuracy to any noticable degree. Thus we have been able to simplify the solution somewhat, and still retain the effect of the a_{ij} being influenced by the initial conditions of the differential equations. This completes the equivalent linearization solution of Holling's model.

3.5 Simulation Study of Holling's Model

We now wish to evaluate the equivalent linearization solution of Holling's model. The equivalent linearization solutions were computed for the same parameters and initial conditions as the linear solution (see section 2.7). The same samples of time plots and phase plane curves are

given in figures 3.1 to 3.6. The corresponding amplitude and frequency error loci are given in figures 3.7 to 3.9. We note that we have an improvement in size of the amplitude error loci, but this is at the expense of the frequency error loci. Thus, as a solution to this apparent trade-off between amplitude and frequency error, we use the amplitude of the equivalent linearized solution, and before computing the solution, we substitute in the frequency of the linear solution, so as to obtain the maximum benefit of both methods. Hence we obtain a solution that is an improvement over the classical linear solution. We now proceed onwards to study the next ecological model discussed in Chapter Two.

3.6 Equivalent Linearization Solution of Rosenzweig's Model

The third model we wish to study is Rosenzweig's (see section 2.8) model. We begin by translating the singularity $(x_{sing}, y_{sing}) = (J, \frac{rJ(1-J/K)}{b(1-\exp(-cJ))})$ to (0,0) to obtain:

$$\dot{x} = rJ(1-J/K) + rx(1-2J/K) - x^2 r/K - b(y + \frac{rJ(1-J/K)}{b(1-e^{-cJ})})\ (1-e^{-c(J+x)})$$

$$\dot{y} = s(y + \frac{Jr(1-J/K)}{b(1-e^{-cJ})})\ (e^{-cJ} - e^{-c(J+x)})$$

Before we can evaluate the a_{ij}, we must pause to evaluate the following intergrals.

$$\int_0^{2\pi} \sin(nx)\, e^{a\cos x}\, dx = 0 \qquad \text{(by symmetry)}$$

$$I_n = \int_0^{2\pi} \cos(nx)\, e^{a\cos x}\, dx = \int_0^{2\pi} \cos(nx) \{ \sum_{K=1}^{\infty} \frac{a^{2K}}{(2K)!} [\frac{1}{2^{2K}} \binom{2K}{K} + \frac{1}{2^{2K-1}}(\cos 2Kx + \ldots + \binom{2K}{K-1}\cos 2x)] + \sum_{K=1}^{\infty} \frac{a^{2K-1}}{(2K-1)!\,2^{2K-2}} [\cos(2K-1)x + \ldots + \binom{2K-1}{K-1}\cos x]\} dx$$

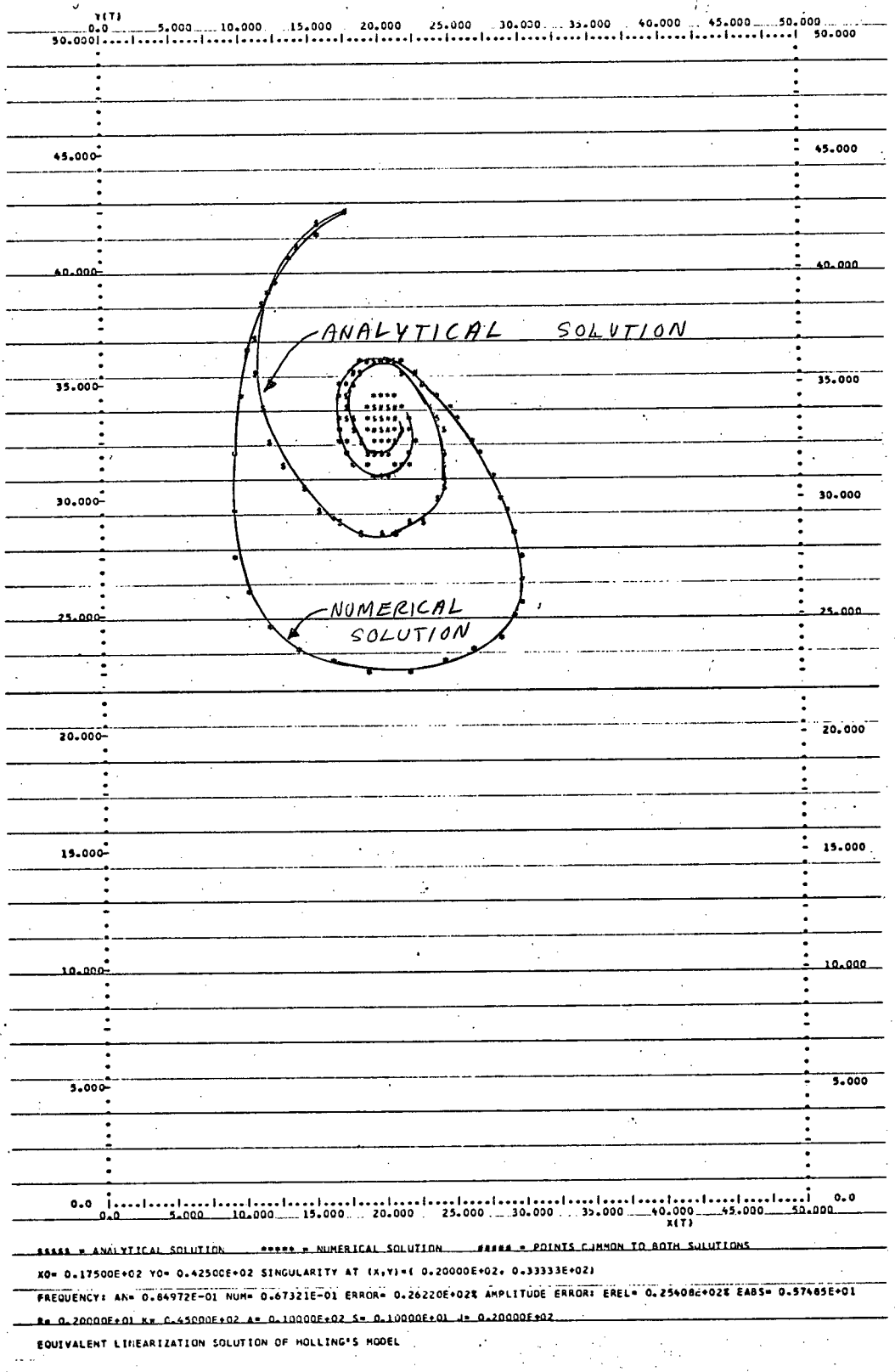

Fig. 3.1 Holling's Model Equivalent Linearization Solution for $(x_o, y_o) = (17.5, 42.5)$

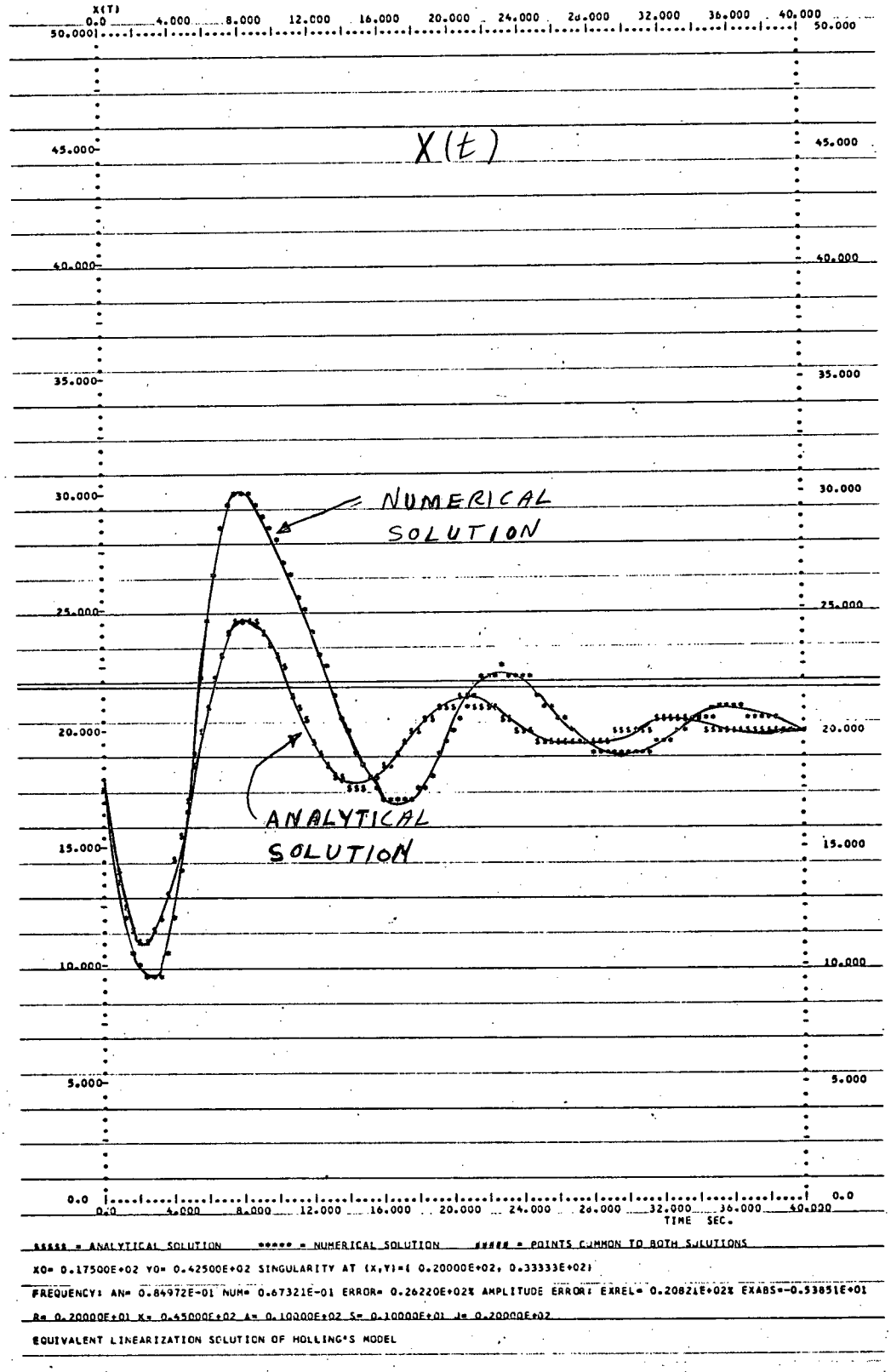

Fig. 3.2 Holling's Model Equivalent Linearization Solution for $(x_o, y_o)=(17.5, 42.5)$

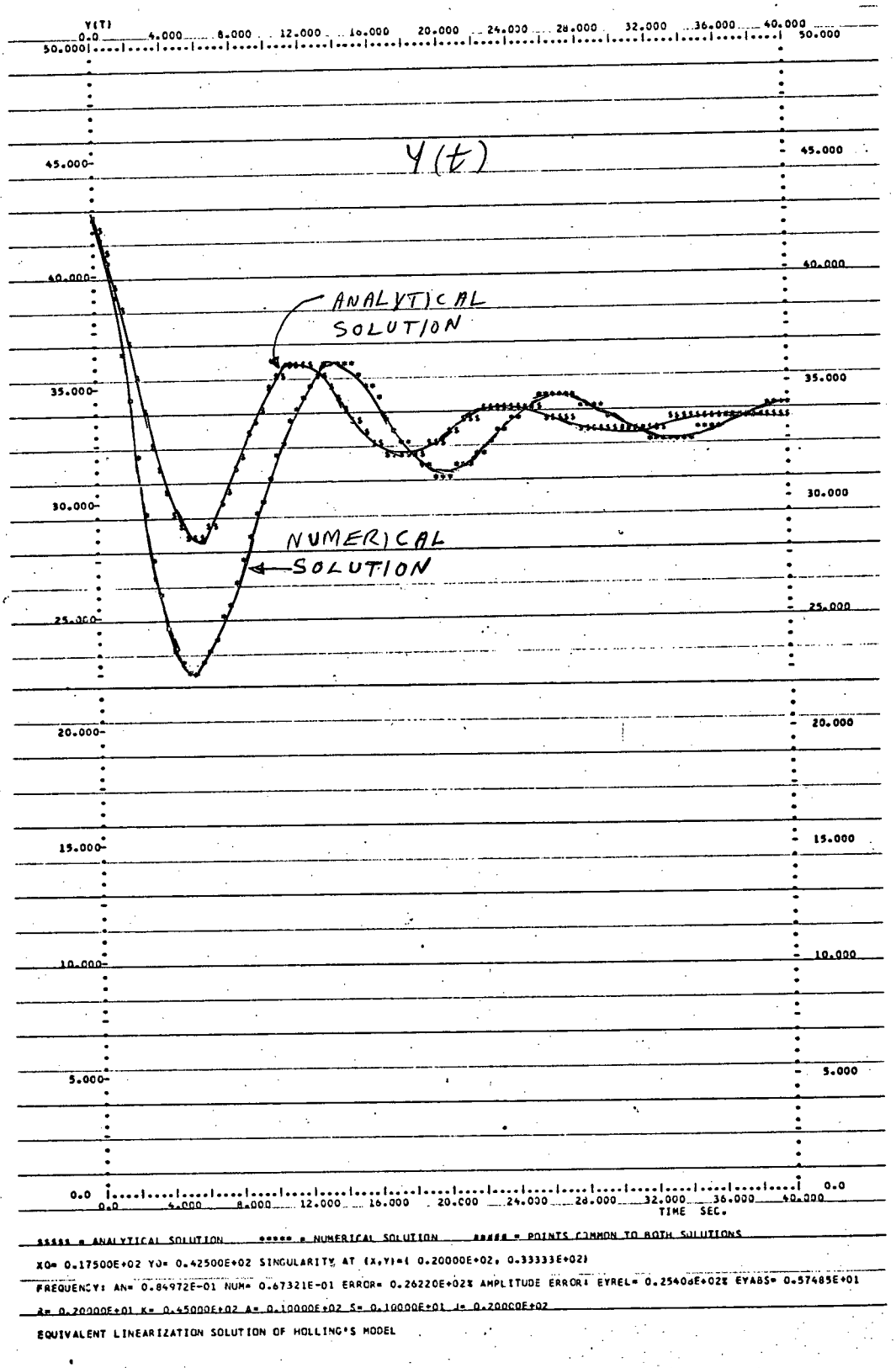

Fig. 3.3 Holling's Model Equivalent Linearization Solution for $(x_o, y_o)=(17.5, 42.5)$

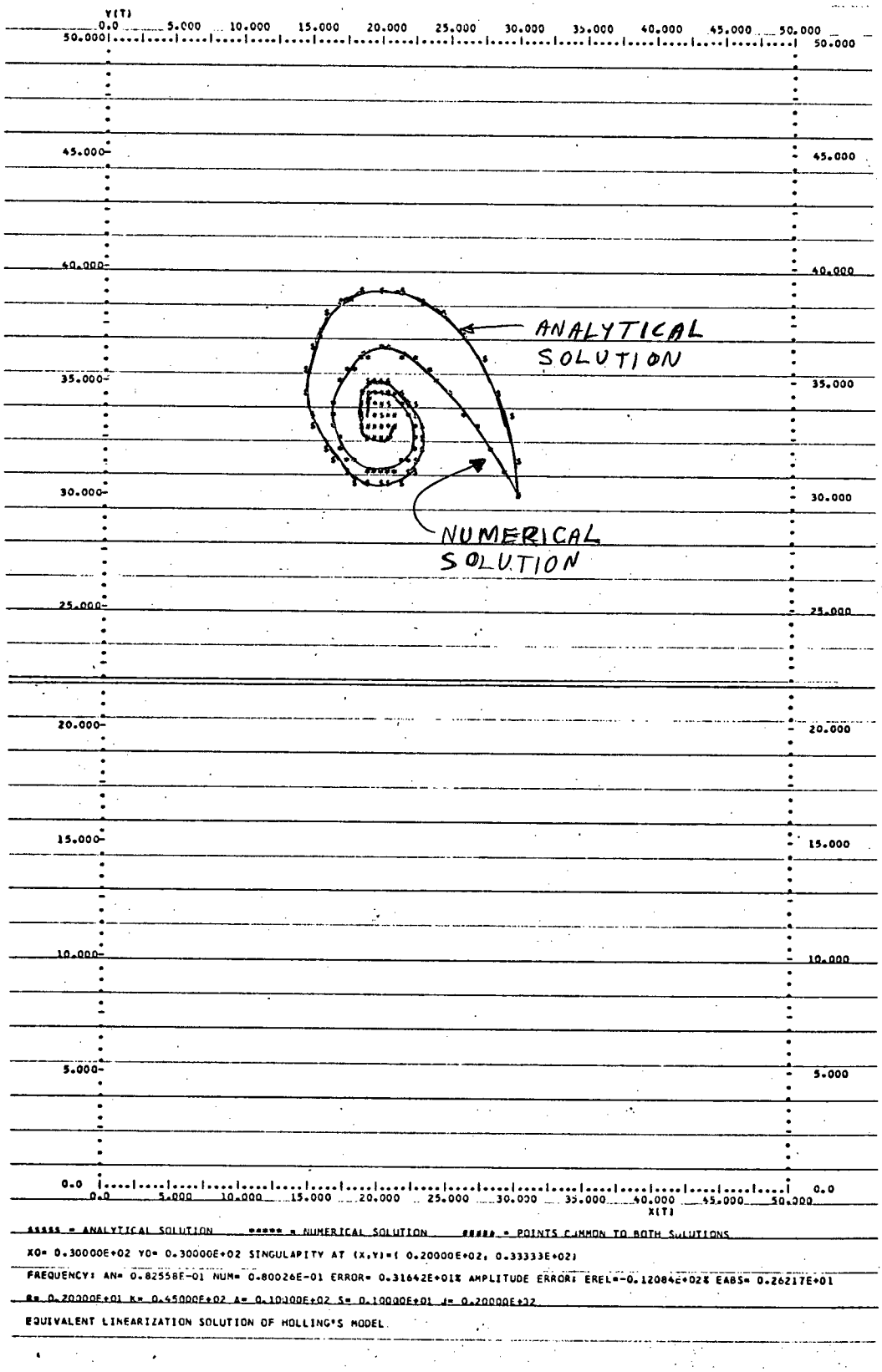

Fig. 3.4 Holling's Model Equivalent Linearization Solution for $(x_o, y_o)=(30,30)$

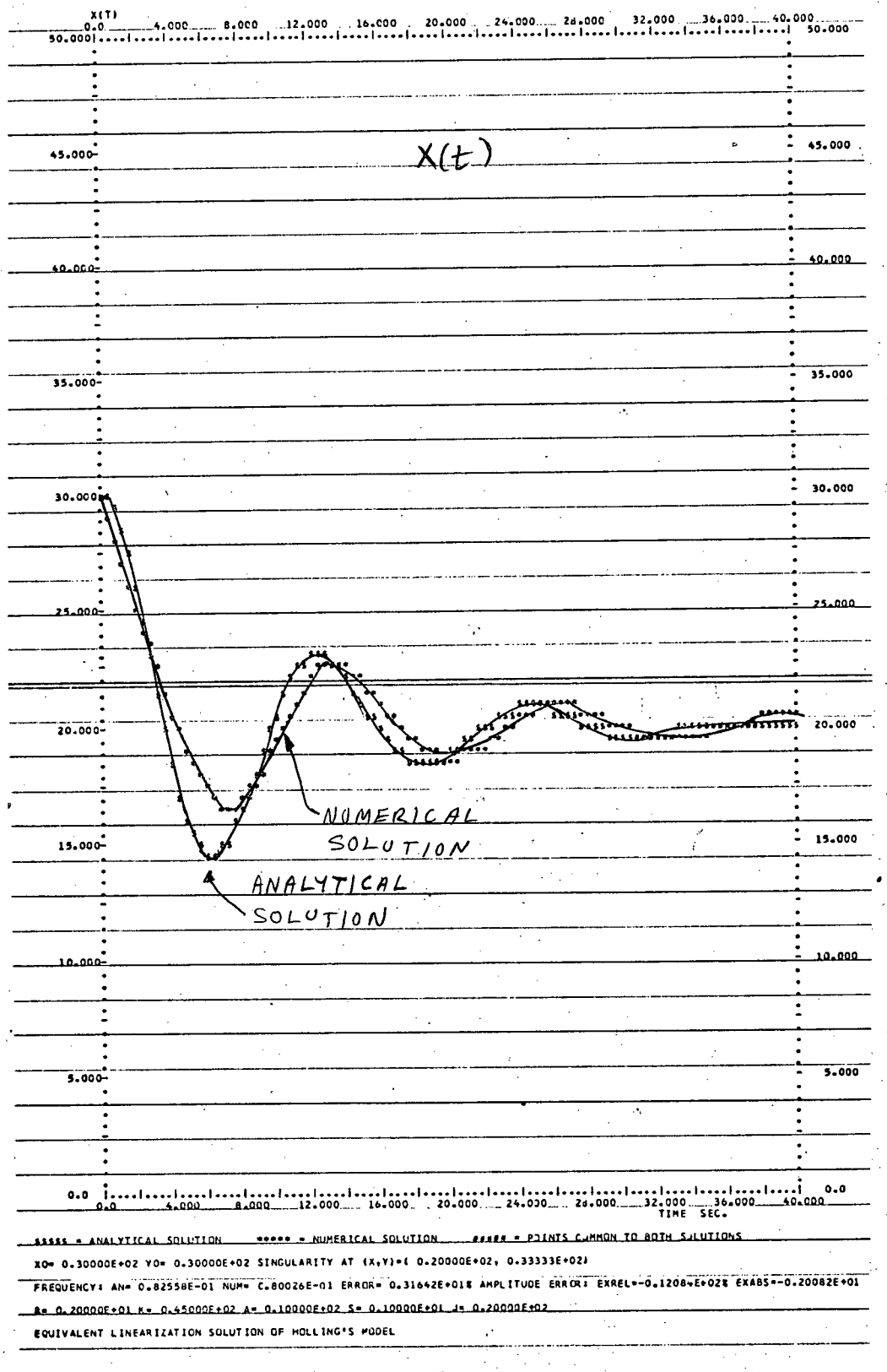

Fig. 3.5 Holling's Model Equivalent Linearization Solution for $(x_o, y_o)=(30,30)$

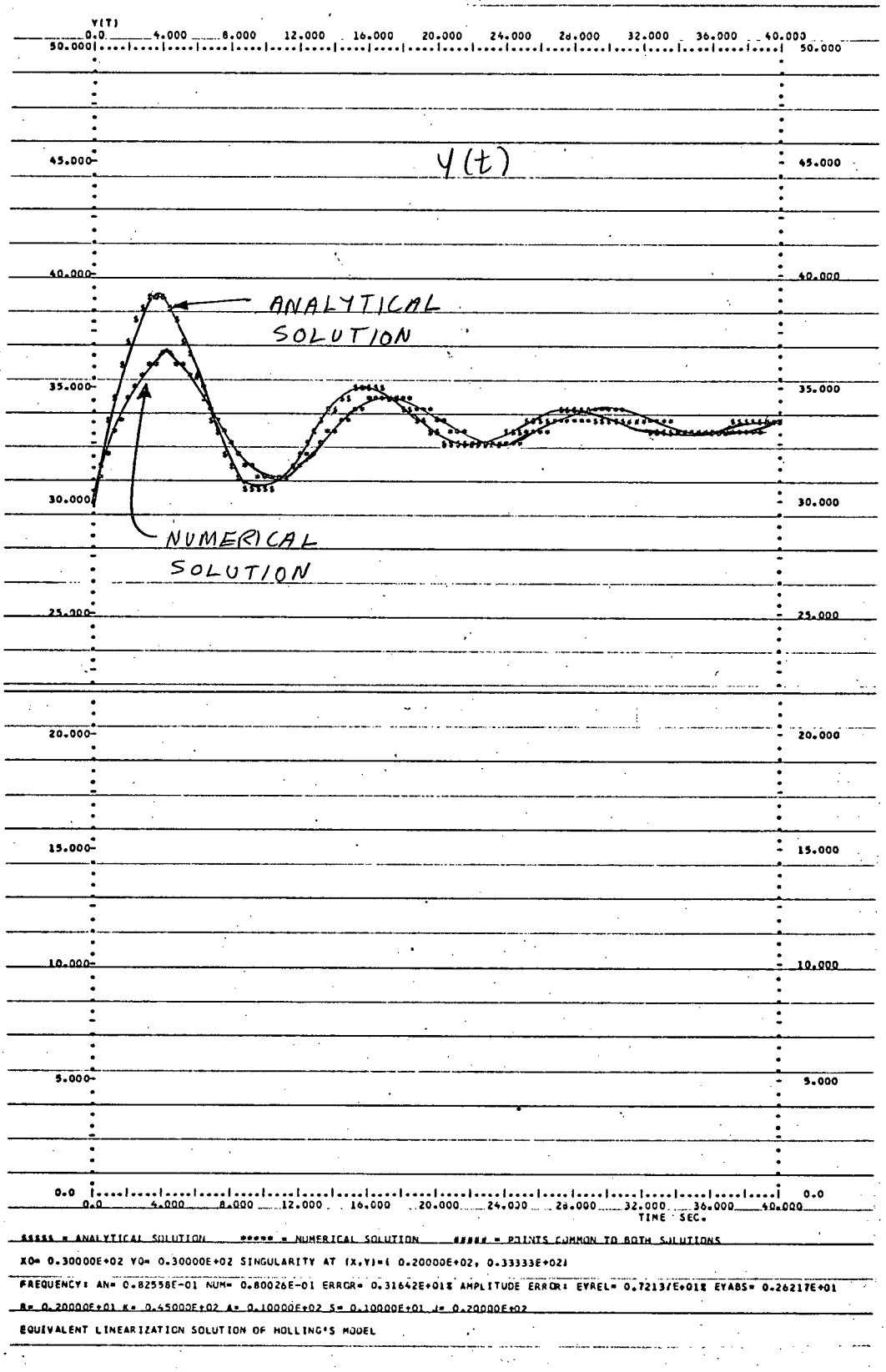

Fig. 3.6 Holling's Model Equivalent Linearization Solution for $(x_o, y_o)=(30,30)$

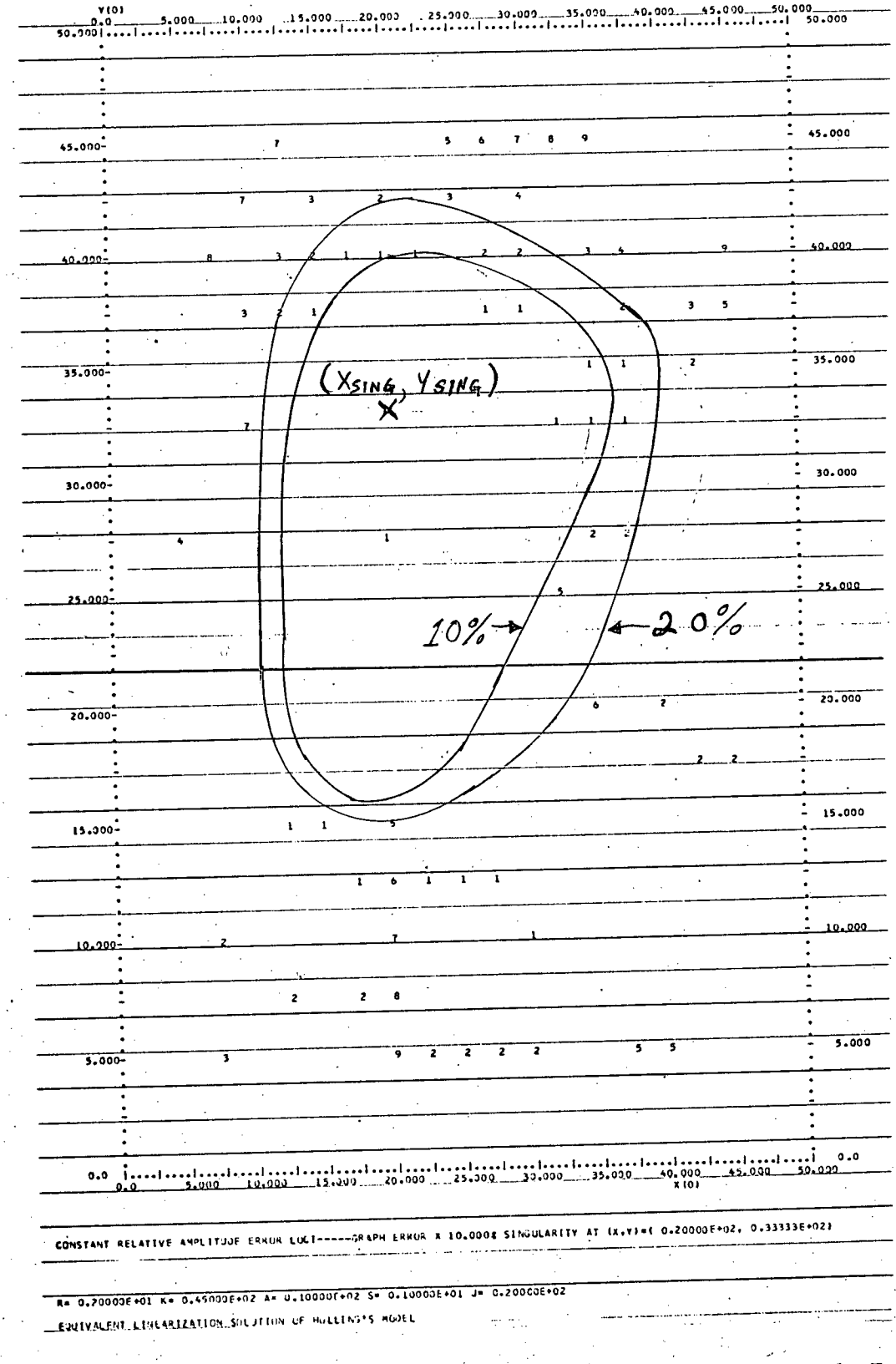

Fig. 3.7 Holling's Model Equivalent Linearization Solution Amplitude Error Loci

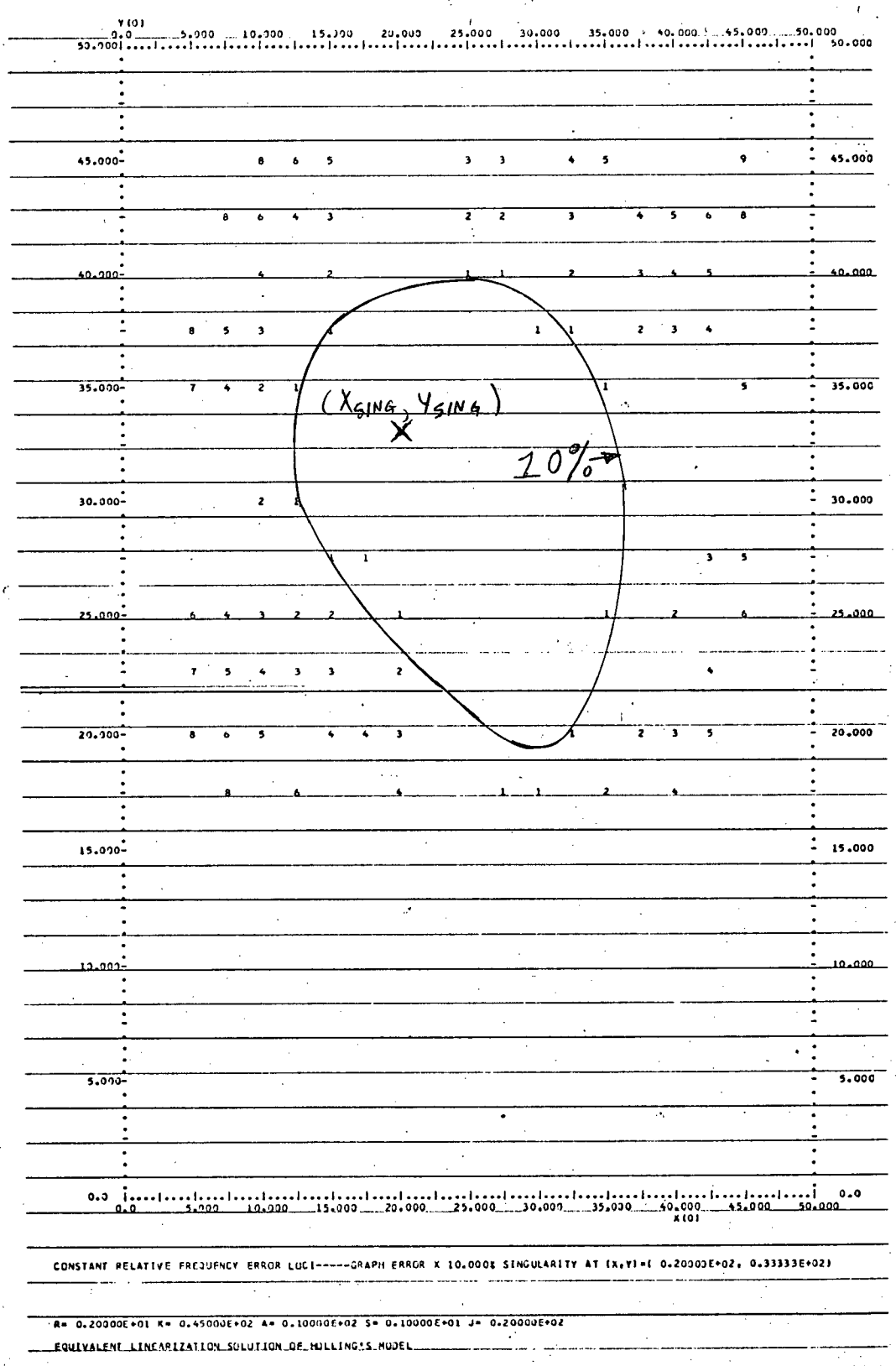

Fig. 3.8 Holling's Model Equivalent Linearization Solution Frequency Error Loci

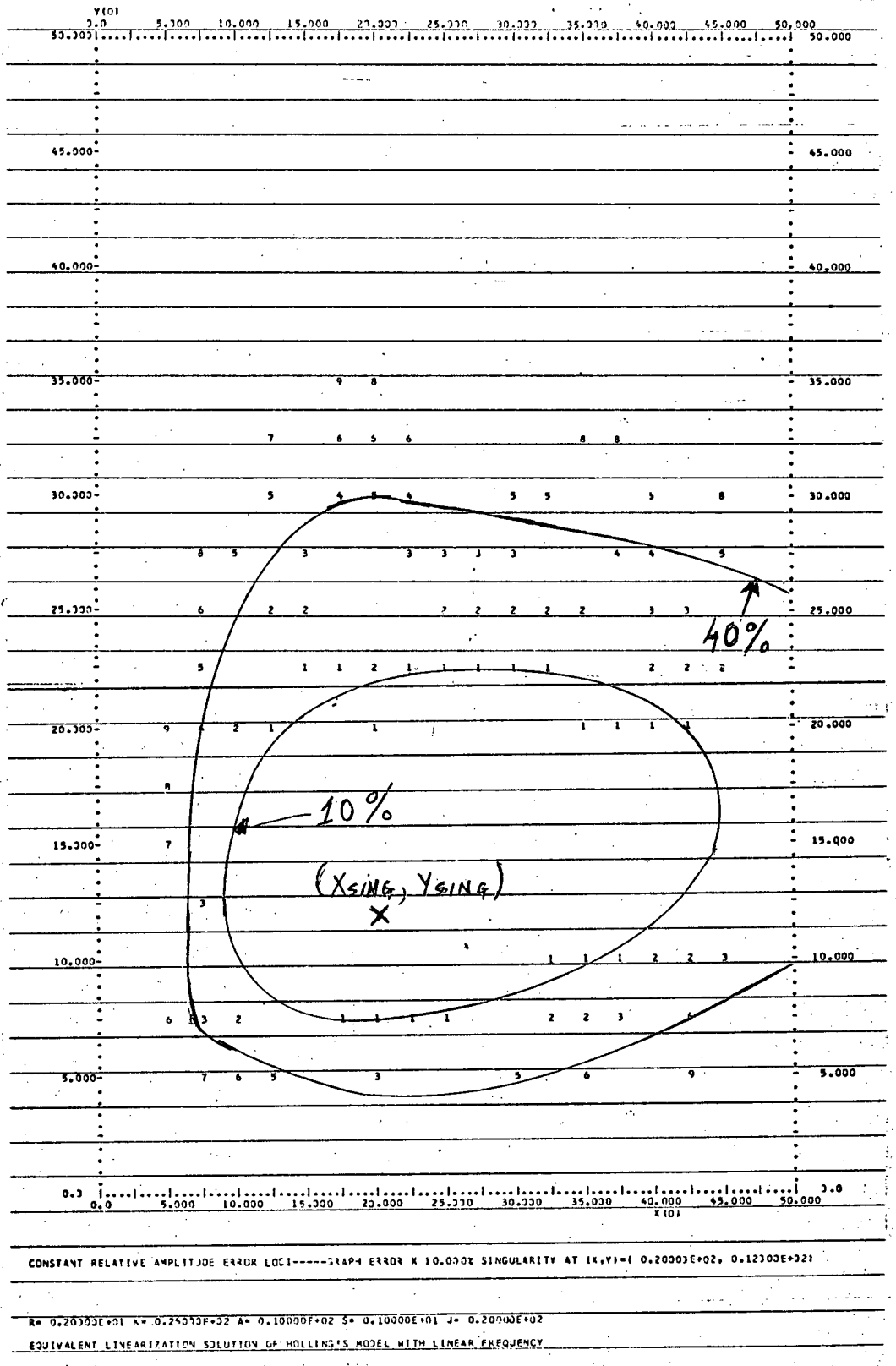

Fig. 3.9 Holling's Model Equivalent Linearization Solution Amplitude Error Loci

We will need the values of I_n for n = 0,1,2. We obtain:

$$n = 0 \qquad I_o = 2\pi\left[1 + \sum_{K=1}^{\infty} \frac{a^{2K}}{(2K)!\,2^{2K}} \binom{2K}{K}\right]$$

$$n = 1 \qquad I_1 = \pi \sum_{K=1}^{\infty} \frac{a^{2K-1}}{(2K-1)!\,2^{2K-2}} \binom{2K-1}{K-1}$$

$$n = 2 \qquad I_2 = \pi \sum_{K=1}^{\infty} \frac{a^{2K}}{(2K)!\,2^{2K-1}} \binom{2K}{K-1}$$

where $$\binom{K}{n} = \frac{K!}{n!(K-n!)}$$

We may now compute the a_{ij} as follows:

$$a_{11} = r(1-2J/K) - \frac{crJ(1-J/K)}{(e^{Jc}-1)}\left[1 + \sum_{K=1}^{\infty} \frac{(-cr_1)^{2K}}{2^{2K}(K+1)!K!}\right]$$

$$a_{12} = b - be^{-Jc}\left[1 + \sum_{K=1}^{\infty} \frac{(-cr_1)^{2K}}{2^{2K}(K+1)!K!}\right]$$

$$a_{21} = \frac{srJc(1-J/K)}{b(e^{Jc}-1)}\left[1 + \sum_{K=1}^{\infty} \frac{(-cr_1)^{2K}}{2^{2K}(K+1)!\ K!}\right]$$

$$a_{22} = se^{-Jc} - se^{-Jc}\left[1 + \sum_{K=1}^{\infty} \frac{(-cr_1)^{2K}}{2^{2K}(K+1)!\ K!}\right]$$

Simulation of the equations show that we may truncate the infinite series to one term if we have $|c| < 1$. As with Holling's model, we define $\xi = a_{12}/a_{21}$. This gives us a quadratic equation for ξ whose solution is given by

$$\xi = \frac{-a_1 + \sqrt{a_1^2 - 4a_2a_o}}{2a_2}$$

where $$a_2 = \frac{srJ(1-J/K)c^3}{8\,b(e^{Jc}-1)}\,(Y_o - Y_{sing})^2$$

$$a_1 = \frac{srJ(1-J/K)}{b(e^{Jc}-1)} \left(c + \frac{c^3}{8}(x_o - x_{sing})^2\right) + \frac{b\, e^{-Jc} c^2}{8} (Y_o - Y_{sing})^2$$

$$a_0 = b\, e^{-Jc} \left[1 + \frac{c^2}{8}(X_o - X_{sing})^2\right] - b$$

Thus we compute ξ, and then the a_{ij}, which completes our solution. As before, when the initial conditions tend to the singularity, the coefficients a_{ij} tend to the values obtained for the linear solution. This completes the equivalent linearization solution of Rosenzweig's model.

3.7 Simulation Study of Rosenzweig's Model

We now wish to evaluate the equivalent linearization solution of Rosenzweig's model. The equivalent linearization solutions were computed for the same parameters and initial conditions as the linear solution (see section 2.10). The corresponding amplitude and frequency error loci are shown in figures 3.10 to 3.12. We note that we have a substantial improvement in the size of the amplitude error loci, but this is again at the expense of the frequency error loci. Thus, for the complete solution, we proceed as with the case of Holling's model, by using the equivalent linearization solution amplitude and the linear solution frequency, and obtain the best of both worlds. Again, we have an improvement over the linear solution. We now proceed onwards to the fourth ecological model discussed in Chapter Two.

3.8 Equivalent Linearization Solution of O'Brien's Model

The last model to be studied is O'Brien's (see section 2.11) model. We begin by translating the singularity $(x_{sing}, y_{sing}) = (J, r(J+A)/J)$ to $(0,0)$ to obtain:

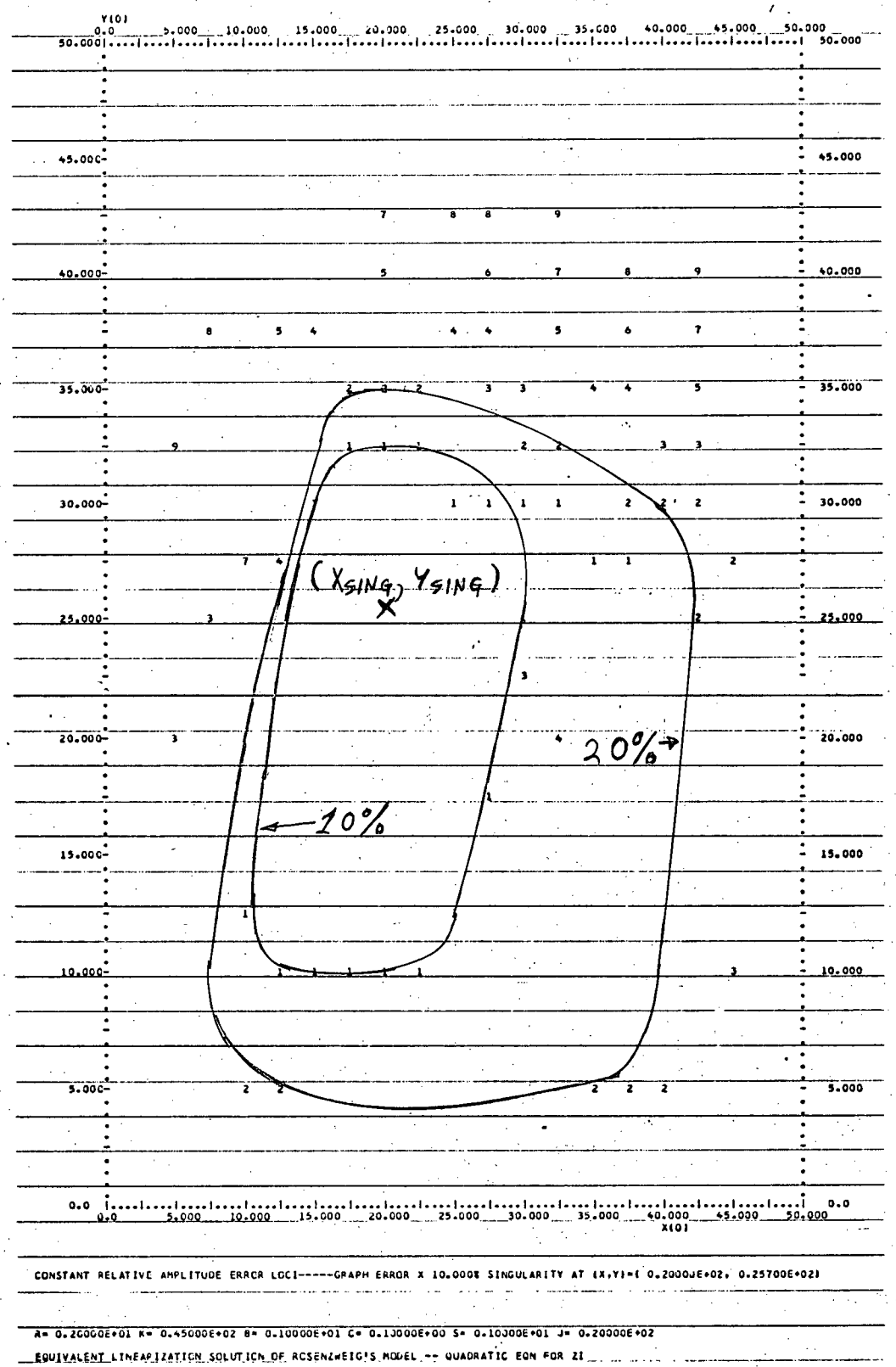

Fig. 3.10 Rosenzweig's Model Equivalent Linearization Solution Amplitude Error Loci

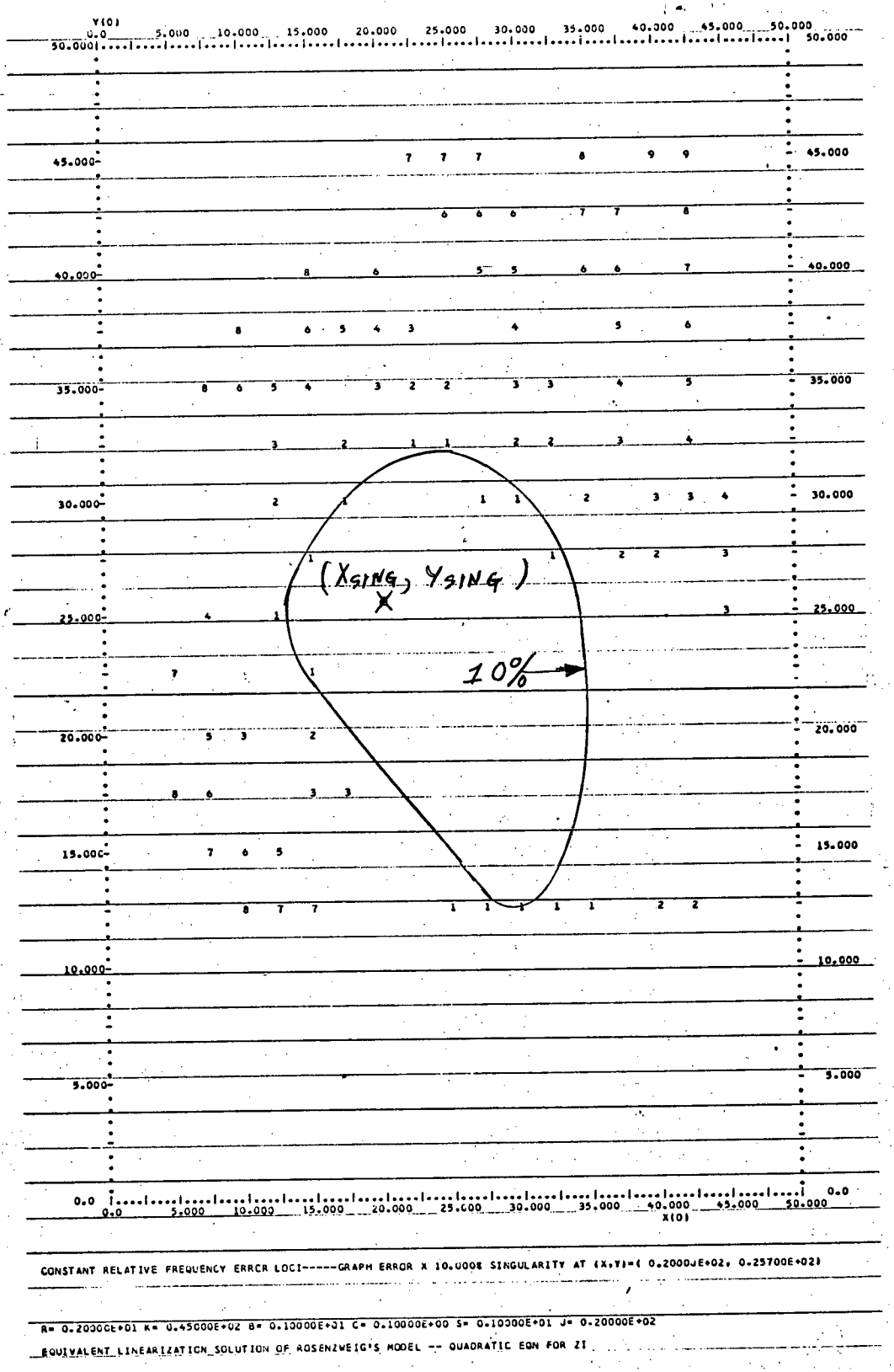

Fig. 3.11 Rosenzweig's Model Equivalent Linearization Solution Frequency Error Loci

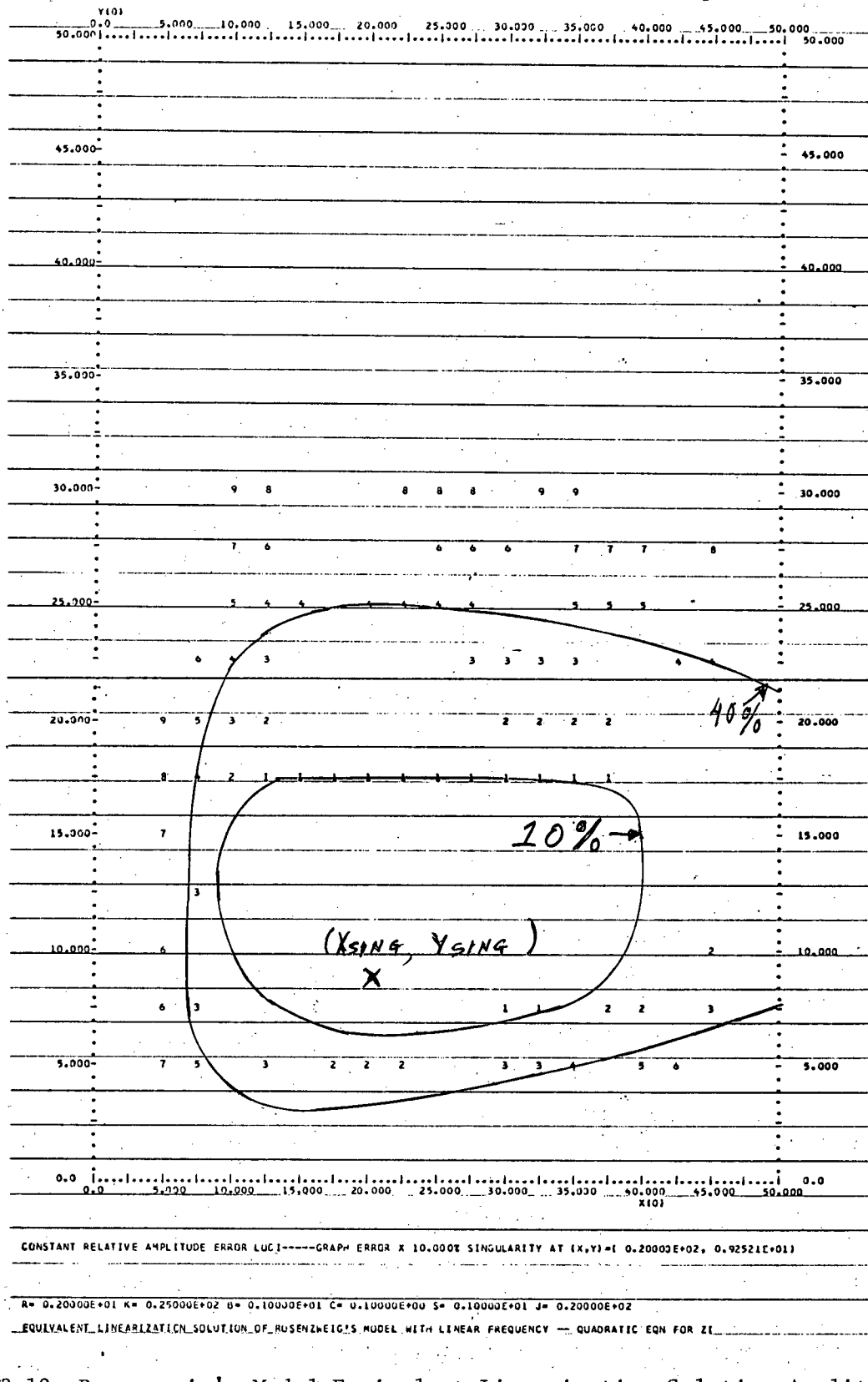

Fig. 3.12 Rosenzweig's Model Equivalent Linearization Solution Amplitude Error Loci

$$\dot{x} = r - \frac{(x+J)(y + r(J+A)/J)}{(J+A+x)}$$

$$\dot{y} = \frac{sAx(y + r(J+A)/J)}{(J+A)(J+A+x)}$$

We may now compute the a_{ij} as follows:

$$a_{11} = \frac{-2r(J+A)}{r_1\sqrt{(J+A)^2-r_1^2}}\left(\sqrt{\frac{(J+A)^2}{r_1^2} - 1} - \frac{(J+A)}{r_1}\right) - \frac{r(J+A)\left\{1+\left(\sqrt{\frac{(J+A)^2}{r_1^2} - 1} - \frac{(J+A)}{r_1}\right)^2\right\}}{\sqrt{(J+A)^2-r_1^2}}$$

The coefficients a_{12}, a_{21} & a_{22} are the same as for Holling's model. Again we may approximate the solution of equations for a_{12} & a_{21}, as previously described in section 3.4. As before, when the initial conditions tend to the singular point of interest, the coefficients a_{ij} tend to the values obtained for the linear solutions. This completes the equivalent linearization solution of O'Brien's model.

3.9 Simulation Study of O'Brien's Model

We now wish to evaluate the equivalent linearization solution of O'Brien's model. The equivalent linearization solutions were computed for the same parameters and initial conditions as the linear solutions (see section 2.13). The corresponding amplitude and frequency error loci are shown in figures 3.13 to 3.15. We note as before, we have an improvement in the size of the amplitude error loci, but again at the expense of the frequency error loci. Thus, as with the other solutions, we use the equivalent linearization solution amplitude and the linear solution frequency. Again, we have an improvement over the linear solutions. This completes our study and evaluation of the method of equivalent linearization of nonlinear differential equations.

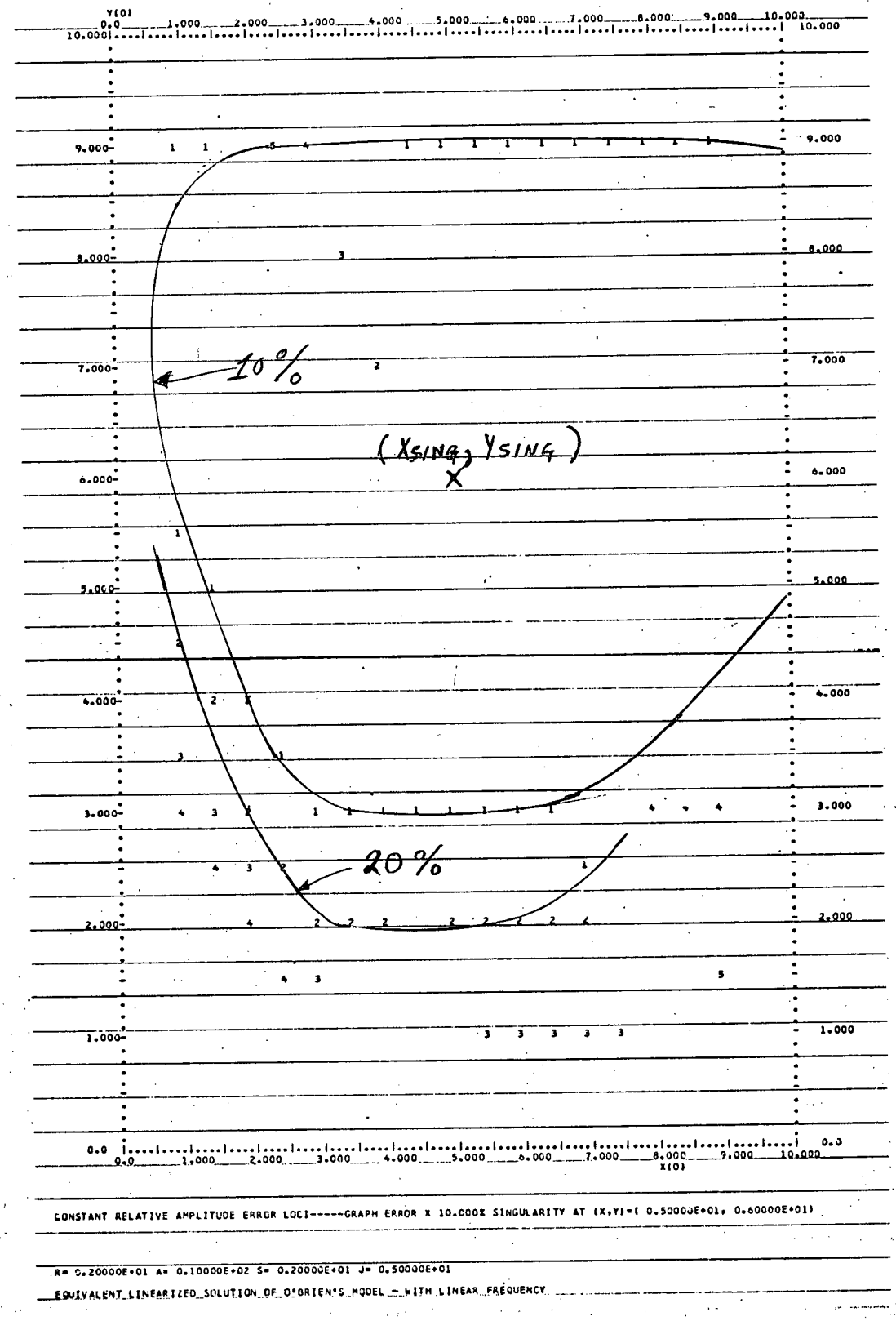

Fig. 3.13 O'Brien's Model Equivalent Linearization Solution Amplitude Error Loci

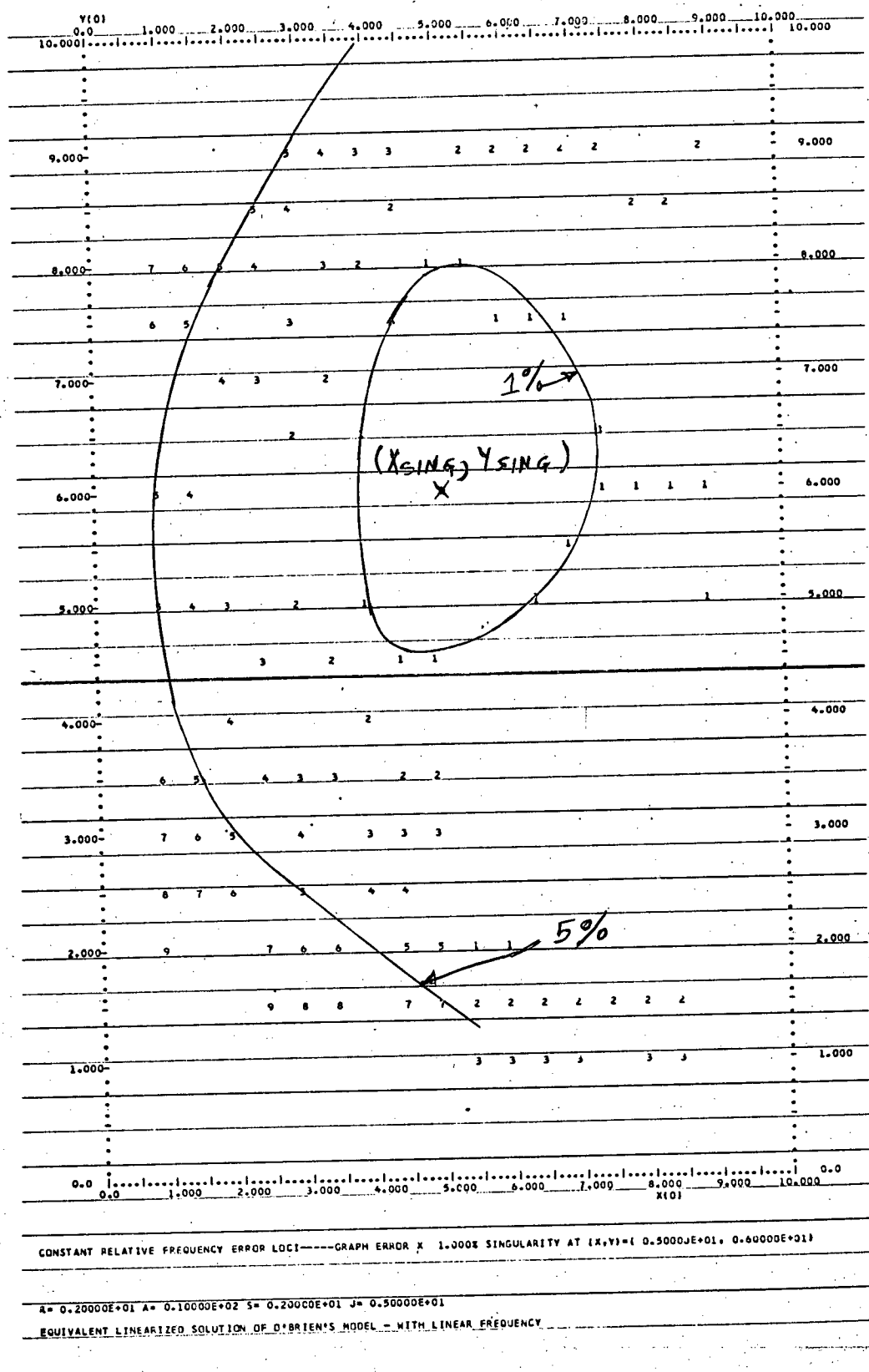

Fig. 3.14 O'Brien's Model Equivalent Linearization Solution Frequency Error Loci

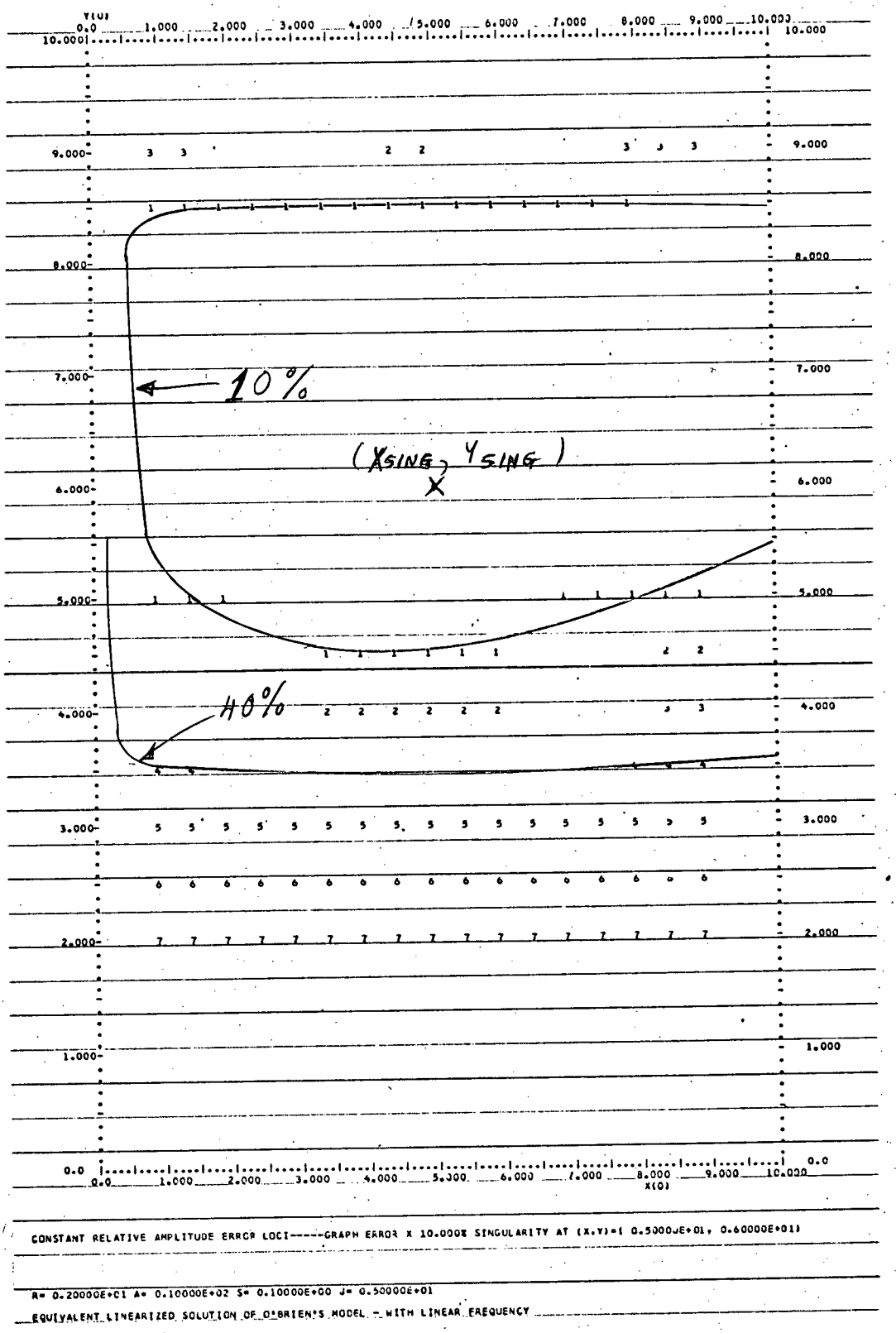

Fig. 3.15 O'Brien's Model Equivalent Linearization Solution Amplitude Error Loci

3.10 Summary

In this chapter we have developed and applied the method of equivalent linearization to the four ecological models that were introduced in chapter two. This method of solution yields an improvement in the accuracy of the amplitudes of the solutions over the classical linear solution. However, the frequency of the equivalent linearized solution is found to be less accurate than that of the linear solution for given initial conditions. This apparent trade-off between amplitude and frequency error was resolved by combining the amplitude of the equivalent linearization solution with the frequency of the linear solution to obtain the best features of both.

The trade-off between amplitude and frequency is not a general occurance, but one that depends on the form of the individual model. If the model produces a large nonsymmetrical oscillation close to the time origin, the minimum mean square error criterion chooses the a_{ij} so that the approximate solution tracks the actual solution very well near the time origin. If the model then continues on to produce symmetrical oscillations, (as the models under consideration do) the original estimate of the a_{ij} is no longer accurate. As the derivatives in the nonsymmetrical oscillations are usually larger than those of the symmetrical oscillations, we find that this gives an estimate of the derivatives that is higher than it actually is, which in turn raises the frequency estimate. This effect will not necessarily occur in all nonlinear differential equation models that employ this method of solution.

It should be noted that for the equivalent linearization solution of Holling's model and O'Brien's model, if the initial conditions are large enough, the denominators of the a_{ij} may become imaginary, in which case the

solution ceases to be meaningful. For initial conditions near the singular point of interest, the equivalent linearization solutions reduce to the linear linear solutions.

With the method of equivalent linearization, we have a complete literal parameter solution, which in general, will depend in a nonlinear manner on the initial conditions. This solution yields a refined estimate of the a_{ij} which may now depend on the initial conditions, an affect not found in linearized solutions. From the equations for the a_{ij}, one can easily determine the influence of initial conditions and variations of parameters on the various components of the solutions. For some parameters combinations, a given a_{ij} will be dominated by only one or two terms and may dominate a component of the solution, indicating which parameters are of major influence on the solution. These formulae save on the trouble of extensive computer sensitivity studies.

Refinements to the method of equivalent linearization will be discussed in the next chapter.

CHAPTER FOUR

REFINEMENT OF THE METHOD OF EQUIVALENT LINEARIZATION

4.1 Introduction

Having completed the application and evaluation of the method of equivalent linearization, we turn our attention to other techniques of obtaining approximate solutions of nonlinear differential equations that yield literal parameter solutions that would be acceptable over a wider range of initial conditions than the previously developed techniques. The first approach taken towards this end was the elliptic functions method. The VGW model was used as a prototype for development of the technique. The results may be briefly summarized by stating that they were, at best, only as good as the previously developed results. A brief summary of the methods used, along with the complications and limitations encountered are given in Appendix A for the interested reader.

The next approach taken to obtain improved solutions is a completely novel method and is described in detail in the next sections.

4.2 The Additive Correction Factor

While evaluating the methods of linearization and equivalent linearization, an interesting phenomenon was observed, but at the time, was ignored. For large initial conditions, the numerical (true) solution typically appeared in the phase plane to be a spiral whose centre of oscillation was slowly shifting down towards the singular point (x_{sing}, y_{sing}). It was conjectured that a transient term in the form of an exponentially damped ramp could be added to the existing solutions to reproduce this effect and hopefully reduce the amplitude errors of the equivalent linearization

solutions.

Numerical studies were done to evaluate the general validity of this idea. Exponentially damped ramps were extracted from the x(t) and y(t) numerical solutions and then added to the approximate analytical solutions. This transient was obtained by numerically fitting (using a least squares method) two pairs of decaying exponentials to the numerical solution maxima and minima, which represent the upper and lower envelopes of each solution. The difference of these two envelope exponentials gives the desired transient. The preliminary studies showed that this was indeed an improvement, and should be investigated further.

4.3 Analytical Determination of the Additive Correction Factor

Having found an idea that exhibits a potential improvement for our existing solutions, we now wish to determine analytically the four parameters of the additive corrections factors,

$$x_c = tA_x e^{\sigma_x t}$$

$$y_c = tA_y e^{\sigma_y t}$$

The initial goal was to be able to compute the exact values of the solution peaks, which would then yield the correction factors in a similar manner to the preliminary numerical studies. A number of ideas for computing the peaks and the correction factors were initially tried, but these yielded spurious results, in terms of accuracy. They are briefly outlined in Appendix B for the interested reader.

As a means of approximating the extrema of the solutions, we used a three term McLaurin expansion:

$$x = x_o + F(x_o, y_o)t + F'(x_o, y_o)t^2/2$$

$$y = y_o + G(x_o, y_o)t + G'(x_o, y_o)t^2/2$$

It was found that this method yielded good results if the peak of the solution was within ¼ cycle of the time origin. Unfortunately, this condition was not met by all combinations of initial conditions. Also, this method would permit computation of only the first peak of the x & y solutions, whereas it was desired to obtain several successive peaks.

These problems were circumvented by using the general Taylor series expansion to obtain:

$$x(t) = \sum_{i=1}^{\infty} x^i(x_{t_a}, y_{t_a})(t-t_a)^i/i!$$

$$y(t) = \sum_{i=1}^{\infty} y^i(x_{t_B}, y_{t_B})(t-t_b)^i/i!$$

where the higher order derivatives are easily obtained from the original differential equations. There is a problem in that the terms in the series are functions of x & y, which are known precisely only at the time origin. This problem may be resolved by using the equivalent linearization solutions as an approximation in evaluating the derivatives in the Taylor series.

We choose the points t_a & t_b, about which we develop a Taylor series, as follows. From Chapters Three and Four, we know that the phase and frequency of the linear solution is accurate, and may use it to predict the location of the peaks of the true solution. To accomplish this, we first rewrite the analytical solutions as follows:

$$x = r_x e^{\sigma t}\cos(\omega t + \theta_x)$$

$$y = r_y e^{\sigma t}\sin(\omega t + \theta_y)$$

where

$$r_x = \sqrt{(x_o - x_{sing})^2 + \frac{((x_o - x_{sing})(a_{11}-\sigma) - a_{12}(y_o - y_{sing}))^2}{\omega^2}}$$

$$r_y = \sqrt{(y_o - y_{sing})^2 + \frac{((y_o - y_{sing})(a_{22}-\sigma) + a_{21}(x_o - x_{sing}))^2}{\omega^2}}$$

$$\theta_x = \tan^{-1}\left[\frac{(y_o-y_{sing})a_{12}-(x_o-x_{sing})(a_{11}-\sigma)}{(x_o-x_{sing})\omega}\right]$$

$$\theta_y = \tan^{-1}\left[\frac{(y_o-y_{sing})\omega}{(y_o-y_{sing})(a_{22}-\sigma)+(x_o-x_{sing})a_{21}}\right]$$

We then locate the extremum points by requiring that $\dot{x}(t_x) = 0$ and $\dot{y}(t_y) = 0$, from which we obtain:

$$t_x = \frac{1}{\omega}\left[\tan^{-1}\left(\frac{\sigma}{\omega}\right) - \theta_x\right]$$

$$t_y = \frac{-1}{\omega}\left[\tan^{-1}\left(\frac{\omega}{\sigma}\right) + \theta_y\right]$$

These formulae give the location of the first peaks of the solutions, and successive ones are located every $\frac{\pi}{\omega}$ time units later in time. We first evaluate our Taylor series at the points $t_a=t_x/2$ & $t_b=t_y/2$, which locates the series at least half way between peaks, and then every $\frac{\pi}{\omega}$ later in time. The reason that we locate our series away from the actual peaks is that the approximate solution is accurate near the singular point and permits accurate prediction of the derivatives in the Taylor series. The peaks of the solution are then given by $x_{peak}=x\quad(t_x/2)$ & $y_{peak}=y(t_y/2)$.

The next question that arises concerns how many terms of the Taylor series are actually needed. Experiments done on the computer showed that terms of order three and higher could be neglected in most cases. For the cases where the terms of order three and higher are significant, it was found that by adding on a term of the form $c_x(t-t_a)^3$ the accuracy of the Taylor series was improved. The coefficient c_x was chosen so that the Taylor series peak value occurred at t_x. This additional term approximates the effects of all the neglected terms of the series. In many cases, this additional term is not neccessary, and when we compute it, it turns out to be zero or negligible. We obtain c_x from:

$$c_x = -(F(x_{t_a}, y_{t_a}) + F'(x_{t_a}, y_{t_a})(t_x - t_a))/3(t_x - t_a)^2$$

We may compute the term c_y in a similar manner. We now have a means of computing the peak values of the solutions. For large initial conditions, when the approximate solutions become inaccurate, so does the Taylor series.

We may now proceed to determine the actual correction factors. We could use the Taylor series to generate numerous points of the solution and then proceed in the manner used in the numerical study. If this were done, the formulae for the correction factors would become cumbersome, and would not yield any practical insight into the system behaviour. Instead a different approach will be pursued.

As the major source of error in the existing solutions usually occurs in the first period of the solution, we propose a correction factor that will correct only the first peak in each solution, which will reduce the overall error somewhat. The additive correction factors will take the form:

$$x_c = A_x t^n e^{-nt/t_x} \qquad \text{where} \qquad x(t) = x_{eq\ lin} + x_c$$

$$y_c = A_y t^n e^{-nt/t_y} \qquad\qquad y(t) = y_{eq\ lin} + y_c$$

These correction factors are n'th order exponentially damped ramps whose peak values occur at t_x & t_y, the times of the first peaks. The correction factors become more like narrow pulses as n becomes larger. The maximum values of the correction factors are given by $A_x t_x^n e^{-n}$ and $A_y t_y^n e^{-n}$, which we would like to be equal to the difference in peak values between the actual and approximate solutions. The peak values of the approximate solutions are given by:

$$x_{peak} = r_x e^{\sigma t_x} \cos(\omega t_x + \theta_x)$$

$$y_{peak} = r_y e^{\sigma t_y} \sin(\omega t_y + \theta_y)$$

Thus we obtain:

$$A_x = (x_{\text{peak Taylor}} - x_{\text{peak Analytic}})(e/t_x)^n$$

$$A_y = (y_{\text{peak Taylor}} - y_{\text{peak Analytic}})(e/t_y)^n$$

We now wish to choose n so that the correction factor will affect only the first peak of the solution. When we take n = 11, the correction factor will be reduced to a maximum of 35% of its peak value by the time the solution has progressed another quarter period forward in time. When the next peak of the solution occurs, the correction factor will be completely negligible.

We may also apply this correction factor to the overdamped solutions. First, we must modify the method whereby we compute the peak times t_x & t_y. We rewrite the overdamped solutions as follows:

$$x(t) = x_{sing} + A_{1x}e^{\sigma_1 t} + A_{2x}e^{\sigma_2 t}$$

$$y(t) = y_{sing} + A_{1y}e^{\sigma_1 t} + A_{2y}e^{\sigma_2 t}$$

where

$$A_{1x} = ((x_o - x_{sing})(a_{11} - \sigma_2) - a_{12}(y_o - y_{sing}))/(\sigma_1 - \sigma_2)$$

$$A_{2x} = ((x_o - x_{sing})(\sigma_1 - a_{11}) + a_{12}(y_o - y_{sing}))/(\sigma_1 - \sigma_2)$$

$$A_{1y} = ((y_o - y_{sing})(a_{22} - \sigma_2) + a_{21}(x_o - x_{sing}))/(\sigma_1 - \sigma_2)$$

$$A_{2y} = ((y_o - y_{sing})(\sigma_1 - a_{22}) - a_{21}(x_o - x_{sing}))/(\sigma_1 - \sigma_2)$$

These solutions exhibit a peak point located at

$$t_x = \frac{1}{(\sigma_1 - \sigma_2)} \ln\left(\frac{-A_{2x}\,\sigma_2}{A_{1x}\,\sigma_1}\right)$$

$$t_y = \frac{1}{(\sigma_1 - \sigma_2)} \ln\left(\frac{-A_{2y}\,\sigma_2}{A_{1y}\,\sigma_1}\right)$$

If t_x is to be greater than zero, we must have $(\sigma_1 - \sigma_2) \gtrless 0$ and $\frac{-A_{2x}\sigma_2}{A_{1x}\sigma_1} \gtrless 1$, with similar restrictions on t_y. Should there be no peak in positive time, we may estimate a point at which we may apply the correction factors. This estimate is given by:

$$t_x = \frac{2(|A_{1x}| + |A_{2x}|)}{(|A_{1x}\sigma_1| + |A_{2x}\sigma_2|)}$$

This estimate locates a point on the solution that is about half way between the initial values and the steady state value. For the overdamped case, we don't need such sharp pulses for correction factors, and thus we may reduce n down to n=4. We then proceed with the correction factors as previously outlined for the underdamped case.

Thus we have developed a correction factor using a modified Taylor series and an exponentially damped ramp that will correct the first peak of the existing equivalent linearization solutions and reduce the overall solution error. We now proceed to apply this method to the four ecological models discussed in chapter two, and evaluate its usefulness.

4.4 Additive Correction Factorfor the VGW Model

The first model we wish to apply the additive correction factor to is the VGW model discussed in section 2.2. For computing the derivatives in the modified Taylor series, we already have the first derivatives, which are the differential equations. The second derivatives may be computed as follows:

$$\ddot{x} = \frac{d}{dt}(\dot{x}) = \frac{\partial F}{\partial x}\dot{x} + \frac{\partial F}{\partial y}\dot{y}$$

$$= \frac{\partial F}{\partial x}F + \frac{\partial F}{\partial y}G$$

and $$\ddot{y} = \frac{\partial G}{\partial x}F + \frac{\partial G}{\partial y}G$$

The partial derivatives are given in the A matrices (see chapter two). We now compute the additive correction factors using the method outlined in section 4.3.

To evaluate the additive correction factors, we compute the corrected solutions for the same parameter choice and ranges of initial conditions as for the linear solutions (see section 2.4). The same samples of time plots and phase plane plots are given in figures 4.1 to 4.3. The corresponding amplitude error loci are given in figure 4.4. We observe that we have an increase in the size of region enclosed by the error loci (compared to that of the uncorrected equivalent linearization solutions), indicating that this method is definitely an improvement. As the correction factor is designed to correct only one peak of the solution, the frequency of the solution will not be affected, and hence the corresponding frequency error loci will be identical to those of the uncorrected solutions, and need not be shown here.

In the computer algorithm, provisions were made so that if error improved by the correction factor was less than 10% of the equivalent linearization solution a correction factor would be applied to the second peak instead of the first. This was to accomodate the cases where the solution started off very close (in time) to the first peak (and incurred little error at that peak)but had a significant error at the second peak. It should be noted that when one peak of the solution is corrected, the next largest error (usually on the next peak) becomes the dominating and limiting error in the solution. If it was so desired, additive correction factors could be applied to more than one peak, but this increases the complexity of the complete solution.

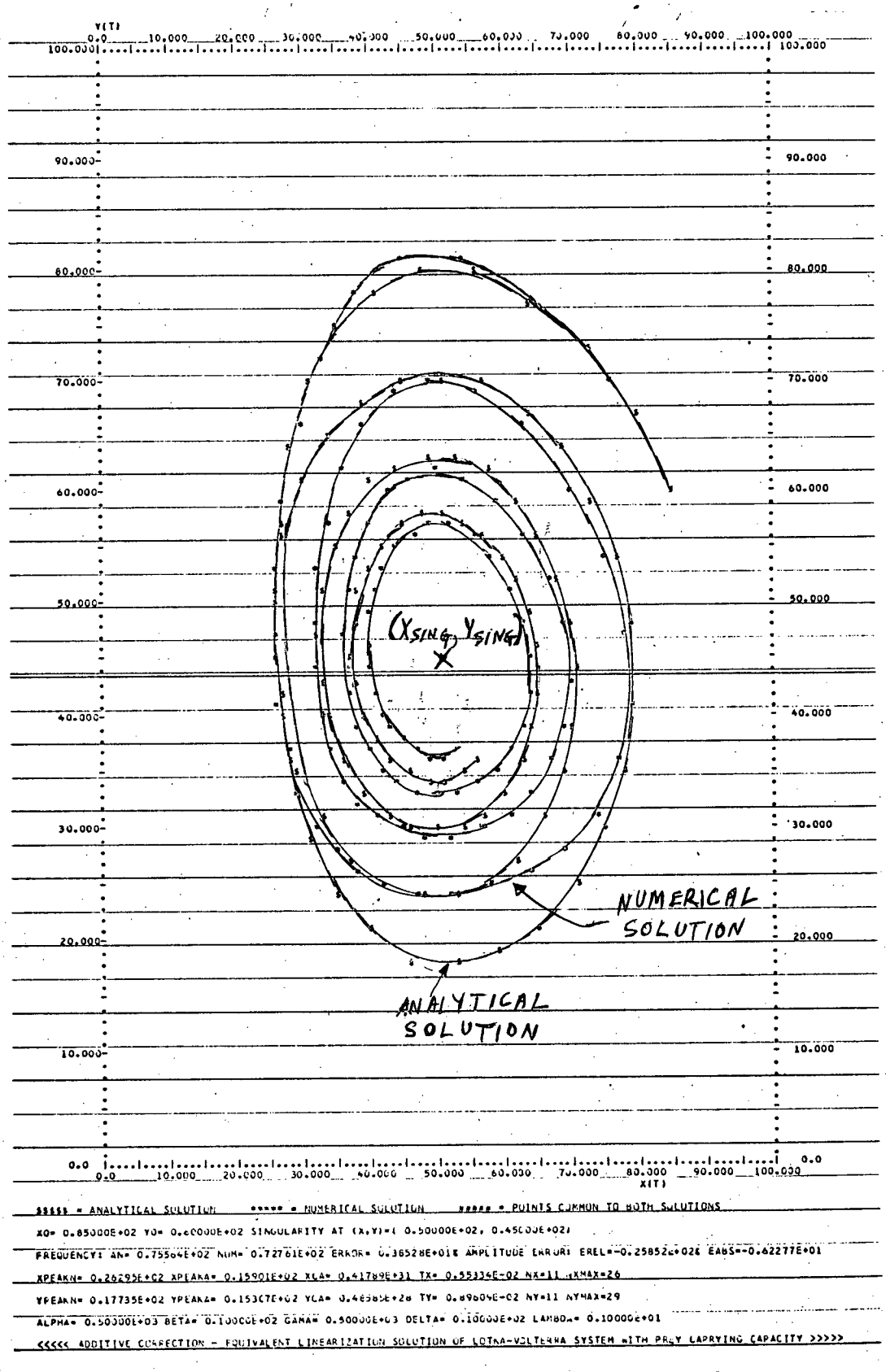

Fig. 4.1 VGW Model: Corrected Equivalent Linearized Solution for $(x_o, y_o)=(85,60)$

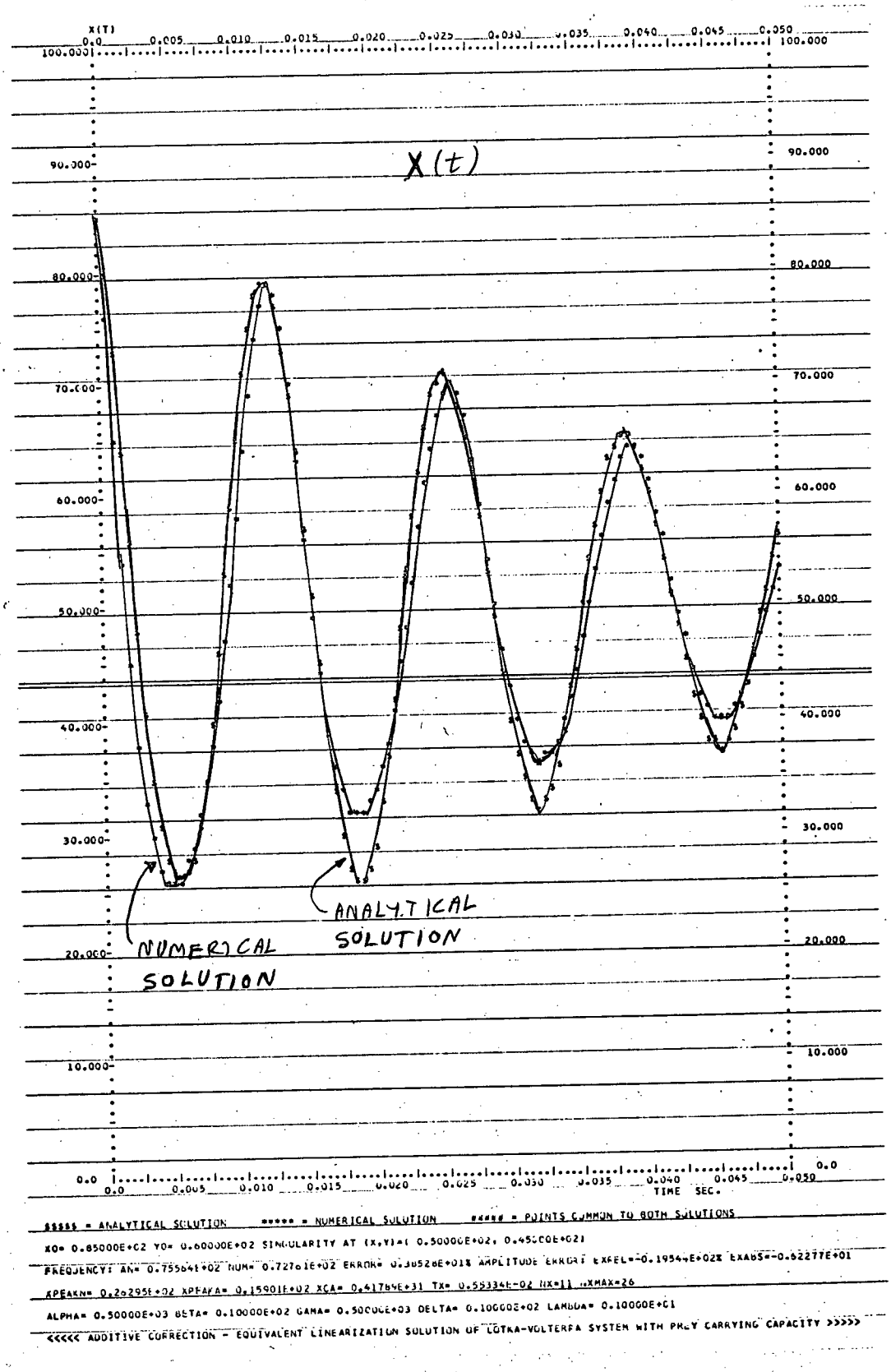

Fig. 4.2 VGW Model Corrected Equivalent Linearization Solution for $(x_o, y_o)=(85,60)$

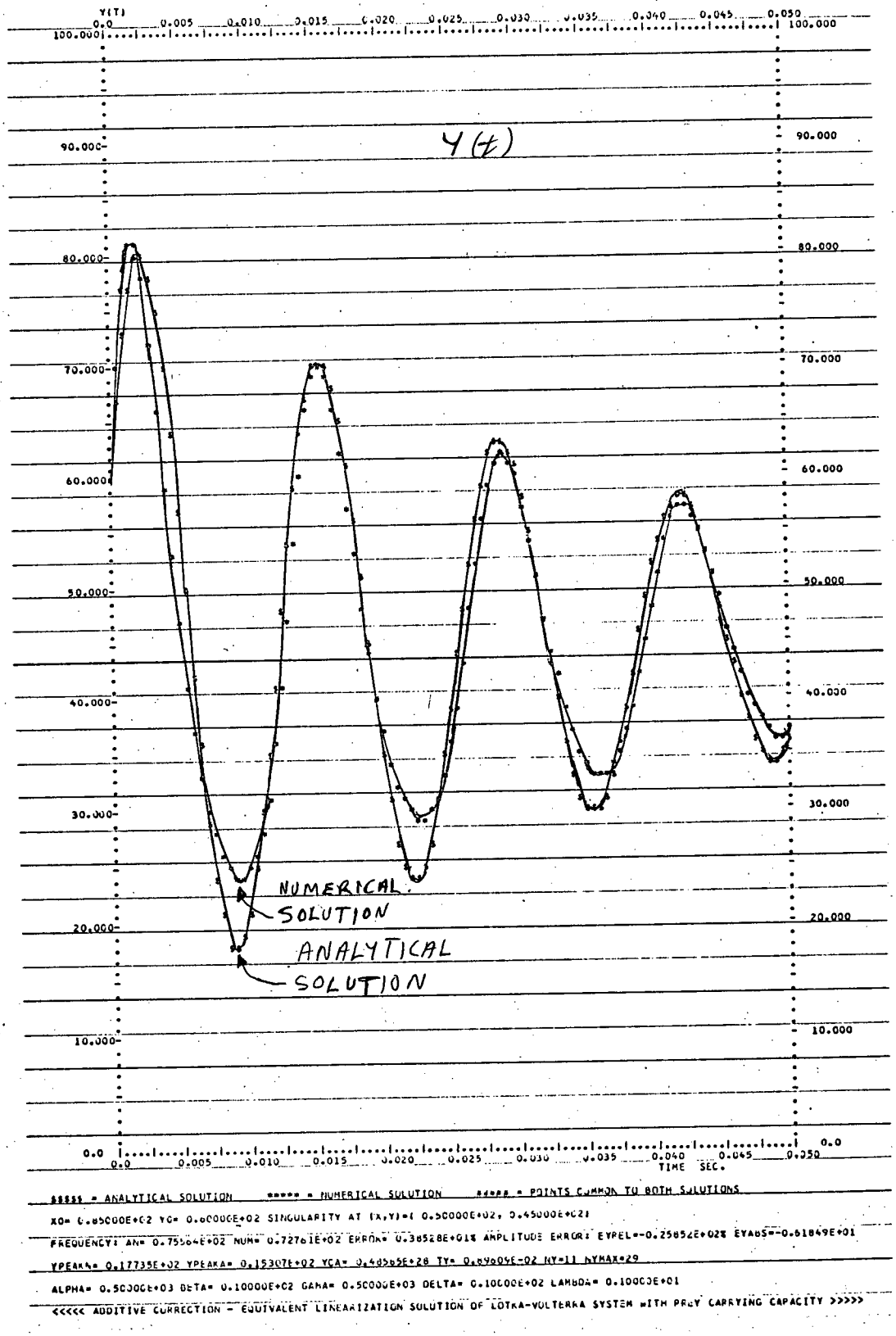

Fig. 4.3 VGW Model Corrected Equivalent Linearization Solution for $(x_o, y_o)=(85,60)$

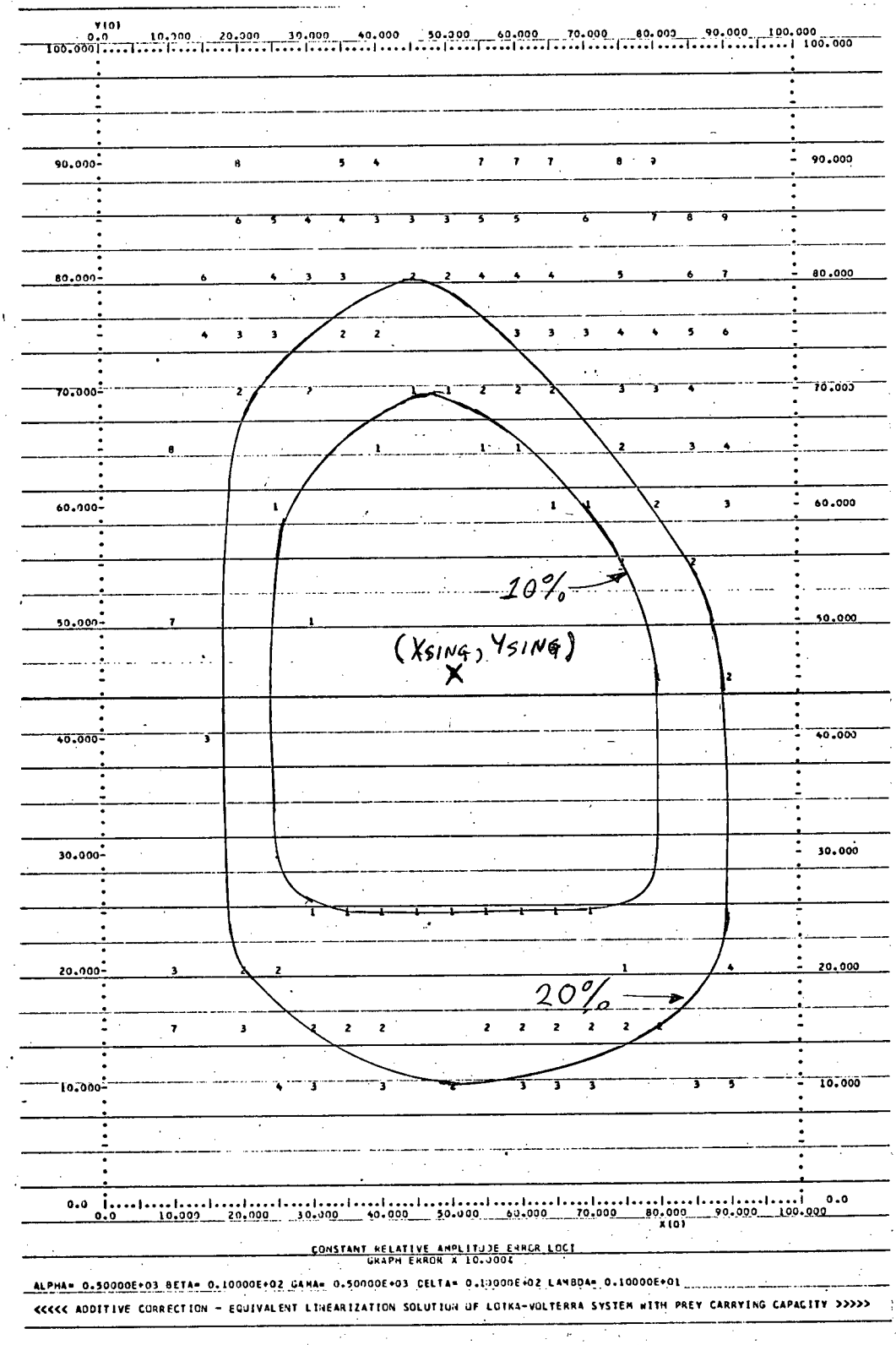

Fig. 4.4 VGW Model Corrected Equivalent Linearization Solution Amplitude Error Loci

The corrected solutions were also computed for the overdamped case, and the same samples of time plots and phase plane curves are shown in figures 4.5 to 4.10. The corresponding amplitude error loci are shown in figure 4.11. Here also, we have an improvement in the size of the amplitude error loci. We now proceed onwards to study the next ecological model.

4.5 Additive Correction Factor for Holling's Model

The second model that we wish to apply an additive correction factor to is Holling's model. The correction factors may be computed in the same manner as outlined for the VGW model.

To evaluate the additive correction factor, the corrected solutions were computed for the same parameter choice and ranges of initial conditions as for the linear solutions (see section 2.7). The same samples of time plots and phase plane curves are given in figures 4.12 to 4.17. The corresponding amplitude error loci for the corrected solutions are given in figure 4.18 and 4.19. In both cases, we note that we have an improvement in the size of the amplitude error loci (compared to the uncorrected equivalent linearized solution). Having found the additive correction factor to be useful improvement for the solutions of Holling's model, we now turn to study the third ecological model.

4.6 Additive Correction Factor for Rosenzweig's Model

The next model we wish to apply the additive correction factor to is Rosenzweig's model. The correction factor may be computed in the same manner as outlined for the VGW model.

To evaluate the additive correction factor, the corrected solutions were computed for the same parameter choice and ranges of initial conditions

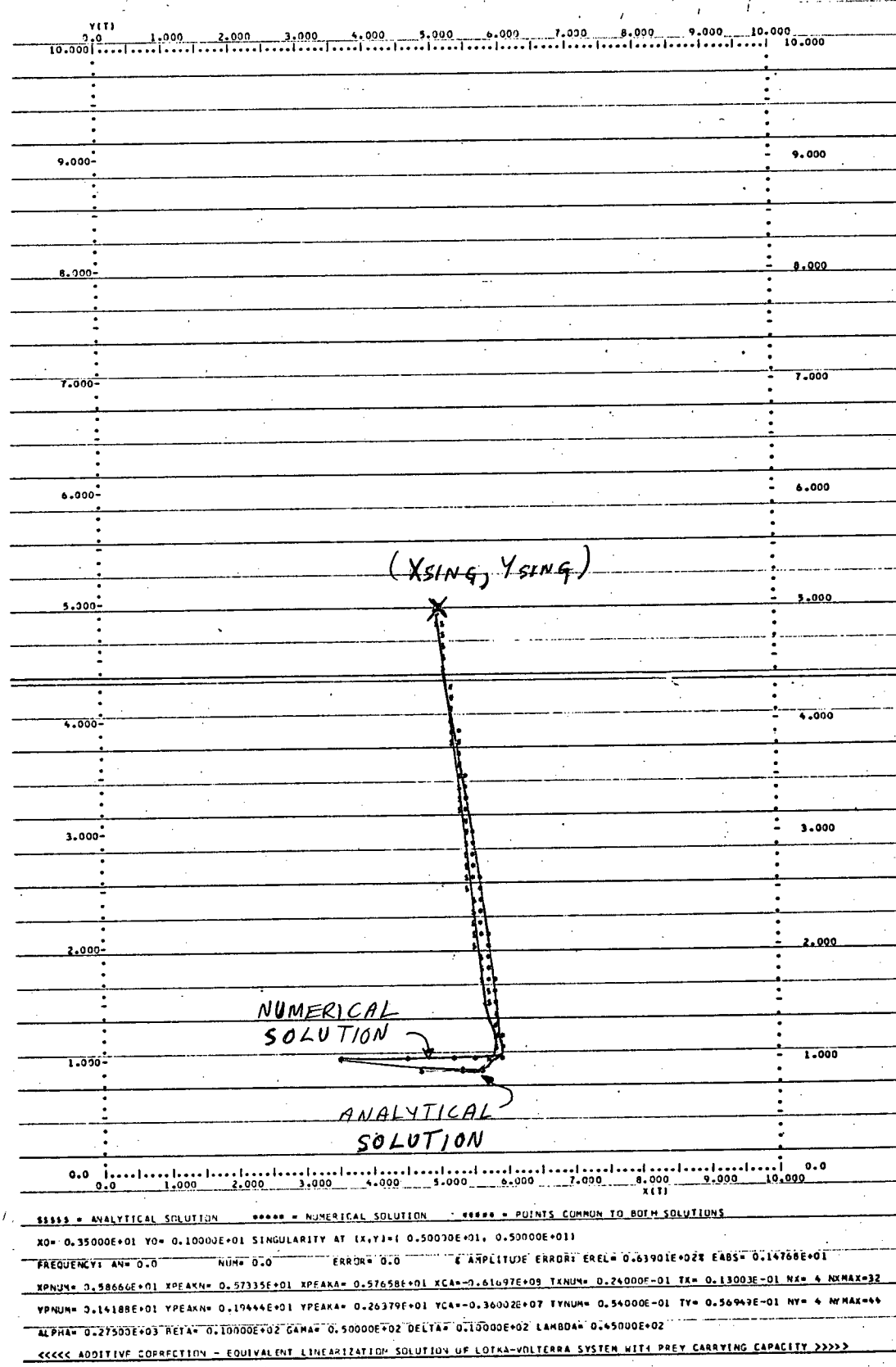

Fig. 4.5 VGW Model Corrected Equivalent Linearization Solution for $(x_o, y_o)=(3.5,1)$

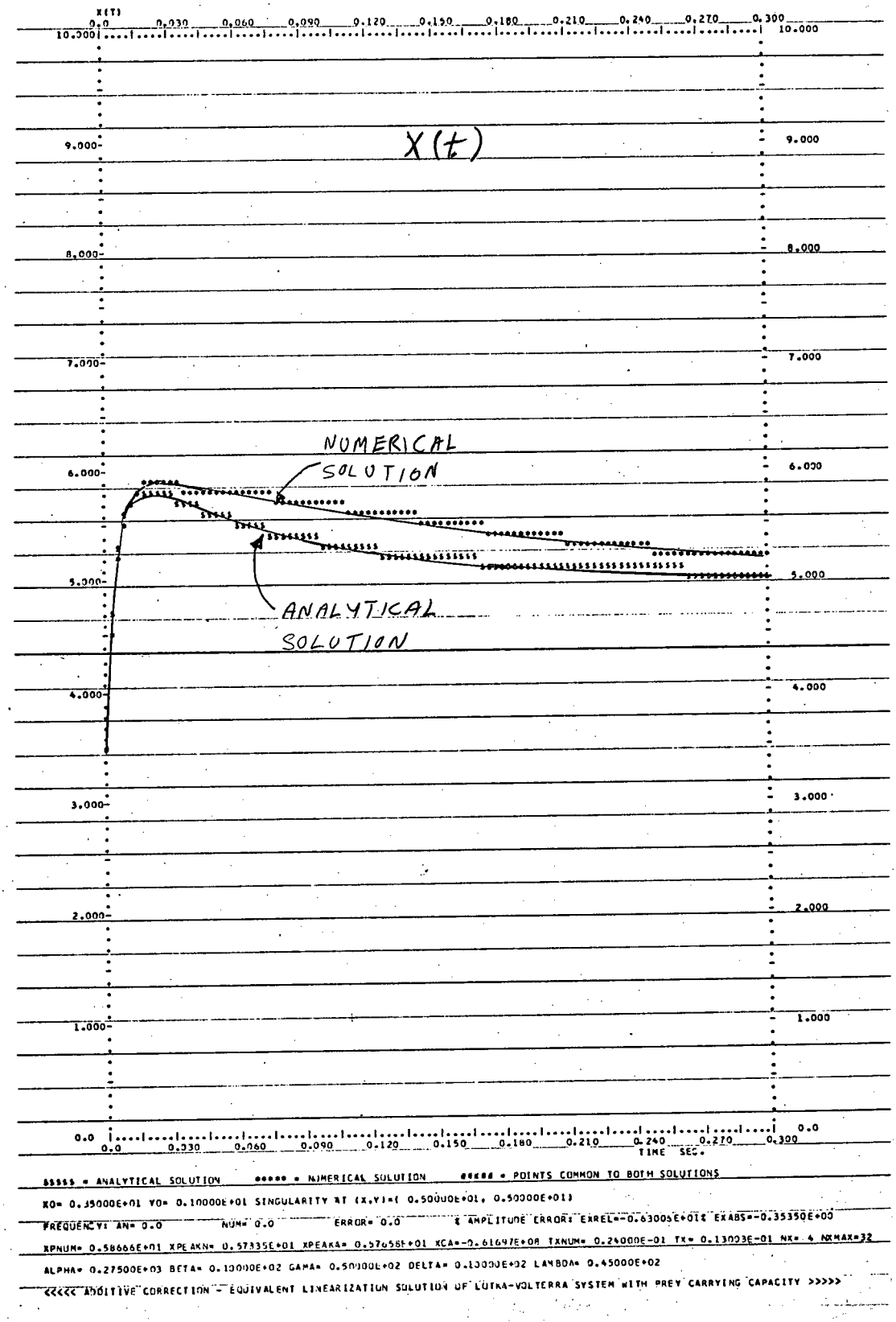

Fig. 4.6 VGW Model Corrected Equivalent Linearized Solution for $(x_o, y_o)=(3.5,1)$

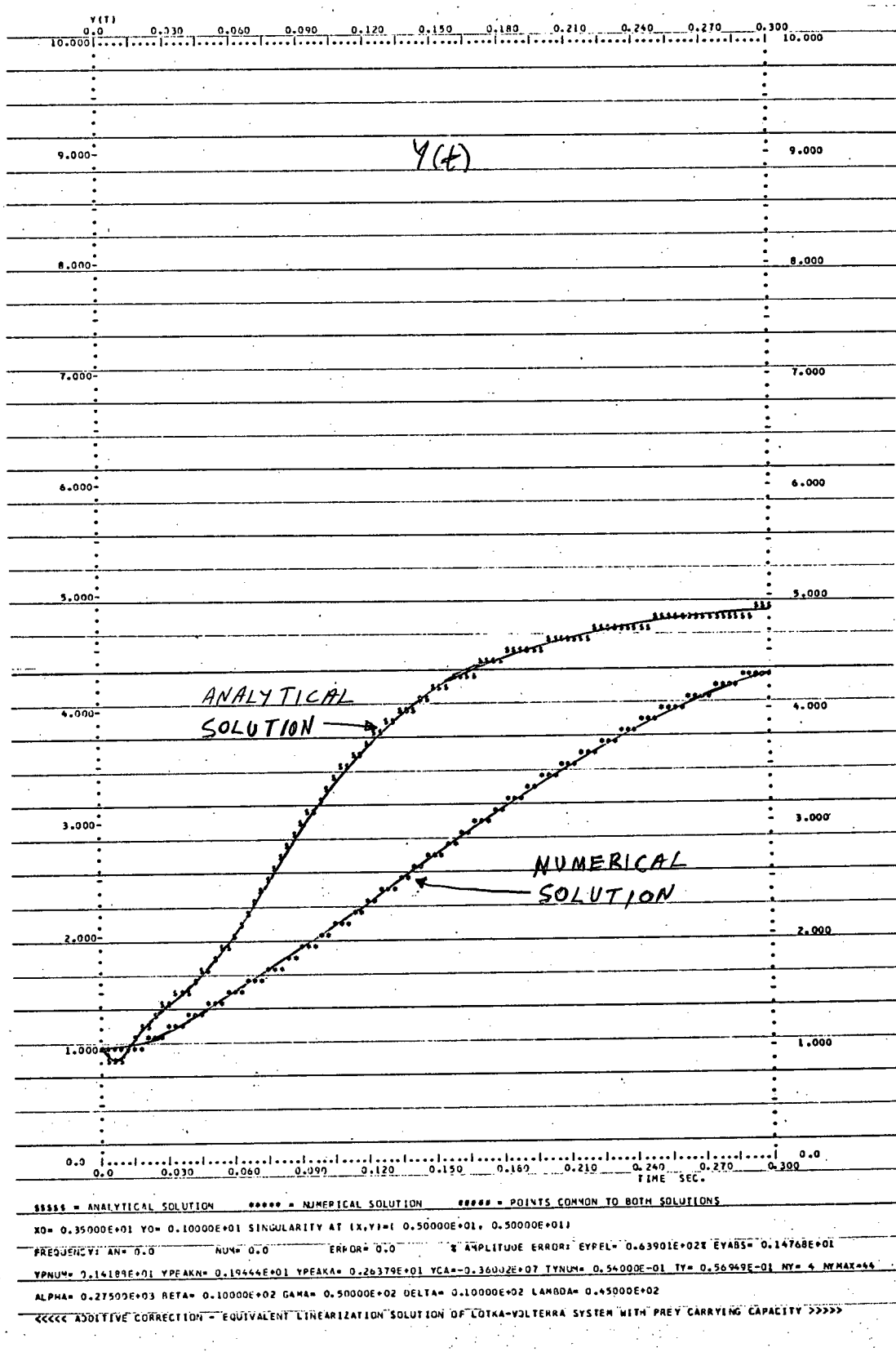

Fig. 4.7 VGW Model Corrected Equivalent Linearization Solution for $(x_o, y_o)=(3.5,1)$

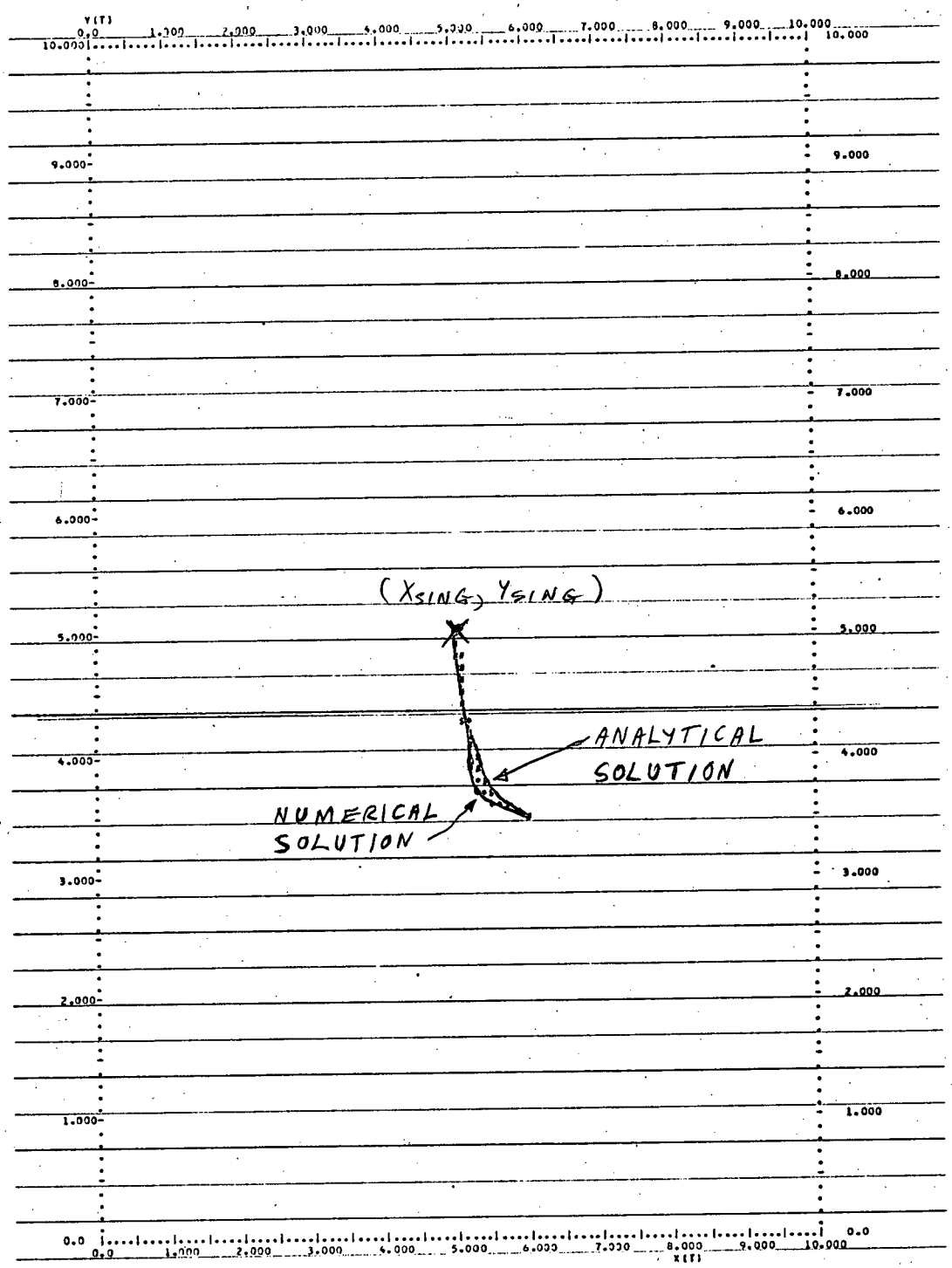

Fig. 4.8 VGW Model Corrected Equivalent Linearized Solution for $(x_o, y_o)=(6, 3.5)$

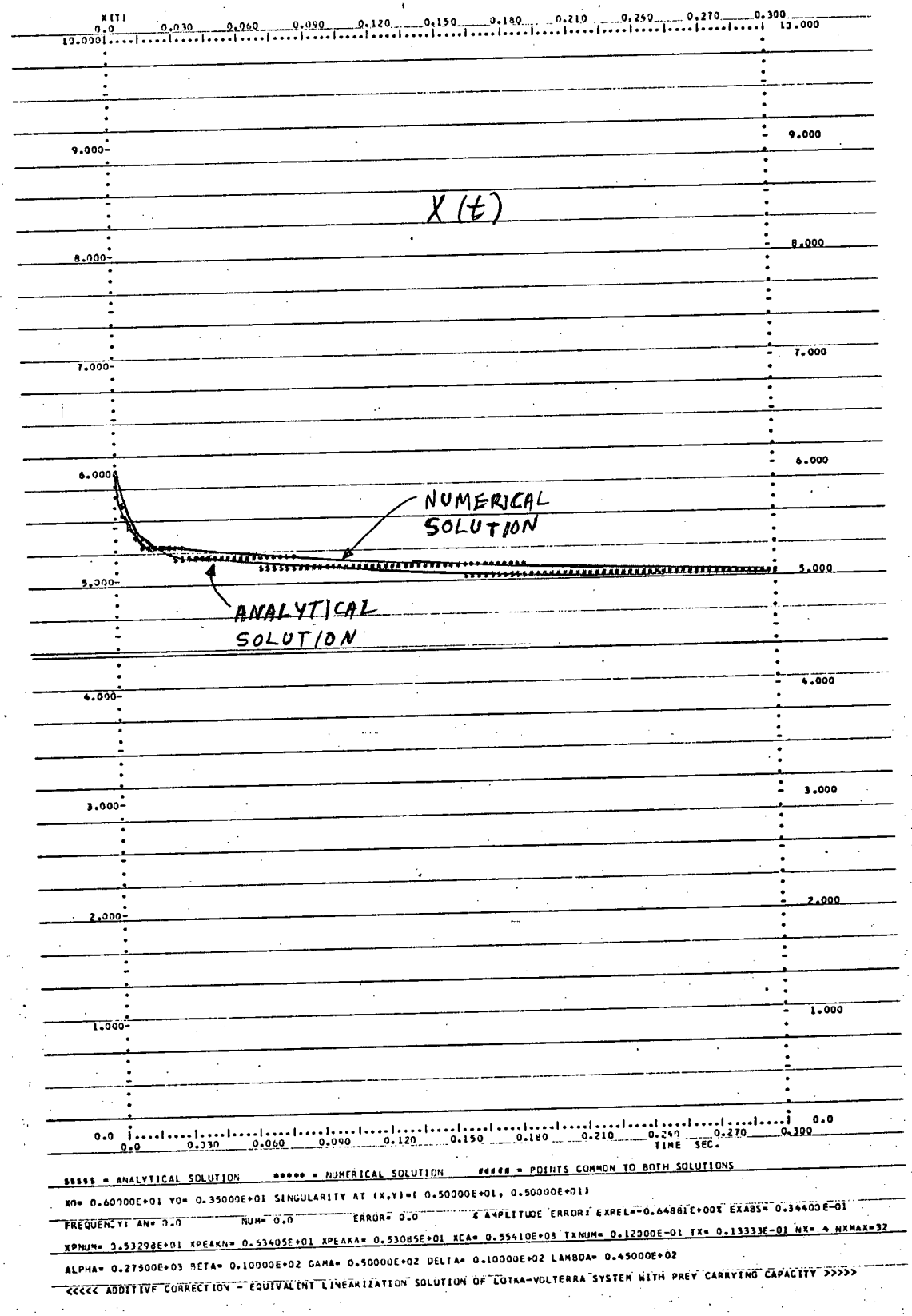

Fig. 4.9 VGW Model Corrected Equivalent Linearization Solution for $(x_o, y_o)=(6, 3.5)$

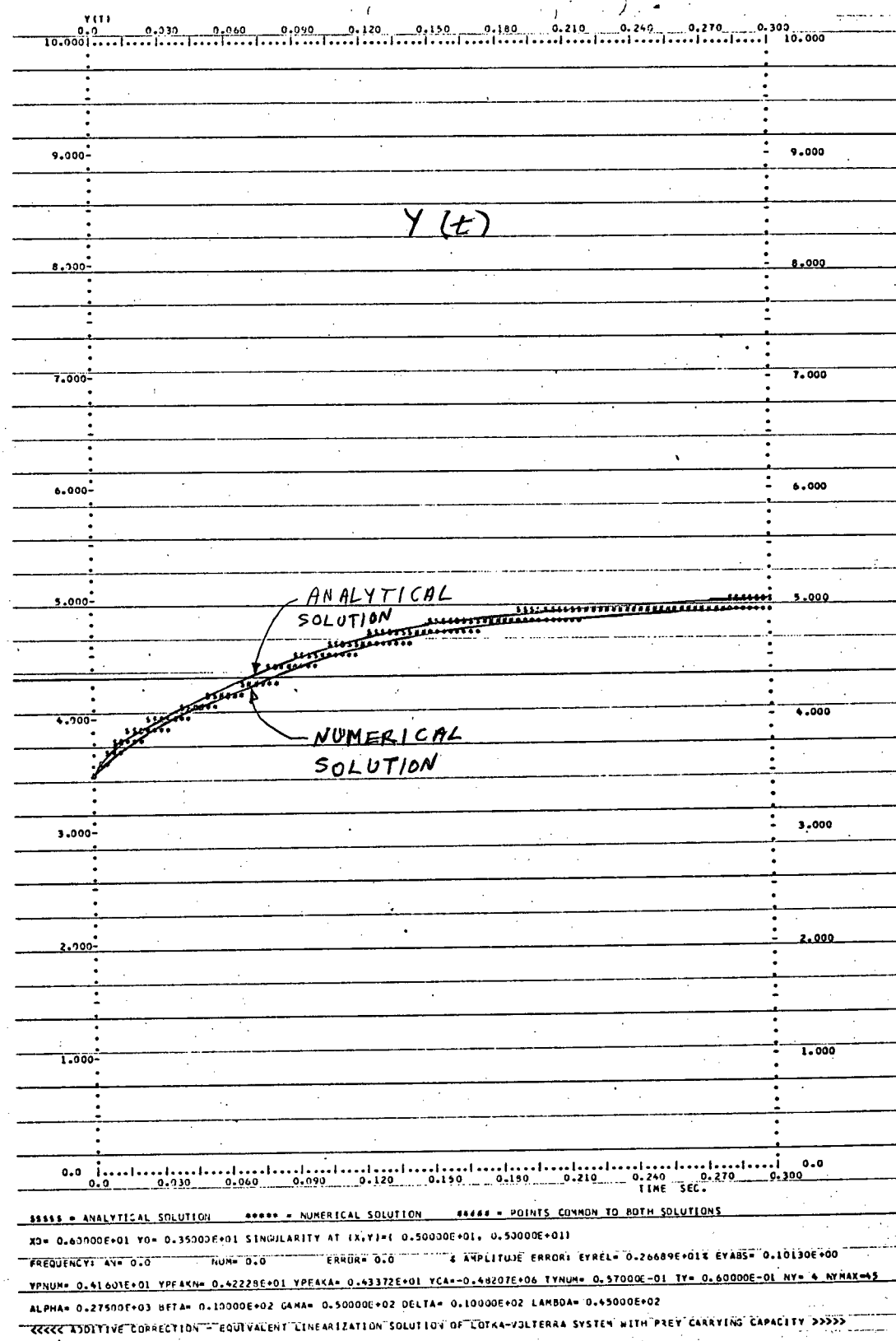

Fig. 4.10 VGW Model Corrected Equivalent Linearization Solution for $(x_o, y_o)=(6,3.5)$

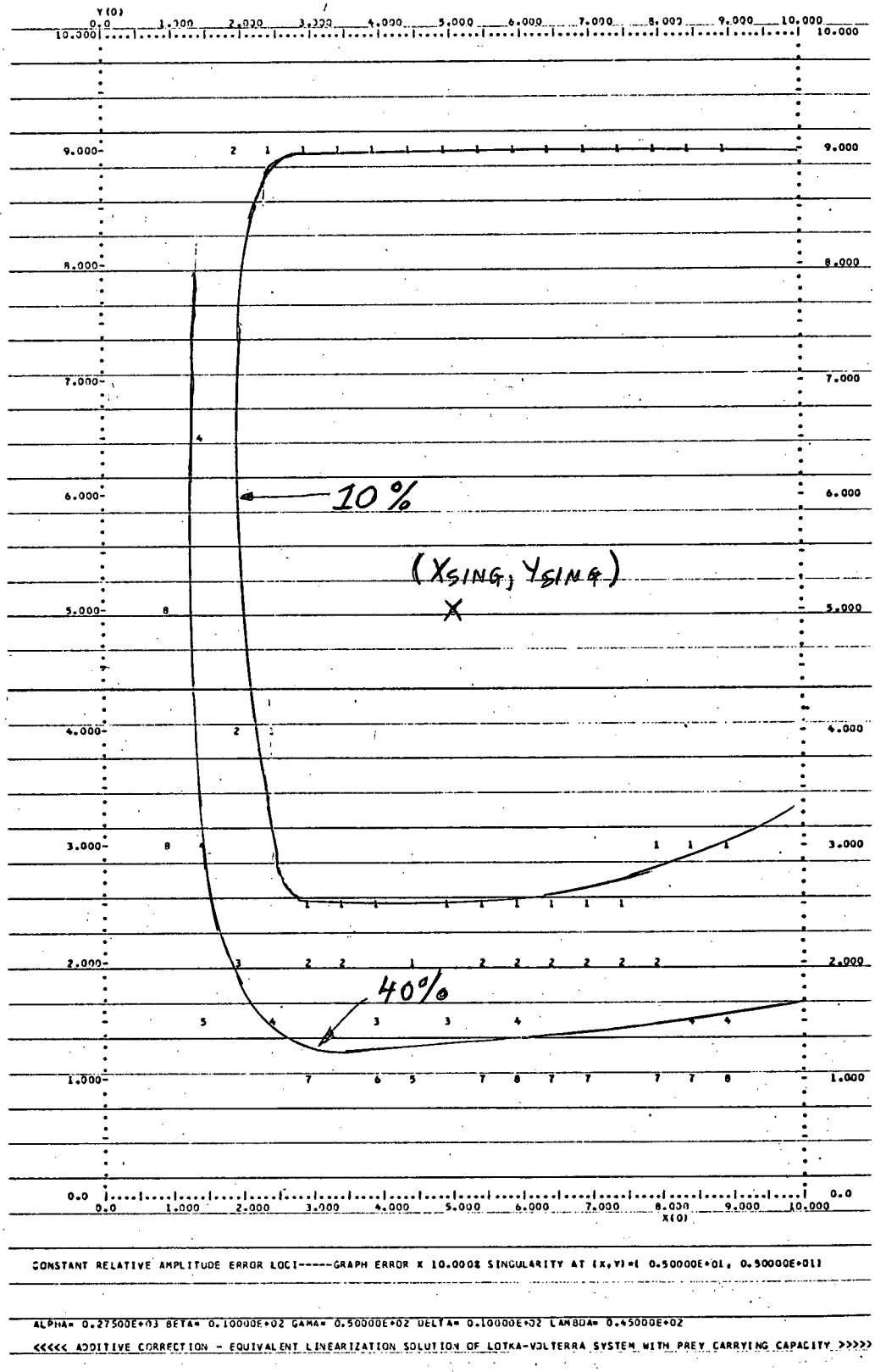

Fig. 4.11 VGW Model Corrected Equivalent Linearization Solution Amplitude Error Loci

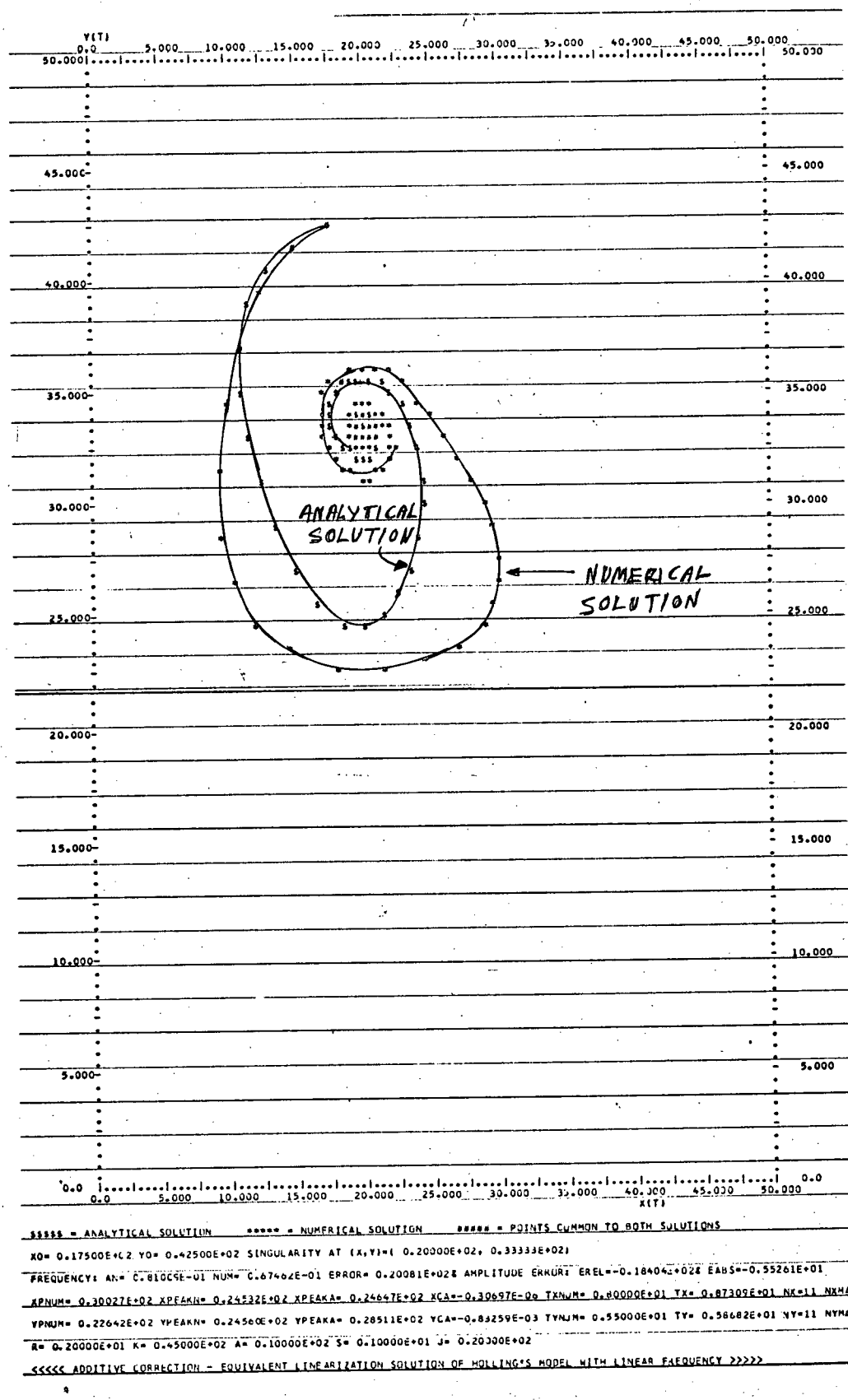

Fig. 4.12 Holling's Model Corrected Equivalent Linearization Solution for $(x_o, y_o) = (17.5, 42.5)$

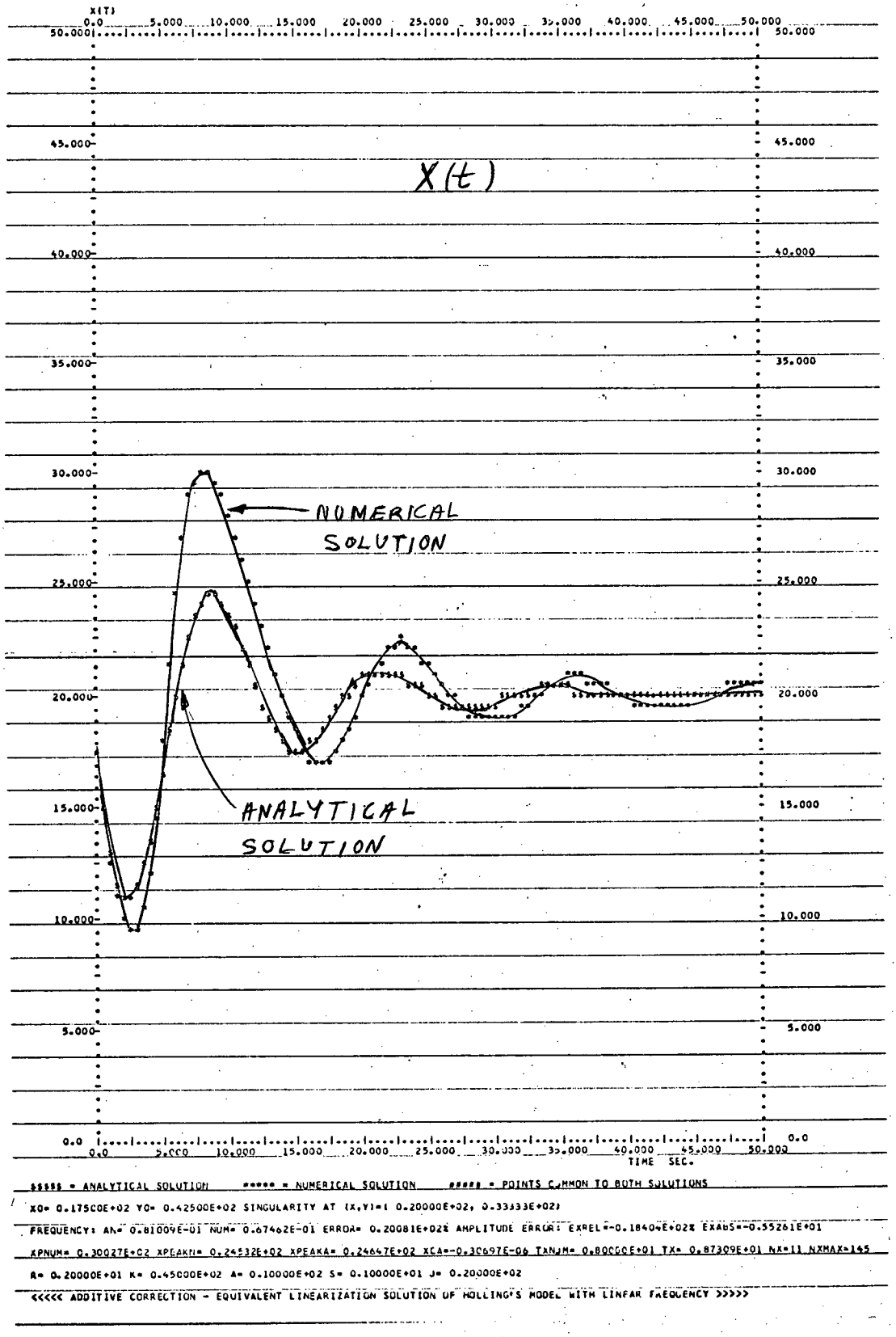

Fig. 4.13 Holling's Model Corrected Equivalent Linearization Solution for $(x_o, y_o) = (17.5, 42.5)$

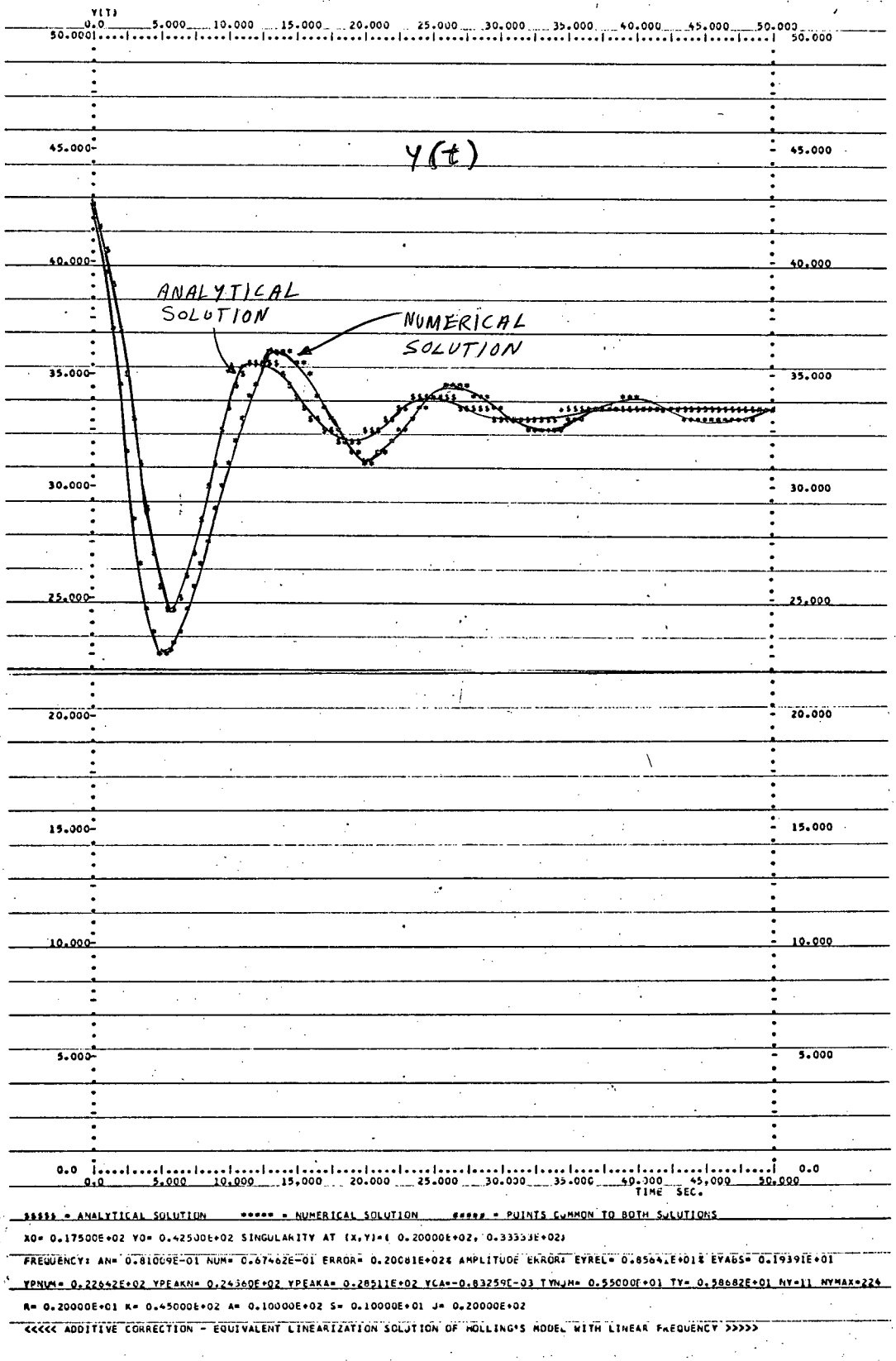

Fig. 4.14 Holling's Model Corrected Equivalent Linearization Solution for $(x_o, y_o) = (17.5, 42.5)$

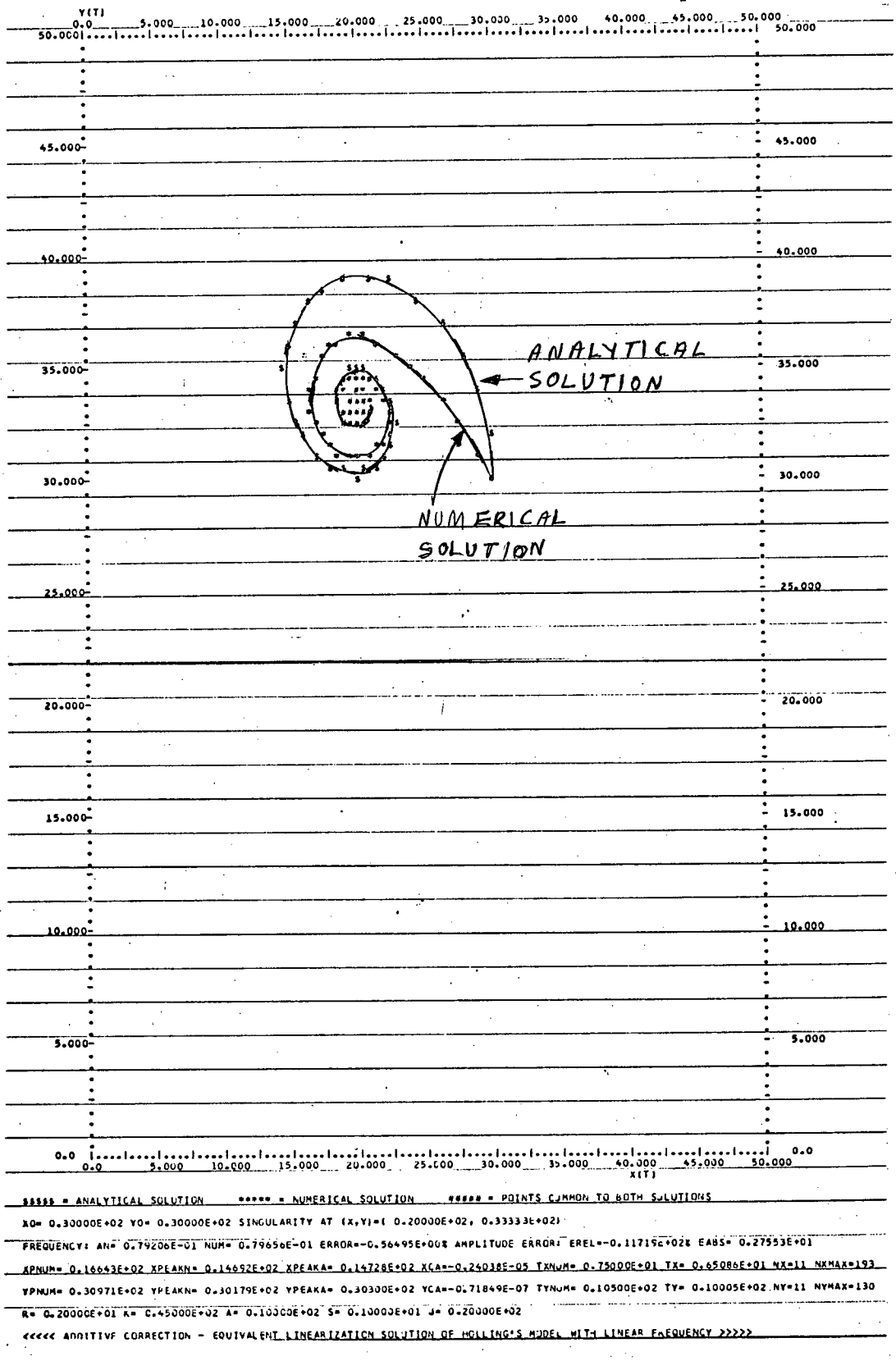

Fig. 4.15 Holling's Model Corrected Equivalent Linearization Solution for $(x_o, y_o) = (30, 30)$

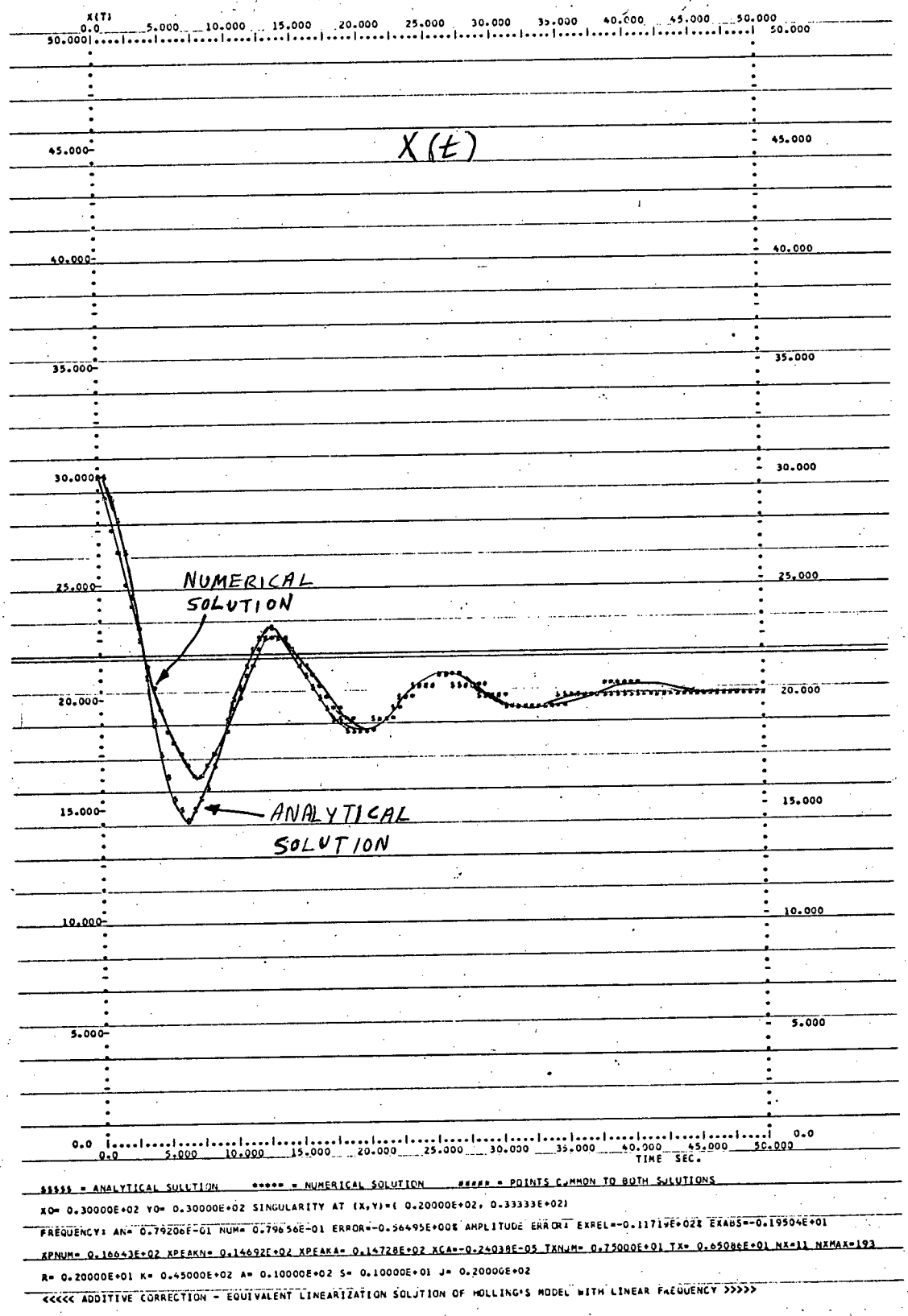

Fig. 4.16 Holling's Model Corrected Equivalent Linearization Solution for $(x_o, y_o) = (30, 30)$

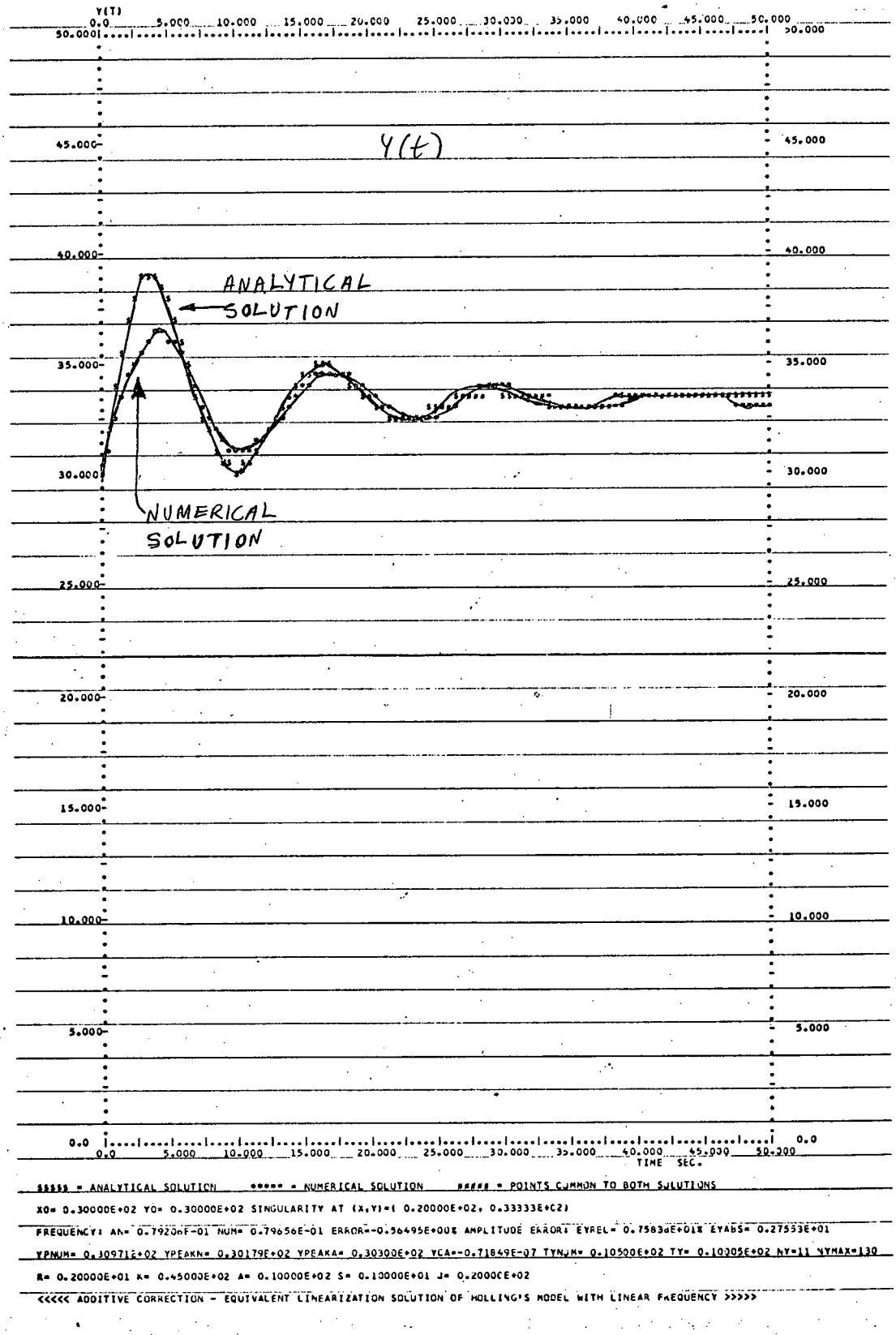

Fig. 4.17 Holling's Model Corrected Equivalent Linearization Solution for $(x_o, y_o) = (30, 30)$

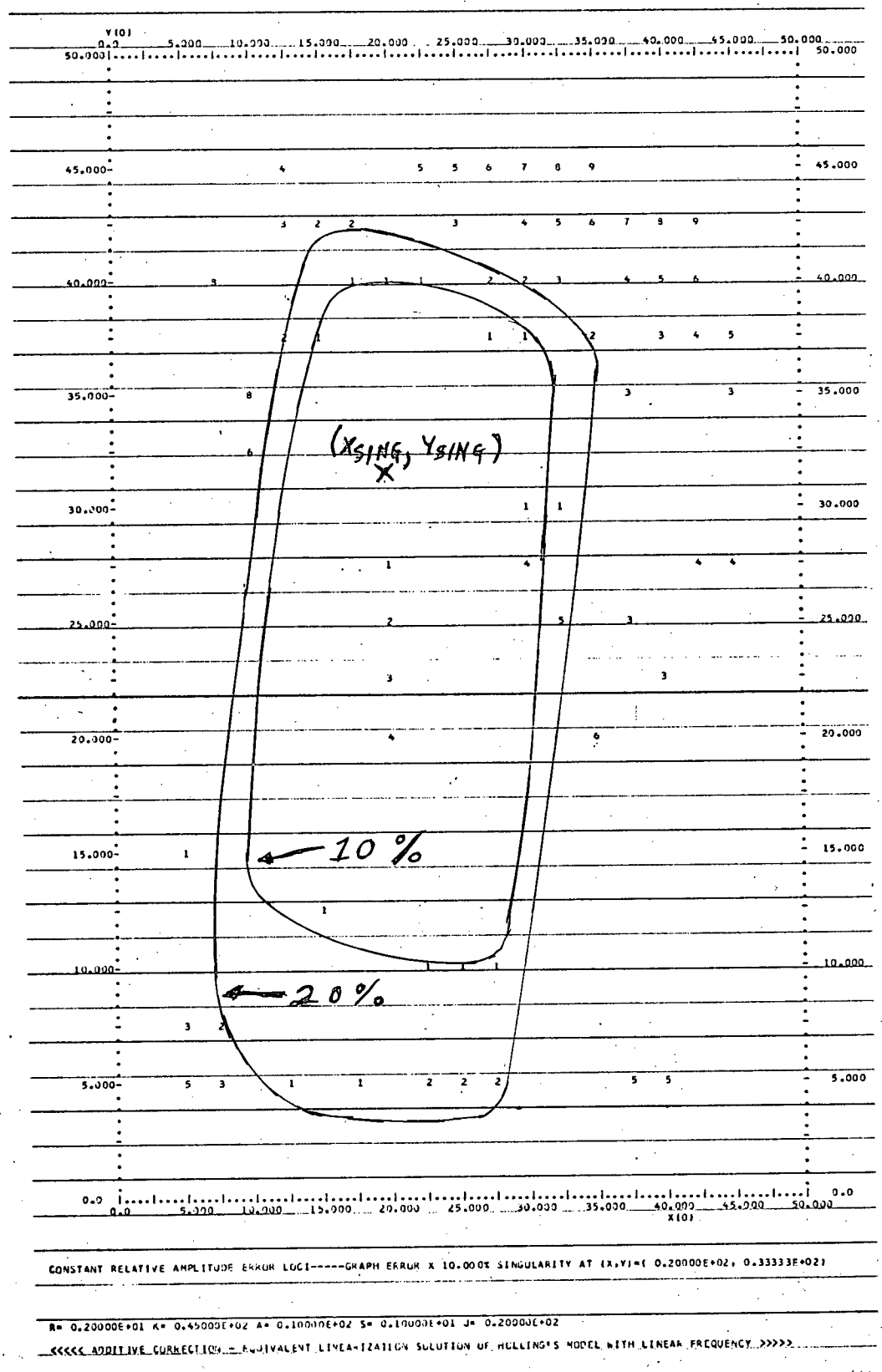

Fig. 4.18 Holling's Model Corrected Equivalent Linearization Solution Amplitude Error Loci

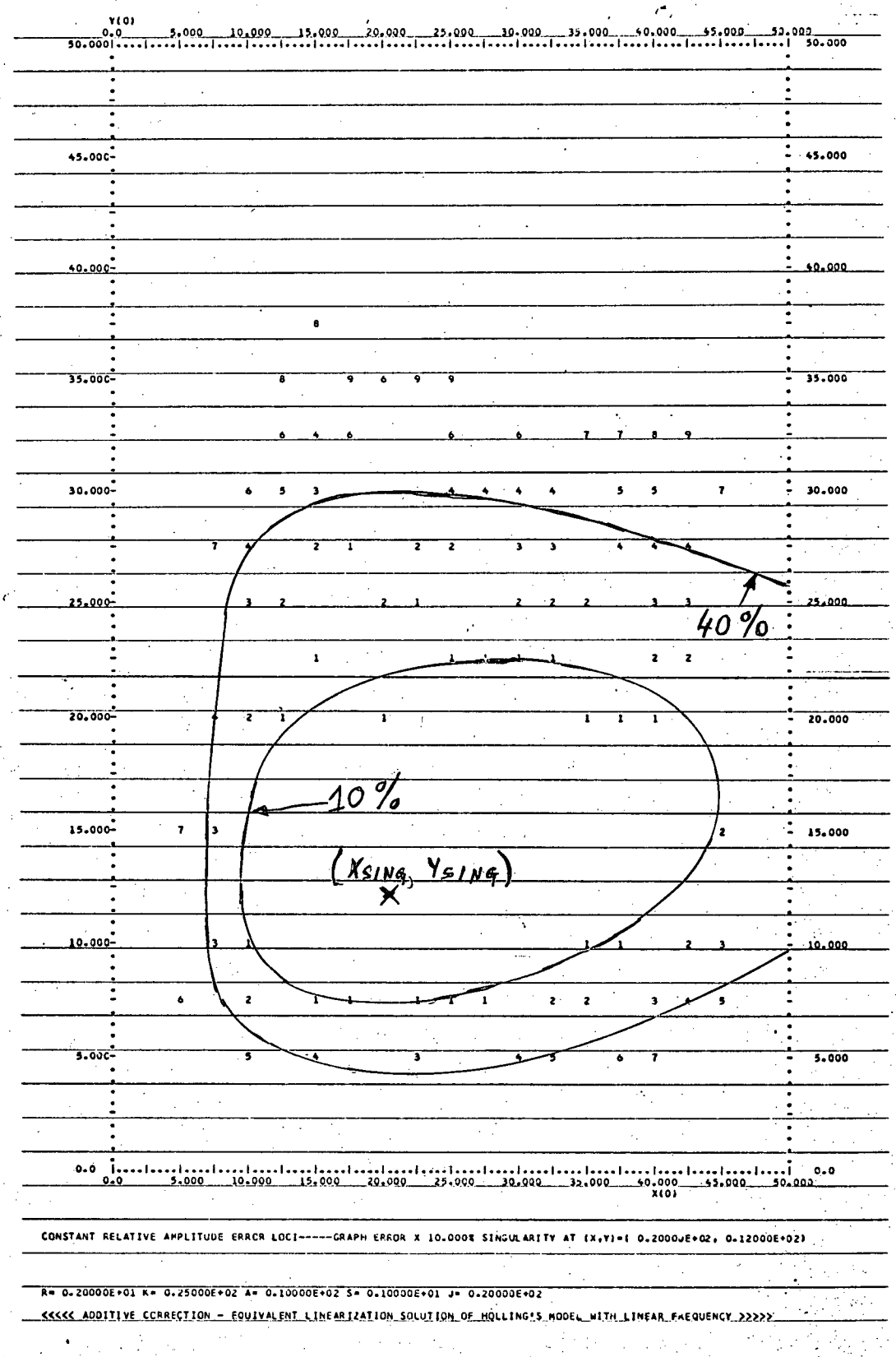

Fig. 4.19 Holling's Model Corrected Equivalent Linearization Solution Amplitude Error Loci

as for the linear solutions (see section 2.10). The amplitude error loci for the corrected underdamped case are given in figure 4.20, while the loci for the corrected overdamped case are given in figure 4.21. In both cases we observed that we have an improvement in the size of the amplitude error loci, compared with the uncorrected equivalent linearized solutions.

Here also we have found the additive correction factor to be a usefull improvement for the solutions of Rosenzweig's model. We now have one remaining model left to study.

4.7 Additive Correction Factor for O'Brien's Model

The final model that we shall apply the additive correction factor to is O'Brien's model. The correction factors may be computed in the same manner as outlined for the VGW model.

To evaluate the additive correction factor, the corrected solutions were computed for the same parameter choice and ranges of initial conditions as for the linear solutions (see section 2.13). The amplitude error loci for the corrected underdamped case are given in figure 4.22, while the loci for the corrected overdamped case are shown in figure 4.23. In both cases, we find that we have only a very small improvement in the size of the amplitude error loci over the uncorrected equivalent linearized solutions. It should be noted, however, that the uncorrected solutions are useful over a comparatively much wider range of initial conditions than the other models previously dicussed, and hence we might not expect that much of an improvement from the correction factors. This completes our evaluation of the additive correction factor as applied to the various ecological models at hand.

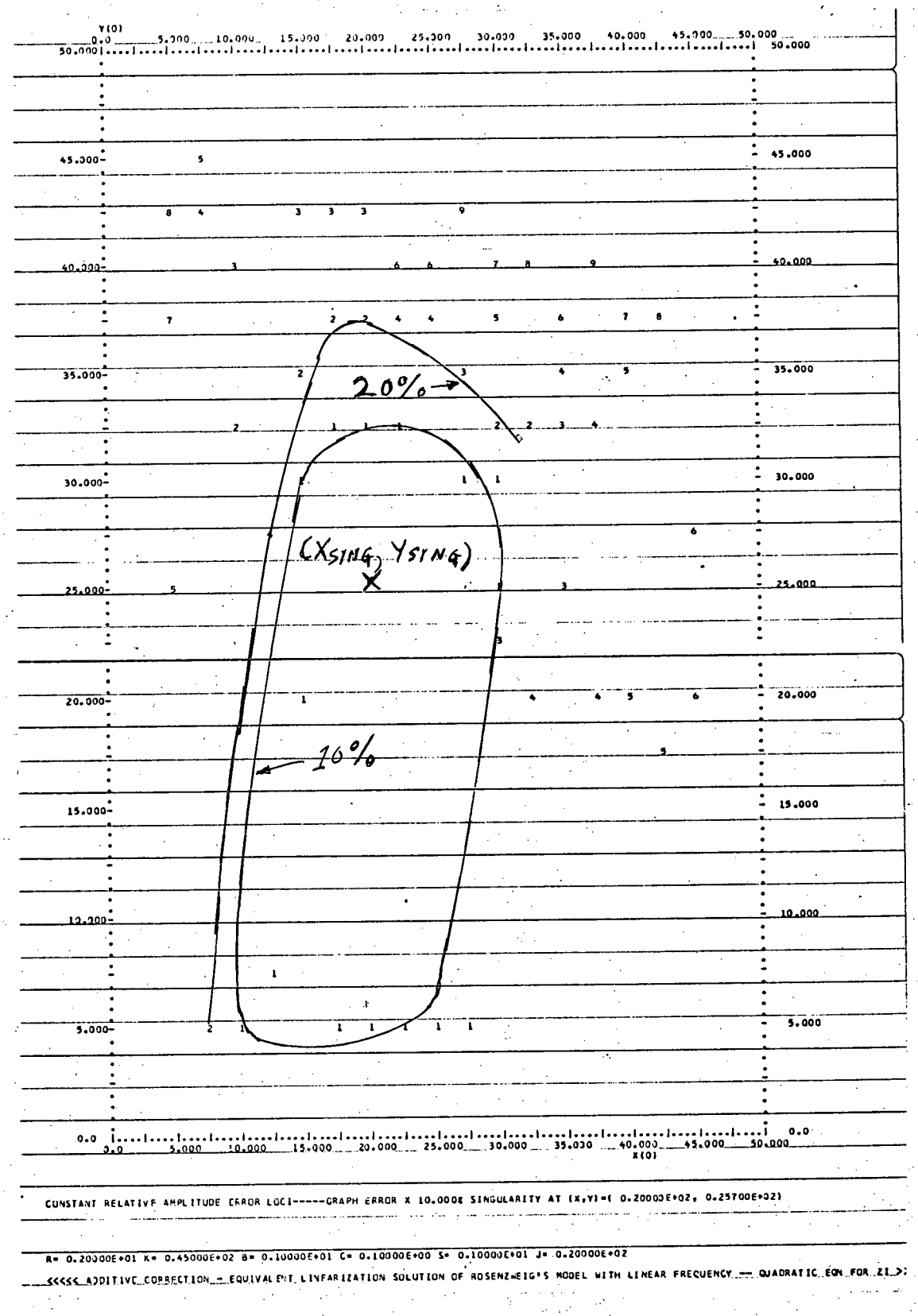

Fig. 4.20 Rosenzweig's Model Corrected Equivalent Linearization Solution Amplitude Error Loci

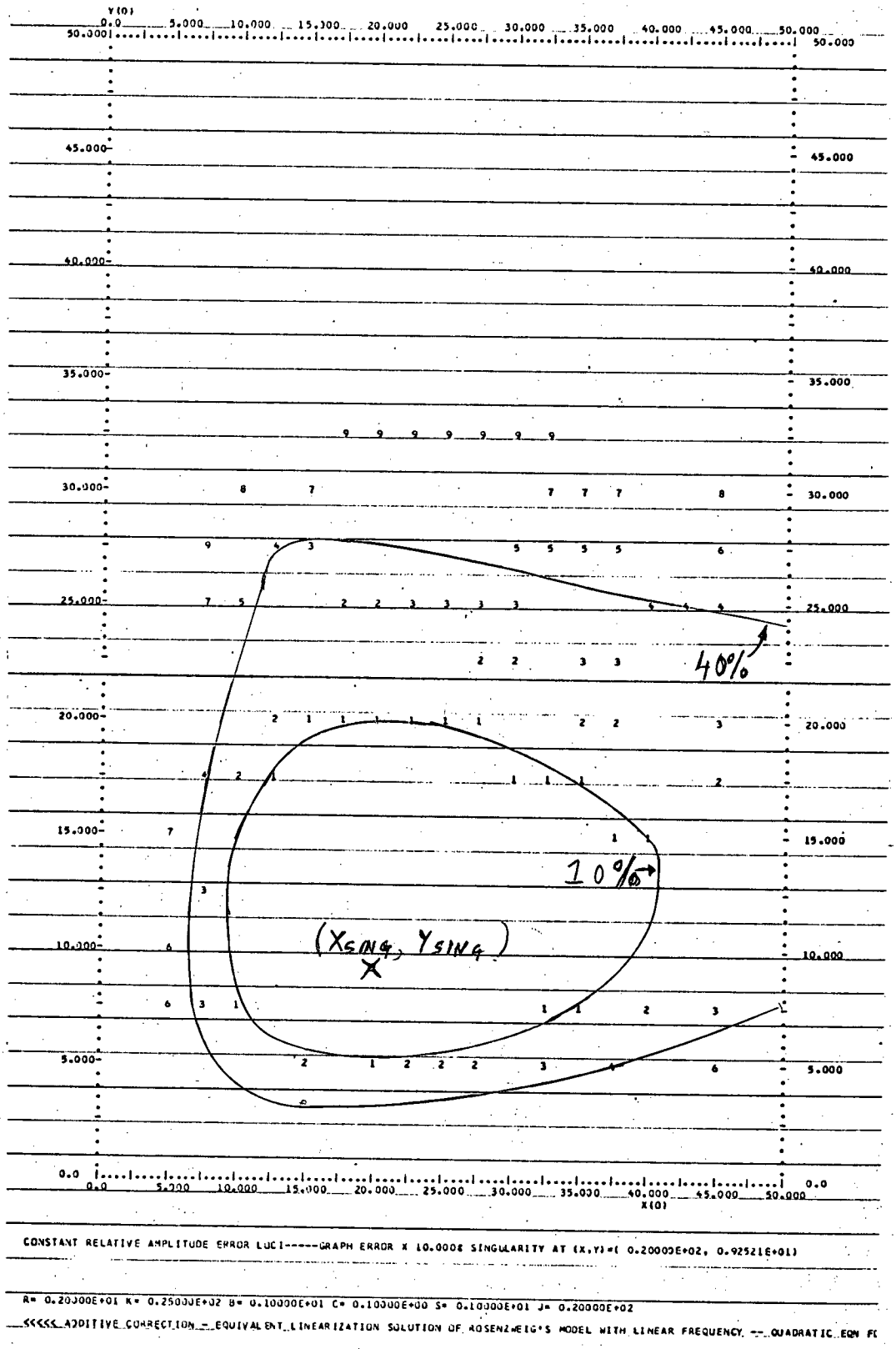

Fig. 4.21 Rosenzweig's Model Corrected Equivalent Linearization Solution Amplitude Error Loci

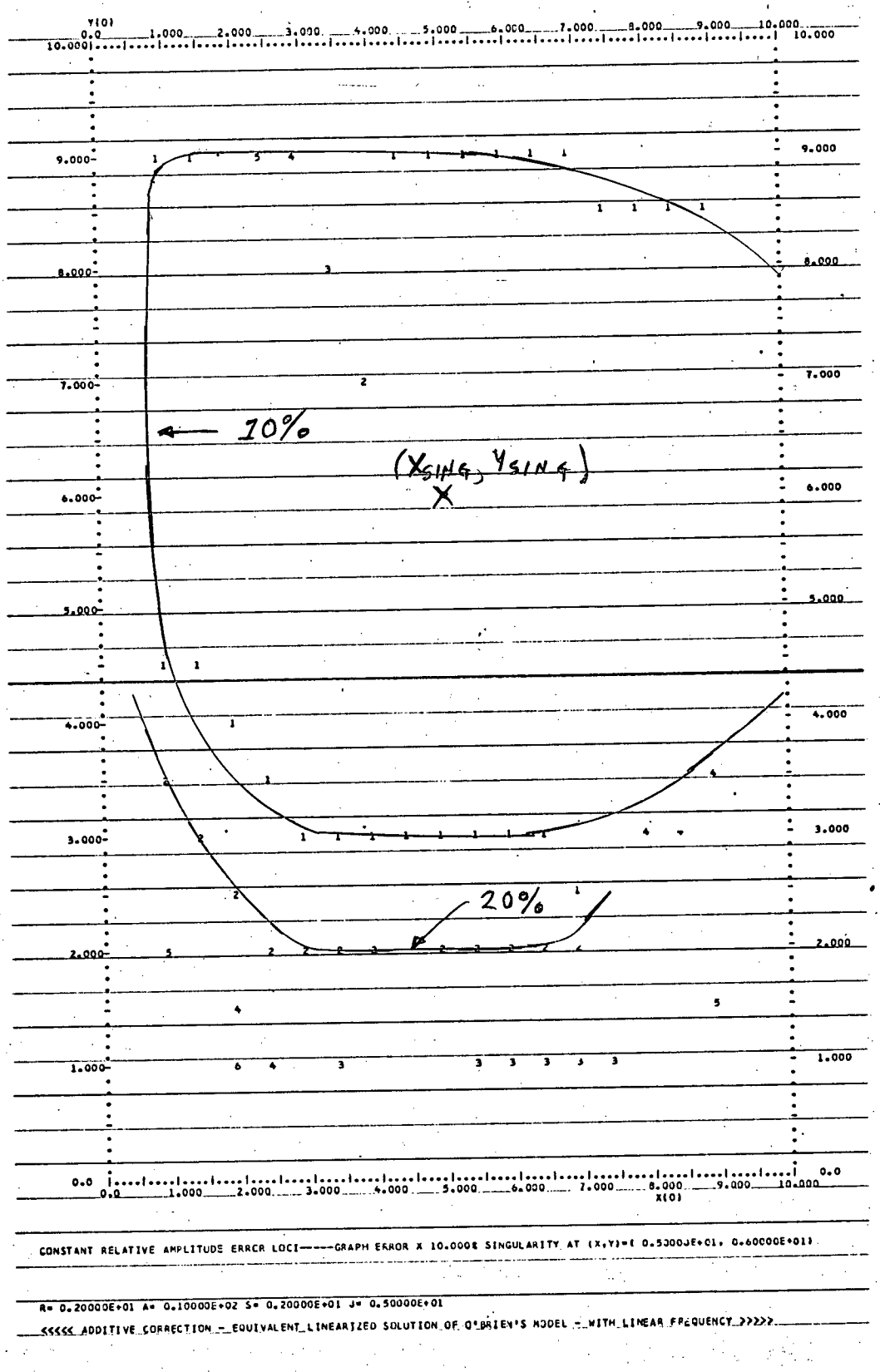

Fig. 4.22 O'Brien's Model Corrected Equivalent Linearization Solution Amplitude Error Loci

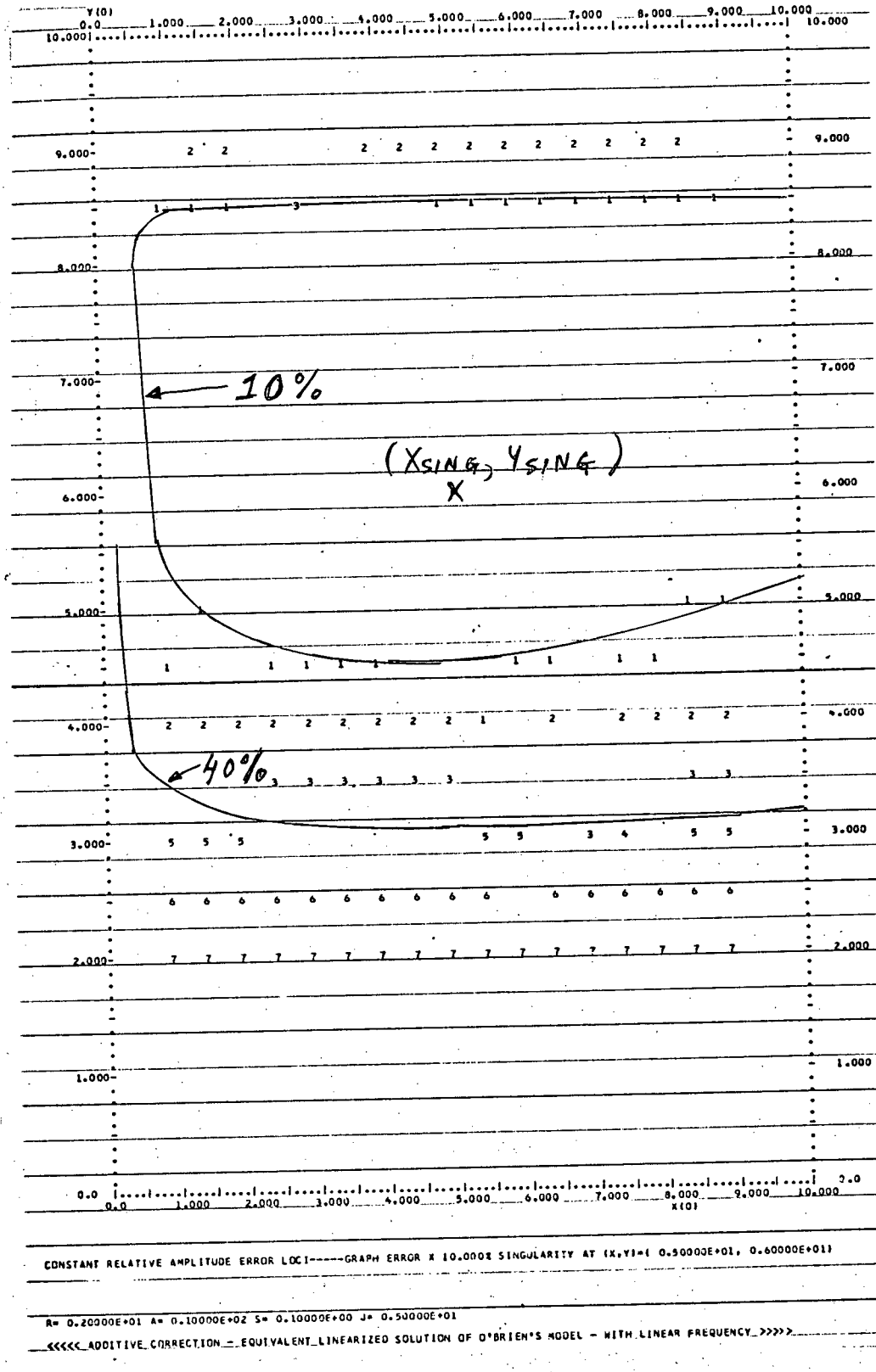

Fig. 4.23 O'Brien's Model Equivalent Linearization Solution Amplitude Error Loci

4.8 Summary

In this chapter, we have developed an additive correction factor as a refinement to the method of equivalent linearization, and it has been applied to the four ecological models discussed in chapter three. This refinement extends the range of initial conditions over which the solutions developed in chapter three are useful by reducing the error of one peak of the solution, which, in turn reduces the overall solution error. The additive correction factor does not affect the frequency of the solution. The additive correction factor increases our understanding of the models behaviour, and the effects of the various model parameters and initial conditions on the peaks of the solution oscillitions.

CHAPTER FIVE

CONCLUSIONS

In this thesis, we have developed and evaluated several different analytical techniques for obtaining literal parameter approximate solutions for pairs of first order, coupled nonlinear differential equations that model ecological systems. These solutions permit insight into the system dynamics without resorting to numerical computer studies. In all the cases considered, the solutions developed were local to the singularity of interest in the model under consideration. All the solutions obtained were usefull over a range of initial conditions larger than a small ϵ region about the singular point, contrary to what one would normally expect for differential equations that are dominated by nonlinearities.

We began by applying the classical Ritz method for dealing with conservative systems (see chapter one) to the first ecological model ever proposed, the Lotka-Volterra model. The solutions obtained by this method were found identical to those obtained by linearizing about the singularity. The results obtained were encouraging, and it was observed that the amplitude errors were the limiting the range of initial conditions over which the solutions were useable. These results motivated the development of a second method of approximating the amplitudes of the solutions. The second method improved the amplitude errors greatly, so that the limiting factor for these solutions became the frequency errors incurred for large initial conditions.

The prototype study of the conservative Lotka-Volterra system was followed by studies of nonconservative systems that incorporated more biological phenomenon than contained in the Lotka-Volterra model. In chapter two, the models of Volterra-Gause-Witt, Holling, Rosenzweig, and O'Brien

were introduced. As a preliminary means of understanding these models, the classical principle of linearization was applied to each model. Again it was found that these literal parameter linear solutions were useful over a large range of initial conditions; much more than the ϵ region about the singularity that one would normally expect. It was also observed that the amplitude error was the limiting factor in determining the range of initial conditions for which these solutions were useable. We then had a practical means of gaining insight into the behaviour of the nonconservative ecological models, without resorting to computer studies.

After completing our preliminary studies of four nonconservative ecological models, it was then desired to obtain literal parameter solutions that were usefull over a wider range of initial conditions than the previously discussed linear solutions. In chapter three, the method of equivalent linearization was developed in detail and then applied to the previously discussed models. These solutions exhibited an amplitude that had less error for given initial conditions than the linear solutions. However, the frequency of the equivalent linearization solutions had a higher error than the linear solutions for given initial conditions. A compromise was made by combining the amplitude of the equivalent linearization solutions with the frequency of the linear solutions to obtain superior solutions that possessed the good features of both techniques of solution. Here again, the amplitude error was the limiting factor for determining the usefull ranges of initial conditions for the solutions.

The results obtained for the method of equivalent linearization of nonlinear differential equations motivated us to develop a method of more accurately computing the amplitudes of the approximate solutions. In chapter four, an additive correction factor for reducing the error of one peak of the

equivalent linearization solution was proposed. This additive correction factor consisted of a modified Taylor series used to compute the actual solution peak value, combined with an n'th order exponentially damped ramp, and was designed to affect only one peak of the solution. Hence the already acceptable frequency of the solution was not interfered with. This refinement of the method of equivalent linearization extended the ranges of initial conditions over which the solutions were useable. It was found that for Rosenzweig's and Holling's models, both the amplitude and frequency errors were significant in determining the ranges of initial conditions for which the solutions were useable.

The value of all of these solutions is seen from the fact that we obtain literal parameter solutions, which also permits the user to determine which terms dominate a given component of the solution, such as frequency, time constant or singular point, and hence would be sensitive to certain parameter changes. The user may also find out which terms are negligible for a given parameter combinations. In some of the solutions, the initial conditions appear in numerous places in the solutions and in a nonlinear manner. The user is thus spared the tedious task of heuristic computer sensitivity studies.

As a comparative illustration of the improvements gained by the more complex methods developed in chapter three and four, the 10% amplitude error loci for Rosenzweig's model are superimposed for easy assessment in figure 5.1. Similar comparisons may be made for the other models studies in this thesis.

In conclusion, we have successfully developed and evaluated some practical techniques for obtaining literal parameter approximate solutions for nonlinear differential equation models of ecological systems. These

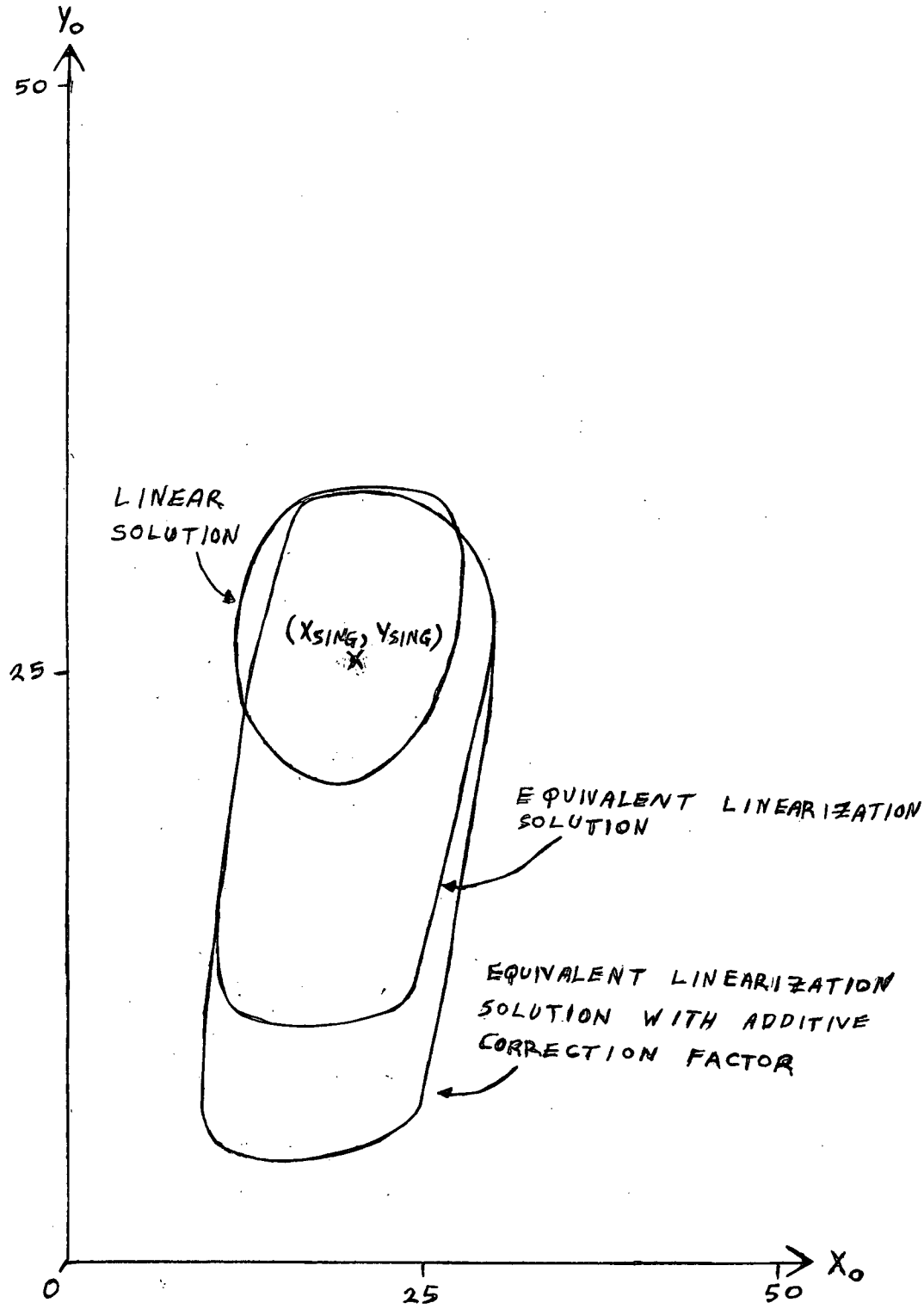

Fig. 5.1 Comparison of the 10% Amplitude Error Loci for Rosenzweig's Model for Three Solution Techniques

solutions permit the reader to rapidly become familiar with the effects of the system parameters and initial conditions on the model behaviour without resorting to the traditional numerical computer studies.

APPENDIX A

ELLIPTIC FUNCTIONS AS APPROXIMATE SOLUTIONS

In this appendix, we will very briefly outline the copious amount of work that was done using elliptic functions to obtain literal parameter approximate solutions of nonlinear differential equations. Solutions of the form

$$x(t) = A(t)Cn(\tilde{\omega}t + \theta_x, k)$$

$$y(t) = B(t)Sn(\omega t + \theta_y, k)$$

are postulated, where Cn & Sn are the elliptic cosine and sine functions, with k being the elliptic modulus, which may be a time varying quantity. The amplitude functions A(t) & B(t) and the frequency ω, may be functions of k. In all the following work, the elliptic functions were computed by the highly efficient computer oriented algorithms described by King (30).

The Lotka-Volterra model (see section 1.3) was selected for a prototype study. The elliptic functions methods developed by Barkham (2,3 and 4), Soudack (53 and 54), Lansdowne (31), and Christopher (10) were studied, and motivated us to attempt to extend them to the systems at hand. For the conservative Lotka-Volterra system, the methods reduced to a form of the Ritz method, except using elliptic functions instead of trigonometric functions. First of all, the centre singularity of the Lotka-Volterra model was translated to (0,0) and the differential equations were rewritten as a single second order differential equation to obtain:

$$\ddot{x} + \alpha\gamma x + \delta\alpha x^2 - \delta x\dot{x} - \dot{x}^2/(x + \gamma/\delta) = 0$$

Upon inserting the approximate solutions in the differential equation, we obtain equations for ω and k by matching like powers of elliptic functions. These equations, are at best, rather clumsy. The parameters ϕ and A (which

are constants in this case) were found by matching initial conditions and first derivatives. The initial major problem encountered with this model was that the parameter k turned out to be greater than unity for all but the smallest of initial conditions, which is not permitted by the definition of the elliptic functions.

In an attempt to resolve this problem, some variations in expanding the terms in the differential equation were made so as to hopefully modify the equations for k and eliminate this problem. Unfortunately, this effort was to little avail.

Following these attempts at an elliptic function solution for the Lotka-Volterra system, a solution of the form

$$x(t) = \frac{A+B\ Cn(\omega t+\phi,k)}{C+Cn(\omega t+\phi,k)}$$

was postulated. This solution would facilitate the previously discussed matching process to obtain the desired equations for the solution parameters. This yielded six huge equations in the six solution parameters, which had to be solved by the computer. The solutions obtained were of next to no improvement over the Ritz method discussed in chapter one, and certainly not worth all the additional effort required. The attemps to develop a practical elliptic function solution for the Lotka-Volterra system were then abandoned.

The next idea for developing elliptic function solutions was to modify the Krylov-Boguluibov techniques for nonconservative systems. The VGW model (see section 2.2) was selected for the prototype study. Solutions of the form

$$x = r(t)\ Cn(\theta(t), k)$$

$$y = r(t)\ Sn(\theta(t), k)$$

were proposed. The system and solutions were put in polar coordinates to

obtain:

$$r(t) = \sqrt{x^2 + y^2}$$

$$\Theta(t) = tn^{-1}[y/x,k]$$

$$\dot{r} = (x\dot{x} - y\dot{y})/r$$

and $$\dot{\Theta} = (x\dot{y} - y\dot{x})/r\sqrt{r^2-k^2y}$$

We then used the averaging techniques discussed by Lin (32) to solve for r(t) and $\Theta(t)$. To obtain a first order solution, we have:

$$\dot{r}_o \simeq F^{(1)}(r_o,\phi_o)$$

$$\dot{\phi} \simeq G^{(1)}(r_o,\phi_o)$$

$$r \simeq r_o$$

$$\Theta \simeq \phi_o$$

where $$F^{(1)}(r_o,\phi_o) = \frac{1}{4K} \int_o^{4K} [F(r_o,\phi_o)Cn(\phi_o,k)+G(r_o,\phi_o)Sn(\phi_o,k)]d\phi_o$$

$$G^{(1)}(r_o,\phi_o) = \frac{1}{4K} \int_o^{4K} \frac{1}{r_o Dn(\phi_o,k)} [G(r_o,\phi_o)Cn(\phi_o,k)-F(r_o,\phi_o)Sn(\phi_o,k)]d\phi_o$$

In the above integrals, we treat r_o and ϕ_o as constants. To simplify the integrals further, we approximate $G^{(1)}(r_o,\phi_o)$ as:

$$G^{(1)}(r_o,\phi_o) = \frac{1}{4Kr_o\overline{Dn}} \int_o^{4K} [G(r_o,\phi_o)Cn(\phi_o,k)-F(r_o,\phi_o)Sn(\phi_o,k)]d\phi_o$$

where $$\overline{Dn} = \pi/2K(k)\sqrt{1-k^2}$$

We still have to determine the parameter k. The first method used to obtain k was to minimize the mean square error of the derivatives with respect to k over one period of the solution, 4K, as follows

$$\frac{\delta}{\delta k}[\frac{1}{4K} \int_o^{4K} \{[F(.,.)- \frac{d}{dt}(rCn\Theta)]^2+[G(\cdot,\cdot) \frac{-d}{dt}(rSn\Theta)]^2\}d\theta] = 0$$

The equations obtained were extremely messy and the corresponding results

were very poor. The problem of k being greater than unity was also encountered again. The equations for k (as determined above) did, however, suggest that k would be of the form $k^2 = pr(t)$, with p being a constant. We then assumed this to be the case, and attempted to find an equation for p. This was done by matching initial derivatives. The solutions obtained were as good as those obtained by the method of equivalent linearization. However, for some initial conditions, the value of p computed caused k to become greater than unity. This idea for computing k was abandoned for lack of better ideas.

As this method of determining elliptic functions solutions for nonlinear differential equations was going through its final deathbed convulsions, one final heuristic attempt to find an equation for k was proposed. It was conjectured that the system at hand was equivalent to a second order differential equation of the form $\ddot{x} + b\dot{x} + \omega^2 x + px^3 = 0$. This differential equation has an elliptic function solution with k being given by $k^2 = pr^2/2(\omega^2 + pr^2)$. This form of k was adopted for use in the solution at hand. Again p was obtained by matching initial first derivatives. Unfortunately, for some initial conditions, p was negative, which caused the denominator of k to become small and hence k exceeded unity. For the initial conditions that this idea worked, the results obtained were only as good as those obtained for the method of equivalent linearization.

At this point, the idea of obtaining elliptic function solutions for the differential equation ecological models was completely abandoned. The problem to be tackled by future researchers is that of obtaining an equation for k such that $k^2 \leq 1$ for all initial conditions.

APPENDIX B

PRELIMINARY DEVELOPMENTS OF THE ADDITIVE CORRECTION FACTOR

In this appendix, we will very briefly outline the chronological attempts to obtain an additive correction factor for the solutions of the method of equivalent linearization. The final version of the additive correction factor is presented in chapter four. In all work, the VGW model (see section 2.2) was used for the prototype study.

The first method evaluated for obtaining the additive correction factors was a modification of the method of equivalent linearization, so that the solutions of the differential equations would contain the desired transient terms. To do this, we started with the desired solutions

$$x(t) = r_x e^{\sigma t}\cos(\omega t + \theta_x) + A_x t\, e^{\sigma_x t}$$

$$y(t) = r_y e^{\sigma t}\sin(\omega t + \theta_y) + A_y t\, e^{\sigma_y t}$$

and used Laplace transforms to work backwards to obtain the differential equations that would generate these solutions. We obtained:

$$\dot{x} = a_{11}x - a_{12}y + A_x e^{\sigma_x t} + (\sigma_x - a_{11})tA_x e^{\sigma_x t} + a_{12}A_y te^{\sigma_y t}$$

$$\dot{y} = a_{21}x + a_{22}y + A_y e^{\sigma_y t} + (\sigma_y - a_{22})tA_y e^{\sigma_y t} - a_{21}A_x te^{\sigma_x t}$$

We then had to determine the parameters of the differential equations.

We followed the method outlined in chapter three, and minimized the mean square derivative error J, over one period of the solution, which gives us eight equations for the eight system parameters, which are:

$$J = \frac{1}{2\pi}\int_0^{2\pi} \{[F(x,y) - \dot{x}]^2 + [G(x,y) - \dot{y}]^2\}\, d\theta$$

$$\frac{\partial J}{\partial a_{11}} = \frac{1}{2\pi}\int_0^{2\pi}[F(x,y)-\dot{x}][r_1\cos\theta - tA_x e^{\sigma_x t}]\,d\theta = 0$$

$$\frac{\partial J}{\partial a_{12}} = \frac{1}{2\pi}\int_0^{2\pi}[F(x,y)-\dot{x}][r_2\sin\theta - tA_y e^{\sigma_y t}]\,d\theta = 0$$

$$\frac{\partial J}{\partial a_{21}} = \frac{1}{2\pi}\int_0^{2\pi}[G(x,y)-\dot{y}][r_1\cos\theta - tA_x e^{\sigma_x t}]\,d\theta = 0$$

$$\frac{\partial J}{\partial a_{22}} = \frac{1}{2\pi}\int_0^{2\pi}[G(x,y)-\dot{y}][r_2\sin\theta - tA_y e^{\sigma_y t}]\,d\theta = 0$$

$$\frac{\partial J}{\partial A_1} = \frac{1}{2\pi}\int_0^{2\pi}\{[F(x,y)-\dot{x}][e^{\sigma_x t} + (\sigma_x - a_{11})te^{\sigma_x t}] + [G(x,y)-\dot{y}][-a_{21}te^{\sigma_y t}]\}\,d\theta = 0$$

$$\frac{\partial J}{\partial A_2} = \frac{1}{2\pi}\int_0^{2\pi}\{[F(x,y)-\dot{x}][a_{12}te^{\sigma_x t}] + [G(x,y)-\dot{y}][e^{\sigma_y t}+(\sigma_y - a_{22})t\,e^{\sigma_y t}]\}\,d\theta = 0$$

$$\frac{\partial J}{\partial \sigma_x} = \frac{1}{2\pi}\int_0^{\pi}\{[F(x,y)-\dot{x}][2\,te^{\sigma_x t} + (\sigma_x - a_{11})t^2 e^{\sigma_x t}] + [G(x,y)-\dot{y}][-a_{21}t^2 e^{\sigma_x t}]\}\,d\theta = 0$$

$$\frac{\partial J}{\partial \sigma_y} = \frac{1}{2\pi}\int_0^{2\pi}\{[F(x,y)-\dot{x}][a_{12}t^2 e^{\sigma_y t}] + [G(x,y)-\dot{y}][2te^{\sigma_y t} + (\sigma_y - a_{22})t^2 e^{\sigma_y t}]\}\,d\theta = 0$$

We make the assumption in evaluating the integrals for the a_{ij} that the transient terms $tA_x e^{\sigma_x t}$ and $tA_y e^{\sigma_y t}$ may be neglected in the computations. Thus, the first four equations reduce to those obtained for the a_{ij} in chapter three.

To evaluate the remaining four integrals, it was assumed that the transients were slowly changing and that we could make the approximation $e^{\sigma_x t} \simeq 1$. We then obtained four huge nonlinear algebraic equations in the four unknowns, A_x, A_y, σ_x, σ_y. Numerical solutions of these equations

yielded (for some initial conditions) $\sigma_x > 0$ and $\sigma_y > 0$, which is not acceptable as we know the models under analysis are stable.

It was then conjectured that the initial assumption that $e^{\sigma_x t} \simeq 1$ and $e^{\sigma_y t} \simeq 1$ was invalid. The last four integrals were recomputed without this assumption to yield even more horrendous equations for the unknowns A_x, A_y, σ_x, and σ_y. However, upon numerical solution of these equations, we obtained reasonable values for σ_x and σ_y, but the values for A_x and A_y were several orders of magnitude to small.

At this juncture, it was decided to try an alternate method for computing the remaining four parameters. By matching initial first and second derivatives of the solution with the original differential equation, we obtain comparatively simple formuae for the parameters. Unfortunately, we run into the problem of σ_x and σ_y being greater than zero for some initial conditions. For lack of more useful ideas, the whole concept of the modified equivalent linearization differential equation was scrapped.

The concept of the peak correction factor was slowly beginning to materialize at this point in time. The first idea for computing the peak values of the solutions was based on an idea taken from the techniques used to numerically solve differential equations, and was as follows. We rewrite our differential equation in form of an integral equation as $x(t) = \int_0^t F(x,y)dt + x_o$. To approximate the integral, we use the previously developed equivalent linearization solutions in the integrand, $F(x,y)$. This method accurately predicts the peak values of the solutions if the peak point is very close to the time origin. This method was not good enough for all values of initial conditions.

The next idea was to approximate the first fraction of a period of the solution by the polynomial $x(t) = x_o + at + bt^2$, where a and b are chosen

so that the first derivatives of the two solutions match, and the polynomial attains its peak value at the time of the actual peak (which is predicted from the phase of the linear solutions). This polynomial was then used in the above integral equation. This idea accurately predicted the peaks for most initial conditions, but not all possible cases.

At this point, it was decided that more terms in the polynomial were needed to accurately predict the solutions peaks for all initial conditions. We then began experimenting with three and four term McLaurin expansions. The reader is now referred back to chapter four for the discussion of this idea and the remainder of the development of the additive correction factor.

REFERENCES

1) Ayala, F.J. & Gilpen, M.E. & Ehrenfeld J.G., 1973 Theor. Pop. Biol. 4 pp. 331-356.

2) Barkham, P.G.D. & Soudack, A.C., 1969 Int. J. Control 4, pp. 377-392.

3) Barkham, P.G.D. & Soudack, A.C., 1970 Int. J . Control 1, pp. 101-114.

4) Barkham, P.G.D. & Soudack, A.C., 1977 Int. J. Control 3, pp. 341-358.

5) Bogoluibov, N.N & Mitropolsky, Y.A., 1961, "Asymptotic Methods in the Theory of Nonlinear Oscillation ", Hindustan Publishing Corp., Delhi.

6) Brauer, F. & Sánchez, D.A., 1975, Theor. Pop. Biol. 1, pp. 12-30.

7) Brauer, F. & Soudack, A.C., & Jarosch, H.S., 1976, Int. J. Control 4, pp. 553-573.

8) Brauer, F. & Soudack A.C., 1976 Math. Research Centre Technical Report #1664, Univ. Wisconsin.

9) Brearley, J.R. & Soudack, A.C., 1978 Int. J. Control to appear.

10) Christopher, P.A.T. 1973, Int. J. Control 3, pp. 597-608.

11) Clark, C.W. "Mathematical Bioeconomics", J. Wiley & Sons, New York, 1976, pp. 194-196.

12) Comins, H.N. & Hassel, M.P., 1976, J. Theor. Biol. 62, pp. 93-114.

13) Cunningham, W.J., 1958, "Introduction to Nonlinear Analysis", McGraw-Hill, New York.

14) Diamond, P., 1976. J. Theor. Biol. 61, pp. 287-306.

15) Dutt, R. & Ghosh, P.K., 1975, Math. Bioscience, 27, pp. 9-16.

16) Dutt, R., Ghosh, P.K., & Karmakar, B.B., 1975, Bulletin of Math. Biol. 37, pp. 139-146.

17) Frame, J.S., 1974, J. Theor. Biol. 43, pp. 73-81.

18) Frederikson, A.G. & Jost, J.L., Tsuchiya, H.M. & Hsu, P.H., 1973, J. Theor. Biol., 38, pp. 487-526.

19) Gause, G.F., 1934, Science, 79, p.16.

20) Gause, G.F., 1934, "The Struggle for Existence" Williams & Wilkin Co., Baltimore.

21) Gilpen, M.E. & Ayala, F.J. 1973, Proc. Nat. Acad. Sci. 70, pp.3590-3593.

22) Gilpen, M.E. & Justice, K.E., 1973, Math. Bioscience 17, pp. 57-63.

23) Grassman, & Veling, E. 1973, Math. Bioscience 18, pp. 185-189.

24) Greenberg, J.M. & Hoppenstead, F. 1975. SIAM. J. Applied Math. 3, pp.662-674.

25) Holling, C.S. 1965, Mem. Ent. Soc. Canada, 45, pp. 5-60.

26) Hoppenstead, F., 1976, Science 194, pp. 335-337.

27) Hoppenstead, F. "Optimal Exploitation of a Spatially Distributed Fishery" preprint.

28) Hoppenstead, F. & Hyman, J.M. "Periodic Solutions of a Logistic Difference Equation", preprint.

29) Ivlev, V.S., 1961, "Experimental Ecology of the Feeding of Fishes", Yale Univ. Press, New Haven.

30) King, L.V. 1924, "On the Direct Numerical Calculation of Elliptic Functions and Integrals", Cambridge at the Univ. Press.

31) Lansdowne, D.L. & Soudack, A.C., 1971, Int. J. Cont. 6, pp.1151-1159.

32) Lin, J. & Kahn, P.B., J. Theor. Biol. 57, p.73-102, 1976.

33) Lotka, A.J. 1924, "Elements of Physical Biology", Williams & Wilkins, Baltimore.

34) May, R.M. 1973, "Stability and Complexity in Model Ecosystems", Princeton Univ. Press, New Jersey.

35) May, R.M., 1974, Science Vol. 186. pp.645-647.

36) May, R.M. , July, 1976 NATO Ecoscience Conference, "Factors Controlling the Stability and Breakdown of Ecosystems".

37) May, R.M. & Oster, G.F. 1976, Amer. Nat., 110 p.573.

38) Mazanov, A. 1974, J. Theor. Biol., 46 pp.271-282.

39) McGehee, R. & Armstrong, R.A., 1977, J. Differential Equations 23, pp.30-52.

40) Mulholland, R.J, & Keener, M.S., 1974, J. Theor. Biol. 44, pp.105-116.

41) Murray, J.D., 1976 Math Biosciences, 30, pp.73-85.

42) Nayfeh, A.H., 1973, "Perturbation Methods", J. Wiley & Sons, New York.

43) Oaten, A., & Murdoch, W.W., 1975, Amer. Nat. 109 pp.289-298.

44) O'Brien, W.J., 1974, Ecology, 55, pp135-141.

45) Oster, G.F., 1975, SIAM Ecosystem Analysis and Prediction.

46) Rapport, D.J. & Turner, J.E., 1975 J. Theor. Biol., 51, pp.169-180.

47) Rosenzweig, M.L., 1969, Amer. Nat. 103, pp.81-87.

48) Rosenzweig, M.L., 1971 Science, 171 , pp.385-387.

49) Rosenzweig, M.L., 1973, Amer. Nat. 107, pp.275-294.

50) Sánchez, D.A., 1977, "Linear Age-Dependant Population Growth with Harvesting" preprint.

51) San Goh, B., Leitmann, G., & Vincent, T.L., 1974, Math. Bioscience, 19, pp.263-286.

52) Smale, S., & Williams, R.F., 1976, J. Math. Biol. 3, p.1-4.

53) Soudack, A.C. & Barkham, P.G.D., 1970, Int. J. Cont. 12, pp.763-767.

54) Soudack, A.C., 1974, Int. J. Cont., 19, pp.841-844.

55) Volterra, V., 1931, "Leçons sur la Theorie Mathamatique de la Lutte pour la Vie", Gauthiers-Villars, Paris.

56) Wayland, H., 1970, "Complex Variable applied in Science and Engineering", pp.137-138, Van Nostrand-Reinholt Co., New York.

57) Zwanzig, R., 1973, Proc. Nat. Acad. Sci., 70, pp.3048-3051.